ABSTRACT

WOOLARD, KEVIN DOUGLAS. Comparative Biology of Glioma Stem Cells and Embryonic Neural Stem Cells in Dogs. (Under the direction of Dr. John Cullen and Dr. Howard A Fine).

In spite of accounting for less than 1.5% of human cancers in the United States, glioma tumors are a leading cause of cancer related mortality, with a dismal median survival time of only 12 months in patients suffering from glioblastoma multiforme (GBM). These tumors are driven by glioma stem cells (GSCs), a subpopulation of cells with similar molecular and functional characteristics to physiologic neural stem cells. Widespread and intensive investigation regarding the biology of these GSCs has nonetheless yielded disappointingly little progress in our understanding of the formation or progression of glioma tumors to date. Confounding attempts at dissecting the complex genomic aberrations in human GBMs are the often-large regions of chromosomal amplification or deletion, frequently involving entire chromosomal arms, in which we are only able to ascribe significant tumor suppressor or oncogene function to a single gene within this large region. In the face of such a complex, heterogeneous genome, efforts at modeling glioblastoma biology in genetically engineered mouse models by deleting or amplifying single genes or small clusters of genes often fails to recapitulate the behavioral, phenotypic, or genomic heterogeneity of spontaneous human glioblastoma tumors. Currently, there is no validated, naturally occurring model for human gliomagenesis. The domestic dog recapitulates every human histologic grade and develops glioma at an equivalent incidence to humans and as such, represents the only feasible model for comparative study of spontaneously occurring glioma tumors.

Here, we have characterized the dramatic similarities between glioma stem cells isolated from a canine anaplastic astrocytoma and our human GSC lines, and follow the canine GSCs as they form serial, orthotopic xenografts in immunocompromised mice. Serial xenotransplantation of our canine GSCs results in a progressive increase in tumor malignancy, expansion of the GSC subpopulation, and progressive genomic alterations strikingly similar to those associated with human secondary GBM formation. Chiefly, canine GSCs exhibit deletions of *CDKN2A*/p16^{Ink4a}, deletion of *PTEN*, and loss of p53 function through amplification of MDM2 and MDM4 and loss of ARF. Importantly, these three pathways are identified as the major alterations driving human gliomagenesis, suggesting significant similarities between the two species at a molecular or genomic level.

In addition to the identification of these highly conserved copy number alterations (CNAs) present in our canine GSCs over serial xenotransplantation, analysis of the comparative genomic alterations between canine and human GSCs identifies numerous additional, putative tumor suppressor genes across both species. The canine genome is organized into 38 autosomes compared to 22 in the human, resulting in the dispersion of human chromosomal regions across multiple syntenic canine genomic segments occupying numerous individual chromosomes and allowing us to focus comparisons on small, highly conserved regions containing tumor suppressor or oncogenes we believe may be relevant to human glioma biology.

Additionally, we have isolated and characterized canine physiologic neural stem cells throughout gestation. Embryonic neural stem cells early in brain development exhibit increased clonogenic growth and proliferation, express higher markers associated

with stem cell biology and perhaps most important, are refractory to differentiation cues- all of which are features shared by glioma stem cells. Global gene expression analysis of these embryonic neural stem cells identifies shared signaling networks to other mammalian neural stem cells. Future analysis of transcriptional networks governing canine neural stem cell self-renewal may reveal novel genes or gene interactions governing the proliferation of canine and human GSCs.

Comparative Biology of Glioma Stem Cells and Embryonic Neural Stem Cells in Dogs

by
Kevin Douglas Woolard

A dissertation submitted to the Graduate Faculty
of North Carolina State University
in partial fulfillment of the
requirements for the degree of
Doctor of Philosophy

Comparative Biomedical Sciences

Raleigh, NC

2011

APPROVED BY:

_____	_____
Dr. John Cullen Chair of Advisory Committee	Dr. Howard A Fine
_____	_____
Dr. R. Mark Simpson Co-Chair of Advisory Committee	Dr. Matthew Breen
_____	
Dr. Dave Malarkey	

DEDICATION

This dissertation is dedicated to my Parents, Don and Liz Woolard, for always being in my corner and offering the kind of unwavering love and support that can still make the world seem right on a cloudy day; to my sister Ashley Woolard for all of her love, friendship, and inspiration; to Heather Shive and Charles Hunt for being my friends always, and my family when i need it; to Sandy, the 9-year-old lab without whom this would not be possible, and to her generous owners that believed in the benefit of this research to both humans and dogs; to the memory of Kyleigh Mahard Geissler, aka The Boss, you will always be missed my good friend; and finally to God, for all of the blessings i receive.

BIOGRAPHY

Kevin Woolard was born and raised in Raleigh, North Carolina, who's parents having found the most beautiful state in the United States, decided not to move away from it. Despite the efforts of an amazing high school physics teacher, he became interested in veterinary medicine while in high school and entered North Carolina State University in 1996 upon graduation from W. G. Enloe High in Raleigh. There, he never met a major that he didn't like at least enough to minor in, but all the while kept his goal of attending veterinary school first and foremost, achieving this in 1999 and leaving undergraduate studies without a degree, proving a high school diploma can still get you places. After quickly learning that his perceived calling as a veterinary surgeon was ill founded at best, he vacillated between internal medicine and pathology until the last possible moment, when all of life's best decisions are made. After graduation from veterinary school in 2003, he entered a combined residency and PhD program through the Graduate Scholars in Molecular Pathology Program at the National Cancer Institute in Bethesda, Maryland under the direction of Dr. R. Mark Simpson, and joined the Neuro-Oncology Branch under Dr. Howard A Fine in July of 2006, where he has lived happily ever since.

ACKNOWLEDGEMENTS

i would like to sincerely thank my entire committee for your time, support, and efforts spent on my behalf through the years. In particular, i would like to thank Dr. Howard Fine for allowing me this opportunity to join the Neuro-Oncology Branch when i showed up one day talking about dogs with brain tumors, and for being a mentor over the last four years. Your devotion to your patients and the lab are truly amazing and inspiring. To Dr. Mark Simpson, who recruited me to the National Cancer Institute and has been nothing short of incredible in offering support, advice, and assistance in any aspect during my entire tenure here. Truly, i cannot thank you enough for all of your help and it will never be forgotten. i would like to thank Dr. John Cullen for his mentorship through veterinary school, an anatomic pathology residency, and then through graduate school. Thank-you for allowing me to work in your laboratory through veterinary school, which ultimately rekindled my passion for basic research-while hepatology is now second fiddle to brain tumors, it's a strong second place. To Dr. Matthew Breen and Dr. Rachael Thomas, for holding my hands through learning the basics of comparative genomic hybridization and for all of your great assistance and insights throughout this study. To Dr. Jeongwu Lee, thank you for having the faith in me that you did and to teach me how to work independently. You are a great scientist and it was a pleasure. To Dr. Wei Zhang, thank you for the support i always feel, even when things are not going as well as i'd like, you are an amazing person and we are all lucky to work with you. i would like to thank Dr. Myung jin Son for her amazing assistance as i joined the lab and

for her friendship over the years, i wish you the best success in life. To Dr. Yuri Kotliarov, i thank you for all of your efforts analyzing the canine SNP arrays and for tolerating my endless iterations of figures. To my fellow lab members, thank you for putting up with me through board exams and everything in between. In particular, i would like to thank (Future Dr.) Chibawanye Ene, Dr. Emely Castro-Rivera, Dr. Ido Nevo, and Dr. Amanda Linkous for your friendship, advice, and support. i gratefully acknowledge the amazing efforts of the Animal Brain Tumor Core here at the Neuro-Oncology Branch for their assistance and care of the mice involved in this study, and to Dr. Galina Belova for her much-appreciated help in culturing an ever-increasing set of tumor stem cells. i would also like to thank Dr. Dragan Maric for his assistance in FACS analysis and for taking the time to help a new graduate student troubleshoot a laundry list of antibodies in a nonstandard species. Additionally, i would like to thank Dr. Maggie Cam for putting together the collaborations needed to complete this work and to help in keeping me off the panic button when things look like they might fall apart. i thank the members of the Comparative Molecular Pathology Unit for all of you assistance, advice, and friendship- to Mrs. Shelley Hoover for all of your technical assistance and support, to Dr. Josh Webster for your truly amazing and tireless efforts trying to get me ready for boards and most of all, for your friendship, and to Ms. Jennifer Edwards for your help and always being a counterweight to my cloud. Finally, i would like to thank the other members of the Graduate Scholars in Molecular Pathology Program, both past and present. You are some of my best friends and i count myself lucky to be included amongst you all.

TABLE OF CONTENTS

LIST OF FIGURES

ISOLATION AND COMPARISON OF CANINE GLIAL AND NON-GLIAL NEUROEPITHELIAL TUMOR STEM CELLS

ISOLATION AND CHARACTERIZATION OF CANINE EMBRYONIC NEURAL STEM CELLS IDENTIFIES TEMPORALLY REGULATED DIFFERENTIATION POTENTIAL THROUGHOUT GESTATION

LIST OF TABLES

1) INTRODUCTION

Despite aggressive multimodality treatment, the overall prognosis for human patients with high-grade gliomas (anaplastic astrocytomas and glioblastoma multiforme (GBM)) remains very poor, with median survival times of those suffering from GBM around 12 months (1). A greater understanding of the biological basis for these tumors offers the best hope for improved therapeutic strategies. The isolation and characterization of cells with stem cell like properties from human glioma (glioma stem cells, or GSCs) has radically altered investigations into the underlying events resulting in glioma formation, attributing the tumorigenicity to this specific sub-population of cells (2-4). For all of the excitement generated by these cells however, significant improvement in our understanding of the salient genomic events and cellular deregulation in the formation and progression of glioma in patients remains elusive. Major questions still persist regarding the cell of origin of these tumors, their relationship to physiologic neural stem cells (NSCs), and the complex molecular events involved in the malignant transformation.

The disappointment in progress towards understanding glioma and particularly glioma stem cell biology may be explained in part by the lack of available nonhuman models for spontaneous glioma development as a base for comparative biological investigation. While genetically engineered mouse models of glioma disease offer unquestionable use for the investigation of single genes or even combinations of particular genes, they fail to

reproduce the pronounced genetic instability and complex genomic rearrangements that are characteristic of spontaneous malignant neoplasia, and GBM tumors in particular (5).

The domestic dog represents the only available model of spontaneous glioma disease suitable for comparative study, as it develops glioma tumors with remarkable histologic and behavioral similarity (all histologic grades identified in human are recapitulated in dogs, including GBM), and tumors occur at a nearly identical reported incidence (6-8). Despite a recent report of GSCs isolated from a canine GBM and comparative genomic analyses between canine and human gliomas however, our understanding of the molecular events driving canine gliomagenesis and in particular, how it relates to humans is lacking (7, 9).

Recent, high throughput analysis of over two hundred human GBMs has identified the most common genomic alterations across these samples, with three pathways that appear to drive tumor formation (10). These commonly altered pathways are the PTEN/PI3K/AKT pathway, the p53 pathway, and the retinoblastoma ($Rb1/p16^{Ink4a}$) pathway. Loss of *PTEN* and the subsequent increase in AKT activity leads to enhanced tumor cell survival, invasion, growth, angiogenesis, and alters the metabolism of the cell. Decreased p53 activity may arise through either mutations in *TP53* or through increased degradation of the p53 protein in human gliomas. Regardless of the mechanism, loss of p53 activity significantly decreases the ability of the cell to initiate apoptosis or perhaps more importantly, to enter senescence due to the increased oncogene activity in tumor

cells (e.g. AKT activity). Finally, inactivation of Rb1 in gliomas increases the overall transcriptional activity of cells, mitigates cell cycle checkpoints, and cooperates with decreased p53 activity to inhibit the ability of a cell with oncogene-induced genomic stress to enter senescence. The culmination of these three commonly altered pathways results in a cooperative state of increased oncogene-mediated cell growth, while decreasing the cell's ability to halt mitosis, leading to increased genomic instability and tumor formation or progression.

While these efforts have identified the aforementioned pathways as critical drivers of human gliomagenesis, the complex genomic alterations present in human GBMs hinders efforts to associate these genes with other putative tumor suppressor genes or oncogenes. GBMs characteristically exhibit amplification or deletion of large chromosomal regions, including entire chromosome arms, which not only contain genes relevant to these pathways, but numerous other genes adjacent to these known tumor suppresor genes or oncogenes (11, 12). Much effort has been spent by many investigators trying to evaluate additional genes within these regions that may function independently of these known pathways. The elucidation of additional genes active in glioma formation or progression within these commonly altered regions would enable investigators to dissect which of these genes may be important "driver mutations" masked by the commonly altered status of those genes already established as tumor suppressor genes or oncogenes, and which genes are merely "passenger mutations" and uninvolved in glioma formation or progression. Many of these approaches to date rely strictly on bioinformatic analysis and

statistical, rather than biologic evidence however, that falls short of definitive evidence and are thus merely speculative.

To this end, the canine genome is a remarkable tool in the analysis of chromosomal regions believed to be biologically relevant in human glioma. The domestic dog contains 38 autosomes compared to the human 22. Therefore, the syntenic genomic material is much more widely dispersed in the dog than in the mouse, with human chromosomal regions spread over sometimes many corresponding canine chromosomes (9, 13). The establishment of canine gliomas as a representative model for both GSC biology and the underlying genomic events driving glioma formation or progression would therefore open a potentially invaluable toolbox for the comparison and definition of minimally altered foci within these comparatively large copy number alterations in human GBMs. The further definition of novel oncogenes or tumor suppressor genes within these regions may in part explain why targeted therapy through these pathways has proven largely unsuccessful in patients, and identify new therapeutic targets.

Finally, GSCs share many functional similarities to physiologic neural stem cells, including the expression of stem cell markers, self-renewal, and multilineage differentiation potential (2, 14, 15). Embryonic NSCs are temporally regulated to enter periods of expansion or proliferation, neuronal, and then glial differentiation (16). As NSCs during the expansion phase are highly proliferative, motile, and resistant to differentiation, they may share similar transcriptional or epigenetic regulatory pathways

with GSCs. Canine embryonic NSCs have not yet been characterized. The evolution of genes involved in brain development in the dog may be more similar to humans than the more commonly used rodent NSC model, and comparison of canine NSCs through periods of gestation to canine GSCs would allow for the first time, a direct comparison of these two related entities within the same species.

Dogs are in many ways the animal with whom we develop a relationship closest to that we share with each other. We invite them into our homes and they share the same environment as we do. They are exposed to similar exogenous and potentially transformative entities such as carcinogenic stimuli, making them an ideal comparative model for human disease. The profound phenotypic similarities between human and canine glioma offer a unique and potentially powerful model to identify and validate new tumor suppressor genes or oncogenes, as well as to investigate functional similarities of glioma stem cells across spontaneously occuring tumors in two species for the first time.

This dissertation will investigate the comparative biology of glioma formation and progression in dogs and in humans by addressing the following:

1) Determine the functional similarities between glioma stem cells isolated from human GBMs and canine glioma tumors and characterize the molecular events driving tumor formation.

2) Characterize the progressive genomic alterations within canine glioma stem cells over serial xenograft tumor formation and compare them to human GBMs through high-density array-based comparative genomic hybridization to identify shared copy number alterations.

3) Determine if canine glioma stem cells may be isolated from low-grade gliomas and other tumors of neuroepithelial origin and compare the functional and molecular similarities to glioma stem cells isolated form high-grade canine gliomas and human glioma stem cells.

4) Isolate canine embryonic neural stem cells from multiple timepoints through gestation to establish periods of temporally regulated neuronal and glial differentiation, and compare the differentiation-resistant neural stem cells isolated early in gestation to canine and human glioma stem cells.

2) **LITERATURE REVIEW**

GLIOMA TUMORS IN HUMANS AND THE DOMESTIC DOG

Gliomas represent the most common brain tumor in humans, forming a histologically diverse spectrum of tumors ranging from grade I pilocytic astrocytomas to grade IV glioblastoma multiforme as defined by the WHO (17, 18). Grade I tumors are considered to be benign tumors curable by local excision. However, invasion of tumor cells is a hallmark of even grade II astrocytoma tumors, rendering them nearly incurable from

surgical excision (19, 20). Grade III tumors, or anaplastic astrocytomas have increased features of malignancy over grade II astrocytoma, such as cellular pleomorphism, increased cell division, and angiogenesis (21). Unfortunately, the most malignant grade IV glioblastoma multiforme (GBM) is also the most common glioma histotype tumor in humans. This tumor is characterized by prominent vascular proliferation, cellular atypia (hence the term multiforme), and large regions of necrosis within the tumor mass (22). Glioma tumors are nearly invariably fatal, with dismal median survival times of around 12 months for GBM and only slightly longer at 2-5 years for patients suffering from grade III anaplastic astrocytomas (1). This poor survival in patients affected by high-grade glioma occurs despite significant advances in surgical technique, imaging and diagnostic capability, radiotherapy, and chemotherapy in the medical field. Therefore, while primary brain tumors are relatively rare forms of cancer, representing fewer than 1.5% of all cancer cases reported in the United States each year, they are the third leading cause of cancer-related deaths in men and the fourth leading cause of cancer-related deaths in women between the ages of 15 and 54 years (23).

Glioblastoma tumors may arise in two clinically distinct fashions (Figure 1)(24, 25). A majority of GBMs present as primary tumors, with no history of prior intracranial tumors. These patients are typically older, with median ages ranging from 54-60 years of age at presentation. In addition to primary tumors, GBMs may arise through malignant progression or transformation of lower-grade tumors. These tumors are termed secondary GBMs and occur in patients with prior history of a grade II or grade III glioma. Patients

presenting with secondary GBMs are often younger in age, typically less than 45 years old. This transformation is not an uncommon event, with approximately three quarters of patients with grade II astrocytomas progressing to high-grade glioma within 5-10 years. Interestingly, despite a diverse clinical history, the histologic and pathologic features of primary and secondary glioblastoma are indistinguishable, reflected in similar survival times (24, 26).

In the face of such poor survival statistics for this tumor, much effort has been spent attempting to elucidate genomic alterations responsible for the formation or progression of glioma tumors, particularly in GBMs. The increased ability of high-throughput genomic sequencing and copy number analysis in human glioma tumors has allowed for widespread, meaningful analyses of tumor samples. This is perhaps best exemplified by the recent analysis performed by The Cancer Genome Atlas, which selected glioblastoma as the first tumor type to examine (10). By comparing over 200 glioblastoma samples, three key pathways were identified as being responsible for driving tumor formation. These pathways (discussed in greater detail below) are A) PTEN/PI3K/AKT, B) p53, and C) the CDKN2A/ CDKN2B/Rb1 pathway. Additional commonly altered pathways include the receptor tyrosine kinase receptors for platelet derived growth factor (PDGFR) and epidermal growth factor (EGFR) (27, 28). Elevated PDGFR expression has been documented in low and high-grade glioma tumors and is believed to be an inciting event, along with *TP53* mutations and loss of the GTPase neurofibromin encoded by the neurofibromatosis 1 gene (*NF1*) function in the initiation of gliomagenesis (29, 30). Co-

expression of both PDGF receptors and PDGF ligand by tumor cells suggests an autocrine or auto-feedback mechanism in glioma cells (31, 32). As with other receptor tyrosine kinases, binding of PDGF induces dimerization of PDGFR, autophosphorylation of the intracellular domains of the receptor and association with adapter proteins such as GRB2 that may bind guanine exchange factors such as SOS, leading to GTP association and activation of the RAS MAP-kinase cascade (33, 34). In contrast to PDGFR, which is detected frequently in low-grade tumors, EGFR activity is most commonly identified in high-grade human gliomas and specifically in GBMs. While a mechanism for PDGFR overexpression in glioma remains elusive, increased EGFR is often associated with genomic amplification of the gene locus on human chromosome 7 (hsa 7) (35, 36). This amplification is most commonly reported in primary glioblastoma and may be present in as many as 40% of GBMs (10). In addition to genomic amplification and the resulting overexpression of EGFR, expression of EGFR mutants is reported in human glioblastoma. The most common EGFR mutant is EGFRvIII or ΔEGFR, which is a mutant allele with an in-frame deletion of exons 2-7 (37). Loss of this region corresponds to the synthesis of a truncated protein lacking an extracellular binding domain and resulting in constitutive autophosphorylation (and subsequent activation) of the receptor. This mutant EGFR allele may be present in as many as 20-30% of GBMs, including a majority of those tumors exhibiting increased EGFR activity (10). Regardless of whether EGFR signaling is enhanced via genomic amplification, mutation, or both, the end result is pro-proliferative signaling through the Ras-MAP kinase cascade or pro-survival signals through activation of phosphatidylinositol-3-kinase (PI3K), and the eventual activation of

AKT (to be discussed more below). Thus, while human glioma tumors often exhibit a complex and heterogeneous genomic landscape, certain key alterations have been identified that are overrepresented or appear to control crucial aspects of tumor biology (e.g. driving mutations).

The domestic dog (*Canis lupus familiaris*) represents the only tenable model for comparative study of spontaneous glioma tumors. Amazingly, the dog develops glioma tumors at a nearly identical estimated incidence, and more astoundingly, develops tumors that recapitulate all salient features of human gliomas, from grade I to grade IV tumors (6, 7, 38). Canine tumors are therefore graded similarly to human gliomas, using identical diagnostic criteria and enabling direct comparisons between human and canine tumor histotypes. Like humans, dogs are typically middle-aged to older at the time of presentation and as in humans the tumor carries a poor prognosis, accounting for an estimated 1-3% of deaths in dogs (39). Canine gliomas express similar markers to human glioma tumors, including glial fibrillary acidic protein (GFAP), vascular endothelial growth factor (VEGF), smooth-muscle actin (SMA), PDGFR, and EGFR (8, 40). While high throughput analysis of genetic mutations has not been performed to date, single cases of *TP53* mutations have also been reported in canine GBMs (6). While the overall relative incidence of glioblastoma tumors compared to other glioma is still unknown in dogs, definite breed predispositions for high-grade glioma and glioblastoma are reported in brachycephalic breeds(41).

Our understanding of the molecular mechanisms driving canine glioma tumor formation, and the comparison to human gliomas remains in its infancy. As improved antemortem imaging capability matriculates into veterinary clinics and increased emphasis is placed on veterinary neurosurgical intervention in dogs with intracranial tumors, greater access to source material will be available. Those reports currently published do reveal significant similarity in chromosomal alterations between canine and human gliomas. In the largest current study, 25 gliomas (of which 2 were diagnosed as glioblastoma) were analyzed for chromosomal copy number alterations by hybridizing DNA isolated from these tumors on custom bacterial artificial chromosome (BAC) arrays (9). This BAC array contained over 2000 mapped clones distributed across all canine chromosomes, resulting in a resolution of approximately 1 megabase (Mb) between individual clones (42). When analyzed, the data revealed significant genomic complexity among canine gliomas as compared to meningioma, with copy number alterations of every chromosome except canine chromosome 6 (cfa 6) identified in at least one glioma sample. When individual chromosomes are examined, both canine GBMs exhibited amplification of canine chromosome 18 (cfa 18), which contains *EGFR* and suggests the importance of *EGFR* amplification in primary GBMs within both species. Additionally, cfa13 was amplified in a majority of canine gliomas, containing the MYC oncogene, which is also frequently amplified in human glioma. Many other commonly reported genomic foci commonly altered in human gliomas however, were not identified in this canine glioma collection. These include most of the tumor suppressor genes, chiefly *p16/Ink4a* and *PTEN*. These results may be explained in part by the low number of high-grade gliomas

in the sample set, containing only two GBMs and one grade III astrocytoma in the twenty-five glioma samples. Many of the analogous alterations (e.g. *PTEN* or *p16/ARF* deletion) in human glioma biology are reported in high-grade astrocytoma samples or GBMs, so it may not be surprising to find that grade II canine astrocytomas or oligodendrogliomas do not exhibit these chromosomal variations. Additionally, sequencing of high-grade tumors for *PTEN* or *TP53* may have revealed mutations and loss of function analogous to those present in human gliomas but that would not be evident on aCGH. Nonetheless, numerous regions of shared copy number alterations were identified between canine and human gliomas, similar to other reports of shared genomic alterations in lymphoma, osteosarcoma, leukemia, and soft-tissue sarcomas in dogs and humans.

The ability to identify shared genomic alterations across two species in spontaneously occurring glioblastoma tumors may help identify minimal foci of alteration surrounding major regulatory genes or chromosomal regions associated with gliomagenesis. As previously stated, high-throughput analysis of human GBMs has identified three pathways that when deregulated are critical to the development or progression of the tumor. These are the receptor tyrosine kinase (RTK)/PI3K/PTEN/AKT, p53, and p16/Ink4a/Rb1 pathways (10). These major pathways, along with other gene mutations or copy number alterations govern cell proliferation, survival, invasion, and angiogenesis- all hallmarks of GBM and accordingly offer the first targets for comparative analysis between canine and human gliomas.

PHOSPHATIDYLINOSITOL-3-KINASE SIGNALING IN GLIOMA

Phosphatidulinositol-3-kinases (PI3Ks) are subdivided into class IA and IB lipid kinase enzymes that are activated by either receptor tyrosine kinases or G-protein coupled receptors, respectively (43). Class 1A PI3Ks are recruited to activated receptors by the adapter proteins p85α, p55α, and p50α. These adapter proteins then recruit the catalytic domains p110α, o110β, and p110δ. Recruitment of a specific catalytic domain define PI3K isoforms, encoded by the genes PI3KCA, PI3KCB, and PI3KCD, respectively (44, 45). As previously mentioned, activation of the EGFR and PDGFR family of receptor tyrosine kinases is prominent in many gliomas. When active, these receptor kinases recruit the catalytic kinase protein (p110) directly or through the binding of adapter proteins (p85). Catalytic kinase domains on p110 then phosphorylate the second messenger, phosphatidylinositol-4,5-bisphosphate (PIP2) at the third position of the inositol ring, producing the active phosphatidylinositol-3,4,5-triphosphate (PIP3) (46). This lipid then serves as a ligand for membrane associated enzymes, chiefly phosphoinositide-dependent kinase 1 (PDK1) and AKT (also known as protein kinase B), by binding of their pleckstrin-homology (PH) domains (47, 48). PDK1 is a serine/threonine kinase that phosphorylates the threonine 308 residue of AKT within the activation T-loop. In addition to PDK1, AKT is also phosphorylated by a separate protein, the mammalian target of rapamycin complex 2 (mTORC2), or the rapamycin-insensitive mTOR complex. This complex phosphorylates the serine 473 residue within the hydrophobic motif and produces a conformational change allowing binding of PDK1

by AKT (49, 50). Complete AKT activation requires phosphorylation of both Thr308 and Ser473 (51). AKT is the major effector enzyme for PI3K signaling, and is encoded by three genes producing the isoforms AKT1, AKT2, and AKT3 (also referred to as PKBα, PKBβ, and PKBγ, respectively). These isoenzymes have some overlapping function, but have tissue-specific differences in expression and distinct functions as well as identified by genomic knockout mice. While AKT1 activation suppresses cell growth and invasion, AKT2 promotes invasion and survival, although there is very high substrate specificity shared between all enzyme isoforms (52-56). Accordingly, AKT2 and AKT3 have been suggested as the most significant AKT isoenzymes relevant to glioma tumor formation, although the extend of tissue-specific (and cancer-specific) AKT activation is still unknown (57).

Downstream effectors of PI3K signaling and AKT activation include an expanding multitude of substrates phosphorylated by AKT. More than 100 nonredundant substrates have been identified across multiple species (58). These substrates in turn regulate significant processes relevant to tumor biology, including cell survival, cell growth or proliferation, cell migration or invasion, metabolism, and angiogenesis, highlighting the complexity and importance of this enzyme pathway to glioma biology.

AKT and Cell Survival

The first recognized role of AKT activity was as an important mediator of cell survival (59). The principle mechanism by which AKT increases cell survival in cells is through

the inhibition or removal of pro-apoptotic signals or mediators. One such family targeted by AKT are the forkhead box O (FOXO) proteins. The FOXO family of transcription factors includes FOXO1, FOXO3a, and FOXO4 (60). Upon phosphorylation by AKT, these transcription factors release their binding to DNA and instead bind to 14-3-3 proteins, which are highly conserved proteins ubiquitous in eukaryotic cells and are highly expressed in human astrocytomas (61-65). Once bound to FOXO proteins, these 14-3-3 proteins mediate the translocation of FOXO proteins to the cytoplasm, removing these transcription factors from the nucleus and thereby inactivating them (63, 66). FOXO transcription factors induce the expression of proapoptotic genes such as Fas-Ligand (Fas-L), tumor necrosis factor-related apoptosis inducing ligand (TRAIL), and Bcl-2 interacting mediator of cell death (Bim) (63, 67, 68). AKT-mediated phosphorylation and subsequent inhibition of FOXO thus not only increases cell proliferation but also decreases apoptosis (increases cell survival).

AKT is also able to inhibit BAD directly through phosphorylating the protein at serine 136, allowing the protein to interact with the 14-3-3 proteins, sequestering BAD from its targets (69-71). BAD is a member of the pro-apoptotic Bcl-2-homology domain (BH3)-only proteins that are responsible for the degradation of the pro-survival Bcl-2 family (72). Therefore, inhibition of BAD allows for accumulation of the pro-survival Bcl-2 proteins and resistance to apoptosis.

In addition to the inhibition of FOXO proteins and the pro-apoptotic BH3-protein families, AKT is also able to promote cell survival by indirect inhibition of p53 function. AKT is responsible for phosphorylation of MDM2, the p53 ubiquitin ligase responsible for the degradation of nuclear p53. Upon phosphorylation of MDM2 at serine residues 166 and 186 by AKT, MDM2 then translocates to the nucleus where it may function as an E3-ubiquitin ligase and result in the nuclear export and proteosome degradation of the p53 protein (73, 74). As discussed later, MDM2 amplification is a common genomic event in human glioblastoma, highlighting the importance of concurrent AKT activity to activate its nuclear transclocation.

Cell Proliferation and Growth

As FOXO transcription factors increase the cell cycle inhibitor p27 (CDKN1B or Kip1) and the retinoblastoma (Rb)-related protein p130, inhibition of FOXO through AKT activity promotes entry to the cell cycle (68). AKT is able to directly phosphorylate p27 at the threonine 157 residue as well, which enables 14-3-3 proteins to bind and sequester p27 within the cytosol, ensuring the complete removal of the inhibitory effects of p27 (75-77). In a manner similar to the p27 Kip1 CDK-inhibitor, AKT is also able to directly phosphorylate the p21 Cip1/WAF1 CDK inhibitor by phosphorylating the threonine 145 residue, again allowing binding of 14-3-3 proteins and cytoplasmic sequestration (78).

In addition to the previously discussed increase in cell proliferation, perhaps the most widely characterized role of AKT signaling in cell function is in the promotion of cell

growth. The major growth-promoting signal via AKT activation is believed to be through the activity of the mTOR complex 1 (mTORC1 or mTOR-Raptor complex). MTORC1 is composed of mTOR, raptor, mLST8, PRAS40, and DEPTOR. AKT activation of mTORC1 results in increased activity of its downstream targets, p70/S6 kinase (S6K) and eukaryotic translation initiation factor 4E binding protein 1 (4EBP1) (79-81). S6 kinase activity phosphorylates the eukaryotic initiation factor 3 (eIF3) where it serves as an on/off switch for the assembly of the pre-initiation complex (PIC) in protein translation. Associated with this is phosphorylation of the S6 protein in the 40S ribosomal subunit and eIF4b by S6K1, which then are then capable of binding with the PIC alongside mTOR and raptor to enhance protein translation. 4EBP1 phosphorylation by AKT also stimulates protein translation, as in its hypophosphorylated state 4EBP1 remains bound to eIF4E, sterically inhibiting its interaction with eIF4G and its incorporation into the PIC. AKT-mediated phosphorylation of 4EBP1 removes this inhibitory binding and releases eIF4E to assemble into the PIC alongside the increased S6K (82-86).

While AKT may directly phosphorylate mTORC1 (and lead to the phosphorylation of S6K and 4EBP1), most evidence suggests that AKT-mediated activation of this complex is instead indirect, through the activation of the tuberous sclerosis complex 2 (TSC2) (87, 88). *TSC2* is a putative tumor suppressor gene and its protein is a crucial inhibitor for mTORC1 signaling, functioning to inhibit the small G protein Ras homolog enriched in brain (RHEB), which is bound to GDP in its inactive state, maintained by TSC2. AKT is able to phosphorylate TSC2 at multiple sites (Ser939, Thr1462, Ser981, Ser1130, and

Ser1132) resulting in inhibition of TSC2 and the accumulation of GTP-bound RHEB, which then activates mTORC1 (89-92).

AKT also phosphorylates other components of the mTORC1, including the proline-rich Akt substrate of 40kDa (PRAS40). PRAS40 functions as an inhibitor of mTORC1 through its binding to 14-3-3 proteins. AKT mediated phosphorylation at threonine 246 on this protein removes this inhibitory effect and indirectly enhances the activity of mTORC1 (93-96). A similar effect has been identified in myeloma cells regarding the other inhibitory element within the mTORC1, DEPTOR (79). While regulation of mTORC1 is complex, it stems from common AKT activation pathways and has been shown to be an important mediator of cell growth in human glioma.

Cell Invasion

Several studies have implicated AKT signaling as a mediator of cell invasion, with increased AKT activity reported in invasive glioma cells in xenograft models and inhibition of AKT2 resulting in decreased invasion (55). The precise role of AKT, or the role of AKT isoforms remains unknown however, with contradicting results regarding the importance of AKT1 versus AKT2 in the promotion of invasion or metastasis. A recent study utilizing mouse xenograft models reported significantly higher AKT phosphorylation within invasive glioma cells as compared to the tumor bulk cells (97). In human breast cancer cell lines, AKT2 has been implicated to promote tumor cell invasion *in vitro*, possibly through increased expression of the transcription factor twist (twist is

involved in the promotion of epithelial to mesenchymal transformation, EMT) (98). While EMT remains a controversial and unproven concept in glioma, twist1 expression has been described within invading glioma cells within orthotopic xenograft models and reduced AKT2 expression correlates with an abrogated invasion ability in glioma cell lines, suggesting a similar role of AKT in invasion (99-101). AKT activation has also been suggested to modulate the extracellular matrix within the scope of cell invasion, increasing the expression of osteopontin by glioma cells, a protein which is associated with cellular migration as well as increasing proteins that interact with the ECM in either a degradative (MMP-2 and MMP-9) or interactive fashion (β1-Integrin, ACAP-1, and Girdin) (102-105). While much of this association between AKT activity and invasion remains indirect or speculative, it has very real clinical relevance to glioma patients, as it has also been suggested to participate in increased cell invasion following irradiation, a standard treatment regimen for nearly all patients suffering from gliomas (104).

Other Functions of AKT: Angiogenesis and Metabolism

A salient feature of many tumors and GBM in particular is an increased vascularity or angiogenesis (106). While AKT activity has been well described in its role driving vascular endothelial precursor proliferation to form new blood vessels within tumors, there is also evidence that AKT activity within tumor cells is able to interact with, and promote vascular proliferation. Most prominently, AKT activation results in increased synthesis of HIF1α and HIF2α (107, 108). Together, these heterodimers form the HIFα transcription factor, which is able to translocates to the nucleus and bind to a hypoxia

responsive element (HRE) within the *VEGF* promoter and drive VEGF production. VEGF has been described as upregulated in both human and canine glioma tumors (40, 109). Nitric oxide synthase (NOS) is constitutively produced by neuronal (nNOS) and endothelial (eNOS) cells and upregulated during angiogenesis. Inducible NOS (iNOS) is also described to exist in human and rodent glioma and is upregulated by AKT, suggesting potential roles for AKT signaling driving angiogenesis in tumors as well (110-113).

While the precise metabolic requirements of tumor cells are complex and are an emerging interest in cancer biology, it is known that cancer cells exhibit significant alterations in metabolic pathways compared to differentiated mammalian cells. As originally described by Otto Warburg in 1924 one of the most intriguing such differences is the preferential utilization of glucose for glycolysis or lactate fermentation over aerobic glycolysis (Warburg effect) (114). AKT stimulates both oxidative and anaerobic metabolism in tumor cells, increasing the expression of glucose transporters along with transporters for other metabolites, such as amino acids (115-117). AKT is also able to phosphorylate and activate phosphofructokinase-2 (PFK-2), which in turn phosphorylates PFK-1 and accelerates the metabolism of glucose-6-phosphate (118). Therefore, AKT activity increases both the uptake and processing of glucose in tumor cells. AKT also phosphorylates and inactivates glycogen synthase kinase 3 (GSK3). GSK3 exerts an inhibitory effect on a number of molecules, including its canonical namesake glycogen synthase as well as the sterol regulatory element-binding proteins (SREBPs), which are

responsible in part for driving cholesterol and fatty acid production by cells. Inhibition of GSK3 by AKT may therefore promote the formation of glycogen and increase the stability of SREBPs (119, 120). The exact role for GSK3 in physiologic or neoplastic scenarios however, is likely far more complex as pharmacologic inhibition of GSK3 may result in apoptosis or growth arrest in glioma cells *in vitro* (121, 122).

Mechanisms of AKT Activation in Glioma Tumors

As previously described, AKT phosphorylates a multitude of target proteins responsible for the regulation of cell survival, cell growth or proliferation, cell migration or invasion, angiogenesis, and metabolism, and AKT activity is increased in over half of all human GBM tumors (123). Gain of function mutations of PI3K have been described in human GBM, with point mutations in PI3KCA (p110α) described in as much as 15% of GBMs (10). These mutations are typically present within the adapter binding domain, the C2 helical, or kinase domain of the subunit. While no mutations have been described in the other catalytic subunits or isoforms, increased expression of PI3KCB (p110β) and PI3KCD (p110δ) have been characterized in GBM as well as other human tumors such as colon and urinary bladder(124-126). Recent sequencing of the PI3K adapter protein p85α indicated that mutations might be present as a relatively common event, as nine of ninety-one GBMs sequenced contained deletion mutations of this gene (10). It is hypothesized that these mutant proteins would be unable to bind and regulate the catalytic domains, and none of the mutations were identified alongside mutated p110α genes. These mechanisms account for a minority of tumors with increased AKT activity however, as

most GBMs exhibiting high levels of AKT do so through the loss of a tumor suppressor gene, phosphatase and tensin homolog deleted on chromosome 10 (*PTEN*) (10, 127). PTEN functions physiologically to directly antagonize PI3K signaling through its non-redundant phosphatase activity, removing the phosphate group from the third position in the inositol ring of PIP3 and converting it to PIP2. Loss of PTEN function is the most commonly identified alteration in human GBM, with up to 75% of tumors losing PTEN activity through either mutation or loss of human chromosome 10q (HSA10q) (25, 128). As mentioned previously, GBMs may arise through either de novo (primary) or progressive (secondary) pathways. PTEN is often inactivated in both primary and secondary GBMs, although there are differences identified between the two groups. Mutations in *PTEN* are found almost exclusively in human primary GBMs and are rare events in secondary GBMs. These mutations are divided between missense (33.3%), deletion or insertional mutations forming stop codons (32.1%), and nonsense mutations (12.8%). Whereas missense mutations occur with a predilection for exons 1-6 in the human *PTEN* gene, premature stop codon or nonsense mutations are evenly distributed throughout the gene. *PTEN* mutations are also rare events in lower grade gliomas, highlighting the importance of PTEN loss and subsequent AKT activation in GBM pathobiology (10, 24, 25).

While mutation of *PTEN* occurs in a subset of (typically) primary human GBMs, chromosomal copy number alterations (CNAs) occur in both primary and secondary GBMs. Copy number alterations in human cancer may occur in two patterns: broad and

focal. Broad copy number alterations encompass large regions of many megabases (Mb) in size and may include whole chromosomal alterations (amplification or deletion). In contrast, focal alterations typically include small regions and may contain single or few genes (129). Human GBMs often contain a large number of broad CNAs in their tumor genome, highlighting a pitfall in the investigation of relevant tumor suppressor genes or oncogenes within regions of chromosomal loss or amplification, respectively. While focal CNAs are comparatively easy to identify and study putative oncogenes or tumor suppressor genes, owing to the large number of genes altered in broad regions, it is difficult to identify and then validate such genes within these areas. Such is the case with *PTEN*, as human GBMs often exhibit loss of heterozygosity (LOH) of either the entire chromosome 10 or the 10q chromosomal arm (11, 12, 130).

The combination of *PTEN* mutations and deletion occurring almost exclusively in glioblastoma (primary or secondary) and not in lower grade glioma suggest that the loss of *PTEN* (and subsequent increase in AKT activity) has a role specific to high-grade glioma or in the case of secondary GBM, glioma progression. LOH of chromosome 10 is more common in GBMs than *PTEN* mutation, and clinically LOH of 10q is associated with poorer survival whereas *PTEN* mutations are not. While far from being conclusive, this suggests additional tumor suppressor genes may be present within chromosome 10 that are also important in human GBMs. Identifying such a tumor suppressor gene however, has proven difficult because of the size of the region deleted containing *PTEN*. Primary GBMs typically have LOH affecting an entire copy of chromosome 10 and

secondary GBMs usually have LOH of the entire long arm, chromosome 10q. Identifying tumor suppressor genes in such broad CNAs is far more difficult than in focal anomalies. Accordingly, while candidate tumor suppressor genes within hsa10q have been identified, isolating the relevance of such genes from the documented importance of *PTEN* deletion relative to AKT activation is difficult (131, 132).

Regardless of whether *PTEN* is inactivated by mutation or deletion, the result is an increased AKT activity with profound, pleotrophic effects on cell proliferation, survival, invasion, and angiogenesis, as described above. Its exact role in gliomagenesis however, remains unclear. While it is a non-redundant tumor suppressor gene and the most common alteration in GBMs, null-function mouse models do not produce glioma tumors, despite their predilection for numerous other tumor types. Possible explanations for such observations include cell senescence from oncogene-induced genomic stress or roles more specific in glioma progression, rather than formation. Thus, while it has been described as potentially outpacing *TP53* as the most commonly altered tumor suppressor gene in human cancer, many questions regarding its regulation and role in glioma persist.

THE ROLE OF P53 IN GLIOMAGENESIS

The p53 protein has been so extensively studied for its role as a tumor suppressor gene that it has been nearly ubiquitously accepted as "the guardian of the genome" (133). Mutations in the *TP53* gene encoding the p53 protein may be the most common sporadic

event in human or veterinary cancers, underscoring its vital role in the control or regulation of cellular proliferation and DNA repair (134-137). It is estimated that up to 50% of human cancers contain inactivating mutations in *TP53*(138). Activation of the p53 protein may arise from a variety of cellular stresses, including DNA damage, oncogene activation, and altered cellular metabolic demands. p53 is subsequently able to induce apoptosis, cellular senescence or cell-cycle arrest, or induce DNA repair mechanisms. Regardless of the cellular outcome, activation of the p53 pathway in physiologic cells renders the cell unable to enter or complete the cell cycle with DNA damage or the potential for DNA damage (e.g. with oncogene activation), thereby removing cells perceived as being damaged from the proliferating pool.

Sensing DNA Damage and p53 Activation

Although DNA replication proceeds at a remarkably efficient and successful rate, with base substitution error ranging from an estimated rate of 10^{-3} to more than 10^{-6}, DNA as a molecule is very susceptible to the accumulation of damaging alterations from a variety of endogenous and exogenous processes over the lifetime of an organism (139). These include ultraviolet and ionizing radiation, chemicals within the environment (and including chemotherapeutics with regards to cancer cells), as well as reactive oxygen species (ROS) generated through metabolic or physiologic processes within cells. These lesions in DNA may result in alteration of base pairs through methylation (alkylation), cross-linkage, deamination, and oxidation among other means (140-142). Subsequently the DNA strand may develop single or double stranded breaks (SSBs or DSBs,

respectively). Single stranded breaks may progress to double stranded breaks through altered replication forks or aberrant DNA replication. Ultimately, these breaks in DNA trigger the DNA damage response (DDR), an evolutionarily conserved mechanism to recruit and activate mediators of DNA repair, including p53. As oncogenic stress is capable of inducing DNA damage through a variety of mechanisms and leads to double stranded DNA breaks, the DDR is a critical step in the development and progression of cancer. Even low-grade human tumors show near constitutive expression of proteins that are markers of the DDR, suggesting that this pathway is active in tumors (143-146).

One of the most prominent mechanisms by which DNA damage is detected and the DDR is initiated is through activation of the ataxia-telangiectasia-mutated (ATM) kinase and its analog, the ATM and Rad3 related kinase (ATR) (147). Single and Double stranded breaks are recognized and bound by the proteins Mre11, Rad50, and Nbs1, forming the MRN complex (148-152). The MRN complex is able to bind DNA in an ATM-independent manner, forming a heterotetramer capable of binding to and stabilizing the ends of a double-stranded DNA break. The Mre11 subunit is responsible for the tethering of the complex to DNA through its DNA binding motifs. As Rad50 is recruited it forms a complex, coiled hinge structure that bridges the double stranded DNA break using Zn^{+2} ions as a cofactor. This interaction between Rad50 and Mre11 activates exo- and endonuclease activities of Mre11 (a similar enhancement of endonuclease activity results from interaction with Nbs1). Ultimately, the MRN complex is capable of binding to and stabilizing DNA breaks, as well as partially unwinding DNA helix in preparation of

repair. The ATM and ATR kinases are functionally related Ser/Thr-Gln-kinases with shared protein substrates, but act to repair DSBs occurring at different times in the cell cycle. ATM is capable of acting at any time during the cell cycle, whereas ATR is active primarily in the S and G2 phase and is dependent on ATM. ATM is recruited to and activated primarily by the C-terminus of the Nbs1 subunit within the MRN complex at the site of double stranded breaks. ATM in turn phosphorylates and activates the checkpoint proteins 1 and 2 (Chk1 and Chk2), which are downstream substrates responsible for activating much of the DDR, including p53 (153-156).

Phosphorylation of p53 by Chk2 is part of the complex regulatory mechanism governing the action of the p53 protein. p53 is a protein comprised of an N-terminal transactivation domain (TAD), a proline rich domain, a large DNA binding domain (DBD), a tetramerization domain, and a C-terminal domain (CTD) (157). Scattered throughout these domains are numerous, conserved serine, threonine, and lysine residues that serve as substrates for post-translational modification and regulation of p53. Known modifications relevant to p53 activation include phosphorylation of serine residues 15 and 20, and phosphorylation of threonine 18 within the TAD(158, 159). ATM and ATR are capable of phosphorylating Ser15 while CHK2 phosphorylate Ser20 and Thr18 (160, 161). Importantly, these kinases are not specific for these residues giving some modicum of redundancy, as multiple kinases are generally capable of modifying any particular amino acid residue. The result of this phosphorylation by DDR kinases on the p53 protein is a conformational change in the protein, accompanied by a reduced affinity for its

principal inhibitory protein, MDM2 (discussed in greater detail later) and an increased affinity for stabilization factors (162-164). Briefly, MDM2 maintains the p53 protein in a poly-ubiquitinated state that targets the protein for degradation and thus exerts a strong repressive function on p53. Removal of this interaction allows nuclear accumulation of the protein leading to the formation of p53 protein tetramers and increased protein stability within the cell by masking the nuclear export signal through this conformational change (tetramerization). Concurrently, the conformational change allows for the association of nuclear p53 with co-activator proteins via the proline rich domain, such as p300 and CREB-binding protein (CBP), which function as histone acetyl transferases (HATs). The activity of these HATs acetylates lysine residues 320, 372, 373, 381, and 382 within the tetramerization (Lys320) and C-terminal domain (Lys 372, 373, 381, and 382) of the p53 protein, removing degradative ubiquitin modifications and allowing p53 to bind chromatin through a combination of the DNA binding domain and the CTD (165-167). p53 binding of DNA is mediated by specific sequences within the promoter of genes activated in the DDR, containing the consensus sequence 5'-PuPuPuC(A/T)(T/A)GPyPyPy-3' that binds the DBD of p53 (p53 response element) (168, 169). Classically, the CTD was believed to be a negative modulator of DNA binding. More recent evidence however, suggests that this domain mediates non-specific binding to DNA in a fashion that may allow for p53 to "search" for the specific consensus sequence within the promoter of target genes (170, 171). Once bound to DNA, p53 is able to transactivate target genes through the recruitment of transcription factors such as the TFIID and Srb/Med complexes (172, 173). The genes that bind p53 within the

promoter region will determine to a varying extent the response of the cell to genomic stress. As mentioned previously, the two primary outcomes of genomic stress and p53 activation are apoptosis or cellular senescence.

p53 mediated Apoptosis

Discovery of the ability of p53 to regulate and drive apoptosis in cells was made through investigations into the effects of irradiation on murine thymocytes (174). Following this observation, the role of p53 in the initiation of apoptosis was expanded to include many targets at both a transcriptional and post-translational level. Transcriptionally, p53 is able to induce the expression of pro-apoptotic genes such as *Bax*, p53-induced gene 3 (*PIG3*), *Killer/DR5, CD95/FAS, Noxa*, and *PUMA* (175-180). Many of the transcriptional targets of p53 encode members of the Bcl-2 family of proteins, although much of the pro-apoptotic function associated with p53 activation is attributed to PUMA. Expressed at very low levels in physiologic scenarios, activation of p53 binds to the two p53 response elements within the promoter and rapidly increases transcription of *PUMA* (181, 182). This highly conserved, BH3-only protein functions in the cytoplasm to remove the inhibition of the pro-apoptotic Bcl-2 proteins by interacting with Bcl-2, Bcl-XL, Mcl-1, Bcl-1, and A1. Through the binding and inhibition of these proteins, they release Bax and Bak, which are then able to interact with the mitochondria and induce the release of cytochrome C to form the apoptosome and SMAC, which removes the inhibitors of apoptosis proteins (IAPs) (183, 184). Ultimately this transition at the mitochondria leads to caspase activation and apoptosis. In addition to the indirect activation of pro-apoptotic

proteins Bax and Bak through the removal of inhibitory proteins (e.g. Bcl-2), PUMA may directly activate Bax as well, although the precise role of this interaction *in vivo* is still under investigation (185).

Additionally, p53 is able to stimulate apoptosis through transcriptionally independent mechanisms, as with high nuclear accumulation of the protein, cytoplasmic translocation may occur and p53 may associate with mitochondria. At the mitochondria, p53 is able to initiate mitochondrial outer membrane permeability (MOMP), thus allowing for the release of cytochrome C. p53 appears to do this in a direct manner, possibly by functioning as a BH3-only protein itself (175, 186, 187). Whether the apoptotic response to p53 activation is generated through direct or indirect mechanisms, the endpoint remains the establishment of the MOMP and release of proapoptotic proteins, namely cytochrome C and SMAC.

p53 and Cellular Senescence

The concept of cellular senescence stems from initial observations regarding *in vitro* investigations into both the replicative ability of physiologic cells and in the transformation of cells. The term of replicative senescence was originally used to describe the cessation of cell division in normal human embryonic fibroblasts *in vitro*, which would proliferate for a finite period of time and then enter permanent growth arrest (188). A similar phenomenon was observed during attempts at transformation of cells, where activation of the oncogene *HRAS* in wild-type cells *in vitro* results in cell

proliferation initially, but is subsequently followed by growth arrest (189). Senescent cells differ from either apoptotic or quiescent cells in that they are able to be maintained long-term as a viable cell population, but remain arrested in G0 at the G1/S checkpoint even if exposed to growth factors. This phenomenon correlates with cellular activation of p53 and Rb pathways (190). Accordingly, concomitant inhibition of these pathways through *TP53* mutations or inactivation of p16 protein (discussed later) with oncogene activation transforms these cells, bypassing cellular senescence (191). Originally, this process was attributed to shortening of telomeres in cells as they age (192, 193). Telomeres are specialized structures present at the terminus of most eukaryotic chromosomes that serve as a nucleoprotein cap protecting the integrity of individual chromosomes during replication, as the chromosomal terminus is typically incompletely replicated during DNA synthesis. Telomeres are maintained by the enzyme telomerase, which is typically expressed in embryonic and compartmental stem cells but is not found or found at very low levels in mature, differentiated cells. Without the activity of telomerase, telomere length is gradually shortened over progressive cellular division, until a critical point is reached, termed the Hayflick limit, at which point a DDR is initiated resulting in activation of the ATM/ATR pathway and p53 (194, 195). This response culminates in growth arrest of cells as they age, preventing them from continuing cell division while containing unstable chromosomes, which may produce chromosomal end fusions and introduce novel chromosomal break points during mitosis or chromosomal translocations. Such events are potentially transformative events and thus cellular senescence is described as a major tumor suppressor mechanism. This

process of telomere-induced cellular senescence explains the mechanism by which cells maintained over time enter growth arrest, but may not explain why expression of oncogenes such as *KRAS*, cause senescence. The mechanism of non-telomere induced senescence is therefore a relevant tumor suppressor mechanism, as even in cells expressing telomerase (as is documented in some human tumor cells), these cells have a finite replicative lifespan and are capable of entering senescence. This mechanism may be mediated in part through activation of oncogenes and through reactive oxygen species (149, 196-198). Both oncogene activation and ROS elicit a DDR within neoplastic cells and activation of p53, which mediates the cellular senescence and serves as a tumor suppressor mechanism to keep proliferative cells within early events of tumor formation in check. This observation is supported by observations of murine and human tumors *in vivo*, where benign tumors contain a majority of cells exhibiting markers of cellular senescence, whereas malignant cells lacking p53 function do not, suggesting that circumvention of this pathway is a major obstacle towards the acquisition of a malignant phenotype in the development of a tumor (199).

Senescence is primarily mediated through the activity of p53 as a transcription factor, inducing the expression of several key proteins that function in cell cycle arrest. Whereas both Rb (discussed later) and p53 control entry and progression through the cell cycle, inactivation of Rb alone is incapable of removing the growth arrest, whereas abrogation of p53 on its own is (200-202). This DDR eliciting p53 activity is initiated by a variety of physiologic stresses, such as oncogene-induced genomic stress, ionizing radiation,

chemotherapeutic agents, or telomere dysfunction, underscoring the central role of p53 in cellular senescence (203-205). One principle effector of this response is the $p21^{Waf1/Cip1}$ protein, a member of the Cip/Kip family of cyclin-dependent kinase (CDK) inhibitors (along with $p27^{Kip1}$ and $p57^{Kip2}$) (206). CDKs are proline-directed serine/threonine kinases that phosphorylate a variety of substrate proteins responsible for the driving of cell division. By inducing p21 expression, p53 is able to inhibit the cell cycle, as p21 binds to and inhibits CDK2 and its interaction with cyclin E, required for entry into S-phase in cell division (207). p53 also induces expression of other proteins mediating cell cycle arrest, including Gadd45 and 14-3-3 proteins. Gadd45 family of proteins include 3 isoforms which are emerging mediators of the DDR, as they are capable of binding to and enhancing p21 activity, binding the proliferating cell nuclear antigen (PCNA) in DNA repair processes, and inhibiting cell cycle progression directly by inhibiting the interaction between Cdc2(CDK1) and cyclin B1 (208-210). As Cdc2 regulates the transition of cells from G2 to mitosis (M) phase during cell division, this provides an additional level of cell cycle regulation in the p53-mediated DDR. As discussed previously, the 14-3-3 family of proteins are highly conserved proteins ubiquitously expressed in eukaryotic cells with pleiotrophic effects on a wide variety of substrates. p53 is able to induce the expression of 14-3-3 proteins, which in turn binds to and sequesters both Cdc2/CDK1 and Cdc25C as well as enhancing the stability of p53 tetramers.

The p53-mediated DNA damage response has emerged as a far-reaching, complex pathway involved in a multitude of cellular processes, including apoptosis and cellular

senescence. While its role in apoptosis was the initial characterization of this protein as a tumor suppressor, the role of p53 in cellular senescence may eventually prove to be just as important, if not more so as a tumor suppressor. The observation that benign tumors remain in senescence until malignant transformation suggest that such cells are merely awaiting the acquisition of an event enabling them to overcome this process. Tumors with intact p53 signaling are also more vulnerable to DDR-mediated senescence in response to chemotherapeutic agents as well, highlighting its importance in the development and maturation of cancer.

Inactivation of p53 in Gliomas

As p53 is capable of acting as a potent tumor suppressor governing cellular senescence or apoptosis in response to oncogene-induced DDR, it is not surprising that altered p53 signaling is present in a majority of GBMs. Indeed, approximately 87% of GBMs are reported to exhibit diminished or absent p53 activity through a combination of *TP53* mutations, deletions, or post-translational mechanisms inhibiting the activity or stability of the p53 protein (10). The importance and role of *TP53* as a tumor suppressor gene relevant to gliomagenesis has been recognized for decades, as human patients affected by Li-Fraumeni syndrome (characterized by inherited genomic mutations in *TP53*) exhibit an increased incidence of glioma formation, although *TP53* is mutated less commonly in gliomas than in many other human tumors (211, 212). Classically, *TP53* mutations in glioma have been associated with low-grade gliomas and those that progress to secondary GBMs, suggesting that p53 loss is an early event in glioma formation. Higher throughput

analysis of primary GBMs however, has recently suggested a significant number of primary GBMs that contain p53 mutations as well, with up to 37.5% of untreated primary GBMs exhibiting mutations in *TP53* (35, 128).

Mutations in *TP53* in human glioma are generally recognized within the DNA-binding domain, clustering between codons 125 and 300 (213, 214). Whereas many of the mutations affecting other tumor suppressor genes identified in cancer are frameshift or nonsense mutations, mutations in *TP53* within the DBD are most commonly missense, affecting single amino acid residues. A great number of missense mutations across this region have therefore been reported in human tumors. Outside of the DBD, the incidence of missense mutations is reduced, representing approximately 40% (215). The remaining mutations are most commonly nonsense or frameshift mutations. Single base mutations are typically transition mutations occurring at CpG sites, with 25% reported as C:G>T:A. There are 22 CpG sites in the DBD, of which codons 175, 248, and 273 are recognized as hotspots for mutation, containing 60% of CpG mutations identified. Five other codons (196, 213, 245, 282, and 306) contain 26% of mutations as well (216, 217). The effect of mutations on p53 function depends on the location of the mutated base. As described previously, p53 contains a DNA binding domain (DBD) located between the proline-rich and tetramerization domains. This domain, in concert with the C-terminal domain (CTD) is responsible for the binding of p53 to DNA, thus enabling its function as a tumor suppressing transcription factor, transactivating its effector genes. Mutations at hot spots within the DBD are so-called because they occur at residues crucial either for contacting

and binding DNA or in the formation of the protein's tertiary and quaternary structure necessary to transactivate its target genes. The inability of mutant p53 to bind p53-response elements in effector genes of the DDR described above would abrogate this response in glioma cells transformed with oncogene activation and confer a significant advantage in neoplastic growth. Alternatively, some mutated p53 proteins outside these hotspots may result in a dominant negative p53 protein, which would also eliminate the ability of p53 to signal as a transcription factor in the DDR (218). As p53 must act through the formation of a tetramer to bind to and transactivate effector genes, any wild-type p53 binding dominant negative mutant p53 results in an aberrant conformational change of this tetramer and therefore an inability to bind DNA. While functional (non-silent) *TP53* mutations are deleterious to the cell harboring them, not all mutations are oncogenic strictly from the loss of its potent tumor-suppressor role. Briefly, *TP53* mutations that function as putative oncogenic transformative events have been described as well, termed gain of function mutations, or GOF (219). Evidence exists that such mutated p53 may interfere with the function of wild-type p53 (or the related p63 and p73) or directly interferes with the ATM/ATR DDR(220). Alternatively, such mutations are hypothesized to activate genes normally repressed by wild-type p53 through altered binding properties at the p53-response element.

While loss of p53 protein function is common in gliomas, typically this is accomplished not through mutation (as it is in many other solid human cancers), but through altered post-translational processing of the p53 protein in glioma cells leading to accelerated

degradation or sequestration of the protein. One such mechanism is through the activity of the murine double minute-2 (MDM2) protein, which functions as the principle ubiquitin E3 ligase for p53 (221). MDM2 is able to specifically bind the N-terminal, hydrophobic pocket of p53, obscuring a crucial N-terminal alpha helix responsible for the binding of co-activators required to transactivate p53 effector genes. MDM2 contains a really interesting new gene (RING) domain at its C-terminus that functions, with a zinc-cofactor as an E3 ubiquitin ligase to transfer ubiquitin residues from E2 enzymes to the six lysine residues present on the C-terminus of p53 (162, 163, 222). Ubiquitin residues ligated to p53 form oligomers linked by lysine 48, which trigger proteosome-mediated degradation of p53. MDM2 is also capable of mono-ubiquitination of p53, a process that modulates the function of p53 and may lead to the nuclear export and cytoplasmic sequestration of the protein. Additionally, MDM2 may actively inhibit the translation of *TP53* mRNA (223). Transcription of *MDM2* is a physiologic target of p53 as a method for p53 to induce its own degradation and prevent excessive accumulation (224). Glioma cells however, often exhibit genomic amplification of *MDM2*, located on human chromosome 12 (hsa 12q14-15). This copy number alteration is identified in 10-15% of human GBMs (10, 225). This *MDM2* amplification is almost exclusively identified in GBMs containing a wild-type *TP53*, thereby providing a method to inhibit p53 activity. This is further enhanced by the increased AKT activity often present in human GBMs, as AKT is capable of phosphorylating MDM2 at serine residues 166 and 186, enhancing its E3 ubiquitin ligase activity (226). A similar gene, *MDM4* (or *MDMX*) has also been identified within amplified genomic segments in human GBMs. This protein has a p53

binding domain highly similar to MDM2 and is capable of binding p53 at its N-terminal transactivation domain as well. While MDM4 also contains a RING domain similar to MDM2, evidence suggests it has a low intrinsic E3 ubiquitin ligase activity in contrast to MDM2 (221, 227). *MDM4* is amplified in approximately 5-7% of human GBMs, and is capable of oligomerizing with MDM2 (10, 221, 228). Studies *in vitro* suggest that while MDM4 is typically monomeric on its own, when it oligomerizes with MDM2 it enhances the E3 ubiquitin ligase of MDM2 over MDM2 oligomers on their own (229). MDM4 activity is also enhanced by increased AKT signaling, as the kinase is reported to phosphorylate MDM4 at serine 367, enhancing its affinity to associate both with p53 and MDM2 (230). Genomic amplifications of *MDM2* and *MDM4* in human GBMs enable inhibition of p53 activity even in the face of wild-type p53 protein. This appears to be through a combination of steric hindrance preventing p53 from functioning as a transcription factor, cytoplasmic sequestration of p53, and through poly-ubiquitination and proteosome-mediated degradation.

The most common mechanism by which p53 function is inhibited in human GBMs however, is most likely through the deletion of the *CDKN2A*/Ink4b/p14^{ARF} (ARF) tumor suppressor gene (231). As discussed later, the ARF tumor suppressor was originally identified through the observation that a segment in human chromosome 9p21 was often deleted on a variety of cancers (232). Sequencing of this region identified two, very similar putative tumor suppressor genes named *Ink4a*/p16^{Ink4a} and *Ink4b*/p15^{Ink4b}. Both genes had sequence homologies suggestive as a role in CDK inhibition, confirming them

as tumor suppressor products. An additional exon, exon 1β was identified however, between *Ink4a* and *Ink4b*. Interestingly, this exon contains no sequence homology to either *Ink4a* or *Ink4b* and is transcribed under control of its own promoter, which also incorporates exons 2 and 3 of *Ink4a*, where exon 2 is translated in an alternative reading frame, producing a unique protein product, ARF. Genomic deletion in human tumors almost invariably encompasses this entire locus, resulting in losses in *Ink4a*, *Ink4b*, as well as *ARF* (10). These genomic deletions are especially common in human GBMs, with loss of this locus identified as the most common homozygous deletion. ARF also functions as a tumor suppressor, but as mentioned in a different manner than the CDK inhibitors of the Ink4a family. As discussed previously, MDM2 is the principle ubiquitin ligase, and thus regulator of degradation, for p53. In physiologic settings, ARF binds to and sequesters MDM2, as well as inhibits this ubiquitin ligase activity. During DDR or stress responses, ARF is upregulated and further reduces MDM2 levels, thereby indirectly enhancing the activity of p53 (233). The loss of ARF, which is present in 50-70% of human high-grade gliomas, thereby removes inhibition of MDM2, allowing unfettered ubiquitination of p53 and increased p53 degradation, potentially confounded by concurrent MDM2 or MDM4 genomic amplification events (10, 25).

THE RETINOBLASTOMA PATHWAY AND GLIOMAGENESIS

The control of cell cycle entry and progression is crucial for the maintenance of regulated cell division and represents a barrier that must be overcome by proliferating neoplastic cells. The mammalian cell cycle, normally tightly maintained in a repressive state must be changed to allow for near constitutive mitogenic signaling within the tumor. Cell cycle progression is regulated by the cyclin dependent kinases (CDKs), serine/threonine kinase proteins that, when bound to specific regulatory cyclin proteins phosphorylate a variety of regulatory proteins involved in cell proliferation. As these cyclins are rapidly synthesized and degraded, they control the temporal activity of CDKs, thereby coordinating the cell cycle. Mitotic activity is initiated by the synthesis of cyclins D1, D2, and D3, which bind to and activate CDK4 and CDK6 during the G1 phase of cell division (234, 235). CDK4 and CDK6 partially phosphorylate key inhibitory proteins retinoblastoma protein 1 (Rb1), p107, and p130 (collectively known as the pocket proteins). The Rb family of proteins (E2F1-5) act as inhibitory regulators of cell division through the binding to and sequestration of the E2F family transcription factors (236, 237). Members of the E2F family are potent activators of genes involved in cell proliferation (such as cyclins), as evidenced by the observation that overexpression of E2F activators force quiescent cells into the G1 phase in a growth factor independent fashion (238, 239). To regulate these factors, Rb is capable of binding E2F through a specific domain between the N- and C-terminus known as the “pocket”, functioning as a molecular tether and blocking E2F from associating with (and activating) promoters of

genes involved in cell division. Additional modes by which Rb antagonizes cellular proliferation include recruitment of chromatin modifying enzymes and inhibition of other, non-E2F family transcription factors (240-242). Phosphorylation of these pocket proteins inactivates them and allows the synthesis of cyclin E1 and E2, which bind to and activate CDK2. CDK2-cyclinE then completely phosphorylates (inhibits) Rb and allows entry into the S phase of cell division. Cyclin A is then synthesized, which interacts with CDK2 to complete S-phase and enter G2 phase (beginning mitosis), which is completed by the association of cyclin A with CDK1 (234). Two key observations emerged from these investigations. First, the identification of the archetypal tumor suppressor gene *Rb1* and second, the characterization of key cell cycle checkpoints- the transition from G1 to S-phase (G1/S checkpoint) and the transition from interphase through mitosis (G2/M checkpoint).

Glioma tumors must therefore develop a mechanism for the circumvention of these checkpoints to allow continued cell proliferation. Recent, high-throughput analysis of human GBMs underscore this by determining that 78% of GBMs exhibit altered Rb pathway or cell cycle signaling (10). An estimated 15% of human high-grade gliomas exhibit genomic amplifications of chromosome 12q13-14, containing the *CDK4* gene. Overexpression of CDK4 in mouse models does induce hyperplastic foci of epithelial tissues, but only after prolonged latency periods (243, 244). *CDK6*, located on hsa7q21-q22 is also frequently amplified and overexpressed in human gliomas. Experimental overexpression of this kinase however, has not produced any phenotype to date.

Determination of the causal roles of these genes in gliomagenesis is further confounded by the presence of other oncogenes with known biological relevance in proximity of both *CDK4* and *CDK6* (235). Amplifications of human chromosome 12q also contain the *MDM2* gene, with known importance in the regulation of p53, as discussed previously. *CDK6* is located on chromosome 7, of which a subset of GBMs with *EGFR* amplification will contain trisomy or whole chromosomal amplification of hsa7 (10, 245). Therefore, while CDKs are often overexpressed in gliomas, additional mutations appear to be required to license continued cell cycle progression.

From the discovery of mutated RB causing pediatric retinoblastoma tumors by Alfred Knudson nearly four decades ago (and the establishment of the two hit theory), much interest has been generated describing inactivating mutations in RB in other tumors (246). As described above, Rb and the other pocket proteins function as a molecular brake against the progression of the cell cycle, primarily in the progression through the G1/S checkpoint. Loss of Rb function leads to deregulated or unchecked activity of E2F transcription factors and thus greater ease by which the cell may enter mitosis, as the G1/S checkpoint is considered the rate limiting step in a quiescent cell entering mitosis. The significance of Rb as a tumor suppressor in regulating cell division has been demonstrated by overexpressing Rb in actively dividing cells, whereby forced expression is capable of arresting dividing cells at G1 (247). Mutations in the RB gene, located on hsa13q14, have been described in human GBMs, estimated to occur in 11-25% of tumors (10, 248). Additionally, a smaller subset exhibits deletion or loss of 13q. The majority of

human GBMs however, escape this restraint on cell proliferation not by CDK amplification or RB mutation, but through an indirect manner involving deletion and loss of a chromosomal locus previously discussed for its simultaneous role in p53 regulation, the Ink4a/ARF locus (248, 249).

As described previously, the *Ink4a/ARF* locus, located on human chromosome 9p21 is often deleted in a variety of cancers. This locus contains a complex arrangement of exons encoding two, very similar tumor suppressor genes *Ink4a*/p16^{Ink4a} and *Ink4b*/p15^{Ink4b} and an additional exon 1β, controlled by its own promoter. Transcription of either exon 1α or 1β (controlled by separate promoters within the locus), coupled with the exons 2 and 3 encodes either the Ink4a or ARF transcript, respectively (although exon 2 is translated in an alternative reading frame in the ARF transcript) (232). While ARF inhibits MDM2 and thus maintains the stability of p53, the p16 protein belongs to the INK4 protein family, which function as key CDK inhibitors controlling cell cycle progression. The INK4 family includes p16^{Ink4a} (encoded by *CDKN2A*), p15^{Ink4b} (encoded by *CDKN2B*), p18^{Ink4c} (encoded by *CDKN2C*), and p19^{Ink4d} (encoded by *CDKN2D*) (231). While the genes for Ink4a and Ink4b are located in close proximity on hsa9p21, Ink4c is located on 1p32 and Ink4d on 19p13.

Ink4a and Ink4b are capable of negatively regulating cell division by binding to the CDK-cyclin complexes, specifically by binding CDK4/6-cyclin D. The Ink4a/p16 protein binds CDK4 opposite of the catalytic cleft, responsible for the binding of cyclin D. This

interaction is important, as p16 is capable of binding CDK4 and CDK6 whether they have associated with cyclin D or not (250, 251). Therefore, Ink4 proteins may bind CDKs even if they are in an active state, complexed with cyclin D. This interaction between Ink4a/p16 and CDK4/6 results in an allosteric conformational change that alters the catalytic cleft of the CDK and prevents cyclin D from binding and thus, activating CDK4 or CDK6. Ink4 also distorts the ATP binding cleft of the CDK, significantly reducing its kinase ability and functionality. This Ink4-mediated inactivation of the CDK4/6-cyclin D complex inhibits G1/S progression in two manners. First, as CDK4 and CDK6 are responsible for the initiation of Rb phosphorylation and inactivation, the removal of this action maintains Rb's inhibitory hypophosphorylated status and therefore sequesters the E2F transcription factors required for cell cycle progression (252). Secondly, at G1/S, a significant portion of the CDK4/6-cyclin D complexes are bound by members of the Cip/Kip CDKIs, $p21^{Cip1}$ and $p27^{Kip1}$. Binding of CDKs by Ink4 proteins however, releases the Cip/Kip proteins from this complex, freeing these proteins to exert an additional inhibitory role by binding to and blocking the activity of CDK2-Cyclin E (253, 254). Therefore, through the Ink4 proteins, cells may inhibit the release of E2F transcription factors from Rb by abrogating both CDK4/6-cyclin D complexes and CDK2-cyclin E. As CDK4/6 are responsible for initiating phosphorylation and inactivation of Rb, and CDK2-cyclinE is responsible for the complete phosphorylation and release of E2F factors, Ink4 both directly and indirectly help to control the G1/S checkpoint, mediated through Rb.

Gliomas however, typically contain deletions of 9p21, affecting both the *CDKN2A* and *CDKN2B* (along with the *ARF*) genes. Approximately 50-70% of high-grade human gliomas exhibit loss of function of this locus, typically through homozygous deletion (10). Tumor cells lacking p16 are thus unable to inhibit the activity of CDK4/6-cyclin D at the G1/S checkpoint. Such a deficiency may be further confounded by the aforementioned amplifications of *CDK4* and *CDK6* that are frequent in GBMs. Finally, loss of function of p53 through either *TP53* mutation, deletion, *ARF* deletion, and/or *MDM2* amplification removes p21, allowing for increased CDK2-cyclinE mediated Rb phosphorylation (255). It is somewhat remarkable from an evolutionary genetics point of view, that the loss of one locus may have such profound effects, through multiple pathways at one cellular event. Ultimately, this common genomic event in gliomas (the loss of the *Ink4a/ARF* locus) removes the G1/S checkpoint through not only the lack of CDK inhibition (Ink4), but through the decreased p53 pathway activity as well (ARF). Thus, glioma cells are frequently capable of deregulating the cell cycle and in particular the Rb pathway, although inactivating mutations in *RB* itself are somewhat less common than other solid tumor types (256-258).

IDENTIFICATION AND CHARACTERIZATION OF HUMAN GLIOMA-DERIVED CANCER STEM CELLS

Since their initial characterization by two separate laboratories in 2003 and 2004, tumor stem cells isolated from pediatric and adult gliomas (glioma stem cells, GSCs), and particularly from GBMs have introduced a new paradigm with far reaching implications regarding their role in the origin, progression, and response to treatment (3, 259). Investigations into cancer stem cells (CSCs) in general were a natural outgrowth following the characterization of physiologic hematopoietic stem cells almost five decades ago (260, 261). The hematopoietic stem cell (HSC) was the first tissue stem cell to be identified through bone marrow reconstitution experiments in irradiated mice. The identification of this HSC and delineation of the two chief tenants of stem cell biology, self-renewal and multilineage differentiation, would come to dominate stem cell and cancer biology at the end of the twentieth century and moving into the twenty-first (262).

This central theme of a tissue stem cell that is capable of unlimited self-renewal and multilineage differentiation established early efforts towards a hierarchical organization in physiologic stem cells. The heterogeneous cell population of the normal bone marrow, through these efforts, could be reconstituted by a single cell and was thus ultimately responsible for the generation of more differentiated progeny with limited replicative potential, forming the erythroid and myelomonocytic cell lines within the marrow (263). These speculations were confirmed during now landmark studies in the 1980s utilizing

molecular labeling of the cell surface markers on marrow cells to more completely identify and map the ontogeny of these cells (264). Investigators could therefore follow the differentiation of HSCs- cells with unlimited replicative potential and the capacity for multilineage differentiation, to multipotential progenitor cells- those with limited replication capacity and early markers of fate (differentiation) commitment and finally, to differentiated blood cells. That this ontogeny of progenitor cells is produced through a common, single cell implies that this process is mediated through epigenetic means, as all cells share a common physiologic (wild-type) genome. Importantly, this organizational scheme also dictates that the tissue stem cell represents a very small percentage of cells within the total marrow population through the exponential expansion associated with the division of these progenitor cells. While this stem cell ontogeny remains best characterized in the HSC population, similar populations have been isolated from the brain (described in greater detail below), intestine, mammary gland, prostate, hair follicle, and other human tissues (2, 265-268).

Cancer has long been theorized to exist as a collection of heterogeneous tumor cell populations, reflected by variable tumorigenic potential between individual cells within the same tumor (269). Early studies regarding the ability of clonal populations derived from human and murine cancer to form tumors in xenograft models suggested significant differences between individual clones in the capacity to proliferate both *in vitro* and *in vivo* (270-272). These studies include efforts to estimate the clonogenic potential of acutely isolated cells from a variety of tumors, including multiple myeloma, non-

Hodgkin's lymphoma, ovarian carcinoma, melanoma, and neuroblastoma. Using soft agar assays, clonogenic cells were reported to constitute a minority of the overall cell population, comprising between 0.02-0.1% of cells isolated (273-277). Demonstrations of varying growth patterns in clonal populations derived from chronic myelogenous leukemia (CML), acute myelogenous leukemia (AML), and other myeloproliferative disorders were reported over several decades (278, 279). Then, in 1997 the identification of a cell isolated from a patient with AML able to recapitulate the identical tumor phenotype of the patient cemented the interest in so-called tumor stem cells (280). For the first time, the investigators were able to demonstrate that the cell population identified shared cell surface markers associated with physiologic hematopoietic stem cells ($CD34^{+}CD38^{-}$), reformed the tumor in xenograft models, and was capable of differentiating into the blast-like cells originally present in the patient (M1-M7), acquired markers of differentiation *in vivo* (CD38, CD117), and did so from clonally-derived, transformed precursors. Estimated frequency of these AML cancer stem cells ranged from 0.00002-0.2% of the original tumor population, reflecting the rare occurrence of these cells and consistent with prior reports. These studies, and others that followed regarding CML and myeloproliferative diseases suggested that, in hematopoietic tumors the heterogeneity and differences in tumorigenic potential between clones from a given tumor were due to a clonal-derived, hierarchically arranged population of tumor cells, similar to the arrangement in physiologic hematopoietic stem cells (281-283).

This tumor stem cell model classically attempts to explain the observed heterogeneity through epigenetic changes involved in some degree of differentiation between the tumor cells (284). The true tumor stem cell, like the physiologic tissue stem cell, constitutes a small percentage of the total population, which is exponentially expanded during tumor formation. Each expansion alters the epigenetic imprinting of the cell, resulting in the generation of progenitor cells either lacking or with limited self-renewal or tumor formation capacity, and expressing markers associated with differentiated cells. Differences in clonal proliferation would be explained therefore, by the irreversible or nearly irreversible epigenetic modifications in restricted tumor progenitor cells, with the rare tumor stem cell populations accounting for the low numbers of clonal cells reported in various tumors (285-288). These epigenetic modulations within the bulk of the tumor population is thus equivalent to differentiated progeny in somatic tissue- forming the majority of cells but incapable of indefinite proliferation. Indeed, investigations into cancer stem cells isolated in leukemia and from germ cell tumors have demonstrated the ability of these cells to generate progeny expressing markers of differentiation, which are incapable of tumorigenesis (289, 290). The existence of such tumor stem cells has since been extended to solid tumors, including glioma, breast, ovarian, intestinal, and prostate cancers (291-295).

In contrast to the tumor stem cell paradigm, which attributes the heterogeneous tumorigenic potential within a neoplasm to epigenetic changes within a hierarchically arranged population, the clonal evolution model stipulates that this heterogeneity is

driven through a combination of epigenetic and genetic alterations that happen spontaneously within the tumor cell, often in a stochastic process (262, 296). This continual process results in particular cells within the entire population accruing additional gene mutations, which ultimately lead to an outgrowth of cells harboring this advantageous (from the vantage point of the neoplastic cell) aberration. Each cell however, maintains a tumorigenic potential, and those cells within the clonal outgrowth are each individually equally capable of tumor formation. The selection process favoring those cells with the highest proliferative capacity is ultimately what drives the phenotypic variation or heterogeneity of the individual tumor.

The clinical implications regarding these two models attempting to explain tumor heterogeneity and propagation are profound. In the tumor stem cell model, a hierarchical organization implies that therapy must be targeted against the true, multipotent stem cell (262, 297). If the progeny constituting the bulk of the tumor are a mixture of replication incompetent or limited progenitor cells, they therefore do not represent a permanent threat to tumor growth. Clonal evolution or stochastic growth however, asserts that each cell within a tumor or a clonal outgrowth of the tumor has an equal capacity to form and propagate the tumor (262, 298). Successful therapy in this case would therefore center on the elimination of every neoplastic cell within a patient. Certain clinical observations would seem to support the tumor stem cell hypothesis, at least superficially. As these cells reside at the pinnacle of the hierarchy governing tumor formation, they- like physiologic stem cells would be presumed to have similar growth characteristics. Both

physiologic and tumor stem cells are assumed to comprise a small percentage of the overall population, with long periods of quiescence between cellular divisions (299). As current cancer therapy lies heavily on radiation therapy or radiomimetic chemotherapy, the mechanism of cell death in these cells is highly dependent upon inducing DNA damage in a proliferative cell, leading to mitotic catastrophe and cell death. Cells that reside in the tumor which are simultaneously quiescent, yet capable of re-entry into the cell cycle would thus be able to repair the DNA damage prior to cell division and may account for the inherent radioresistance of many tumors, including GBM. Indeed, some groups have reported increased DNA repair capacity in tumor stem cells isolated form human GBMs (156). Similarly, tumor stem cells are hypothesized by some investigators to possess an intrinsic resistance to chemotherapeutics through increased expression of drug antiporter/efflux pump proteins (300-305). Resistance to therapy however, is not an exclusive feature to tumor stem cells. Within the clonal evolution theory, tumor cells may acquire through genetic mutations increased abilities to repair DNA or export exogenous compounds (chemotherapeutics). Additionally, tumor cells in both models exist within a highly variable microenvironment known as the tumor cell niche. As radiation-induced damage is greatly dependent upon the presence of oxygen to generate free-radical damage, the relative tissue oxygen tension may be of vital importance for localized tissue damage and tumor cell death. As many tumors contain regions of necrosis, characterized by low oxygen tension (especially true in GBM), differences in microenvironment are theorized to contribute to the differential therapeutic response in both the tumor stem cell and clonal evolution models (302, 303).

The evaluation of hierarchical organization in tumor stem cells also presents a demanding challenge. The establishment and measurement of tumor cell heterogeneity depends ultimately upon the demonstration that a subpopulation of cells within the total cell mass possesses a greater tumorigenic capacity than the mass as a whole. To assert this heterogeneity is hierarchically arranged, as in the tumor stem cell model, investigators must first validate specific markers that consistently identify this tumor subpopulation, such as CD34 in the HSC or leukemia tumor stem cells (280). Secondly, utilizing such markers it must be demonstrated that these tumor stem cells are able to divide asymmetrically. To constitute hierarchical arrangement a single cell must recapitulate the ontogeny of the original tumor- to be able to divide such that it gives rise to more differentiated, replication impaired progeny while maintaining a small pool of stem cells (262, 299). While the knowledge and investigations into the markers and hierarchical arrangement of physiologic HSCs aided greatly the ability of investigators to apply these criteria to tumor stem cells in AML and CML, such knowledge of physiologic stem cell equivalents in solid tumors is by in large, extremely lacking. Such is the case in glioma, where efforts comparing stem cell markers and hierarchy in these cells to neural stem cells have been unrewarding thus far.

Putative Markers Identifying Neural and Glioma Stem Cells

Unlike the HSC compartment, which appears to be rather strictly ordered in a linearly arranged, fluid phase compartment continually producing progeny within a relatively

well-defined microenvironment of the marrow, physiologic neural stem cells in the adult are far less defined. These cells do not exist in any known linear organization, arranged instead spatially within three specific anatomic locations of the brain- the olfactory bulb, the subventricular zone (SVZ) of the lateral ventricles, and the dentate gyrus of the hippocampus (15, 306). These cells are still poorly characterized, but are grouped into three categories known as Type B, Type C, and Type A cells (307). Type B cells are tentatively referred to as neural stem cells, as they are slowly cycling and tend to localize only within the SVZ, producing type C cells as progeny, which are often referred to as transient amplifying (TAP) cells (308). These cells rapidly migrate along the rostral migratory stream (RMS) towards the olfactory bulb where they form neuroblasts both within the RMS and at the olfactory bulb, termed type A cells. Markers identifying these cells however have proven to be much more elusive than in the HSC compartment. Attempts at prospectively isolating these physiologic NSCs utilizing expression of the intermediate filaments GFAP and nestin, as well as expression of EGFR, among others have been made (309-312). Unfortunately, none of these markers are specific to the brain, let alone the NSC subpopulation and are therefore ineffective at defining glioma tumor stem cell hierarchy. Rather than following the lead of the identification of leukemic tumor stem cells therefore, attempts of isolating glioma stem cells have largely been through the identification of markers that enrich tumorigenicity in these populations, with attempts at "reverse engineering," applying these markers towards physiologic cells. The two principle such markers are CD133 (also known as Promonin-1) and CD15 (also known as Lewis X/Lex or stage-specific embryonic antigen 1/SSEA-1). While CD133 is

expressed on neural stem or progenitor cells, it is also expressed by numerous other tissues, and currently has no known function (313-316). Initial reports characterized a dramatically increased tumorigenic potential in CD133+ GSCs, going so far to ascribe these cells as being the exclusive tumor-forming compartment within the cell population (317, 318). Further study of this marker however, rapidly dissolved this tenant, suggesting that CD133-negative cells are also capable of forming xenograft tumors (319, 320). The role of CD133 positive cells in radio- and chemotherapeutic resistance is similarly confusing, with conflicting reports suggesting these cells are either more resistant to or more susceptible these treatments. The surface marker CD15 also contains no known function, but is expressed by embryonic neural stem cells during brain development (16, 321). GSCs not expressing CD133 often express CD15 (although the expression of these markers is not mutually exclusive) and, like those cells expressing CD133, exhibit trends towards greater tumor forming capacity using xenograft mouse models (322, 323). Physiologic correlates of either marker towards the adult stem cell compartment remains difficult, however. Type B cells, the putative neural stem cell frequently does not express either marker, and in comparative studies CD133 or CD15-negative cells are more clonogenic *in vitro* than positive cells (324). Furthermore, any fashion of hierarchical arrangement between negatively labeled cells, CD133+, or CD15+ cells within glioma is still far on the horizon, if it exists at all. Other attempts at sorting glioma cells to establish a hierarchical arrangement using the expression of either the ATP-dependent transport protein ABCG2 or through dye exclusion studies (side population) have been similarly inconsistent (325, 326). Finally, the measurement of

tumorigenic potential within the hierarchical arrangement of glioma cells may itself represent a difficulty in defining the tumor stem cell population. Separating a heterogeneous population into tumorigenic and nontumorigenic subpopulations necessarily involves the accurate assessment of tumor forming capacity, often using xenograft models. While serial transplantation of cells capable of reforming the original tumor across multiple xenograft animals remains the gold standard measurement of tumor stem cell subpopulations as compared to *in vitro* estimates, recent studies have questioned the accuracy of xenograft models as models of tumor-forming capacity (327).

Physiologic Similarities between Glioma and Neural Stem Cells

With the above limitations regarding the definition of glioma stem cells, much of the evidence for their existence remains empirical. Chiefly, the remarkable similarities in how these cells are isolated, cultured, and the expression of similar markers of either self-renewal or differentiation led many to speculate they share a similar physiology. Both glioma and neural stem cells have been isolated in an identical manner (2). Following tissue homogenization, these cells are routinely placed into serum-free media containing the mitogens basic fibroblast growth factor (bFGF or FGF2) and epidermal growth factor (EGF). In this environment, both neural and glioma stem cells proliferate as non-adherent, spherical structures termed neurospheres. These neurospheres are composed of a mixed population, containing undifferentiated stem cells as well as more differentiated progeny, although in serum-free conditions more mature cells are reported to die-off during subculture or expansion (328, 329).

When cultured in serum free media (NBE media), both populations express similar markers of both stem cell (undifferentiated) and differentiated status. Undifferentiated neural and glioma stem cells commonly express the intermediate filament nestin. This structural protein was originally described in 1990 from rat neuroepithelial stem cell populations and initially attributed with highly specific localization to neural stem cells (330, 331). Subsequent studies however, have identified nestin expression in hair follicle, pancreatic, and vascular cells, among others (332-334). It is nonetheless highly expressed in both cell types, and at least in neural stem cells nestin$^{-/-}$ mice exhibit deficiencies in neural stem cell numbers, with increased apoptosis, suggesting a relevant functional role to this protein with regards to neural stem cell self-renewal (311).

Along with nestin, neural and glioma stem cells both commonly express the protein sox2 (335, 336). This member of the high mobility group (HMG) transcription factor family is highly expressed in both embryonic and tissue stem cells, and is a component of the four transcription factors described by Yamanaka and colleagues to induce pluripotency in mature fibroblasts (337). Its expression in developing neuroepithelial tissue is highly conserved across species, further suggesting its role as a central transcription factor important for the maintenance of an undifferentiated state (338-340). The exact role of sox2 in neural stem cell maintenance however, appears far more complicated. Mice expressing a hypomorphic allele of sox2 do not develop any overt CNS defects, although complete ablation of sox2 expression at embryonic day 12.5 (E12.5) does produce mice

with hypocallosity and significant reductions in proliferating neural progenitors in the post-natal period (341). Expression of sox2 early in development coincides with expression of other members of the SoxB1 subgroup, sox1 and sox3 (342, 343). While unknown, it is speculated that these members may have some degree of overlapping function. The expression of sox2 is clearly involved in neural stem cell proliferation and/or self-renewal, but its expression also correlates with the onset of neuronal differentiation (344). Inhibition of sox2 activity decreases neuronal differentiation and migration in both the eye and the brain, as evidenced by the previous mention of hypocallosity in sox2 mutants. The role of sox2 in neural stem cell development is thus somewhat muddled, as it is expressed both in undifferentiated progenitor cells and differentiating neural stem cells. Its expression is well documented in glioma tumors as well, and in glioma stem cells, where it is presumed to function in an analogous manner regulating self-renewal. Accordingly, downregulation of sox2 in GSCs reduces their tumorigenicity and clonal proliferation, without significantly altering the expression of differentiation markers, suggesting a role specific to self-renewal (335, 345). Sox2 appears to function in both neural and glioma stem cells in a dose-dependent fashion, and may be regulated post-transcriptionally by the eukaryotic translation initiation factor eIF4E, which as previously mentioned is regulated in part by mTOR and S6K expression, frequently elevated in glioma tissue (335, 345). This suggests that sox2 expression may be maintained at a high level in glioma tissue and contribute significantly to self-renewal, perhaps in a fashion analogous to the maintenance of pluripotency in iPS cells. Thus, the

expression of nestin and sox2 are two of the most frequent and reliable indicators of an undifferentiated state in both neural and glioma stem cells.

Other markers associated with the maintenance of a stem cell state include the basic helix-loop-helix (bHLH) transcription factor Olig2 and members of the Polycomb Group of genes responsible for chromatin remodeling, Bmi1 and EZH2 (346-350). Olig2 is exclusively expressed within the central nervous system. Originally identified along with the structurally related Olig1 as important transcription factors mediating neuronal and oligodendroglial differentiation, separate functions of Olig2 as a mediator for neural and glioma stem cell self-renewal have recently been investigated. Expression of Olig2 in adult rodents is typically high in regions of neurogenesis, with both type B and type C cells expressing detectable levels (307). When exposed to the mitogens EGF or bFGF, these type B cells give rise to a rapid burst of proliferative, type C/TAP cells, which express high levels of olig2. Gliomas commonly express olig2 as well, detectable in both low- and high-grade tumors (351). In engineered mouse models of glioma, olig2 null mice are incapable of forming glioma tumors, suggesting a significant role of this transcription factor in glioma stem cell biology (352). In this study, olig2 appears to function by directly repressing the expression of the p53 effector p21. As p21 is a principle mediator of p53-induced cellular senescence, inhibition of this pathway in both neural and glioma stem cells may increase self-renewal capacity and in the case of glioma tumors, dampen the DDR associated with oncogene-induced cellular stress.

Bmi1 and EZH2 belong to a large family of genes referred to as the Polycomb Group (PcG). These proteins function in concert with numerous others to form large complexes that bind to and inhibit expression of target genes through epigenetic chromatin modulation (353). Briefly, these proteins are grouped into two sub-complexes, termed Polycomb Repressive Complex 1 and 2 (PRC1 and PRC2). PRC1 contains a RING1 subunit that functions as a monoubiquitination E3 ligase (similar to that described previously in MDM2 and MDM4 domains) (354). The RING domain in PRC1 specifically (singly) ubiquitinates lysine 119 of the histone protein H2A, conferring a repressive chromatin structure, thus inhibiting transcription of any gene in which PRC1 binds within its promoter region (355). This function of PRC1 appears to be modulated to some extent by the specific cofactors comprising the PRC1 complex, with Bmi-1 expressed during cell proliferation while the Bmi-1 analog PCGF2/MEL18 represses cell growth (356). Bmi-1 therefore serves in part to target the PRC1 complex to repress the expression of genes inhibitory to cell growth. Bmi-1 is expressed highly in embryonic and adult neural stem cells as well as many glioma stem cells (357). Bmi1-bound PRC1 is capable of binding to and ubiquitinating Geminin, an inhibitor of DNA replication that must be degraded prior to entry into S phase (358). PRC1 ubiquitination of Geminin results in the proteosome-mediated degradation of this protein and allows the cell to enter S phase. Additionally, Bmi-1 directs PRC1 to inhibit the Ink4a/ARF locus in embryonic neural stem cells- a vital control mechanism for the G1/S checkpoint (359). As previously discussed, this locus is often homozygously deleted in GBMs, suggesting a different relevance to Bmi-1 overexpression may be present in these cells, supported by findings

that in p16 null models of glioma stem cells, Bmi-1 still governs cell self-renewal and tumorigenic potential (352). Indeed, Bmi-1 is also able to inhibit p21 in both neural and glioma stem cells by directly binding to and inhibiting the p21 promoter with the cooperation of the Foxg1 transcription factor (360). Perhaps through this inhibition of p21 and the DDR, bmi-1 expression appears to contribute to radioresistance and resistance to apoptosis in neural stem cells. The PRC2 complex contains the histone methyltransferases EZH1 or EZH2 complexed to the cofactor SUZ12 and other proteins (361-363). EZH2 acts to silence gene expression through trimethylation of lysine 27 on the histone H3 protein (H3K27me3). The activity of PRC2 roughly corresponds to the proliferative status of cells *in vitro*, most highly expressed during periods of rapid cell proliferation, suggesting this complex represses growth inhibitory genes in a manner analogous to PRC1. Similarly, EZH2 is capable of catalyzing the repressive H3K27me3 mark on the p16/Ink4 locus, as well as the $p15^{Ink4b}$ promoter (364).

Finally, neural and glioma stem cells also share markers of differentiation. In the developing and adult CNS, neural stem cells are capable of tripotential differentiation-forming cells of neuronal, astrocytic, and oligodendroglial lineage, although in adulthood most actively proliferating cells within the NSC niche may give rise to neuroblasts or neuronal cells (365). Similarly, glioma stem cells are capable of expressing identical markers of differentiation, although the pathways governing differentiation may be altered through the often-significant genomic and epigenetic aberrations characteristic of human GBMs. Nonetheless, both neuronal and glioma stem cells downregulate the

expression of the aforementioned "stem cell" markers and increase the expression of β-III-tubulin (TuJ-1), glial fibrillary acidic protein (GFAP), and O4 in response to a variety of differentiation cues, chiefly with exposure to fetal bovine serum (serum) or through the removal of growth factors (2, 366, 367). TuJ-1 is an intermediate filament that serves as a marker of immature or recently differentiated neuronal cells both *in vivo* and *in vitro* (368). In contrast, GFAP is an intermediate filament most commonly associated with astroglial cells, although it is also highly expressed by type B neural precursor cells and by glioma stem cells in undifferentiated conditions (306, 369). O4 is a cell surface marker that is associated with oligodendrocytes, although these cells may also express markers shared by astrocytes (370).

NEURAL STEM CELLS IN EMBRYONIC AND ADULT NEUROGENESIS

As described above, glioma stem cells and neural stem or progenitor cells from the embryonic and adult mammalian brain share numerous similarities. Both GSCs and neural stem cells express similar surface markers, are capable of multilineage differentiation, and are isolated and expanded similarly *in vitro*. Moreover, regardless of whether gliomas originate from either a stochastic or tumor stem cell paradigm, the cell initiating the tumor must arise through the accumulation of sufficient genomic alterations allowing for uncontrolled and independent cell proliferation. At once the neural stem cell appears as an attractive model for this malignant transformation, given the long-lived status of these cells and the inherent similarities to GSCs. The discovery and

characterization of neural stem cells that persist in the adult mammalian brain over the previous three decades has fueled investigations regarding this hypothesis. While no evidence currently exists to establish a causal link between neural stem cells and GSCs, the comparison of embryonic and adult neural stem cells to GSCs may reveal common pathways of cellular self-renewal, differentiation (or blockade of differentiation in GSCs), migration or invasion, and ultimately aid in establishing the elusive cellular hierarchy of glioma stem cells.

Embryonic Neural Stem Cells and Brain Development

Brain development from embryonic stem cells is often viewed as a default programming event, as neural speciation from the gastrulating embryo is caused not by the induction of a pathway, but by the inhibition of embryonic signaling at a localized niche (371). The prime pathways that must be inhibited to allow for neural induction are the bone morphogenetic protein (BMP) and other related pathways within the transforming growth factor-β (TGF-β) superfamily (372-374). BMP produced during gastrulation causes the differentiation of primitive ectodermal cells towards epidermal tissue. A collection of cells on the dorsal aspect of the embryo (Spemann's organizer) however, blocks this signaling thorugh the secretion of paracrine acting compounds such as Noggin, Chordin, Follistatin, Nodal, Cerberus and others (375, 376). Concurrently, the developing neuroectoderm secretes members of the fibroblast growth factor (FGF) family that act as mitogens and morphogens, promoting neural speciation (377, 378). Ultimately, this collective inhibition of BMP signaling (specifically BMP2 and BMP4) in combination

with FGF signaling establishes dorsal-ventral patterning in the developing embryo and the existence of the neural plate, the first collection of neuroectoderm, which will eventually form the neural groove and ultimately the neural tube(379). The neural tube closes at embryonic day 30 in humans, 18.5 in dogs, and 9.5 in the mouse (380-382). Once closed, the neuroectoderm proliferates, creating a germinal structure that gives rise to the ventricular zone (VZ). This structure is composed of primitive neural stem cells arranged in a pseudo-stratified arrangement with radial processes on the cells (383-385). During this developmental period, cells are refractory to differentiation, dividing symmetrically to populate the VZ, and highly migratory (386-388). NSCs within the VZ are polarized, exhibiting pronounced nuclear migration during cell division, as the nucleus moves towards the surface of the cortex during DNA synthesis. Some NSCs within the ventricular zone display a characteristic nuclear migration, termed interkinetic nuclear migration (INM). This feature is an aspect of early NSCs and this pronounced cellular polarity identifies them as radial glia (386, 387, 389). These cells maintain contacts with both the ventricle and the pial surface, and exhibit pronounced lengthening of these processes as the cells divide and populate the developing neocortex. This polarity appears to be chiefly organized through interactions of the Notch pathway, specifically with the expression of Numb and Numb-ligand (NumbL), which result in basolateral expression of cadherins and maintenance of cellular adherens junctions (residual properties of the more immature neuroepithelial cells) (390, 391). Interkinetic nuclear migration is a complex mitotic property that is specific for early NSCs, as this is lost as cells switch from symmetric to asymmetric cell divisions(392, 393). During this process,

S-phase nuclei align themselves along the apical aspect of the ventricle, forming a cell population several layers in thickness, separated from the ventricular surface. As cells move to M-phase, nuclei migrate to the ventricular surface, with G1 and G2 cells present in between the apical and ventricular surface. Although the precise role of interkinetic nuclear migration in NSC development remains unknown, disruption of this process inhibits cell division and neurogenesis, suggesting it has an important role in the regulation of early NSCs and the maintenance of asymmetric cell division (394, 395). Proliferation and maintenance of a differentiation-incompetent state within this cell population is associated with expression of the β1 family of Sox proteins (Sox1-3), the Zic family (zinc-finger containing transcription factors), Geminin, Notch ligands, Iroquois family proteins, the cell surface marker CD133, integrin-α_6, and the intermediate filament nestin (342, 379, 390, 396, 397). As previously stated, many of these markers are also upregulated or expressed on glioma stem cells.

Following this initial phase of proliferation, neural stem cells enter into temporally regulated patterns of first neuronal, then astrocytic, and then oligodendroglial differentiation (398-400). This onset of neurogenesis is associated with the switching of cells from symmetric cell divisions within the proliferative phase to asymmetric cell division that generates differentiated progeny. This event occurs at embryonic day 33 in humans, day 10 in mice, and is currently undefined in dogs (390). During this switch, NSCs or radial glia do not exhibit interkinetic nuclear migration, instead producing basilar, restricted neuronal progenitor cells that do not contact the ventricular surface.

These restricted progenitor cells then proliferate to mark the onset of neurogenesis, in a fashion resembling transient amplifying cells (TAPs) in adult NSCs (described in further detail below). Early neuronal differentiation is associated with expression of several important genes in NSCs, including paired box 6 (Pax6), forkhead box G1 (FOXG1), LIM homeobox 2 (LHX2), and empty spiracles homologue 2 (EMX2) (401). Signaling through the contact of early NSCs or radial glia with the developing meninges may be important temporal regulators as well, as expression of all-trans retinoic acid (ATRA) at the meninges appears to correlate with the onset of neurogenesis (402, 403). Terminal neuronal differentiation is then characterized by progressive downregulation of Pax6 and upregulation with the transcription factors TBR2, neurogenin 2 (NGN2), and cut-like homeobox 1 (CUX1) and 2 (CUX2) (387, 404). The intermediate filaments nestin is also downregulated with differentiation, with cells instead expressing neuronal filaments beta-III-tubulin (TuJ-1) and microtubule associated protein 2 (MAP2) (396, 398).

Cytokine signaling is also crucial for NSC regulation and differentiation, again involving members of the TGF-β superfamily such as BMP. As previously discussed, inhibition of BMP signaling is the initial step in neural speciation. This is followed by the upregulation of the BMPR-1A receptor early during neurogenesis. Expression of BMPR-1A in turn results in the expression of BMPR-1B which, when bound to BMP ligands leads to activation of the bHLH transcription factor MASH1 in differentiating neurons (405-407). BMP receptors signal through the formation of heterotetramers and serine/threonine kinase activity. This serine/threonine kinase phosphorylates serine residues present within

the carboxy-terminus of homologues to mothers against decapentaplegic proteins (SMADs). BMP triggers phosphorylation of activating SMADs, SMAD1, SMAD3, and SMAD5 that bind to co-SMAD/SMAD4 and translocate to the nucleus where they induce transcription of target genes and trigger neurogenesis (408).

Glial differentiation follows neuronal patterning and is regulated by a combination of cytokine signaling and changes in gene expression. BMP signaling through BMPR-1B, in addition to causing terminal differentiation of NSCs to neurons results in the fate-switching from neuronal to astrocytic differentiation. BMP signaling induces inhibitory bHLH transcription factors such as Hes-5, Id1, and Id3 (409-411). These factors rapidly downregulate the expression of Mash1 and neurogenin and thus inhibit neuronal differentiation. Hes1 and Hes5 expression is also upregulated during this fate-switch by Notch signaling (412). Coincident with this BMP-mediated inhibition of neuronal progenitor cell proliferation is an increase in STAT3 activation. Receptors for cytokines such as leukemia inhibitory factor (LIF) and ciliary neurotrophic factor (CNTF) dimerize with glycoprotein 130 (gp130) upon binding of their ligand (413-415). This heterodimer is able to then recruit Janus Activated Kinase (JAK) to the receptor where it in turns phosphorylates members of the signal transducer and activator of transcription (STAT) family by acting as a serine/threonine kinase. Specifically, phosphorylation of tyrosine residue 720 of STAT3 results in the nuclear translocation and activation of genes involved in glial differentiation. Epigenetic regulation of chromatin helps in the coordination of these signaling events as opening or compaction of chromatin structures

may reveal or conceal binding sites for STAT3. One such example is the promoter for the glial intermediate filament protein, glial fibrillary acidic protein (GFAP), which contains a STAT3 binding element. This promoter is methylated prior to glial differentiation and expression of GFAP is induced only after this repressive mark is removed (416).

Neural Stem Cells in the Adult Mammalial Brain

Neural stem cells persist from the post-natal period into adulthood in mammals, with niches present in the subventricular zone and dentate gyrus of the hippocampus that have similarities to the developing neocortex of embryonic NSCs (417). Within the lateral ventricles, NSCs are located in the subventricular zone (SVZ). Quiescent NSCs within the SVZ are termed type B cells, which then divide asymmetrically to generate a highly proliferative type C cell population that further differentiates to type A cells. These type A cells are capable of rapid migration along the rostral migratory stream towards the olfactory bulb. There, type A cells further differentiate to neuroblasts or interneurons. Type B cells, believed to be the NSC compartment, express similar features of embryonic NSCs (eNSCs). Type B cells express nestin and sox2, and develop cellular process which move through the ependymal layer to contact the ventricle surface, similar to that identified in radial glia or eNSCs. These cells also express markers of differentiation however, including astrocytic markers GFAP and GLAST (306-308). Targeted disruption of type B cells leads to a dramatic reduction in neurogenesis in mouse models, and depletion of type C and A cells indicates that these type B cells are capable of regenerating this population, suggesting a hierarchical arrangement and that these type B

cells are the adult NSC (15, 370, 418). Type C cells are in turn produced through asymmetric divisions of type B cells and constitute the majority of actively dividing cells as they undergo both limited symmetric cell divisions and asymmetric cell divisions during maturation. As these cells are highly mitotic, but have a finite replicative potential, these cells are also referred to as transient amplifying progenitor (TAP) cells (308). TAP cells are clearly important for the expansion of the NSC pool during neurogenesis, but remain a poorly defined entity, as their precise role and physiologic regulation *in vivo* remains unknown. These cells produce type A cells through asymmetric cell division however, and it is these cells, which migrate through the rostral migratory stream towards the olfactory bulb where they acquire neuronal markers (TuJ-1, Neural Cell Adhesion Molecules/NCAMs, MAP2) as they differentiate into neuroblasts and interneurons (307).

The other major NSC niche and site for neurogenesis in the adult mammalian brain is the hippocampus, specifically the subgranular zone of the dentate gyrus (DG) (419, 420). Similar to both eNSCs and the type B cells of the SVZ, NSCs within the DG possess a prominent cell process, cellular polarity, and are termed radial astrocytes or type I progenitors (421, 422). This radial process spans the subgranular zone and contact multiple cell layers throughout the DG. These cells express sox2 and nestin but like type B cells in the SVZ also express markers of astrocytic differentiation, including GFAP (421). Type I cells are capable of asymmetric cell division to give rise to lineage restricted type II, or type D neuronal progenitor cells in an analogous fashion to the type C or A cells in the SVZ. Type D cells in turn produce differentiated progeny, the type G

or granular neurons that functionally integrate into the granular layer of the hippocampus (421, 423). Accordingly, NSC division in the dentate gyrus is affected by a multitude of physiologic stimuli. Mitotic activity is upregulated during inflammation, seizures, and glutamate receptor activation. Activity is also significantly reduced during depression and reversed following administration of antidepressant medication (424-427).

Neural stem cells from either the SVZ or DG express similar markers to both each other and to eNSCs, and exist in similar microenvironments. Both type B and type I cells may express CD133, and CD15 is expressed by progenitor cells within the SVZ as well (428-431). Functional differences between cells expressing these markers over negatively expressing cells have yet to be demonstrated however, and the role of these markers *in vivo* is still unclear, further hindering attempts at a hierarchical ordering. Both type B and type I cells are also found in NSC niches intimately associated with extensive vascularity, suggesting a role of NSC-endothelial cell signaling in the maintenance of these NSC niches, although this too remains speculative (432, 433).

Summary

In spite of comprising only 1.5% of new cancer cases, gliomas are a leading cause of cancer-related death in the United States, with a dismal median survival time of only 12 months. The most malignant gliomas, glioblastoma multiforme (GBM) may arise in either a primary (no prior history of intracranial tumor) or secondary (malignant

progression of low-grade glioma) manner. Despite this difference in clinical presentation and some differences in genomic alterations identified between these two groups, these tumors are phenotypically identical and have nearly identical median survival times. Both primary and secondary human GBMs commonly exhibit profound alterations in the PTEN/PI3K/AKT pathway, the p53 pathway, and the Rb1/$p16^{Ink4a}$ pathway.

The domestic dog (*Canis familiaris*) develops glioma tumors that are phenotypically identical to human glioma, recapitulating every histologic grade, with similar biologic behavior and a nearly identical incidence rate, suggesting significant similarities between these spontaneously occurring tumors across both species. While recent investigations have identified GSCs within a canine GBM and some similarities have been identified at a genomic level, the relatedness of canine glioma to human glioma, in particular in relation to glioma stem cell biology and genomic alterations is still largely unknown.

The tumor stem cell hypothesis attributes the formation and maintenance of the tumor (i.e. the tumorigenic potential) to a specific subpopulation within the tumor as a whole. Originally identified in leukemia, with strong correlates to physiologic hematopoietic stem cells, the concept has been pushed forward to numerous solid tumors as well over the last decade. The application of the tumor stem cell hypothesis to human gliomas remains an evolving theory. There are clear and significant similarities in the growth and molecular profiles between physiologic neural stem cells and the purported GSCs that are expanded from human glioma tissue. In studies involving animal xenograft tumor

models, these cells clearly most accurately replicate the salient features of the parental tumor, chiefly in cell invasion, as compared to traditional cell line models. The true defining characteristic of a glioma stem cell is still unproven however, as no definitive hierarchical organization has been elucidated. The tumor stem cell hypothesis and clonal evolution are far from mutually exclusive, with components of each likely occurring in both the initiation and progression of disease. Tumor cells likely acquire additional genetic aberrations over time that may confer a selective advantage independent of epigenetic regulation, forcing a somewhat more liberal interpretation of the stem cell hypothesis. Ultimately however, the tumor stem cell theory emphasizes the existence of this hierarchy, and the significance of identifying tumor cell subpopulations within a heterogeneous tumor mass that are responsible for the maintenance of the tumor, with particular regards towards tumor recurrence after therapy. In other words, the pathways used to create a hierarchical arrangement within a tumor, be they genomic or epigenetic may be less important therapeutically than being able to understand the arrangement itself, and target the most upstream cell population.

Neural stem cells are regulated in a temporal manner *in vivo* to enter periods of proliferation, neuronal, and then glial differentiation. Early NSCs isolated prior to neuronal fate commitment *in vivo* are proliferative cells, are highly migratory *in situ* within the developing brain, and are refractory to differentiation- all features attributed to glioma tumors and specifically to glioma TSCs. Similarly, GSCs often express markers of both neuronal and glial differentiation status. While significant differences obviously

exist between the tumor-derived GSCs and physiologic eNSCs, understanding these differences within the light of their equally significant similarities may aid in the elucidation of how GSCs maintain their tumorigenic potential and are refractory to terminal differentiation.

References

1. Tait, M.J., et al., *Survival of patients with glioblastoma multiforme has not improved between 1993 and 2004: analysis of 625 cases.* Br J Neurosurg, 2007. **21**(5): p. 496-500.

2. Vescovi, A.L., R. Galli, and B.A. Reynolds, *Brain tumour stem cells.* Nat Rev Cancer, 2006. **6**(6): p. 425-36.

3. Galli, R., et al., *Isolation and characterization of tumorigenic, stem-like neural precursors from human glioblastoma.* Cancer Res, 2004. **64**(19): p. 7011-21.

4. Singh, S.K., et al., *Identification of human brain tumour initiating cells.* Nature, 2004. **432**(7015): p. 396-401.

5. Frese, K.K. and D.A. Tuveson, *Maximizing mouse cancer models.* Nat Rev Cancer, 2007. **7**(9): p. 645-58.

6. Stoica, G., et al., *Morphology, immunohistochemistry, and genetic alterations in dog astrocytomas.* Vet Pathol, 2004. **41**(1): p. 10-9.

7. Stoica, G., et al., *Identification of cancer stem cells in dog glioblastoma.* Vet Pathol, 2009. **46**(3): p. 391-406.

8. Lipsitz, D., et al., *Glioblastoma multiforme: clinical findings, magnetic resonance imaging, and pathology in five dogs.* Vet Pathol, 2003. **40**(6): p. 659-69.

9. Thomas, R., et al., *'Putting our heads together': insights into genomic conservation between human and canine intracranial tumors.* J Neurooncol, 2009. **94**(3): p. 333-49.

10. TCGA, *Comprehensive genomic characterization defines human glioblastoma genes and core pathways.* Nature, 2008. **455**(7216): p. 1061-8.

11. Freire, P., et al., *Exploratory analysis of the copy number alterations in glioblastoma multiforme.* PLoS One, 2008. **3**(12): p. e4076.

12. Rapaport, F. and C. Leslie, *Determining frequent patterns of copy number alterations in cancer.* PLoS One, 2007. **5**(8): p. e12028.

13. Lindblad-Toh, K., et al., *Genome sequence, comparative analysis and haplotype structure of the domestic dog.* Nature, 2005. **438**(7069): p. 803-19.

14. Liu, W., et al., *Brain tumour stem cells and neural stem cells: still explored by the same approach?* J Int Med Res, 2008. **36**(5): p. 890-5.

15. Sanai, N., A. Alvarez-Buylla, and M.S. Berger, *Neural stem cells and the origin of gliomas.* N Engl J Med, 2005. **353**(8): p. 811-22.

16. Abramova, N., et al., *Stage-specific changes in gene expression in acutely isolated mouse CNS progenitor cells.* Dev Biol, 2005. **283**(2): p. 269-81.

17. Louis, D.N., et al., *The 2007 WHO classification of tumours of the central nervous system.* Acta Neuropathol, 2007. **114**(2): p. 97-109.

18. Michotte, A., et al., *Neuropathological and molecular aspects of low-grade and high-grade gliomas.* Acta Neurol Belg, 2004. **104**(4): p. 148-53.

19. Huang, H., et al., *Gene expression profiling of low-grade diffuse astrocytomas by cDNA arrays.* Cancer Res, 2000. **60**(24): p. 6868-74.

20. Bourne, T.D. and D. Schiff, *Update on molecular findings, management and outcome in low-grade gliomas.* Nat Rev Neurol.

21. Dreyfuss, J.M., M.D. Johnson, and P.J. Park, *Meta-analysis of glioblastoma multiforme versus anaplastic astrocytoma identifies robust gene markers.* Mol Cancer, 2009. **8**: p. 71.

22. Ohgaki, H., *Epidemiology of brain tumors.* Methods Mol Biol, 2009. **472**: p. 323-42.

23. Deorah, S., et al., *Trends in brain cancer incidence and survival in the United States: Surveillance, Epidemiology, and End Results Program, 1973 to 2001.* Neurosurg Focus, 2006. **20**(4): p. E1.

24. Maher, E.A., et al., *Marked genomic differences characterize primary and secondary glioblastoma subtypes and identify two distinct molecular and clinical secondary glioblastoma entities.* Cancer Res, 2006. **66**(23): p. 11502-13.

25. Ohgaki, H. and P. Kleihues, *Genetic pathways to primary and secondary glioblastoma.* Am J Pathol, 2007. **170**(5): p. 1445-53.

26. Phillips, H.S., et al., *Molecular subclasses of high-grade glioma predict prognosis, delineate a pattern of disease progression, and resemble stages in neurogenesis.* Cancer Cell, 2006. **9**(3): p. 157-73.

27. Shinojima, N., et al., *Prognostic value of epidermal growth factor receptor in patients with glioblastoma multiforme.* Cancer Res, 2003. **63**(20): p. 6962-70.

28. Heimberger, A.B., et al., *Prognostic effect of epidermal growth factor receptor and EGFRvIII in glioblastoma multiforme patients.* Clin Cancer Res, 2005. **11**(4): p. 1462-6.

29. Zhu, Y., et al., *Early inactivation of p53 tumor suppressor gene cooperating with NF1 loss induces malignant astrocytoma.* Cancer Cell, 2005. **8**(2): p. 119-30.

30. Jackson, E.L., et al., *PDGFR alpha-positive B cells are neural stem cells in the adult SVZ that form glioma-like growths in response to increased PDGF signaling.* Neuron, 2006. **51**(2): p. 187-99.

31. Dai, C., et al., *PDGF autocrine stimulation dedifferentiates cultured astrocytes and induces oligodendrogliomas and oligoastrocytomas from neural progenitors and astrocytes in vivo.* Genes Dev, 2001. **15**(15): p. 1913-25.

32. Ma, D., et al., *Autocrine platelet-derived growth factor-dependent gene expression in glioblastoma cells is mediated largely by activation of the transcription factor sterol regulatory element binding protein and is associated with altered genotype and patient survival in human brain tumors.* Cancer Res, 2005. **65**(13): p. 5523-34.

33. Hunter, T., *Signaling--2000 and beyond.* Cell, 2000. **100**(1): p. 113-27.

34. Schlessinger, J., *Cell signaling by receptor tyrosine kinases.* Cell, 2000. **103**(2): p. 211-25.

35. Ohgaki, H., et al., *Genetic pathways to glioblastoma: a population-based study.* Cancer Res, 2004. **64**(19): p. 6892-9.

36. Watanabe, K., et al., *Overexpression of the EGF receptor and p53 mutations are mutually exclusive in the evolution of primary and secondary glioblastomas.* Brain Pathol, 1996. **6**(3): p. 217-23; discussion 23-4.

37. Ekstrand, A.J., et al., *Amplified and rearranged epidermal growth factor receptor genes in human glioblastomas reveal deletions of sequences encoding portions of*

the N- and/or C-terminal tails. Proc Natl Acad Sci U S A, 1992. **89**(10): p. 4309-13.

38. Fankhauser, R., H. Luginbuhl, and J.T. McGrath, *Tumours of the nervous system.* Bull World Health Organ, 1974. **50**(1-2): p. 53-69.

39. Koestner A, H.R., *Tumors of the nervous syste. In: Meuten D (ed) Tumors in Domestic Animals.* Blackwell Publishing, 2002: p. 697.

40. Dickinson, P.J., et al., *Vascular endothelial growth factor mRNA expression and peritumoral edema in canine primary central nervous system tumors.* Vet Pathol, 2008. **45**(2): p. 131-9.

41. Obermaier, G., et al., *Rhinencephalic glial cell nests and their possible role in glioma formation: morphometric studies do not reveal significant differences between brachycephalic and dolichocephalic dogs.* Acta Neuropathol, 1995. **89**(3): p. 258-61.

42. Thomas, R., et al., *A genome assembly-integrated dog 1 Mb BAC microarray: a cytogenetic resource for canine cancer studies and comparative genomic analysis.* Cytogenet Genome Res, 2008. **122**(2): p. 110-21.

43. Engelman, J.A., J. Luo, and L.C. Cantley, *The evolution of phosphatidylinositol 3-kinases as regulators of growth and metabolism.* Nat Rev Genet, 2006. **7**(8): p. 606-19.

44. Easton, R.M., et al., *Role for Akt3/protein kinase Bgamma in attainment of normal brain size.* Mol Cell Biol, 2005. **25**(5): p. 1869-78.

45. Tschopp, O., et al., *Essential role of protein kinase B gamma (PKB gamma/Akt3) in postnatal brain development but not in glucose homeostasis.* Development, 2005. **132**(13): p. 2943-54.

46. Franca-Koh, J., Y. Kamimura, and P.N. Devreotes, *Leading-edge research: PtdIns(3,4,5)P3 and directed migration.* Nat Cell Biol, 2007. **9**(1): p. 15-7.

47. Alessi, D.R., et al., *3-Phosphoinositide-dependent protein kinase-1 (PDK1): structural and functional homology with the Drosophila DSTPK61 kinase.* Curr Biol, 1997. **7**(10): p. 776-89.

48. Alessi, D.R., et al., *Characterization of a 3-phosphoinositide-dependent protein kinase which phosphorylates and activates protein kinase Balpha.* Curr Biol, 1997. **7**(4): p. 261-9.

49. Sarbassov, D.D., et al., *Phosphorylation and regulation of Akt/PKB by the rictor-mTOR complex.* Science, 2005. **307**(5712): p. 1098-101.

50. Mora, A., et al., *PDK1, the master regulator of AGC kinase signal transduction.* Semin Cell Dev Biol, 2004. **15**(2): p. 161-70.

51. Yang, L., et al., *TCR-induced Akt serine 473 phosphorylation is regulated by protein kinase C-alpha.* Biochem Biophys Res Commun, 2010. **400**(1): p. 16-20.

52. Cross, D.A., et al., *Inhibition of glycogen synthase kinase-3 by insulin mediated by protein kinase B.* Nature, 1995. **378**(6559): p. 785-9.

53. Alessi, D.R., et al., *Molecular basis for the substrate specificity of protein kinase B; comparison with MAPKAP kinase-1 and p70 S6 kinase.* FEBS Lett, 1996. **399**(3): p. 333-8.

54. Hutchinson, J.N., et al., *Activation of Akt-1 (PKB-alpha) can accelerate ErbB-2-mediated mammary tumorigenesis but suppresses tumor invasion.* Cancer Res, 2004. **64**(9): p. 3171-8.

55. Arboleda, M.J., et al., *Overexpression of AKT2/protein kinase Bbeta leads to up-regulation of beta1 integrins, increased invasion, and metastasis of human breast and ovarian cancer cells.* Cancer Res, 2003. **63**(1): p. 196-206.

56. Yoeli-Lerner, M., et al., *Akt blocks breast cancer cell motility and invasion through the transcription factor NFAT.* Mol Cell, 2005. **20**(4): p. 539-50.

57. Mure, H., et al., *Akt2 and Akt3 play a pivotal role in malignant gliomas.* Neuro Oncol, 2010. **12**(3): p. 221-32.

58. Manning, B.D. and L.C. Cantley, *AKT/PKB signaling: navigating downstream.* Cell, 2007. **129**(7): p. 1261-74.

59. Marte, B.M. and J. Downward, *PKB/Akt: connecting phosphoinositide 3-kinase to cell survival and beyond.* Trends Biochem Sci, 1997. **22**(9): p. 355-8.

60. Wang, M., et al., *FoxO gene family evolution in vertebrates.* BMC Evol Biol, 2009. **9**: p. 222.

61. Hoekman, M.F., et al., *Spatial and temporal expression of FoxO transcription factors in the developing and adult murine brain.* Gene Expr Patterns, 2006. **6**(2): p. 134-40.

62. Lein, E.S., et al., *Genome-wide atlas of gene expression in the adult mouse brain.* Nature, 2007. **445**(7124): p. 168-76.

63. Brunet, A., et al., *Akt promotes cell survival by phosphorylating and inhibiting a Forkhead transcription factor.* Cell, 1999. **96**(6): p. 857-68.

64. Yang, X., et al., *Isoform-specific expression of 14-3-3 proteins in human astrocytoma.* J Neurol Sci, 2009. **276**(1-2): p. 54-9.

65. Cao, L., et al., *Identification of 14-3-3 protein isoforms in human astrocytoma by immunohistochemistry.* Neurosci Lett, 2008. **432**(2): p. 94-9.

66. Maiese, K., Z.Z. Chong, and Y.C. Shang, *OutFOXOing disease and disability: the therapeutic potential of targeting FoxO proteins.* Trends Mol Med, 2008. **14**(5): p. 219-27.

67. Dijkers, P.F., et al., *FKHR-L1 can act as a critical effector of cell death induced by cytokine withdrawal: protein kinase B-enhanced cell survival through maintenance of mitochondrial integrity.* J Cell Biol, 2002. **156**(3): p. 531-42.

68. Medema, R.H., et al., *AFX-like Forkhead transcription factors mediate cell-cycle regulation by Ras and PKB through p27kip1.* Nature, 2000. **404**(6779): p. 782-7.

69. Datta, S.R., et al., *Akt phosphorylation of BAD couples survival signals to the cell-intrinsic death machinery.* Cell, 1997. **91**(2): p. 231-41.

70. Datta, S.R., et al., *14-3-3 proteins and survival kinases cooperate to inactivate BAD by BH3 domain phosphorylation.* Mol Cell, 2000. **6**(1): p. 41-51.

71. del Peso, L., et al., *Interleukin-3-induced phosphorylation of BAD through the protein kinase Akt.* Science, 1997. **278**(5338): p. 687-9.

72. Danial, N.N., *BAD: undertaker by night, candyman by day.* Oncogene, 2008. **27 Suppl 1**: p. S53-70.

73. Mayo, L.D. and D.B. Donner, *A phosphatidylinositol 3-kinase/Akt pathway promotes translocation of Mdm2 from the cytoplasm to the nucleus.* Proc Natl Acad Sci U S A, 2001. **98**(20): p. 11598-603.

74. Zhou, B.P., et al., *HER-2/neu induces p53 ubiquitination via Akt-mediated MDM2 phosphorylation.* Nat Cell Biol, 2001. **3**(11): p. 973-82.

75. Liang, J., et al., *PKB/Akt phosphorylates p27, impairs nuclear import of p27 and opposes p27-mediated G1 arrest.* Nat Med, 2002. **8**(10): p. 1153-60.

76. Viglietto, G., et al., *Cytoplasmic relocalization and inhibition of the cyclin-dependent kinase inhibitor p27(Kip1) by PKB/Akt-mediated phosphorylation in breast cancer.* Nat Med, 2002. **8**(10): p. 1136-44.

77. Sekimoto, T., M. Fukumoto, and Y. Yoneda, *14-3-3 suppresses the nuclear localization of threonine 157-phosphorylated p27(Kip1).* EMBO J, 2004. **23**(9): p. 1934-42.

78. Rossig, L., et al., *Glycogen synthase kinase-3 couples AKT-dependent signaling to the regulation of p21Cip1 degradation.* J Biol Chem, 2002. **277**(12): p. 9684-9.

79. Peterson, T.R., et al., *DEPTOR is an mTOR inhibitor frequently overexpressed in multiple myeloma cells and required for their survival.* Cell, 2009. **137**(5): p. 873-86.

80. Hara, K., et al., *Raptor, a binding partner of target of rapamycin (TOR), mediates TOR action.* Cell, 2002. **110**(2): p. 177-89.

81. Kim, D.H., et al., *mTOR interacts with raptor to form a nutrient-sensitive complex that signals to the cell growth machinery.* Cell, 2002. **110**(2): p. 163-75.

82. Gingras, A.C., B. Raught, and N. Sonenberg, *eIF4 initiation factors: effectors of mRNA recruitment to ribosomes and regulators of translation.* Annu Rev Biochem, 1999. **68**: p. 913-63.

83. Rousseau, D., et al., *The eIF4E-binding proteins 1 and 2 are negative regulators of cell growth.* Oncogene, 1996. **13**(11): p. 2415-20.

84. Corradetti, M.N., K. Inoki, and K.L. Guan, *The stress-inducted proteins RTP801 and RTP801L are negative regulators of the mammalian target of rapamycin pathway.* J Biol Chem, 2005. **280**(11): p. 9769-72.

85. Shahbazian, D., et al., *The mTOR/PI3K and MAPK pathways converge on eIF4B to control its phosphorylation and activity.* EMBO J, 2006. **25**(12): p. 2781-91.

86. Acosta-Jaquez, H.A., et al., *Site-specific mTOR phosphorylation promotes mTORC1-mediated signaling and cell growth.* Mol Cell Biol, 2009. **29**(15): p. 4308-24.

87. Inoki, K., et al., *TSC2 is phosphorylated and inhibited by Akt and suppresses mTOR signalling.* Nat Cell Biol, 2002. **4**(9): p. 648-57.

88. Manning, B.D., et al., *Identification of the tuberous sclerosis complex-2 tumor suppressor gene product tuberin as a target of the phosphoinositide 3-kinase/akt pathway.* Mol Cell, 2002. **10**(1): p. 151-62.

89. Cai, S.L., et al., *Activity of TSC2 is inhibited by AKT-mediated phosphorylation and membrane partitioning.* J Cell Biol, 2006. **173**(2): p. 279-89.

90. Huang, J., et al., *The TSC1-TSC2 complex is required for proper activation of mTOR complex 2.* Mol Cell Biol, 2008. **28**(12): p. 4104-15.

91. Tee, A.R., R. Anjum, and J. Blenis, *Inactivation of the tuberous sclerosis complex-1 and -2 gene products occurs by phosphoinositide 3-kinase/Akt-dependent and -independent phosphorylation of tuberin.* J Biol Chem, 2003. **278**(39): p. 37288-96.

92. Ghosh, H.S., M. McBurney, and P.D. Robbins, *SIRT1 negatively regulates the mammalian target of rapamycin.* PLoS One, 2010. **5**(2): p. e9199.

93. McBride, S.M., et al., *Activation of PI3K/mTOR pathway occurs in most adult low-grade gliomas and predicts patient survival.* J Neurooncol, 2010. **97**(1): p. 33-40.

94. Wang, L., T.E. Harris, and J.C. Lawrence, Jr., *Regulation of proline-rich Akt substrate of 40 kDa (PRAS40) function by mammalian target of rapamycin complex 1 (mTORC1)-mediated phosphorylation.* J Biol Chem, 2008. **283**(23): p. 15619-27.

95. Wang, L., et al., *PRAS40 regulates mTORC1 kinase activity by functioning as a direct inhibitor of substrate binding.* J Biol Chem, 2007. **282**(27): p. 20036-44.

96. Sanchez Canedo, C., et al., *Activation of the cardiac mTOR/p70(S6K) pathway by leucine requires PDK1 and correlates with PRAS40 phosphorylation.* Am J Physiol Endocrinol Metab, 2010. **298**(4): p. E761-9.

97. Molina, J.R., et al., *Invasive glioblastoma cells acquire stemness and increased Akt activation.* Neoplasia, 2010. **12**(6): p. 453-63.

98. Cheng, G.Z., et al., *Twist transcriptionally up-regulates AKT2 in breast cancer cells leading to increased migration, invasion, and resistance to paclitaxel.* Cancer Res, 2007. **67**(5): p. 1979-87.

99. Elias, M.C., et al., *TWIST is expressed in human gliomas and promotes invasion.* Neoplasia, 2005. **7**(9): p. 824-37.

100. Zhang, J., et al., *AKT2 expression is associated with glioma malignant progression and required for cell survival and invasion.* Oncol Rep, 2010. **24**(1): p. 65-72.

101. Zhang, B., et al., *Reduction of Akt2 inhibits migration and invasion of glioma cells.* Int J Cancer, 2009. **125**(3): p. 585-95.

102. Yan, W., et al., *Expression pattern of osteopontin splice variants and its functions on cell apoptosis and invasion in glioma cells.* Neuro Oncol, 2010. **12**(8): p. 765-75.

103. Fu, Y., et al., *Inhibitory effects of adenovirus mediated Akt1 and PIK3R1 shRNA on the growth of malignant tumor cells in vitro and in vivo.* Cancer Biol Ther, 2009. **8**(11): p. 1002-9.

104. Park, C.M., et al., *Ionizing radiation enhances matrix metalloproteinase-2 secretion and invasion of glioma cells through Src/epidermal growth factor receptor-mediated p38/Akt and phosphatidylinositol 3-kinase/Akt signaling pathways.* Cancer Res, 2006. **66**(17): p. 8511-9.

105. Kubiatowski, T., et al., *Association of increased phosphatidylinositol 3-kinase signaling with increased invasiveness and gelatinase activity in malignant gliomas.* J Neurosurg, 2001. **95**(3): p. 480-8.

106. Brunckhorst, M.K., et al., *Angiopoietin-4 promotes glioblastoma progression by enhancing tumor cell viability and angiogenesis.* Cancer Res, 2010. **70**(18): p. 7283-93.

107. Gordan, J.D. and M.C. Simon, *Hypoxia-inducible factors: central regulators of the tumor phenotype.* Curr Opin Genet Dev, 2007. **17**(1): p. 71-7.

108. Semenza, G.L., *Targeting HIF-1 for cancer therapy.* Nat Rev Cancer, 2003. **3**(10): p. 721-32.

109. Maiuri, F., et al., *Expression of growth factors in brain tumors: correlation with tumor grade, recurrence and survival.* Clin Neuropathol, 2010. **29**(2): p. 109-14.

110. Dimmeler, S., et al., *Activation of nitric oxide synthase in endothelial cells by Akt-dependent phosphorylation.* Nature, 1999. **399**(6736): p. 601-5.

111. Fulton, D., et al., *Regulation of endothelium-derived nitric oxide production by the protein kinase Akt.* Nature, 1999. **399**(6736): p. 597-601.

112. Towner, R.A., et al., *In vivo detection of inducible nitric oxide synthase in rodent gliomas.* Free Radic Biol Med, 2010. **48**(5): p. 691-703.

113. Broholm, H., et al., *Nitric oxide synthase expression and enzymatic activity in human brain tumors.* Clin Neuropathol, 2003. **22**(6): p. 273-81.

114. Warburg, O., *On the origin of cancer cells.* Science, 1956. **123**(3191): p. 309-14.

115. Calera, M.R., et al., *Insulin increases the association of Akt-2 with Glut4-containing vesicles.* J Biol Chem, 1998. **273**(13): p. 7201-4.

116. Kohn, A.D., et al., *Expression of a constitutively active Akt Ser/Thr kinase in 3T3-L1 adipocytes stimulates glucose uptake and glucose transporter 4 translocation.* J Biol Chem, 1996. **271**(49): p. 31372-8.

117. Eguez, L., et al., *Full intracellular retention of GLUT4 requires AS160 Rab GTPase activating protein.* Cell Metab, 2005. **2**(4): p. 263-72.

118. Deprez, J., et al., *Phosphorylation and activation of heart 6-phosphofructo-2-kinase by protein kinase B and other protein kinases of the insulin signaling cascades.* J Biol Chem, 1997. **272**(28): p. 17269-75.

119. Sundqvist, A., et al., *Control of lipid metabolism by phosphorylation-dependent degradation of the SREBP family of transcription factors by SCF(Fbw7).* Cell Metab, 2005. **1**(6): p. 379-91.

120. Berwick, D.C., et al., *The identification of ATP-citrate lyase as a protein kinase B (Akt) substrate in primary adipocytes.* J Biol Chem, 2002. **277**(37): p. 33895-900.

121. Kotliarova, S., et al., *Glycogen synthase kinase-3 inhibition induces glioma cell death through c-MYC, nuclear factor-kappaB, and glucose regulation.* Cancer Res, 2008. **68**(16): p. 6643-51.

122. Korur, S., et al., *GSK3beta regulates differentiation and growth arrest in glioblastoma.* PLoS One, 2009. **4**(10): p. e7443.

123. Chakravarti, A., et al., *Prognostic and pathologic significance of quantitative protein expression profiling in human gliomas.* Clin Cancer Res, 2001. **7**(8): p. 2387-95.

124. Broderick, D.K., et al., *Mutations of PIK3CA in anaplastic oligodendrogliomas, high-grade astrocytomas, and medulloblastomas.* Cancer Res, 2004. **64**(15): p. 5048-50.

125. Samuels, Y., et al., *High frequency of mutations of the PIK3CA gene in human cancers.* Science, 2004. **304**(5670): p. 554.

126. Knobbe, C.B. and G. Reifenberger, *Genetic alterations and aberrant expression of genes related to the phosphatidyl-inositol-3'-kinase/protein kinase B (Akt) signal transduction pathway in glioblastomas.* Brain Pathol, 2003. **13**(4): p. 507-18.

127. Endersby, R. and S.J. Baker, *PTEN signaling in brain: neuropathology and tumorigenesis.* Oncogene, 2008. **27**(41): p. 5416-30.

128. Zheng, H., et al., *p53 and Pten control neural and glioma stem/progenitor cell renewal and differentiation.* Nature, 2008. **455**(7216): p. 1129-33.

129. Taylor, B.S., et al., *Functional copy-number alterations in cancer.* PLoS One, 2008. **3**(9): p. e3179.

130. Beroukhim, R., et al., *Assessing the significance of chromosomal aberrations in cancer: methodology and application to glioma.* Proc Natl Acad Sci U S A, 2007. **104**(50): p. 20007-12.

131. Yadav, A.K., et al., *Monosomy of chromosome 10 associated with dysregulation of epidermal growth factor signaling in glioblastomas.* JAMA, 2009. **302**(3): p. 276-89.

132. Bredel, M., et al., *A network model of a cooperative genetic landscape in brain tumors.* JAMA, 2009. **302**(3): p. 261-75.

133. Lane, D.P., *Cancer. p53, guardian of the genome.* Nature, 1992. **358**(6381): p. 15-6.

134. Kirpensteijn, J., et al., *TP53 gene mutations in canine osteosarcoma.* Vet Surg, 2008. **37**(5): p. 454-60.

135. Yonemaru, K., et al., *The significance of p53 and retinoblastoma pathways in canine hemangiosarcoma.* J Vet Med Sci, 2007. **69**(3): p. 271-8.

136. Lee, C.H., et al., *Mutation and overexpression of p53 as a prognostic factor in canine mammary tumors.* J Vet Sci, 2004. **5**(1): p. 63-9.

137. Talos, F. and U.M. Moll, *Role of the p53 family in stabilizing the genome and preventing polyploidization.* Adv Exp Med Biol, 2010. **676**: p. 73-91.

138. Soussi, T., et al., *Locus-specific mutation databases: pitfalls and good practice based on the p53 experience.* Nat Rev Cancer, 2006. **6**(1): p. 83-90.

139. Daee, D.L., T.M. Mertz, and P.V. Shcherbakova, *A cancer-associated DNA polymerase delta variant modeled in yeast causes a catastrophic increase in genomic instability.* Proc Natl Acad Sci U S A, 2010. **107**(1): p. 157-62.

140. Robertson, A.B., et al., *DNA repair in mammalian cells: Base excision repair: the long and short of it.* Cell Mol Life Sci, 2009. **66**(6): p. 981-93.

141. Baute, J. and A. Depicker, *Base excision repair and its role in maintaining genome stability.* Crit Rev Biochem Mol Biol, 2008. **43**(4): p. 239-76.

142. Weissman, L., et al., *DNA repair, mitochondria, and neurodegeneration.* Neuroscience, 2007. **145**(4): p. 1318-29.

143. Campisi, J. and F. d'Adda di Fagagna, *Cellular senescence: when bad things happen to good cells.* Nat Rev Mol Cell Biol, 2007. **8**(9): p. 729-40.

144. Finkel, T., M. Serrano, and M.A. Blasco, *The common biology of cancer and ageing.* Nature, 2007. **448**(7155): p. 767-74.

145. Gorgoulis, V.G., et al., *Activation of the DNA damage checkpoint and genomic instability in human precancerous lesions.* Nature, 2005. **434**(7035): p. 907-13.

146. Bartkova, J., et al., *DNA damage response as a candidate anti-cancer barrier in early human tumorigenesis.* Nature, 2005. **434**(7035): p. 864-70.

147. Smith, J., et al., *The ATM-Chk2 and ATR-Chk1 pathways in DNA damage signaling and cancer.* Adv Cancer Res, 2010. **108**: p. 73-112.

148. Limbo, O., et al., *Mre11 Nuclease Activity and Ctp1 Regulate Chk1 Activation by Rad3ATR and Tel1ATM Checkpoint Kinases at Double-Strand Breaks.* Mol Cell Biol, 2010.

149. Guo, Z., et al., *ATM activation by oxidative stress.* Science, 2010. **330**(6003): p. 517-21.

150. Lamarche, B.J., N.I. Orazio, and M.D. Weitzman, *The MRN complex in double-strand break repair and telomere maintenance.* FEBS Lett, 2010. **584**(17): p. 3682-95.

151. Williams, R.S., et al., *Nbs1 flexibly tethers Ctp1 and Mre11-Rad50 to coordinate DNA double-strand break processing and repair.* Cell, 2009. **139**(1): p. 87-99.

152. Yoo, H.Y., et al., *The Mre11-Rad50-Nbs1 complex mediates activation of TopBP1 by ATM.* Mol Biol Cell, 2009. **20**(9): p. 2351-60.

153. Wilsker, D. and F. Bunz, *Chk1 phosphorylation during mitosis: a new role for a master regulator.* Cell Cycle, 2009. **8**(8): p. 1161-3.

154. Fragkos, M., J. Jurvansuu, and P. Beard, *H2AX is required for cell cycle arrest via the p53/p21 pathway.* Mol Cell Biol, 2009. **29**(10): p. 2828-40.

155. Carlessi, L., et al., *DNA-damage response, survival and differentiation in vitro of a human neural stem cell line in relation to ATM expression.* Cell Death Differ, 2009. **16**(6): p. 795-806.

156. Bao, S., et al., *Glioma stem cells promote radioresistance by preferential activation of the DNA damage response.* Nature, 2006. **444**(7120): p. 756-60.

157. Ashcroft, M., M.H. Kubbutat, and K.H. Vousden, *Regulation of p53 function and stability by phosphorylation.* Mol Cell Biol, 1999. **19**(3): p. 1751-8.

158. Hublarova, P., et al., *Switching p53-dependent growth arrest to apoptosis via the inhibition of DNA damage-activated kinases.* Cell Mol Biol Lett, 2010. **15**(3): p. 473-84.

159. Helt, C.E., et al., *Ataxia telangiectasia mutated (ATM) and ATM and Rad3-related protein exhibit selective target specificities in response to different forms of DNA damage.* J Biol Chem, 2005. **280**(2): p. 1186-92.

160. Brooks, C.L. and W. Gu, *Ubiquitination, phosphorylation and acetylation: the molecular basis for p53 regulation.* Curr Opin Cell Biol, 2003. **15**(2): p. 164-71.

161. Bode, A.M. and Z. Dong, *Post-translational modification of p53 in tumorigenesis.* Nat Rev Cancer, 2004. **4**(10): p. 793-805.

162. Nie, L., M. Sasaki, and C.G. Maki, *Regulation of p53 nuclear export through sequential changes in conformation and ubiquitination.* J Biol Chem, 2007. **282**(19): p. 14616-25.

163. Sasaki, M., L. Nie, and C.G. Maki, *MDM2 binding induces a conformational change in p53 that is opposed by heat-shock protein 90 and precedes p53 proteasomal degradation.* J Biol Chem, 2007. **282**(19): p. 14626-34.

164. Shieh, S.Y., et al., *DNA damage-induced phosphorylation of p53 alleviates inhibition by MDM2.* Cell, 1997. **91**(3): p. 325-34.

165. Di Stefano, V., et al., *HIPK2 contributes to PCAF-mediated p53 acetylation and selective transactivation of p21Waf1 after nonapoptotic DNA damage.* Oncogene, 2005. **24**(35): p. 5431-42.

166. Knights, C.D., et al., *Distinct p53 acetylation cassettes differentially influence gene-expression patterns and cell fate.* J Cell Biol, 2006. **173**(4): p. 533-44.

167. Sakaguchi, K., et al., *DNA damage activates p53 through a phosphorylation-acetylation cascade.* Genes Dev, 1998. **12**(18): p. 2831-41.

168. Millau, J.F., et al., *p53 Pre- and post-binding event theories revisited: stresses reveal specific and dynamic p53-binding patterns on the p21 gene promoter.* Cancer Res, 2009. **69**(21): p. 8463-71.

169. Menendez, D., A. Inga, and M.A. Resnick, *The expanding universe of p53 targets.* Nat Rev Cancer, 2009. **9**(10): p. 724-37.

170. Sauer, M., et al., *C-terminal diversity within the p53 family accounts for differences in DNA binding and transcriptional activity.* Nucleic Acids Res, 2008. **36**(6): p. 1900-12.

171. Yakovleva, T., et al., *p53 Latency. C-terminal domain prevents binding of p53 core to target but not to nonspecific DNA sequences.* J Biol Chem, 2001. **276**(19): p. 15650-8.

172. Gu, W., et al., *A novel human SRB/MED-containing cofactor complex, SMCC, involved in transcription regulation.* Mol Cell, 1999. **3**(1): p. 97-108.

173. Xing, J., et al., *p53 Stimulates TFIID-TFIIA-promoter complex assembly, and p53-T antigen complex inhibits TATA binding protein-TATA interaction.* Mol Cell Biol, 2001. **21**(11): p. 3652-61.

174. Maltzman, W. and L. Czyzyk, *UV irradiation stimulates levels of p53 cellular tumor antigen in nontransformed mouse cells.* Mol Cell Biol, 1984. **4**(9): p. 1689-94.

175. Vaseva, A.V. and U.M. Moll, *The mitochondrial p53 pathway.* Biochim Biophys Acta, 2009. **1787**(5): p. 414-20.

176. Li, Y.Z., et al., *p53 initiates apoptosis by transcriptionally targeting the antiapoptotic protein ARC.* Mol Cell Biol, 2008. **28**(2): p. 564-74.

177. Lee, J.H., et al., *The p53-inducible gene 3 (PIG3) contributes to early cellular response to DNA damage.* Oncogene, 2010. **29**(10): p. 1431-50.

178. Haupt, S., et al., *Apoptosis - the p53 network.* J Cell Sci, 2003. **116**(Pt 20): p. 4077-85.

179. Kuribayashi, K., et al., *TNFSF10 (TRAIL), a p53 target gene that mediates p53-dependent cell death.* Cancer Biol Ther, 2008. **7**(12): p. 2034-8.

180. Hung, A.C. and A.G. Porter, *p53 mediates nitric oxide-induced apoptosis in murine neural progenitor cells.* Neurosci Lett, 2009. **467**(3): p. 241-6.

181. Wang, P., J. Yu, and L. Zhang, *The nuclear function of p53 is required for PUMA-mediated apoptosis induced by DNA damage.* Proc Natl Acad Sci U S A, 2007. **104**(10): p. 4054-9.

182. Yu, J., et al., *PUMA induces the rapid apoptosis of colorectal cancer cells.* Mol Cell, 2001. **7**(3): p. 673-82.

183. Kuwana, T., et al., *BH3 domains of BH3-only proteins differentially regulate Bax-mediated mitochondrial membrane permeabilization both directly and indirectly.* Mol Cell, 2005. **17**(4): p. 525-35.

184. Chen, L., et al., *Differential targeting of prosurvival Bcl-2 proteins by their BH3-only ligands allows complementary apoptotic function.* Mol Cell, 2005. **17**(3): p. 393-403.

185. Letai, A., et al., *Distinct BH3 domains either sensitize or activate mitochondrial apoptosis, serving as prototype cancer therapeutics.* Cancer Cell, 2002. **2**(3): p. 183-92.

186. Moll, U.M., et al., *Transcription-independent pro-apoptotic functions of p53.* Curr Opin Cell Biol, 2005. **17**(6): p. 631-6.

187. Green, D.R. and G. Kroemer, *Cytoplasmic functions of the tumour suppressor p53.* Nature, 2009. **458**(7242): p. 1127-30.

188. Hayflick, L., *The Limited in Vitro Lifetime of Human Diploid Cell Strains.* Exp Cell Res, 1965. **37**: p. 614-36.

189. Serrano, M., et al., *Oncogenic ras provokes premature cell senescence associated with accumulation of p53 and p16INK4a.* Cell, 1997. **88**(5): p. 593-602.

190. Dimri, G.P., *What has senescence got to do with cancer?* Cancer Cell, 2005. **7**(6): p. 505-12.

191. Campisi, J., *Suppressing cancer: the importance of being senescent.* Science, 2005. **309**(5736): p. 886-7.

192. d'Adda di Fagagna, F., et al., *A DNA damage checkpoint response in telomere-initiated senescence.* Nature, 2003. **426**(6963): p. 194-8.

193. Herbig, U., et al., *Telomere shortening triggers senescence of human cells through a pathway involving ATM, p53, and p21(CIP1), but not p16(INK4a).* Mol Cell, 2004. **14**(4): p. 501-13.

194. Tkemaladze, J. and K. Chichinadze, *Centriole, differentiation, and senescence.* Rejuvenation Res, 2010. **13**(2-3): p. 339-42.

195. Sahin, E. and R.A. Depinho, *Linking functional decline of telomeres, mitochondria and stem cells during ageing.* Nature, 2010. **464**(7288): p. 520-8.

196. Liu, D. and Y. Xu, *p53, oxidative stress and aging.* Antioxid Redox Signal, 2010.

197. Hunziker, A., M.H. Jensen, and S. Krishna, *Stress-specific response of the p53-Mdm2 feedback loop.* BMC Syst Biol, 2010. **4**: p. 94.

198. Bondar, T. and R. Medzhitov, *p53-mediated hematopoietic stem and progenitor cell competition.* Cell Stem Cell, 2010. **6**(4): p. 309-22.

199. Collado, M., et al., *Tumour biology: senescence in premalignant tumours.* Nature, 2005. **436**(7051): p. 642.

200. Dannenberg, J.H., et al., *Ablation of the retinoblastoma gene family deregulates G(1) control causing immortalization and increased cell turnover under growth-restricting conditions.* Genes Dev, 2000. **14**(23): p. 3051-64.

201. Sage, J., et al., *Acute mutation of retinoblastoma gene function is sufficient for cell cycle re-entry.* Nature, 2003. **424**(6945): p. 223-8.

202. Harvey, M., et al., *In vitro growth characteristics of embryo fibroblasts isolated from p53-deficient mice.* Oncogene, 1993. **8**(9): p. 2457-67.

203. Warmerdam, D.O., et al., *Cell cycle-dependent processing of DNA lesions controls localization of Rad9 to sites of genotoxic stress.* Cell Cycle, 2009. **8**(11): p. 1765-74.

204. Bhatia, P., et al., *Mitotic DNA damage targets the Aurora A/TPX2 complex.* Cell Cycle, 2010. **9**(22).

205. Meyer, M., et al., *Oncogenic RAS enables DNA damage- and p53-dependent differentiation of acute myeloid leukemia cells in response to chemotherapy.* PLoS One, 2009. **4**(11): p. e7768.

206. Smogorzewska, A. and T. de Lange, *Different telomere damage signaling pathways in human and mouse cells.* EMBO J, 2002. **21**(16): p. 4338-48.

207. Chan, Y.W., et al., *The kinetics of p53 activation versus cyclin E accumulation underlies the relationship between the spindle-assembly checkpoint and the postmitotic checkpoint.* J Biol Chem, 2008. **283**(23): p. 15716-23.

208. Levine, A.J., W. Hu, and Z. Feng, *The P53 pathway: what questions remain to be explored?* Cell Death Differ, 2006. **13**(6): p. 1027-36.

209. Jin, S., et al., *The GADD45 inhibition of Cdc2 kinase correlates with GADD45-mediated growth suppression.* J Biol Chem, 2000. **275**(22): p. 16602-8.

210. Zhan, Q., et al., *Association with Cdc2 and inhibition of Cdc2/Cyclin B1 kinase activity by the p53-regulated protein Gadd45.* Oncogene, 1999. **18**(18): p. 2892-900.

211. Malkin, D., et al., *Germ line p53 mutations in a familial syndrome of breast cancer, sarcomas, and other neoplasms.* Science, 1990. **250**(4985): p. 1233-8.

212. Louis, D.N., *The p53 gene and protein in human brain tumors.* J Neuropathol Exp Neurol, 1994. **53**(1): p. 11-21.

213. Soussi, T., *The p53 pathway and human cancer.* Br J Surg, 2005. **92**(11): p. 1331-2.

214. Kato, S., et al., *Understanding the function-structure and function-mutation relationships of p53 tumor suppressor protein by high-resolution missense mutation analysis.* Proc Natl Acad Sci U S A, 2003. **100**(14): p. 8424-9.

215. Jones, P.A., et al., *Methylation, mutation and cancer.* Bioessays, 1992. **14**(1): p. 33-6.

216. Hainaut, P. and M. Hollstein, *p53 and human cancer: the first ten thousand mutations.* Adv Cancer Res, 2000. **77**: p. 81-137.

217. Olivier, M., et al., *TP53 mutation spectra and load: a tool for generating hypotheses on the etiology of cancer.* IARC Sci Publ, 2004(157): p. 247-70.

218. Hinds, P.W., et al., *Mutant p53 DNA clones from human colon carcinomas cooperate with ras in transforming primary rat cells: a comparison of the "hot spot" mutant phenotypes.* Cell Growth Differ, 1990. **1**(12): p. 571-80.

219. Lang, G.A., et al., *Gain of function of a p53 hot spot mutation in a mouse model of Li-Fraumeni syndrome.* Cell, 2004. **119**(6): p. 861-72.

220. Oren, M. and V. Rotter, *Mutant p53 gain-of-function in cancer.* Cold Spring Harb Perspect Biol, 2010. **2**(2): p. a001107.

221. Gu, J., et al., *Mutual dependence of MDM2 and MDMX in their functional inactivation of p53.* J Biol Chem, 2002. **277**(22): p. 19251-4.

222. Carter, S., et al., *C-terminal modifications regulate MDM2 dissociation and nuclear export of p53.* Nat Cell Biol, 2007. **9**(4): p. 428-35.

223. Candeias, M.M., et al., *P53 mRNA controls p53 activity by managing Mdm2 functions.* Nat Cell Biol, 2008. **10**(9): p. 1098-105.

224. Giono, L.E. and J.J. Manfredi, *Mdm2 is required for inhibition of Cdk2 activity by p21, thereby contributing to p53-dependent cell cycle arrest.* Mol Cell Biol, 2007. **27**(11): p. 4166-78.

225. Reifenberger, G., et al., *Amplification of multiple genes from chromosomal region 12q13-14 in human malignant gliomas: preliminary mapping of the amplicons shows preferential involvement of CDK4, SAS, and MDM2.* Cancer Res, 1994. **54**(16): p. 4299-303.

226. Wood, N.T., D.W. Meek, and C. Mackintosh, *14-3-3 Binding to Pim-phosphorylated Ser166 and Ser186 of human Mdm2--Potential interplay with the PKB/Akt pathway and p14(ARF).* FEBS Lett, 2009. **583**(4): p. 615-20.

227. Kawai, H., et al., *RING domain-mediated interaction is a requirement for MDM2's E3 ligase activity.* Cancer Res, 2007. **67**(13): p. 6026-30.

228. Riemenschneider, M.J., et al., *Amplification and overexpression of the MDM4 (MDMX) gene from 1q32 in a subset of malignant gliomas without TP53 mutation or MDM2 amplification.* Cancer Res, 1999. **59**(24): p. 6091-6.

229. Tanimura, S., et al., *MDM2 interacts with MDMX through their RING finger domains.* FEBS Lett, 1999. **447**(1): p. 5-9.

230. Okamoto, K., et al., *DNA damage-induced phosphorylation of MdmX at serine 367 activates p53 by targeting MdmX for Mdm2-dependent degradation.* Mol Cell Biol, 2005. **25**(21): p. 9608-20.

231. Solomon, D.A., et al., *Conspirators in a capital crime: co-deletion of p18INK4c and p16INK4a/p14ARF/p15INK4b in glioblastoma multiforme.* Cancer Res, 2008. **68**(21): p. 8657-60.

232. Quelle, D.E., et al., *Alternative reading frames of the INK4a tumor suppressor gene encode two unrelated proteins capable of inducing cell cycle arrest.* Cell, 1995. **83**(6): p. 993-1000.

233. Wang, S., et al., *ARF-dependent regulation of ATM and p53 associated KZNF (Apak) protein activity in response to oncogenic stress.* FEBS Lett, 2010. **584**(18): p. 3909-15.

234. Hochegger, H., S. Takeda, and T. Hunt, *Cyclin-dependent kinases and cell-cycle transitions: does one fit all?* Nat Rev Mol Cell Biol, 2008. **9**(11): p. 910-6.

235. Malumbres, M. and M. Barbacid, *Mammalian cyclin-dependent kinases.* Trends Biochem Sci, 2005. **30**(11): p. 630-41.

236. Harbour, J.W., et al., *Cdk phosphorylation triggers sequential intramolecular interactions that progressively block Rb functions as cells move through G1.* Cell, 1999. **98**(6): p. 859-69.

237. Lundberg, A.S. and R.A. Weinberg, *Functional inactivation of the retinoblastoma protein requires sequential modification by at least two distinct cyclin-cdk complexes.* Mol Cell Biol, 1998. **18**(2): p. 753-61.

238. Johnson, D.G., et al., *Expression of transcription factor E2F1 induces quiescent cells to enter S phase.* Nature, 1993. **365**(6444): p. 349-52.

239. Murray, A.W., *Recycling the cell cycle: cyclins revisited.* Cell, 2004. **116**(2): p. 221-34.

240. DeGregori, J. and D.G. Johnson, *Distinct and Overlapping Roles for E2F Family Members in Transcription, Proliferation and Apoptosis.* Curr Mol Med, 2006. **6**(7): p. 739-48.

241. Dimova, D.K. and N.J. Dyson, *The E2F transcriptional network: old acquaintances with new faces.* Oncogene, 2005. **24**(17): p. 2810-26.

242. Gaubatz, S., et al., *E2F4 and E2F5 play an essential role in pocket protein-mediated G1 control.* Mol Cell, 2000. **6**(3): p. 729-35.

243. Rane, S.G., et al., *Germ line transmission of the Cdk4(R24C) mutation facilitates tumorigenesis and escape from cellular senescence.* Mol Cell Biol, 2002. **22**(2): p. 644-56.

244. Sotillo, R., et al., *Wide spectrum of tumors in knock-in mice carrying a Cdk4 protein insensitive to INK4 inhibitors.* EMBO J, 2001. **20**(23): p. 6637-47.

245. Malumbres, M. and M. Barbacid, *To cycle or not to cycle: a critical decision in cancer.* Nat Rev Cancer, 2001. **1**(3): p. 222-31.

246. Knudson, A.G., Jr., *Mutation and cancer: statistical study of retinoblastoma.* Proc Natl Acad Sci U S A, 1971. **68**(4): p. 820-3.

247. Cobrinik, D., et al., *Rb induces a proliferative arrest and curtails Brn-2 expression in retinoblastoma cells.* Mol Cancer, 2006. **5**: p. 72.

248. Serrano, M., G.J. Hannon, and D. Beach, *A new regulatory motif in cell-cycle control causing specific inhibition of cyclin D/CDK4.* Nature, 1993. **366**(6456): p. 704-7.

249. Schmidt, E.E., et al., *CDKN2 (p16/MTS1) gene deletion or CDK4 amplification occurs in the majority of glioblastomas.* Cancer Res, 1994. **54**(24): p. 6321-4.

250. Jeffrey, P.D., L. Tong, and N.P. Pavletich, *Structural basis of inhibition of CDK-cyclin complexes by INK4 inhibitors.* Genes Dev, 2000. **14**(24): p. 3115-25.

251. Russo, A.A., et al., *Structural basis for inhibition of the cyclin-dependent kinase Cdk6 by the tumour suppressor p16INK4a.* Nature, 1998. **395**(6699): p. 237-43.

252. Ortega, S., M. Malumbres, and M. Barbacid, *Cyclin D-dependent kinases, INK4 inhibitors and cancer.* Biochim Biophys Acta, 2002. **1602**(1): p. 73-87.

253. Pavletich, N.P., *Mechanisms of cyclin-dependent kinase regulation: structures of Cdks, their cyclin activators, and Cip and INK4 inhibitors.* J Mol Biol, 1999. **287**(5): p. 821-8.

254. Sherr, C.J., *The Pezcoller lecture: cancer cell cycles revisited.* Cancer Res, 2000. **60**(14): p. 3689-95.

255. Foijer, F., et al., *Mitogen requirement for cell cycle progression in the absence of pocket protein activity.* Cancer Cell, 2005. **8**(6): p. 455-66.

256. Meuwissen, R., et al., *Induction of small cell lung cancer by somatic inactivation of both Trp53 and Rb1 in a conditional mouse model.* Cancer Cell, 2003. **4**(3): p. 181-9.

257. Munakata, T., et al., *Hepatitis C virus induces E6AP-dependent degradation of the retinoblastoma protein.* PLoS Pathog, 2007. **3**(9): p. 1335-47.

258. Ranade, K., et al., *Mutations associated with familial melanoma impair p16INK4 function.* Nat Genet, 1995. **10**(1): p. 114-6.

259. Singh, S.K., et al., *Identification of a cancer stem cell in human brain tumors.* Cancer Res, 2003. **63**(18): p. 5821-8.

260. Becker, A.J., C.E. Mc, and J.E. Till, *Cytological demonstration of the clonal nature of spleen colonies derived from transplanted mouse marrow cells.* Nature, 1963. **197**: p. 452-4.

261. Siminovitch, L., E.A. McCulloch, and J.E. Till, *The Distribution of Colony-Forming Cells among Spleen Colonies.* J Cell Physiol, 1963. **62**: p. 327-36.

262. Reya, T., et al., *Stem cells, cancer, and cancer stem cells.* Nature, 2001. **414**(6859): p. 105-11.

263. Wu, A.M., et al., *Cytological evidence for a relationship between normal hemotopoietic colony-forming cells and cells of the lymphoid system.* J Exp Med, 1968. **127**(3): p. 455-64.

264. Spangrude, G.J., S. Heimfeld, and I.L. Weissman, *Purification and characterization of mouse hematopoietic stem cells.* Science, 1988. **241**(4861): p. 58-62.

265. Lang, S.H., et al., *Modeling the prostate stem cell niche: an evaluation of stem cell survival and expansion in vitro.* Stem Cells Dev, 2010. **19**(4): p. 537-46.

266. Liu, S., G. Dontu, and M.S. Wicha, *Mammary stem cells, self-renewal pathways, and carcinogenesis.* Breast Cancer Res, 2005. **7**(3): p. 86-95.

267. Vries, R.G., M. Huch, and H. Clevers, *Stem cells and cancer of the stomach and intestine.* Mol Oncol, 2010. **4**(5): p. 373-84.

268. Waters, J.M., G.D. Richardson, and C.A. Jahoda, *Hair follicle stem cells.* Semin Cell Dev Biol, 2007. **18**(2): p. 245-54.

269. Shackleton, M., et al., *Heterogeneity in cancer: cancer stem cells versus clonal evolution.* Cell, 2009. **138**(5): p. 822-9.

270. Coons, S.W. and P.C. Johnson, *Regional heterogeneity in the DNA content of human gliomas.* Cancer, 1993. **72**(10): p. 3052-60.

271. Fey, M.F., et al., *Studying clonal heterogeneity in human cancers.* Cancer Res, 1993. **53**(4): p. 921.

272. Hill, S.A., S. Wilson, and A.F. Chambers, *Clonal heterogeneity, experimental metastatic ability, and p21 expression in H-ras-transformed NIH 3T3 cells.* J Natl Cancer Inst, 1988. **80**(7): p. 484-90.

273. Benard, J., J. Da Silva, and G. Riou, *Culture of clonogenic cells from various human tumors: drug sensitivity assay.* Eur J Cancer Clin Oncol, 1983. **19**(1): p. 65-72.

274. Boccadoro, M., et al., *Kinetics of circulating B lymphocytes in human myeloma.* Blood, 1983. **61**(4): p. 812-4.

275. Durie, B.G., L.A. Young, and S.E. Salmon, *Human myeloma in vitro colony growth: interrelationships between drug sensitivity, cell kinetics, and patient survival duration.* Blood, 1983. **61**(5): p. 929-34.

276. Hamburger, A.W. and S.E. Salmon, *Primary bioassay of human tumor stem cells.* Science, 1977. **197**(4302): p. 461-3.

277. Nomura, Y., H. Tashiro, and K. Hisamatsu, *In vitro clonogenic growth and metastatic potential of human operable breast cancer.* Cancer Res, 1989. **49**(19): p. 5288-93.

278. Fialkow, P.J., et al., *Evidence that essential thrombocythemia is a clonal disorder with origin in a multipotent stem cell.* Blood, 1981. **58**(5): p. 916-9.

279. Griffin, J.D. and B. Lowenberg, *Clonogenic cells in acute myeloblastic leukemia.* Blood, 1986. **68**(6): p. 1185-95.

280. Bonnet, D. and J.E. Dick, *Human acute myeloid leukemia is organized as a hierarchy that originates from a primitive hematopoietic cell.* Nat Med, 1997. **3**(7): p. 730-7.

281. Blair, A., D.E. Hogge, and H.J. Sutherland, *Most acute myeloid leukemia progenitor cells with long-term proliferative ability in vitro and in vivo have the phenotype CD34(+)/CD71(-)/HLA-DR.* Blood, 1998. **92**(11): p. 4325-35.

282. Cobaleda, C., et al., *A primitive hematopoietic cell is the target for the leukemic transformation in human philadelphia-positive acute lymphoblastic leukemia.* Blood, 2000. **95**(3): p. 1007-13.

283. Cox, C.V., et al., *Characterization of acute lymphoblastic leukemia progenitor cells.* Blood, 2004. **104**(9): p. 2919-25.

284. Sell, S., *On the stem cell origin of cancer.* Am J Pathol, 2010. **176**(6): p. 2584-494.

285. Neumuller, R.A. and J.A. Knoblich, *Dividing cellular asymmetry: asymmetric cell division and its implications for stem cells and cancer.* Genes Dev, 2009. **23**(23): p. 2675-99.

286. Quintana, E., et al., *Efficient tumour formation by single human melanoma cells.* Nature, 2008. **456**(7222): p. 593-8.

287. Shah, N.P., et al., *Sequential ABL kinase inhibitor therapy selects for compound drug-resistant BCR-ABL mutations with altered oncogenic potency.* J Clin Invest, 2007. **117**(9): p. 2562-9.

288. Tomasetti, C. and D. Levy, *Role of symmetric and asymmetric division of stem cells in developing drug resistance.* Proc Natl Acad Sci U S A, 2010. **107**(39): p. 16766-71.

289. Barabe, F., et al., *Modeling the initiation and progression of human acute leukemia in mice.* Science, 2007. **316**(5824): p. 600-4.

290. van de Geijn, G.J., R. Hersmus, and L.H. Looijenga, *Recent developments in testicular germ cell tumor research.* Birth Defects Res C Embryo Today, 2009. **87**(1): p. 96-113.

291. Baba, T., et al., *Epigenetic regulation of CD133 and tumorigenicity of CD133+ ovarian cancer cells.* Oncogene, 2009. **28**(2): p. 209-18.

292. Li, C., C.J. Lee, and D.M. Simeone, *Identification of human pancreatic cancer stem cells.* Methods Mol Biol, 2009. **568**: p. 161-73.

293. Lukacs, R.U., et al., *Bmi-1 is a crucial regulator of prostate stem cell self-renewal and malignant transformation.* Cell Stem Cell, 2010. **7**(6): p. 682-93.

294. Shipitsin, M., et al., *Molecular definition of breast tumor heterogeneity.* Cancer Cell, 2007. **11**(3): p. 259-73.

295. Yeung, T.M., et al., *Cancer stem cells from colorectal cancer-derived cell lines.* Proc Natl Acad Sci U S A, 2010. **107**(8): p. 3722-7.

296. Greaves, M., *Cancer stem cells: back to Darwin?* Semin Cancer Biol, 2010. **20**(2): p. 65-70.

297. Dick, J.E., *Stem cell concepts renew cancer research.* Blood, 2008. **112**(13): p. 4793-807.

298. Dick, J.E., *Looking ahead in cancer stem cell research.* Nat Biotechnol, 2009. **27**(1): p. 44-6.

299. Jordan, C.T., M.L. Guzman, and M. Noble, *Cancer stem cells.* N Engl J Med, 2006. **355**(12): p. 1253-61.

300. Baguley, B.C., *Multiple drug resistance mechanisms in cancer.* Mol Biotechnol, 2010. **46**(3): p. 308-16.

301. Bleau, A.M., et al., *PTEN/PI3K/Akt pathway regulates the side population phenotype and ABCG2 activity in glioma tumor stem-like cells.* Cell Stem Cell, 2009. **4**(3): p. 226-35.

302. Charles, N. and E.C. Holland, *The perivascular niche microenvironment in brain tumor progression.* Cell Cycle, 2010. **9**(15): p. 3012-21.

303. Jamal, M., et al., *Microenvironmental regulation of glioblastoma radioresponse.* Clin Cancer Res, 2010.

304. Peng, H., et al., *A novel two mode-acting inhibitor of ABCG2-mediated multidrug transport and resistance in cancer chemotherapy.* PLoS One, 2009. **4**(5): p. e5676.

305. Scharenberg, C.W., M.A. Harkey, and B. Torok-Storb, *The ABCG2 transporter is an efficient Hoechst 33342 efflux pump and is preferentially expressed by immature human hematopoietic progenitors.* Blood, 2002. **99**(2): p. 507-12.

306. Quinones-Hinojosa, A., et al., *Cellular composition and cytoarchitecture of the adult human subventricular zone: a niche of neural stem cells.* J Comp Neurol, 2006. **494**(3): p. 415-34.

307. Alvarez-Buylla, A., et al., *The heterogeneity of adult neural stem cells and the emerging complexity of their niche.* Cold Spring Harb Symp Quant Biol, 2008. **73**: p. 357-65.

308. Doetsch, F., J.M. Garcia-Verdugo, and A. Alvarez-Buylla, *Cellular composition and three-dimensional organization of the subventricular germinal zone in the adult mammalian brain.* J Neurosci, 1997. **17**(13): p. 5046-61.

309. Aguirre, A., M.E. Rubio, and V. Gallo, *Notch and EGFR pathway interaction regulates neural stem cell number and self-renewal.* Nature, 2010. **467**(7313): p. 323-7.

310. Garcia, A.D., et al., *GFAP-expressing progenitors are the principal source of constitutive neurogenesis in adult mouse forebrain.* Nat Neurosci, 2004. **7**(11): p. 1233-41.

311. Park, D., et al., *Nestin is Required for the Proper Self-Renewal of Neural Stem Cells.* Stem Cells, 2010.

312. Witusik, M., et al., *Neuronal and astrocytic cells, obtained after differentiation of human neural GFAP-positive progenitors, present heterogeneous expression of PrPc.* Brain Res, 2007. **1186**: p. 65-73.

313. Fusi, A., et al., *Expression of the Stem Cell Markers Nestin and CD133 on Circulating Melanoma Cells.* J Invest Dermatol, 2010.

314. Guo, R., et al., *Description of the CD133+ subpopulation of the human ovarian cancer cell line OVCAR3.* Oncol Rep, 2011. **25**(1): p. 141-6.

315. Hou, N.Y., et al., *CD133(+)CD44 (+) subgroups may be human small intestinal stem cells.* Mol Biol Rep, 2010.

316. Krupkova, O., Jr., et al., *Nestin expression in human tumors and tumor cell lines.* Neoplasma, 2010. **57**(4): p. 291-8.

317. Bidlingmaier, S., X. Zhu, and B. Liu, *The utility and limitations of glycosylated human CD133 epitopes in defining cancer stem cells.* J Mol Med, 2008. **86**(9): p. 1025-32.

318. Liu, G., et al., *Analysis of gene expression and chemoresistance of CD133+ cancer stem cells in glioblastoma.* Mol Cancer, 2006. **5**: p. 67.

319. Beier, D., et al., *CD133(+) and CD133(-) glioblastoma-derived cancer stem cells show differential growth characteristics and molecular profiles.* Cancer Res, 2007. **67**(9): p. 4010-5.

320. Ogden, A.T., et al., *Identification of A2B5+CD133- tumor-initiating cells in adult human gliomas.* Neurosurgery, 2008. **62**(2): p. 505-14; discussion 514-5.

321. Capela, A. and S. Temple, *LeX is expressed by principle progenitor cells in the embryonic nervous system, is secreted into their environment and binds Wnt-1.* Dev Biol, 2006. **291**(2): p. 300-13.

322. Mao, X.G., et al., *Brain Tumor Stem-Like Cells Identified by Neural Stem Cell Marker CD15.* Transl Oncol, 2009. **2**(4): p. 247-57.

323. Son, M.J., et al., *SSEA-1 is an enrichment marker for tumor-initiating cells in human glioblastoma.* Cell Stem Cell, 2009. **4**(5): p. 440-52.

324. Sun, Y., et al., *CD133 (Prominin) negative human neural stem cells are clonogenic and tripotent.* PLoS One, 2009. **4**(5): p. e5498.

325. Lin, T., O. Islam, and K. Heese, *ABC transporters, neural stem cells and neurogenesis--a different perspective.* Cell Res, 2006. **16**(11): p. 857-71.

326. Mouthon, M.A., et al., *Neural stem cells from mouse forebrain are contained in a population distinct from the 'side population'.* J Neurochem, 2006. **99**(3): p. 807-17.

327. Kelly, P.N., et al., *Tumor growth need not be driven by rare cancer stem cells.* Science, 2007. **317**(5836): p. 337.

328. Guerrero-Cazares, H., K.L. Chaichana, and A. Quinones-Hinojosa, *Neurosphere culture and human organotypic model to evaluate brain tumor stem cells.* Methods Mol Biol, 2009. **568**: p. 73-83.

329. Pollard, S.M., et al., *Adherent neural stem (NS) cells from fetal and adult forebrain.* Cereb Cortex, 2006. **16 Suppl 1**: p. i112-20.

330. Lendahl, U., L.B. Zimmerman, and R.D. McKay, *CNS stem cells express a new class of intermediate filament protein.* Cell, 1990. **60**(4): p. 585-95.

331. Zhang, M., et al., *Nestin and CD133: valuable stem cell-specific markers for determining clinical outcome of glioma patients.* J Exp Clin Cancer Res, 2008. **27**: p. 85.

332. Amoh, Y., et al., *Human hair follicle pluripotent stem (hfPS) cells promote regeneration of peripheral-nerve injury: an advantageous alternative to ES and iPS cells.* J Cell Biochem, 2009. **107**(5): p. 1016-20.

333. Kim, S.Y., et al., *Nestin action during insulin-secreting cell differentiation.* J Histochem Cytochem, 2010. **58**(6): p. 567-76.

334. Suzuki, S., et al., *The neural stem/progenitor cell marker nestin is expressed in proliferative endothelial cells, but not in mature vasculature.* J Histochem Cytochem, 2010. **58**(8): p. 721-30.

335. Gangemi, R.M., et al., *SOX2 silencing in glioblastoma tumor-initiating cells causes stop of proliferation and loss of tumorigenicity.* Stem Cells, 2009. **27**(1): p. 40-8.

336. Pevny, L.H. and S.K. Nicolis, *Sox2 roles in neural stem cells.* Int J Biochem Cell Biol, 2010. **42**(3): p. 421-4.

337. Takahashi, K., et al., *Induction of pluripotent stem cells from adult human fibroblasts by defined factors.* Cell, 2007. **131**(5): p. 861-72.

338. Agathocleous, M., et al., *A directional Wnt/beta-catenin-Sox2-proneural pathway regulates the transition from proliferation to differentiation in the Xenopus retina.* Development, 2009. **136**(19): p. 3289-99.

339. Germana, A., et al., *Developmental changes in the expression of sox2 in the zebrafish brain.* Microsc Res Tech, 2010.

340. Lim, J.H., et al., *Generation and characterization of neurospheres from canine adipose tissue-derived stromal cells.* Cell Reprogram, 2010. **12**(4): p. 417-25.

341. Favaro, R., et al., *Hippocampal development and neural stem cell maintenance require Sox2-dependent regulation of Shh.* Nat Neurosci, 2009. **12**(10): p. 1248-56.

342. Pevny, L. and M. Placzek, *SOX genes and neural progenitor identity.* Curr Opin Neurobiol, 2005. **15**(1): p. 7-13.

343. Wegner, M. and C.C. Stolt, *From stem cells to neurons and glia: a Soxist's view of neural development.* Trends Neurosci, 2005. **28**(11): p. 583-8.

344. Cavallaro, M., et al., *Impaired generation of mature neurons by neural stem cells from hypomorphic Sox2 mutants.* Development, 2008. **135**(3): p. 541-57.

345. Ge, Y., et al., *Sox2 is translationally activated by eukaryotic initiation factor 4E in human glioma-initiating cells.* Biochem Biophys Res Commun, 2010. **397**(4): p. 711-7.

346. Lu, Q.R., et al., *Common developmental requirement for Olig function indicates a motor neuron/oligodendrocyte connection.* Cell, 2002. **109**(1): p. 75-86.

347. Molofsky, A.V., et al., *Bmi-1 promotes neural stem cell self-renewal and neural development but not mouse growth and survival by repressing the p16Ink4a and p19Arf senescence pathways.* Genes Dev, 2005. **19**(12): p. 1432-7.

348. Molofsky, A.V., et al., *Bmi-1 dependence distinguishes neural stem cell self-renewal from progenitor proliferation.* Nature, 2003. **425**(6961): p. 962-7.

349. Zhou, Q. and D.J. Anderson, *The bHLH transcription factors OLIG2 and OLIG1 couple neuronal and glial subtype specification.* Cell, 2002. **109**(1): p. 61-73.

350. Orzan, F., et al., *Enhancer of Zeste 2 (Ezh2) Is up-Regulated in Malignant Gliomas and in Glioma Stem-Like Cells.* Neuropathol Appl Neurobiol, 2010.

351. Rhee, W., et al., *Quantitative analysis of mitotic Olig2 cells in adult human brain and gliomas: implications for glioma histogenesis and biology.* Glia, 2009. **57**(5): p. 510-23.

352. Bruggeman, S.W., et al., *Bmi1 controls tumor development in an Ink4a/Arf-independent manner in a mouse model for glioma.* Cancer Cell, 2007. **12**(4): p. 328-41.

353. Schwartz, Y.B. and V. Pirrotta, *Polycomb silencing mechanisms and the management of genomic programmes.* Nat Rev Genet, 2007. **8**(1): p. 9-22.

354. Valk-Lingbeek, M.E., S.W. Bruggeman, and M. van Lohuizen, *Stem cells and cancer; the polycomb connection.* Cell, 2004. **118**(4): p. 409-18.

355. Wang, H., et al., *Role of histone H2A ubiquitination in Polycomb silencing.* Nature, 2004. **431**(7010): p. 873-8.

356. Guo, W.J., et al., *Mel-18 acts as a tumor suppressor by repressing Bmi-1 expression and down-regulating Akt activity in breast cancer cells.* Cancer Res, 2007. **67**(11): p. 5083-9.

357. Abdouh, M., et al., *BMI1 sustains human glioblastoma multiforme stem cell renewal.* J Neurosci, 2009. **29**(28): p. 8884-96.

358. Ohtsubo, M., et al., *Polycomb-group complex 1 acts as an E3 ubiquitin ligase for Geminin to sustain hematopoietic stem cell activity.* Proc Natl Acad Sci U S A, 2008. **105**(30): p. 10396-401.

359. Maertens, G.N., et al., *Several distinct polycomb complexes regulate and co-localize on the INK4a tumor suppressor locus.* PLoS One, 2009. **4**(7): p. e6380.

360. Fasano, C.A., et al., *Bmi-1 cooperates with Foxg1 to maintain neural stem cell self-renewal in the forebrain.* Genes Dev, 2009. **23**(5): p. 561-74.

361. Cao, R., et al., *Role of histone H3 lysine 27 methylation in Polycomb-group silencing.* Science, 2002. **298**(5595): p. 1039-43.

362. Czermin, B., et al., *Drosophila enhancer of Zeste/ESC complexes have a histone H3 methyltransferase activity that marks chromosomal Polycomb sites.* Cell, 2002. **111**(2): p. 185-96.

363. Kirmizis, A., et al., *Silencing of human polycomb target genes is associated with methylation of histone H3 Lys 27.* Genes Dev, 2004. **18**(13): p. 1592-605.

364. Zhang, Y., et al., *Mechanism of Polycomb group gene silencing.* Cold Spring Harb Symp Quant Biol, 2004. **69**: p. 309-17.

365. Zhao, S., X. Chai, and M. Frotscher, *Balance between neurogenesis and gliogenesis in the adult hippocampus: role for reelin.* Dev Neurosci, 2007. **29**(1-2): p. 84-90.

366. Piccirillo, S.G., et al., *Bone morphogenetic proteins inhibit the tumorigenic potential of human brain tumour-initiating cells.* Nature, 2006. **444**(7120): p. 761-5.

367. Lee, J., et al., *Tumor stem cells derived from glioblastomas cultured in bFGF and EGF more closely mirror the phenotype and genotype of primary tumors than do serum-cultured cell lines.* Cancer Cell, 2006. **9**(5): p. 391-403.

368. von Bohlen Und Halbach, O., *Immunohistological markers for staging neurogenesis in adult hippocampus.* Cell Tissue Res, 2007. **329**(3): p. 409-20.

369. Prestegarden, L., et al., *Glioma cell populations grouped by different cell type markers drive brain tumor growth.* Cancer Res, 2010. **70**(11): p. 4274-9.

370. Menn, B., et al., *Origin of oligodendrocytes in the subventricular zone of the adult brain.* J Neurosci, 2006. **26**(30): p. 7907-18.

371. Levine, A.J. and A.H. Brivanlou, *Proposal of a model of mammalian neural induction.* Dev Biol, 2007. **308**(2): p. 247-56.

372. Pera, M.F., et al., *Regulation of human embryonic stem cell differentiation by BMP-2 and its antagonist noggin.* J Cell Sci, 2004. **117**(Pt 7): p. 1269-80.

373. Kawasaki, H., et al., *Induction of midbrain dopaminergic neurons from ES cells by stromal cell-derived inducing activity.* Neuron, 2000. **28**(1): p. 31-40.

374. Chambers, S.M., et al., *Highly efficient neural conversion of human ES and iPS cells by dual inhibition of SMAD signaling.* Nat Biotechnol, 2009. **27**(3): p. 275-80.

375. Ben-Zvi, D., et al., *Scaling of the BMP activation gradient in Xenopus embryos.* Nature, 2008. **453**(7199): p. 1205-11.

376. Fan, X., et al., *Spatial and temporal patterns of expression of Noggin and BMP4 in embryonic and postnatal rat hippocampus.* Brain Res Dev Brain Res, 2003. **146**(1-2): p. 51-8.

377. Sterneckert, J., et al., *Neural induction intermediates exhibit distinct roles of Fgf signaling.* Stem Cells, 2010. **28**(10): p. 1772-81.

378. Maric, D., et al., *Self-renewing and differentiating properties of cortical neural stem cells are selectively regulated by basic fibroblast growth factor (FGF) signaling via specific FGF receptors.* J Neurosci, 2007. **27**(8): p. 1836-52.

379. Gaspard, N. and P. Vanderhaeghen, *Mechanisms of neural specification from embryonic stem cells.* Curr Opin Neurobiol, 2010. **20**(1): p. 37-43.

380. O'Rahilly, R. and F. Muller, *Neurulation in the normal human embryo.* Ciba Found Symp, 1994. **181**: p. 70-82; discussion 82-9.

381. Juriloff, D.M., et al., *Normal mouse strains differ in the site of initiation of closure of the cranial neural tube.* Teratology, 1991. **44**(2): p. 225-33.

382. Houston, M.L., *The early brain development of the dog.* J Comp Neurol, 1968. **134**(3): p. 371-84.

383. Ajioka, I., T. Maeda, and K. Nakajima, *Identification of ventricular-side-enriched molecules regulated in a stage-dependent manner during cerebral cortical development.* Eur J Neurosci, 2006. **23**(2): p. 296-308.

384. Committee, T.B., *Embryonic vertebrate central nervous system: revised terminology. The Boulder Committee.* Anat Rec, 1970. **166**(2): p. 257-61.

385. Rakic, P., *Specification of cerebral cortical areas.* Science, 1988. **241**(4862): p. 170-6.

386. Caviness, V.S., Jr. and P. Rakic, *Mechanisms of cortical development: a view from mutations in mice.* Annu Rev Neurosci, 1978. **1**: p. 297-326.

387. Gotz, M. and W.B. Huttner, *The cell biology of neurogenesis.* Nat Rev Mol Cell Biol, 2005. **6**(10): p. 777-88.

388. Iacopetti, P., et al., *Expression of the antiproliferative gene TIS21 at the onset of neurogenesis identifies single neuroepithelial cells that switch from proliferative to neuron-generating division.* Proc Natl Acad Sci U S A, 1999. **96**(8): p. 4639-44.

389. Malatesta, P., I. Appolloni, and F. Calzolari, *Radial glia and neural stem cells.* Cell Tissue Res, 2008. **331**(1): p. 165-78.

390. Bystron, I., C. Blakemore, and P. Rakic, *Development of the human cerebral cortex: Boulder Committee revisited.* Nat Rev Neurosci, 2008. **9**(2): p. 110-22.

391. Zhong, W., et al., *Differential expression of mammalian Numb, Numblike and Notch1 suggests distinct roles during mouse cortical neurogenesis.* Development, 1997. **124**(10): p. 1887-97.

392. Rakic, P., *A small step for the cell, a giant leap for mankind: a hypothesis of neocortical expansion during evolution.* Trends Neurosci, 1995. **18**(9): p. 383-8.

393. Chenn, A. and S.K. McConnell, *Cleavage orientation and the asymmetric inheritance of Notch1 immunoreactivity in mammalian neurogenesis.* Cell, 1995. **82**(4): p. 631-41.

394. Taverna, E. and W.B. Huttner, *Neural progenitor nuclei IN motion.* Neuron, 2010. **67**(6): p. 906-14.

395. Del Bene, F., et al., *Regulation of neurogenesis by interkinetic nuclear migration through an apical-basal notch gradient.* Cell, 2008. **134**(6): p. 1055-65.

396. Corbin, J.G., et al., *Regulation of neural progenitor cell development in the nervous system.* J Neurochem, 2008. **106**(6): p. 2272-87.

397. Clay, M.R. and M.C. Halloran, *Regulation of cell adhesions and motility during initiation of neural crest migration.* Curr Opin Neurobiol, 2010.

398. Okano, H. and S. Temple, *Cell types to order: temporal specification of CNS stem cells.* Curr Opin Neurobiol, 2009. **19**(2): p. 112-9.

399. Noctor, S.C., V. Martinez-Cerdeno, and A.R. Kriegstein, *Neural stem and progenitor cells in cortical development.* Novartis Found Symp, 2007. **288**: p. 59-73; discussion 73-8, 96-8.

400. Brody, T. and W.F. Odenwald, *Cellular diversity in the developing nervous system: a temporal view from Drosophila.* Development, 2002. **129**(16): p. 3763-70.

401. Molyneaux, B.J., et al., *Neuronal subtype specification in the cerebral cortex.* Nat Rev Neurosci, 2007. **8**(6): p. 427-37.

402. Engberg, N., et al., *Retinoic acid synthesis promotes development of neural progenitors from mouse embryonic stem cells by suppressing endogenous, Wnt-dependent nodal signaling.* Stem Cells, 2010. **28**(9): p. 1498-509.

403. Siegenthaler, J.A., et al., *Retinoic acid from the meninges regulates cortical neuron generation.* Cell, 2009. **139**(3): p. 597-609.

404. Englund, C., et al., *Pax6, Tbr2, and Tbr1 are expressed sequentially by radial glia, intermediate progenitor cells, and postmitotic neurons in developing neocortex.* J Neurosci, 2005. **25**(1): p. 247-51.

405. Mira, H., et al., *Signaling through BMPR-IA regulates quiescence and long-term activity of neural stem cells in the adult hippocampus.* Cell Stem Cell, 2010. **7**(1): p. 78-89.

406. Di-Gregorio, A., et al., *BMP signalling inhibits premature neural differentiation in the mouse embryo.* Development, 2007. **134**(18): p. 3359-69.

407. Brederlau, A., et al., *The bone morphogenetic protein type Ib receptor is a major mediator of glial differentiation and cell survival in adult hippocampal progenitor cell culture.* Mol Biol Cell, 2004. **15**(8): p. 3863-75.

408. Fei, T., et al., *Genome-wide mapping of SMAD target genes reveals the role of BMP signaling in embryonic stem cell fate determination.* Genome Res, 2010. **20**(1): p. 36-44.

409. Takizawa, T., et al., *Enhanced gene activation by Notch and BMP signaling cross-talk.* Nucleic Acids Res, 2003. **31**(19): p. 5723-31.

410. Vinals, F., et al., *BMP-2 decreases Mash1 stability by increasing Id1 expression.* EMBO J, 2004. **23**(17): p. 3527-37.

411. Hollnagel, A., et al., *Id genes are direct targets of bone morphogenetic protein induction in embryonic stem cells.* J Biol Chem, 1999. **274**(28): p. 19838-45.

412. Imayoshi, I., et al., *Essential roles of Notch signaling in maintenance of neural stem cells in developing and adult brains.* J Neurosci, 2010. **30**(9): p. 3489-98.

413. Asano, H., et al., *Astrocyte differentiation of neural precursor cells is enhanced by retinoic acid through a change in epigenetic modification.* Stem Cells, 2009. **27**(11): p. 2744-52.

414. Androutsellis-Theotokis, A., et al., *Notch signalling regulates stem cell numbers in vitro and in vivo.* Nature, 2006. **442**(7104): p. 823-6.

415. He, F., et al., *A positive autoregulatory loop of Jak-STAT signaling controls the onset of astrogliogenesis.* Nat Neurosci, 2005. **8**(5): p. 616-25.

416. Fan, G., et al., *DNA methylation controls the timing of astrogliogenesis through regulation of JAK-STAT signaling.* Development, 2005. **132**(15): p. 3345-56.

417. Nottebohm, F., *The road we travelled: discovery, choreography, and significance of brain replaceable neurons.* Ann N Y Acad Sci, 2004. **1016**: p. 628-58.

418. Breunig, J.J., et al., *Everything that glitters isn't gold: a critical review of postnatal neural precursor analyses.* Cell Stem Cell, 2007. **1**(6): p. 612-27.

419. Song, H., C.F. Stevens, and F.H. Gage, *Astroglia induce neurogenesis from adult neural stem cells.* Nature, 2002. **417**(6884): p. 39-44.

420. Lie, D.C., et al., *Wnt signalling regulates adult hippocampal neurogenesis.* Nature, 2005. **437**(7063): p. 1370-5.

421. Filippov, V., et al., *Subpopulation of nestin-expressing progenitor cells in the adult murine hippocampus shows electrophysiological and morphological characteristics of astrocytes.* Mol Cell Neurosci, 2003. **23**(3): p. 373-82.

422. Fukuda, S., et al., *Two distinct subpopulations of nestin-positive cells in adult mouse dentate gyrus.* J Neurosci, 2003. **23**(28): p. 9357-66.

423. Seri, B., et al., *Cell types, lineage, and architecture of the germinal zone in the adult dentate gyrus.* J Comp Neurol, 2004. **478**(4): p. 359-78.

424. Cameron, H.A., P. Tanapat, and E. Gould, *Adrenal steroids and N-methyl-D-aspartate receptor activation regulate neurogenesis in the dentate gyrus of adult rats through a common pathway.* Neuroscience, 1998. **82**(2): p. 349-54.

425. Gould, E., H.A. Cameron, and B.S. McEwen, *Blockade of NMDA receptors increases cell death and birth in the developing rat dentate gyrus.* J Comp Neurol, 1994. **340**(4): p. 551-65.

426. Monje, M.L., H. Toda, and T.D. Palmer, *Inflammatory blockade restores adult hippocampal neurogenesis.* Science, 2003. **302**(5651): p. 1760-5.

427. Santarelli, L., et al., *Requirement of hippocampal neurogenesis for the behavioral effects of antidepressants.* Science, 2003. **301**(5634): p. 805-9.

428. Coskun, V., et al., *CD133+ neural stem cells in the ependyma of mammalian postnatal forebrain.* Proc Natl Acad Sci U S A, 2008. **105**(3): p. 1026-31.

429. Corti, S., et al., *Isolation and characterization of murine neural stem/progenitor cells based on Prominin-1 expression.* Exp Neurol, 2007. **205**(2): p. 547-62.

430. Dromard, C., et al., *Adult human spinal cord harbors neural precursor cells that generate neurons and glial cells in vitro.* J Neurosci Res, 2008. **86**(9): p. 1916-26.

431. Capela, A. and S. Temple, *LeX/ssea-1 is expressed by adult mouse CNS stem cells, identifying them as nonependymal.* Neuron, 2002. **35**(5): p. 865-75.

432. Yang, X.T., Y.Y. Bi, and D.F. Feng, *From the vascular microenvironment to neurogenesis.* Brain Res Bull, 2010.

433. Kokovay, E., et al., *Adult SVZ lineage cells home to and leave the vascular niche via differential responses to SDF1/CXCR4 signaling.* Cell Stem Cell, 2010. **7**(2): p. 163-73.

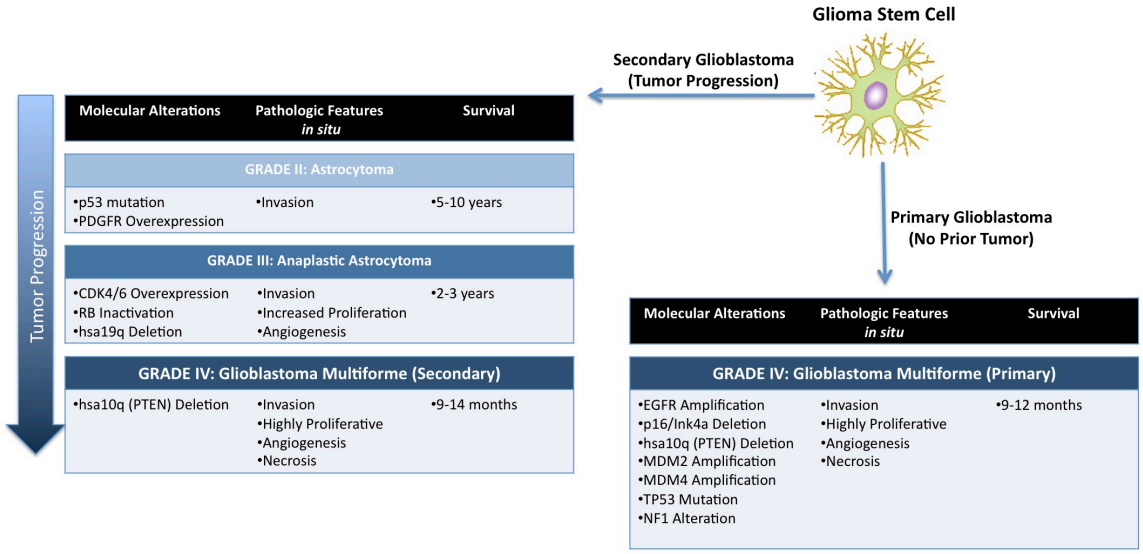

Figure 1. Human Glioblastoma may arise through either primary (*de novo*) or secondary (malignant transformation) pathways. Malignant transformation in secondary GBM formation is associated with the acquisition of more malignant phenotypes and progressive genomic alterations. Modified from Furnari et al. (434)

3) CONVERGENCE OF TUMOR BIOLOGY BETWEEN CANINE AND HUMAN GLIOMA STEM CELLS: SHARED GENOMIC CHANGES DRIVING GLIOMA PROGRESSION

Kevin Woolard[1], Rachael Thomas[2,3], Yuri Kotliarov[1], Matthew Breen[2,3], Mariam Totonchy[1], Maggie Cam[1], Myung jin Son[1], Jeongwu Lee[1], Maureen Beederman[1], Galina Belova[1], James Robinson[4], Amy Hutchinson[5], Wei Zhang[1], Howard A. Fine[1].

[1]Neuro-Oncology Branch, National Cancer Institute, National Institutes of Neurological Disorders and Stroke, Bethesda MD, 2College of Veterinary Medicine, North Carolina State University, Raleigh, NC 3Center for Comparative Medicine and Translational Research, North Carolina State University, Raleigh, NC 4The Broad Institute of MIT and Harvard, Cambridge, MA. 5Core Genotyping Facility, National Cancer Institute, Frederick, MD, National Institutes of Health, Bethesda MD

ABSTRACT

The domestic dog develops spontaneous glial tumors that recapitulate every histologic type and grade found in humans. Here, we characterize the extensive genomic and biological similarities shared by human glioma stem cell (GSC) lines and GSCs isolated from a canine anaplastic astrocytoma. Serial xenotransplantation of our canine GSCs results in a progressive increase in tumor malignancy, expansion of the GSC subpopulation, and progressive genomic alterations orthologous to those associated with human secondary glioblastoma, including deletions of *p16/ARF*, loss of *PTEN* and loss of p53 function. Finally, comparative analysis of the genomic landscape of the canine GSC-derived xenografts and human glioblastomas identifies putative tumor suppressor genes and oncogenes within these syntenic regions that are deleted/amplified across separate canine chromosomes. This convergence of biology in a naturally occurring model of a human tumor allows the interrogation of both genomes for the purpose of identifying new candidate oncogenes and tumor suppressor genes operative in gliomagenesis. The dramatic similarities in biology and genomic changes between two naturally and spontaneously occurring tumors across species suggests a limited number of preferred pathways toward tumorigenesis in nature in contrast to the numerous ways to induce tumors in experimental models.

Introduction

Despite aggressive multimodality treatment, the overall prognosis for patients with high-grade gliomas (anaplastic astrocytomas and glioblastoma multiforme (GBM)) remains very poor. A greater understanding of the biological basis of these tumors offers the best hope for improved therapeutic strategies. The cancer stem cell hypothesis attributes tumorigenicity to a specific sub-population of cells within the tumor (299, 435). In many cases, these cancer stem cells share certain functional properties with normal tissue-restricted and embryonic stem cells (15, 262, 436). Others and we have demonstrated the existence of a subpopulation of tumor-derived glioma cells that self-renew, have the potential for both glial and neuronal differentiation and possess significantly increased tumorigenic potential in immunocompromised orthotopic xenograft mouse models (4, 156, 367). Many key questions persist, however, regarding the relatedness of these "glioma stem cells" (GSCs) to normal neural stem cells and their exact role in GBM progression in patients. A spontaneous non-human glioma model that accurately recapitulates the disease would significantly enhance our ability to find answers to these questions. Although genetically engineered mouse (GEM) models of gliomas are valuable tools in studying gliomagenesis, such models are nonetheless limited to evaluating the effects of one or several genes in gliomagenesis and do not address the profoundly altered genomic landscape and genetic instability found within high-grade human glial neoplasms (5).

The domestic dog represents a unique and potentially powerful opportunity for the study of spontaneously occurring intracranial tumors, particularly glioma. It has long been recognized that canine glial tumors are remarkably similar in growth and histologic appearance to their human counterpart (6, 38). Canine gliomas range from grade I pilocytic to grade IV GBMs, faithfully reproducing the salient histopathologic and clinical features of each grade of human gliomas. Additionally, the incidence of intracranial tumors in both humans and dogs is remarkably similar and has recently been associated with the presence of glioma stem cells (437). Furthermore, brachycephalic breeds of dogs exhibit a significantly higher incidence of gliomas, providing an excellent opportunity for studying polymorphic gene variation controlling disease susceptibility (6). In these respects, the dog represents the only non-human species that is currently suitable for comparative study of naturally occurring gliomagenesis.

Here, we report the isolation and characterization of GSCs from a canine anaplastic astrocytoma and demonstrate their remarkable similarities to human glioma GSCs. These canine GSCs exhibit shared markers of neural stem cells, are capable of differentiating along both glial and neuronal cell lineages, and form invasive serial xenografts when orthotopically transplanted into immunocompromised mice. These xenografts progress in malignancy over serial xenotransplantation and this transformation is associated with stepwise genomic aberrations of key oncogenes and tumor suppressor genes implicated in the progression of low-grade human astrocytomas to secondary GBMs. Most notably, canine glioma GSCs with an initial genomic deletion of *p16/ARF* further develop deletion of *PTEN* and deregulation of the p53 pathway through genomic amplification and

overexpression of MDM2 and MDM4, events functionally equivalent to those seen in the progression of low grade human gliomas to secondary GBMs. This study documents, for the first time, the key role of specific, serial genetic aberrations across two species in naturally occurring analogous tumor types and is the first study to demonstrate that these genetic aberrations occur within the GSC population during the progression of glial tumors.

Materials and Methods

GSC and NSC Cultures

Following identification of a spontaneously occurring intracranial mass by MRI, the owner of a 9 year-old female Labrador Retriever elected humane euthanasia. Immediately after death, the brain was removed and the tumor sectioned. Additional samples were microdissected from the olfactory bulb, dentate gyrus of the hippocampus, and contralateral subventricular zone. All samples were briefly enzymatically dissociated into single cells. Red blood cells and cellular debris were removed by ACK lysis buffer and differential centrifugation. Cells from either GSC or NSC samples were each placed into culture in NBE medium comprised of Neurobasal-A medium (Invitrogen), N2 and B27 supplements (0.5x concentration, each; Invitrogen), heparin (2ug/mL, Sigma), and recombinant human bFGF and EGF (25ng/mL each; R&D systems). Differentiation was induced by either growth factor withdrawal or by culturing cells in DMEM medium (Invitrogen) containing 10% fetal bovine serum (Invitrogen). Cells were cultured as

neurospheres in uncoated tissue culture flasks or as adherent cells on plates pre-coated with a poly-ornithine/poly-D-lysine mixture.

Intracranial Tumor Cell Injection into SCID Mice

Canine GSCs were orthotopically implanted as previously described(367). Cells were enzymatically dissociated and resuspended in 40-80ul of HBSS containing EDTA (Invitrogen). Cells were then injected stereotactically into the striatum of anesthetized adult mice using a stereotactic frame (coordinates: 2 mm anterior, 2 mm lateral, 2.5 mm depth from bregma). There was no injection-procedure-related animal mortality. Animals were sacrificed at given time points for the analysis of tumor histology and immunohistochemistry or for culture of cells from the xenograft tumor. Brains were perfused with 4% paraformaldehyde by cardiac perfusion and further fixed at 4 ℃ overnight.

FACS Analysis

Patient GBM -and xenograft-derived tumor cells as well as *in vitro* cultured cells were dissociated into single-cell suspensions and labeled with the following antibodies; anti-CD133 (Santa Cruz sc-30220), CD-15-FITC (MMA clone, BD), Sox2 (R&D systems: MAB2018), GFAP (Invitrogen), Tuj1 (Covance) antibody as previously described. Staining for CD133 was performed by labeling one million cells with 2ug of antibody at 4ºC for 10 minutes. Concentrations of other antibodies and the staining conditions were followed per the manufacturers recommendation. Non-conjugated primary antibodies

were subsequently labeled with PE- or FITC-conjugated secondary antibodies (BD). Antibodies against mouse immunoglobulin conjugated to PE or FITC were used as antibody isotype controls (BD). The stained cells were analyzed on the FACS Vantage SE flow cytometer (BD).

Soft Agar Colony Forming Assay

Soft agar colony forming assays were performed as previously described(323). Briefly, low melting point agar (Difco) was melted and mixed with NBE media to a final concentration of 0.8% (bottom layer) and 0.4% (top layer).

Limiting Dilution Assay

In vitro NBE-cultured cells and xenograft-derived tumor cells were dissociated into single-cell suspensions and then plated into 96 well plates with various seeding densities (1 to 50 cells per well). Cells were incubated at 37 ℃ for two to three weeks. At the time of quantification, each well was examined for the formation of spheres.

Antibodies for Western Blot Analysis and Immunohistochemistry

The following antibodies were used as primary antibodies: CD133 (Santa Cruz), Nestin (IBL America and Covance), Sox2 (R&D Systems and Santa Cruz Biotechnology; sc-20088), Bmi1 (Upstate), Ezh2 (Pharmingen), Olig2 (Santa Cruz Biotechnology; sc-48817), a-tubulin (Sigma), CD-15-FITC (BD), GFAP (Dako), Tuj1 (Covance), p16

(Pharmingen), Pten (Cell Signaling), Akt (Cell Signaling), MDM2 (Santa Cruz Biotechnology), MDM4 (Santa Cruz Biotechnology).

Comparative Genomic Hybridization

Genomic DNA was extracted from canine GSC samples according to manufacturer's protocol (Qiagen) and processed at the Core Genotyping Laboratory at NCI. Copy number analysis was performed with the CanineHD Whole-Genome BeadChip, a SNP-based microarray for whole-genome genotyping and CNV analysis with more than 170,000 markers on the CanFam2.0 reference sequence (Illumina, Inc.). Data were analyzed using CNV partition v.2.4, based on log R ratio and B-allele frequency (Illumina GenomeStudio software). Due to various noise levels in different samples the segmented data were post-processed in MATLAB (R2010a) to apply sample-specific threshold to averaged log R ratio of each segment. Segmented data were imported into the Integrative Genomics Viewer (Broad Institute, http://www.broadinstitute.org/igv/) and aligned using a syntenic map of CanFam2.0 to the human genome (hg18).

Polymerase Chain Reaction and Sequencing

p53 exons 5, 6, 7, and 8 (DNA binding domain) were amplified from intron-based PCR primer pairs as previously reported (438). PCR products were ligated into TOPO PCR cloning vector (Invitrogen) and sequenced using a T7 primer.

Statistical Analysis

All values are shown as mean ± standard deviation (SD). Kaplan-Meier survival analysis was performed in Prism 4.0 software.

Results

Canine glioma GSC efficiently form serially transplantable tumors

GSCs are broadly defined functionally as a population of cells that form spheres, are clonogenic *in vitro*, and have the ability to form serially transplantable xenograft tumors *in vivo* that recapitulate the genetic, pathologic and clinical features of the original tumor (439). To determine if canine GSCs may be cultured from primary tumors, we dissociated tissue from a spontaneous grade III canine anaplastic astrocytoma (Figure 1) and plated cells in serum free Neurobasal medium supplemented with N2 and B27 supplements in the presence of basic FGF and EGF (NBE medium) as we have previously reported for the characterization of human GSCs (367). Canine GSCs grow in an analogous fashion to their human counterparts, forming non-adherent spheres in NBE conditions. We next sought to determine the ability of these neurosphere-forming canine glioma cells to serially produce tumors in an orthotopic immunocompromised mouse model, consistent with our prior characterizations of human GSCs (323, 367). We injected a small number of canine glioma neurosphere-derived cells (5000 cells per mouse) into the periventricular cortex of five adult mice, resulting in the formation of

primary xenografts in all mice injected. To minimize any *in vitro* artifact associated with prolonged culture, xenograft tumor-derived cells from primary and secondary xenograft tumors were isolated and re-injected into identical SCID mice within 7 to 14 days of xenograft tumor harvest, forming secondary and ultimately tertiary xenograft tumors in 100% of mice injected, respectively. Interestingly, secondary and tertiary xenografts revealed a progression in features of malignancy within xenograft tumors, exhibiting both increased tumor burden within the ipsilateral and contralateral cortex as well as pronounced infiltration along white matter tracts in the mouse brain. There was also a corresponding increase in cellular pleomorphism, vascular proliferation, and necrosis (Figure 2A). Immunofluorescence of xenograft-containing brains using an antibody against canine-specific nucleolin confirms the extent of cell invasion and the pronounced increase in tumor burden between primary and tertiary xenografts (Figure 2B). This pronounced tumor cell infiltration along white matter in the secondary and tertiary canine GSC-derived xenograft tumors is similar to that seen with human GBM-derived GSC xenografts, and represents the major mechanism of tumor progression in naturally occurring human and canine gliomas, but is not seen in xenografts from standard established glioma cell lines (440). Coincident with the increase in malignancy of our serial xenografts was a decreased latency in tumor formation in the immunocompromised mice. While an identical number of primary, secondary, and tertiary cells were injected into identical stereotactic locations, tertiary tumors developed at a dramatically accelerated rate compared to either primary or secondary xenograft tumors (Figure 2C).

Similar to human gliomas, our canine parental and xenograft tumors ubiquitously expressed high levels of markers associated with neural stem cells (sox2, nestin, EGFR), exhibited scattered CD15 positive cells and were intensely immunoreactive for GFAP *in vivo* (Figure 2D). Attempts at immunolabeling CD133 in our tissue sections proved unsuccessful. No appreciable difference in sox2, nestin, or EGFR immunoreactivity was identified over serial xenograft tumors although there was an increase in the number of CD15 labeled cells. Additionally, PDGFR-a was expressed in the parental tumor and in both primary and secondary xenografts but was notably absent in tertiary xenografts. Immunoblots for PDGFR-a and the phosphorylated active PDGFR-a confirm this and suggest that the PDGFR is only actively signaling in cells derived from the primary xenograft tumors (Figure 2E). This pattern appears to correlate with the suspected role of PDGFR signaling early in the progression of lower grade human gliomas, giving way to more dominant signaling through other mitogenic and/or survival pathways such as the EGFR pathway in GBM (441, 442).

Establishment of canine glioma GSCs and evaluation of differentiation potential

Given their ability to form glioma xenografts, we sought next to more fully characterize the canine GSCs. Immediately upon the development of neurological signs, mice bearing intracerebral xenograft tumors were sacrificed and the tumor microdissected from the brain and expanded in NBE conditions. GSC samples isolated from primary xenografts are designated as "0123-A", secondary xenograft GSCs as "0123-B", and tertiary xenograft tumors as "0123-C" samples. Canine GSCs grew in an analogous fashion to

human GSCs, forming non-adherent spheres in NBE conditions and expressing neural stem cell markers sox2, olig2 and nestin. Upon removal of growth factors or exposure to fetal bovine serum however, cells rapidly lost their proliferative capacity and exhibited a dramatic decrease in the stem cell markers and a significant upregulation of the differentiation markers, TuJ-1 and GFAP (Figure 3). Additionally, neural stem cell markers were similarly or more highly expressed in the GSCs than in canine patient-matched dentate gyrus-derived normal NSCs. Interstingly, there was a progressive increase in proteins associated with stem cell renewal (bmi-1) and human glioma progression (olig2) in canine GSCs from serial transplanted xenografts, suggesting the presence of self-renewal signaling pathways in canine GSCs in a manner analogous to that seen in human GSCs and other tumor populations (352, 357, 443-447).

Characterization of GSCs across serial xenografts

As a widely accepted single marker for GSCs remains elusive, we combined the expression of two well-known GSC cell surface markers (CD133 and CD15) and functional assays to evaluate the relative number of GSCs per tumor across serial xenotransplantation. The cell surface markers CD133 and CD15 have been reported to enrich for cells exhibiting enhanced tumorigenic potential, and in the case of CD15, have biologic relevance to developmental neural stem cells (323, 431). Given that the expression of both surface markers may change dramatically over time *in vitro*, we analyzed all cells at an identical number of days *in vitro* (21 d.i.v.) following isolation from the xenograft. Whereas <2% of cells expressed CD133 in the primary xenograft

tumor, secondary and tertiary xenografts contained 9% and 7% CD133 positive cells, respectively. Even more striking was the finding that the percentage of CD15 positive cells progressively increased in the primary, secondary and tertiary tumor from 20%, to 32% to 58%, respectively (Figure 4A). Consistent with the expression of these surface markers, both the soft agar and serial dilution assays demonstrated a progressive increase in clonogenic potential over serial xenograft formation (Figures 4B and 4C). Finally, in a pattern identical to that seen in our human GSCs, canine GSCs expressing either CD133 or CD15 were significantly more clonogenic and had a higher expression of stem cell markers than those cells failing to express either marker, which were less clonogenic and preferentially expressed markers of neuronal and/or glial differentiation. (Figures 4D and 4E) (323). The demonstration that serial xenotransplantation of small numbers of primary canine glioma cells, cultured in stem cell conditions, enriches for a sub-population of cells with both stem cell surface markers and *in vitro* and *in vivo* functional properties of tumor-initiating cells, fulfills the most stringent definition of a tumor stem cell (i.e. GSCs.).

Progression of Canine Xenograft Tumor Malignancy is Reflected in Progressive Genomic DNA Copy Number Alterations Also Found in Human Glioblastoma.

We have demonstrated that GSCs derived from a canine anaplastic astrocytoma form serially transplantable xenograft tumors that recapitulate the heterogeneity, pleomorphism, transformability (to higher grade gliomas) and invasive growth of the parental tumor. A major question in the applicability and relevance of the dog as a model

for spontaneous human gliomagenesis however, lies in whether the genetics driving both the initiation and progression of this tumor is similar to that operative in human gliomas. To examine whether genetic alterations found in our canine glioma GSCs over serial xenograft formation are analogous to those found in human GBM, we performed array comparative genomic hybridization (aCGH) analysis of total genomic DNA isolated from the primary (0123-A), secondary (0123-B), and three different tertiary xenografts (0123-C-1, -2, and -3) against genomic DNA isolated from patient-matched normal brain parenchyma, using a canine SNP array.

Serial comparison of genomic DNA copy number alterations (CNAs) across our canine GSC samples revealed a progressive increase in both genomic amplifications and deletions (Figure 5A). Primary xenograft tumors, which demonstrated the least malignant phenotype, were associated with a small number of focal anomalies in the canine genome but did include key regions with known relevance to human gliomas. Chiefly, canine chromosome 11 (CFA 11) had a focal deletion containing the *CDKN2A/CDKN2B* locus. Loss of *p16*, along with the other tumor suppressors in the INK4a locus, is found in a majority of human high-grade gliomas (448, 449). Additionally, the regions of CFA 10 and 38 containing the genes *MDM2* and *MDM4*, respectively, are amplified, as is true in a subset (~10%) of high-grade human gliomas and consistent with previous reports of canine intracranial tumors (9, 450). We also found that the canine GSCs contained focal amplifications of CFA 10 within a region that contains the *CDK2* and *CDK4* genes, both of which are known to be amplified in up to 15% of human high grade gliomas (225).

Consistent with clonal evolution of a tumor stem cell subpopulation, nearly all CNAs present in the primary GSCs were maintained or expanded in the secondary and tertiary GSCs. As the xenograft tumors increase in malignancy over serial xenotransplantation however, we identified numerous additional or progressive CNAs associated with this malignant progression, in a manner analogous to human secondary glioblastoma development. Chiefly, we identified a deletion in CFA 26 that contains the tumor suppressor gene *PTEN*. *PTEN* is deleted in approximately 70% of GBMs and loss of PTEN function, with the subsequent activation of the downstream effector Akt, is believed to be a critical genomic signature in the progression of human glioma tumors (i.e. in secondary GBM formation) (451-453). The malignant progression of our serial xenograft tumors was also associated with progressive amplifications of CFA 38 (containing mdm4) in our tertiary GSCs, which when coupled with increased MDM2 and AKT signaling, further abrogates p53 function. Sequencing of genomic *p53* in both the parental tumor and GSC samples revealed wild-type sequence, suggesting that loss of p53 function in our canine GSCs may instead be mediated through deletion of ARF and progressive amplification of *MDM2* and *MDM4*. This finding is also analogous to human GBMs where loss of p53 function occurs in 30-70% of human GBMs either through *p53* mutations, *MDM2/4* amplification and/or *ARF* deletions (225, 454).

The domestic dog genome contains 38 autosomes and so the genomic material comprising the 22 human autosomes is dispersed over numerous shared regions across separate canine chromosomes. This physical distribution of shared genomic material

makes the dog an ideal comparative genomic model to investigate small regions of CNAs, as large, commonly amplified or deleted regions in human GBM samples are likely to be syntenic to multiple, individual canine chromosomes. The co-deletion or amplification of separate, individual canine chromosomes syntenic to common human glioma CNAs would suggest relevant tumor suppressor genes or oncogenes are present within those regions, and enable the definition of small, minimally altered foci relative to the comparatively large CNAs currently defined as common alterations in human GBMs.

In order to compare the CNAs of our canine GSCs directly to those regions commonly altered in human GBMs, we first developed an algorithm to map our canine CNAs to their appropriate syntenic human coordinates (Figure 5B). Common CNAs in human GBM tumor populations are defined by Genomic Identification of Significant Targets in Cancer (GISTIC) from the TCGA GBM database, as reported previously (130). In this comparison, we were able to identify seven CNA regions in our tertiary canine GSCs that share significant homology to common CNAs in human GBM. Most notably, focal alterations corresponding to human chromosome 7 (HSA 7q, 62.9-76.6Mb and 97.5-102.3Mb), HSA 9p (19.5-22.4Mb), HSA 10q (35.4-40.3Mb, 59.6-88.7Mb, and 89.2-90.9Mb), and HSA 12q (54.3-74.1Mb) are shared between our canine GSCs and human GBMs. In addition to these CNAs with known tumor suppressor or oncogenes, other commonly altered regions such as HSA 6q (116.6-170.1Mb) and HSA 13p (19.1Mb-24.3Mb and 25.6-40.2Mb) are also deleted in both populations, highlighting the genomic similarity in glioma formation and progression in both species.

Minimal Regions of Alteration are defined by Multiple, Separate Canine Chromosomes.

In order to more completely define minimal regions of alteration within large chromosomal amplifications or deletions often found in human glioblastoma, we identified regions of shared CNAs (between human GBMs and canine GSCs) and mapped these regions to the corresponding canine chromosomes (Figures 6-12, Tables 1-7). *PTEN* (located on HSA 10q.23.3) is usually deleted along with large segments of HSA 10q in human glioblastoma (10, 35). A long-standing question in glioma genetics is whether the target of HSA 10q deletion is *PTEN* alone or whether there are additional target genes that are co-deleted with *PTEN* that contribute to the tumorigenic phenotype. In the dog, *PTEN* is located at the telomeric end of CFA 26, which was deleted in the GSCs derived from the secondary and tertiary xenografts (Fig 5A and 5B, Fig 6, Table 1). Genes co-deleted in our canine GSCs alongside *PTEN* in CFA 26 included *Dkk1*, which functions to inhibit Wnt signaling and may function to inhibit differentiation potential or clonogenic growth potential (455). Additionally, cyclic guanosine monophosphate (cGMP)-dependent kinase (*PRKG1)* was also co-deleted with *PTEN* in the canine tertiary tumors and, alongside *PRKG2*, has been suggested to be potential tumor suppressor genes in colon carcinoma and glioma (456, 457). *PRKG1* also functions to inhibit angiogenesis through vasodilator-stimulated phosphoprotein (*VASP*). Thus, the deletion *PRKG1* in both canine and human GSCs may have a mechanistic role in the aberrant cell cycle control and angiogenic phenotype of malignant gliomas (458).

In addition to the deletions in CFA 26 containing *PTEN* (HSA 10q 89.2-90.9Mb), the canine tertiary xenograft tumors also exhibit an expanded deletion in CFA 4 that is syntenic to areas of HSA 10 that flank the *PTEN* loci and are often deleted in human GBMs (HSA 10q, 59.6-88.7 and 91-91.16Mb) (Figure 6, Table 1). Therefore, while the secondary and tertiary canine GSCs exhibit loss at CFA 26 corresponding to *PTEN*, progression of xenograft malignancy in our canine GSC population is associated with an additional, separate chromosomal deletion of CFA 4 that contains a syntenic region in immediate proximity to *PTEN* on the human genome. We examined genes present within this co-deleted segment of CFA 4 corresponding to HSA 10 and identified several genes within this region that have suspected roles in gliomagenesis. *ANXA7* (located on HSA 10q21.1-q21.2), which is frequently deleted in human GBMs, has been previously suggested as a tumor suppressor gene independent of its human chromosomal proximity to *PTEN*. It has been hypothesized that loss of *ANXA7* stabilizes and thus augments *EGFR* signaling and is negatively associated with patient survival (131). The loss of *ANXA7* secondary to deletion of CFA 4, and separate from that containing *PTEN* (CFA 26), in canine gliomas supports an independent and important role for both genes as potential tumor suppressors in GBMs and demonstrates the power of the dog as a predictive model for interrogating the glioma genome.

Additional genes co-deleted within CFA 4 and corresponding to the syntenic regions of HSA 10q involve other tumor suppressor gene candidates including *BMPR1A*, and *CCAR1*. We, and others have shown that disruptions in BMP signaling may impact the

tumorigenic potential and capacity for differentiation in GSCs, and *BMPR1A* deletions are known to predispose individuals to colon cancer formation (366, 459, 460). *CCAR1*, or cell cycle and apoptosis regulator 1 (also referred to as cell cycle and apoptosis regulatory protein 1 or CARP-1) is located on HSA 10q21-q22 and has been reported to suppress the clonogenic growth, tumorigenicity, and invasion of human breast cancer cells and is integral to the induction of apoptosis following EGFR inhibition (461, 462). Loss of *CCAR1* may explain in part the failure of some patients to respond to EGFR inhibition therapeutically or enable tumor cells to survive in conditions of low growth factor concentration.

We performed similar analyses on the other commonly altered genomic foci shared between our canine GSCs and human GBMs. The canine GSC genomic deletion containing *CDK2NA* is evolutionarily related to a very small region of HSA 9p21-p22, highlighting the importance of *CDKN2A* in glioma biology and diminishing the potential importance of a large number of other genes ("passenger genes") that are co-deleted in the large CNAs found in HSA 9 (Figure 7, Supplemental Table 2). Indeed, the canine chromosomal regions flanking the small locus containing *CDKN2A* are amplified, suggesting a specific role of *CDKN2A* deletion in glioma biology while potentially excluding a number of linked co-deleted genes in HSA 9. Within that minimally deleted region containing the p16/Ink4a locus in our canine GSCs are several interferon genes (*IFNB1, IFNA5, IFNA13*, and *IFNA7*) that are also deleted. This may be of interest for the *IFNAR1* gene was recently identified by Cerami et al. as a linker gene in the PIK3R1

module through an automated network analysis (Human Interaction Network). This module, linking several IFNA genes and *IFNB1* to *IFNAR1*, was found altered in 25% of GBMs in the TCGA database, but as the authors express, was of unknown significance due to the close proximity of IFN genes to *CDKN2A* (463). The co-deletion of *CDKN2A* and the *IFNAR1* gene in both canine and human gliomas strengthens the argument that *IFNAR1* is a potentially significant gene in the biology of GBMs.

An additional chromosomal amplification associated with the more malignant xenograft gliomas is seen in CFA 6, which shares evolutionarily conserved synteny with HSA 7. This is of particular interest since trisomy HSA 7 is a common finding in GBMs (Figures 5, 8, Table 3). This region contains the gene, Glioblastoma Amplified Sequence (*GBAS*), which is amplified in up to 40% of human GBMs (464). Other commonly altered foci in human GBMs show striking conservation in our canine GSCs including those surrounding amplification of *MDM4* (Figure 9, Table 4), *MDM2* (Figure 10, Table 5), and in the genomic regions commonly deleted in HSA 6 (Figure 11, Table 6) and 13 (Figure 12, Table 7). A number of these CNAs that are conserved across both species contain well-known potential tumor suppressor or oncogenes. One such example is Gli1, a transcription factor involved in the transduction of sonic hedgehog signaling and that may have a role in the promotion of tumor cell invasion. The *Gli1* gene (HSA 12q13.2-13.3) is amplified both in a subset of human GBMs as well as in our canine glioma (CFA 10) (465). By contrast, it is of interest that amplification of the epidermal growth factor receptor (*EGFR*) seen in primary human GBMs was not seen in our canine tertiary

tumors, consistent with its lack of amplification in secondary human GBMs (35). Thus, these foci of shared genomic alterations allow us to identify a series of genomic events responsible for driving both human and canine gliomagenesis with more certainty than would be possible through the genomic study of gliomas from only one species

Progressive Genomic Alterations are Critical for Increased Self Renewal and Cell Survival in Tertiary Canine GSCs.

We next examined whether the copy number changes of select genes within specific canine glioma CNAs are associated with alterations in protein expression. The results indicate that aCGH accurately predicted the lack of p16/CDKN2A protein expression and the progressive loss of PTEN function (and resulting increased AKT activity) in our canine GSCs over serial xenograft formation (Figure 13). Furthermore, similar to that seen in human gliomas, the lack of p16 expression results in inhibition of Rb-1, possibly compounded by increased AKT activity over serial xenotransplantation. We also found diminished p53 expression and function, as reflected by decreasing p21 levels, in our tertiary 0123-C canine GSCs consistent with the aCGH analysis showing genomic amplification of the MDM2 and MDM4 genes (Figure 13B).

To investigate the significance of these alterations *in vitro*, we examined the response of primary canine GSCs (0123-A, PTEN intact) and tertiary canine GSCs (0123-C, PTEN null) to growth factor withdrawal (N2B27). Removal of growth factors rapidly induces apoptosis and cell senescence in primary 0123-A GSCs, while tertiary 0123-C GSCs

maintain a viable phenotype. By contrast, concurrent growth factor withdrawal and inhibition of PI3K activity through the addition of wortmannin mitigates the resistance to apoptosis in tertiary 0123-C cells and both cell types acquire a similar phenotype (Figure 13C, E). Cell cycle analysis and TUNEL labeling of 0123-A and 0123-C cells confirms the selective increase in cell cycle arrest and apoptosis in 0123-C cells when AKT signaling is inhibited (Figure 13D). This suggests the relative resistance to apoptosis and increased cell survival in our canine tertiary GSCs compared to the primary GSCs is in large part mediated through activation of the PI3K pathway secondary to PTEN deletion in the tertiary GSCs. This is consistent with evidence in human GBM suggesting PTEN deletion is a key, gate-keeping genomic alteration in the progression of low grade to high-grade gliomas.

Discussion

As the only species to spontaneously develop gliomas with a phenotype identical to humans, the domestic dog represents an attractive comparative model for the study of glioma biology. Despite their striking pathological and clinical resemblance to human gliomas, however, little is known about the biology of canine gliomas, the characterization of canine glioma stem cells, or their genetics. In this study we have documented the *in vitro* characterization of canine glioma-derived GSCs and performed a detailed phenotypic and genomic analysis of the tumors they form *in vivo*.

The importance of GSCs in the pathogenesis of human gliomas remains controversial. Consistent with a prior study reporting the presence of a CD133 population of GSC-like cells in a canine GBM, we have isolated GSCs from a canine anaplastic astrocytoma (437). We were able to demonstrate that these cells are highly proliferative, capable of self-renewal, and effectively form serially transplantable xenograft tumors in immunodeficient animals. Like human GSCs, these canine GSCs express NSC markers and are capable of differentiation along both neuronal and glial pathways. We were also able to demonstrate that sorting for CD133 and CD15-positive cells enriched for a subpopulation of canine glioma cells with NSC-like properties and enhanced clonogenic and tumorigenic potential, as others and we have demonstrated for human GSCs (4, 156, 367). The fact that a very similar subpopulation of cells with NSC-like features that drives the tumorigenic process in xenotransplantation studies can be isolated from tumors in two species of animals that develop naturally occurring gliomas, supports the argument that these GSCs may be intrinsically important to the pathogenesis of the disease.

In addition to demonstrating the presence of GSCs within canine gliomas and their similarity to human GSCs, we have shown that canine GSCs recapitulate the human disease in two other important ways: the ability to form tumors that "transform" to higher-grade malignancies and to form tumors with similar genomic alterations to human gliomas. Approximately 70% of low-grade human gliomas will ultimately transform to higher-grade tumors during the lifetime of the patient. These higher-grade tumors have been termed "secondary GBMs" to differentiate them from primary GBMs, which are not

known to have progressed from an early low-grade precursor stage. It has been demonstrated that the secondary GBMs acquire additional genetic aberrations compared to the parental low-grade tumor (and different from primary GBMs) and thus presumably reflect clonal evolution (466). It is difficult to confirm this hypothesis or study glioma transformation in the laboratory, however, for there are few (if any) animal models that spontaneously recapitulate this biology. We have now shown that serial transplantation of our canine GSCs from *in vivo* propagated tumors spontaneously results in progressively higher grade and more malignant tumors much in the same way that successive human glioma recurrences in the clinical setting are more likely to result in more aggressive and higher grade tumors than the parental tumor. Furthermore, the serially transplanted tumors harbor increasingly larger number of GSCs with greater proliferative and clonogenic properties *in vitro*. The enrichment of GSCs during serial xenotransplantation resulting in the formation of tumors with a shorter latency period and in tumors with greater malignancy suggests a relationship between the percentage of GSCs per tumor and the degree of tumor malignancy. The fact that these observations were made following minimal *in vitro* manipulation or tissue culture of dissociated tumor xenograft-derived cells, and without pre-selection of any putative GSC subpopulations, implies that the relationship between the percentage of GSC per tumor, tumor latency and degree of malignancy is an inherent feature of GSCs in glioma biology.

Genomic analysis of several hundred human GBMs from the recently published Cancer Genome Atlas (TCGA) database have demonstrated inactivation or deregulation of the

p53, Rb and PI3K canonical pathways regardless of the specific genetic aberrations within any given tumor. It is therefore of great interest to find that the canine glioma follows a similar natural history. While our primary canine GSCs exhibit Rb inactivation through p16 deletion and diminished p53 activity through MDM2 genomic amplification, full transformation of the xenograft requires the progressive amplification of MDM4 and the loss of PTEN. This is identical to the situation seen in human secondary GBMs where transformation of a lower grade glioma with p53 mutations and RB inactivation is accompanied by deregulation of the PI3K pathway, usually by PTEN deletion. Therefore, our canine GSCs reiterate the vital role of the Rb, p53 and PI3K pathways in the pathogenesis of naturally occurring malignant gliomas and for the first time demonstrate that glioma clonal evolution can be carried within the GSC compartment.

Some of the minor CNAs within the primary canine GSCs are not found in the tertiary GSCs. It is therefore reasonable to assume that the initial tumor contained a heterogeneous population of GSCs, and that the genotype that ultimately came to dominate following serial passage of the tumor *in vivo* represents the selection of GSCs with progressive genomic (and probably epigenetic) changes that endowed them with greater tumorigenic potential. Although it is plausible that the GSC clonal selection occurred during the *in vitro* propagation of the GSCs prior to intracerebral implantation, we attempted to minimize this possibility by genotyping each population of GSC just prior to intracerebral implantation and by limiting the amount of time the GSCs were in

culture to just a few days. We therefore believe that the successive genomic changes and selection for a GSC population containing the salient mutations that lead to transformation to a higher-grade tumor, was driven within the biologically relevant microenvironment of the central nervous system and not as an artifact of prolonged *in vitro* culture.

Thus, this is one of the first demonstrations that *in vivo* transformation of a naturally occurring glioma likely occurs through clonal evolution and selection within the GSC subpopulation. If true, these observations have significant clinical implications for it suggests that targeting of late genetic alterations (i.e. the PI3K pathway through inhibitors of AKT, mTOR) would still leave intact a population of earlier stage proliferating GSCs prone to subsequent malignant transformation. Our *in vitro* data demonstrating the sensitivity of our tertiary GSCs, compared to our primary GSCs, to PI3K inhibition following the stress of growth factor withdrawal clearly demonstrates this concept. These observations, therefore, theoretically argue for targeting signaling pathways important in the earlier pathogenesis of the disease, but one must be cautious of the possibility that advanced clonal evolution may inherently produce GSC populations no longer dependent on those early genetic/epigenetic signaling aberrations. This indeed represents the complexity of treating a naturally evolving system like human cancer, and demonstrates the potential power of this canine glioma model to study such a complex system

The utility of the dog as a model for human gliomagenesis will depend in many ways on the extent of the similarity between the canine and human tumors at a genetic and chromosomal level. To that end, we have found significant similarity between the genotypes of our canine GSCs and human GBMs, with conservation of commonly reported CNAs corresponding to HSA 1q, 6q, q, 9p, 10q, 12q, and 13p over malignant progression in our canine GSCs. Our data demonstrate that canine gliomas offer a valuable naturally occurring experimental model in comparative glioma genomics. It appears clear from human glioma data, mouse modeling data, and now our canine data that deregulation of the p53, RB and PI3K pathways are common pathways to formation of malignant gliomas (10, 301). Nevertheless the frequent occurrence of other nonrandom CNAs, the finding that high-grade gliomas can be sub-classified into distinct subgroups based on gene expression profiles, and the heterogeneous nature of the clinical disease all suggest that there are other genetic and epigenetic changes within gliomas that can significantly alter their biological and clinical behavior. A proportion of these genetic mutations have been known for some time (i.e. EGFR) and several new ones have been identified through various recent high-throughput sequencing initiatives (i.e. NF1, IDH1/2, PIK3CA) (10, 463, 467). Nevertheless, the occurrence of frequent nonrandom CNAs among different glioma specimens suggest the presence of other target genes of importance. Unfortunately, these CNAs are often large making the search for the relevant target gene(s) within these areas difficult. Our CGH data identify numerous, focal CNAs found within human gliomas that may contain unknown but relevant oncogenes or tumor suppressor genes. We believe that with future, higher density

platforms specific to the canine genome, canine glioma and glioma GSCs may help identify new genetic mutations important for gliomagenesis.

In summary, we have presented the first detailed genomic characterization of canine glioma GSCs, and have validated their use as a comparative model for studying various aspects of human glioma biology. Additionally, we have shown that serial xenograft transplantation of a canine glioma mimics the malignant progression seen clinically in human patients and follows similar genomic deletions and amplifications identified as crucial driving forces within malignant transformation. This significant convergence of tumor biology suggests that despite the numerous genetic alterations that can generate malignant gliomas in experimental animal model systems, nature prefers a limited number of pathways for spontaneously occurring gliomas. Through further detailed genomic and functional interrogation, canine gliomas may help unravel the meaning of the genomic landscape of their human counterparts.

References

1. Jordan, C.T., M.L. Guzman, and M. Noble, *Cancer stem cells.* N Engl J Med, 2006. **355**(12): p. 1253-61.

2. Chen, R., et al., *A hierarchy of self-renewing tumor-initiating cell types in glioblastoma.* Cancer Cell, 2010. **17**(4): p. 362-75.

3. Reya, T., et al., *Stem cells, cancer, and cancer stem cells.* Nature, 2001. **414**(6859): p. 105-11.

4. Sanai, N., A. Alvarez-Buylla, and M.S. Berger, *Neural stem cells and the origin of gliomas.* N Engl J Med, 2005. **353**(8): p. 811-22.

5. Xie, Z. and L.S. Chin, *Molecular and cell biology of brain tumor stem cells: lessons from neural progenitor/stem cells.* Neurosurg Focus, 2008. **24**(3-4): p. E25.

6. Singh, S.K., et al., *Identification of human brain tumour initiating cells.* Nature, 2004. **432**(7015): p. 396-401.

7. Bao, S., et al., *Glioma stem cells promote radioresistance by preferential activation of the DNA damage response.* Nature, 2006. **444**(7120): p. 756-60.

8. Lee, J., et al., *Tumor stem cells derived from glioblastomas cultured in bFGF and EGF more closely mirror the phenotype and genotype of primary tumors than do serum-cultured cell lines.* Cancer Cell, 2006. **9**(5): p. 391-403.

9. Frese, K.K. and D.A. Tuveson, *Maximizing mouse cancer models.* Nat Rev Cancer, 2007. **7**(9): p. 645-58.

10. Fankhauser, R., H. Luginbuhl, and J.T. McGrath, *Tumours of the nervous system.* Bull World Health Organ, 1974. **50**(1-2): p. 53-69.

11. Stoica, G., et al., *Morphology, immunohistochemistry, and genetic alterations in dog astrocytomas.* Vet Pathol, 2004. **41**(1): p. 10-9.

12. Stoica, G., et al., *Identification of cancer stem cells in dog glioblastoma.* Vet Pathol, 2009.

13. Son, M.J., et al., *SSEA-1 is an enrichment marker for tumor-initiating cells in human glioblastoma.* Cell Stem Cell, 2009. **4**(5): p. 440-52.

14. Chu, L.L., et al., *Genomic organization of the canine p53 gene and its mutational status in canine mammary neoplasia.* Breast Cancer Res Treat, 1998. **50**(1): p. 11-25.

15. Piccirillo, S.G., et al., *Brain cancer stem cells.* J Mol Med, 2009. **87**(11): p. 1087-95.

16. Tate, M.C. and M.K. Aghi, *Biology of angiogenesis and invasion in glioma.* Neurotherapeutics, 2009. **6**(3): p. 447-57.

17. Tchougounova, E., et al., *Loss of Arf causes tumor progression of PDGFB-induced oligodendroglioma.* Oncogene, 2007. **26**(43): p. 6289-96.

18. Martinho, O., et al., *Expression, mutation and copy number analysis of platelet-derived growth factor receptor A (PDGFRA) and its ligand PDGFA in gliomas.* Br J Cancer, 2009. **101**(6): p. 973-82.

19. Fan, X., et al., *NOTCH pathway blockade depletes CD133-positive glioblastoma cells and inhibits growth of tumor neurospheres and xenografts.* Stem Cells. **28**(1): p. 5-16.

20. Chiba, T., et al., *Bmi1 promotes hepatic stem cell expansion and tumorigenicity in both Ink4a/Arf-dependent and -independent manners in Mice.* Hepatology.

21. Facchino, S., et al., *BMI1 confers radioresistance to normal and cancerous neural stem cells through recruitment of the DNA damage response machinery.* J Neurosci. **30**(30): p. 10096-111.

22. Bruggeman, S.W., et al., *Bmi1 controls tumor development in an Ink4a/Arf-independent manner in a mouse model for glioma.* Cancer Cell, 2007. **12**(4): p. 328-41.

23. Ligon, K.L., et al., *Olig2-regulated lineage-restricted pathway controls replication competence in neural stem cells and malignant glioma.* Neuron, 2007. **53**(4): p. 503-17.

24. Abdouh, M., et al., *BMI1 sustains human glioblastoma multiforme stem cell renewal.* J Neurosci, 2009. **29**(28): p. 8884-96.

25. Hoenerhoff, M.J., et al., *BMI1 cooperates with H-RAS to induce an aggressive breast cancer phenotype with brain metastases.* Oncogene, 2009. **28**(34): p. 3022-32.

26. Capela, A. and S. Temple, *LeX/ssea-1 is expressed by adult mouse CNS stem cells, identifying them as nonependymal.* Neuron, 2002. **35**(5): p. 865-75.

27. Jen, J., et al., *Deletion of p16 and p15 genes in brain tumors.* Cancer Res, 1994. **54**(24): p. 6353-8.

28. Sherr, C.J. and F. McCormick, *The RB and p53 pathways in cancer.* Cancer Cell, 2002. **2**(2): p. 103-12.

29. Rao, S.K., et al., *A survey of glioblastoma genomic amplifications and deletions.* J Neurooncol. **96**(2): p. 169-79.

30. Thomas, R., et al., *'Putting our heads together': insights into genomic conservation between human and canine intracranial tumors.* J Neurooncol, 2009. **94**(3): p. 333-49.

31. Reifenberger, G., et al., *Amplification of multiple genes from chromosomal region 12q13-14 in human malignant gliomas: preliminary mapping of the amplicons*

shows preferential involvement of CDK4, SAS, and MDM2. Cancer Res, 1994. **54**(16): p. 4299-303.

32. Ali, I.U., L.M. Schriml, and M. Dean, *Mutational spectra of PTEN/MMAC1 gene: a tumor suppressor with lipid phosphatase activity.* J Natl Cancer Inst, 1999. **91**(22): p. 1922-32.

33. Kwon, C.H., et al., *Pten haploinsufficiency accelerates formation of high-grade astrocytomas.* Cancer Res, 2008. **68**(9): p. 3286-94.

34. Salmena, L., A. Carracedo, and P.P. Pandolfi, *Tenets of PTEN tumor suppression.* Cell, 2008. **133**(3): p. 403-14.

35. Parsons, D.W., et al., *An integrated genomic analysis of human glioblastoma multiforme.* Science, 2008. **321**(5897): p. 1807-12.

36. Beroukhim, R., et al., *Assessing the significance of chromosomal aberrations in cancer: methodology and application to glioma.* Proc Natl Acad Sci U S A, 2007. **104**(50): p. 20007-12.

37. TCGA, *Comprehensive genomic characterization defines human glioblastoma genes and core pathways.* Nature, 2008. **455**(7216): p. 1061-8.

38. Ohgaki, H., et al., *Genetic pathways to glioblastoma: a population-based study.* Cancer Res, 2004. **64**(19): p. 6892-9.

39. Zheng, H., et al., *PLAGL2 regulates Wnt signaling to impede differentiation in neural stem cells and gliomas.* Cancer Cell. **17**(5): p. 497-509.

40. Hou, Y., et al., *An anti-tumor role for cGMP-dependent protein kinase.* Cancer Lett, 2006. **240**(1): p. 60-8.

41. Swartling, F.J., et al., *Cyclic GMP-dependent protein kinase II inhibits cell proliferation, Sox9 expression and Akt phosphorylation in human glioma cell lines.* Oncogene, 2009. **28**(35): p. 3121-31.

42. Chen, L., et al., *Vasodilator-stimulated phosphoprotein regulates proliferation and growth inhibition by nitric oxide in vascular smooth muscle cells.* Arterioscler Thromb Vasc Biol, 2004. **24**(8): p. 1403-8.

43. Yadav, A.K., et al., *Monosomy of chromosome 10 associated with dysregulation of epidermal growth factor signaling in glioblastomas.* JAMA, 2009. **302**(3): p. 276-89.

44. Kodach, L.L., et al., *The bone morphogenetic protein pathway is active in human colon adenomas and inactivated in colorectal cancer.* Cancer, 2008. **112**(2): p. 300-6.

45. Lee, J., et al., *Epigenetic-mediated dysfunction of the bone morphogenetic protein pathway inhibits differentiation of glioblastoma-initiating cells.* Cancer Cell, 2008. **13**(1): p. 69-80.

46. Piccirillo, S.G., et al., *Bone morphogenetic proteins inhibit the tumorigenic potential of human brain tumour-initiating cells.* Nature, 2006. **444**(7120): p. 761-5.

47. Downey, C., et al., *Pressure stimulates breast cancer cell adhesion independently of cell cycle and apoptosis regulatory protein (CARP)-1 regulation of focal adhesion kinase.* Am J Surg, 2006. **192**(5): p. 631-5.

48. Rishi, A.K., et al., *Cell cycle- and apoptosis-regulatory protein-1 is involved in apoptosis signaling by epidermal growth factor receptor.* J Biol Chem, 2006. **281**(19): p. 13188-98.

49. Cerami, E., et al., *Automated network analysis identifies core pathways in glioblastoma.* PLoS One, 2010. **5**(2): p. e8918.

50. Wang, X.Y., et al., *GBAS, a novel gene encoding a protein with tyrosine phosphorylation sites and a transmembrane domain, is co-amplified with EGFR.* Genomics, 1998. **49**(3): p. 448-51.

51. Lo, H.W., et al., *A novel splice variant of GLI1 that promotes glioblastoma cell migration and invasion.* Cancer Res, 2009. **69**(17): p. 6790-8.

52. Sidransky, D., et al., *Clonal expansion of p53 mutant cells is associated with brain tumour progression.* Nature, 1992. **355**(6363): p. 846-7.

53. Bleau, A.M., et al., *PTEN/PI3K/Akt pathway regulates the side population phenotype and ABCG2 activity in glioma tumor stem-like cells.* Cell Stem Cell, 2009. **4**(3): p. 226-35.

54. Noushmehr, H., et al., *Identification of a CpG island methylator phenotype that defines a distinct subgroup of glioma.* Cancer Cell. **17**(5): p. 510-22.

Figure 1

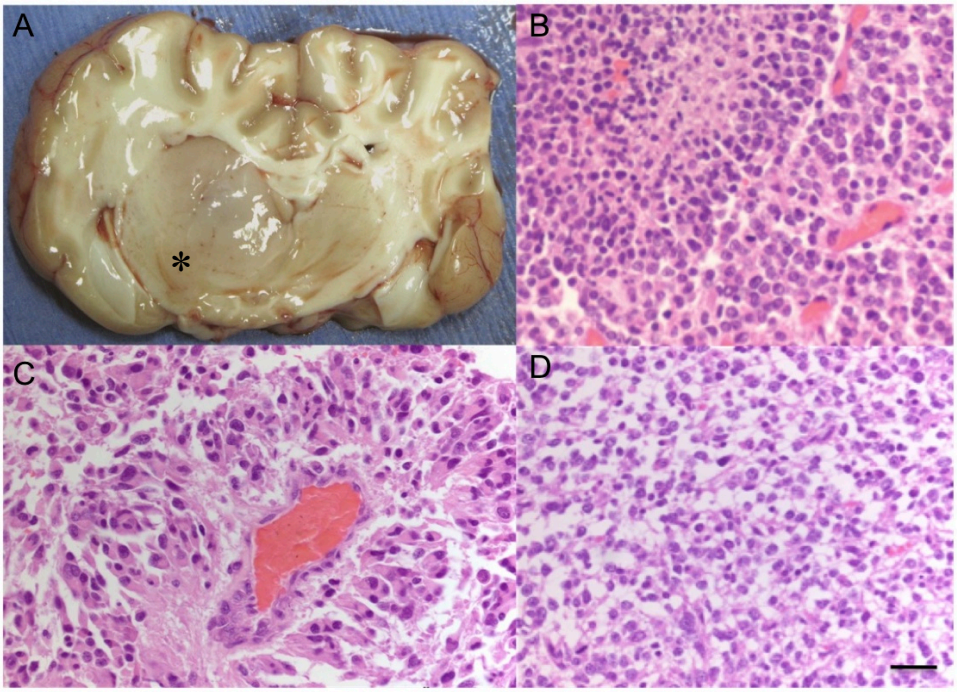

Figure 1. The Parental 0123 Canine Tumor Exhibits Morphologic Features Consistent with a Human Anaplastic Astrocytoma. A) The parental tumor (*) originated from the right periventricular region and was composed of B) sheets of round to C) angular neoplastic astrocytes. D) As occurs in human glioma tumors, focal regions consistent with oligodendroglial morphology were identified within the tumor, as well.

Figure 2

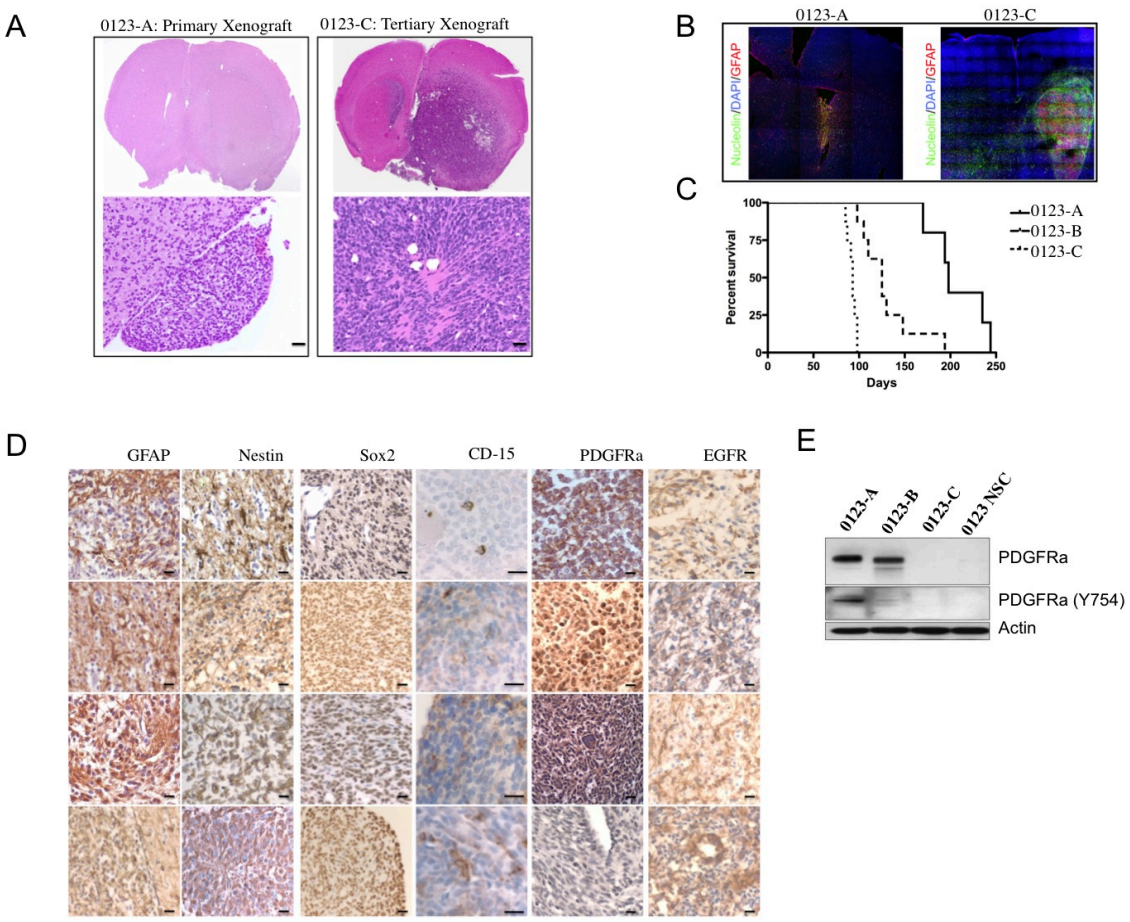

Figure 2. Canine GSCs Form Serially Transplantable Xenograft Tumors. A) Xenograft tumors from canine GSCs exhibit a progressive increase in malignancy over serial transplantation (H&E, bar equals 50μm). B) A canine-specific antibody demonstrates increased tumor burden in the tertiary xenografts. C) Tertiary xenografts decelop at a decreased latency, with median survival times of 93d, 125d, and 198d, respectively (log rank test, $p<0.0001$). D) Xenograft tumors show equivocal immunoreactivity with GFAP, Nestin, sox2, and EGFR, and an increase in CD-15 reactive cells in the 0123-B and 0123-C tumors compared to the parental tumor while PDGFRa is decreased in tertiary xenografts (bar equals 50μm), reflected in E) immunoblot indicating GSCs derived from primary and secondary, but not tertiary tumors express PDGFRa. However, the receptor is only strongly active (as measured by phosphorylation) in primary GSCs

Figure 3

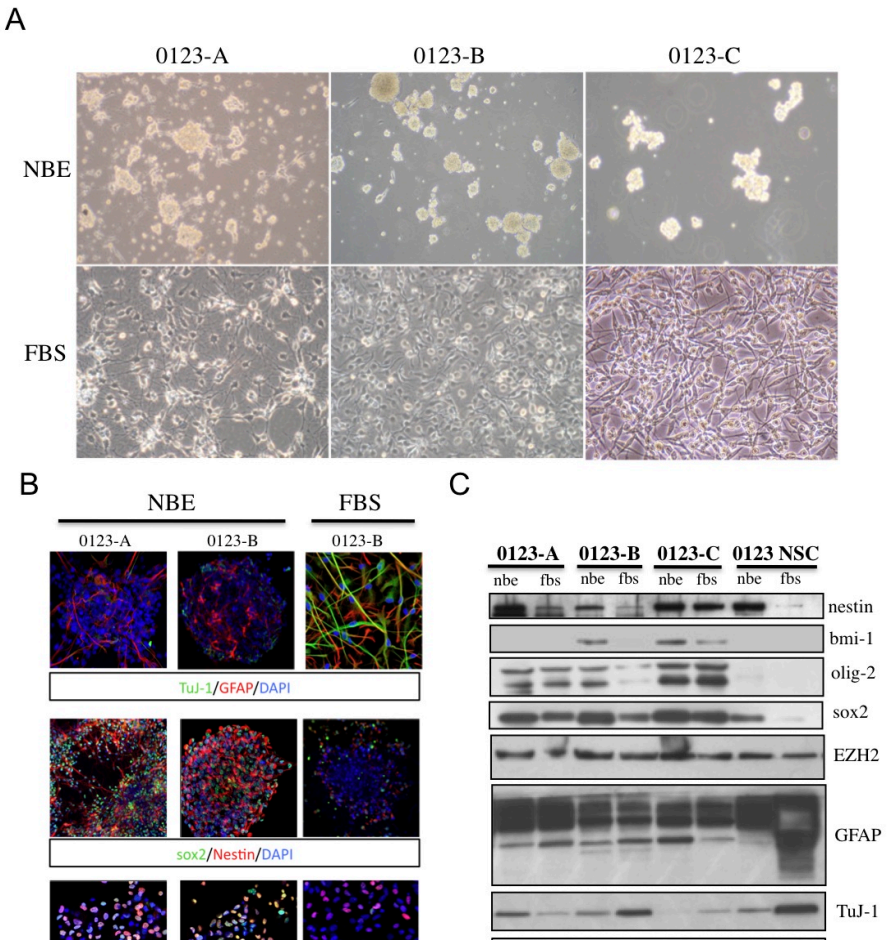

Figure 3. Canine GSCs Exhibit Similar Properties to Human GSCs *in vitro*. A) Canine GSCs grow as non-adherent, neurosphere-like structures when cultured in serum free NBE media. Conversely, in the presence of serum, cells assume an adherent, astrocytic morphology. B) Like human GSCs, canine GSCs express markers of neural stem cells (sox2, olig2, nestin) in NBE, with reduction of these markers and increased differentiation markers in the presence of serum. C) Immunoblot shows increases in proteins associated with stem cell renewal over serial xenografts (Bmi-1, Olig2) and in relation to physiologic neural stem cells, suggesting increased self renewal capacity.

Figure 4

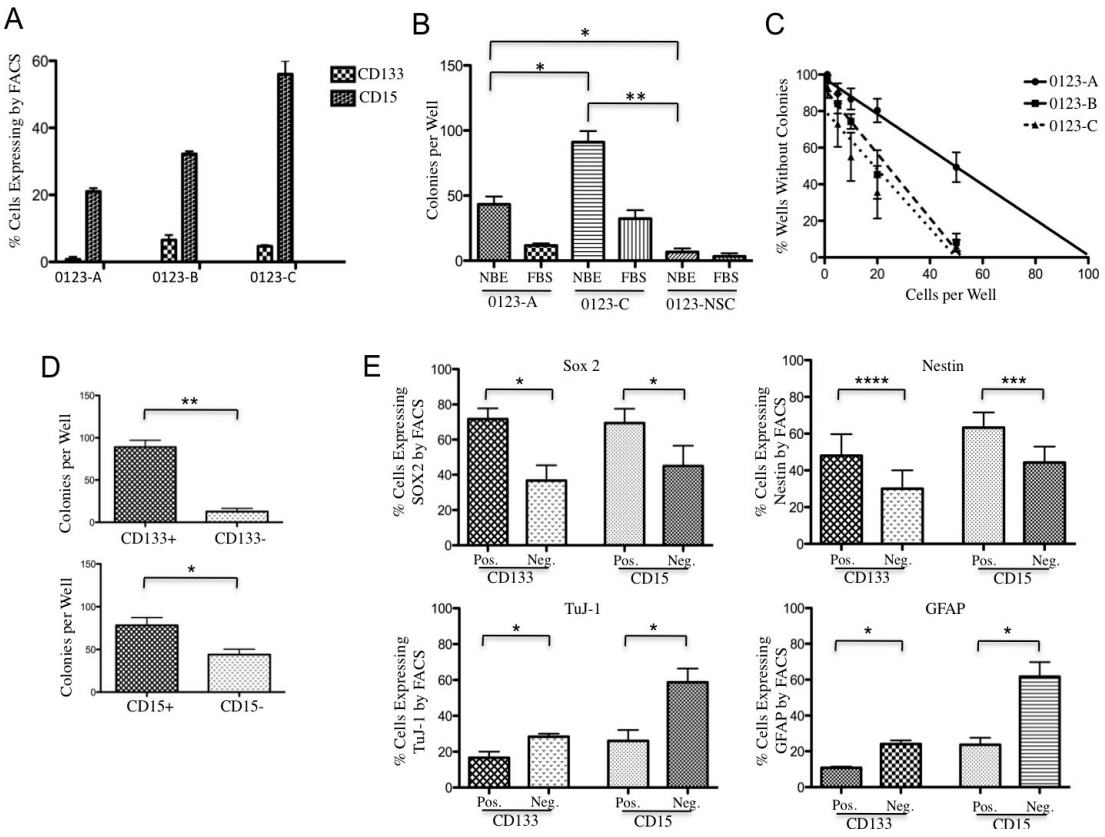

Figure 4. Serial Xenotransplantation Enhances Features of Stem Cell Self-Renewal Measured *in vitro*. A) Canine GSCs express increased CD133 and CD15 over serial xenograft formation. These increases are reflected in an increased clonogenic potential in vitro, as measured by B) soft agar forming assay and C) limiting dilution assay. D) CD133 or CD15 positively labeled cells have significantly increased clonogenic potential compared to negatively labeled cells as measured by soft agar colony formation. E) Cells co-expressing CD133 or CD-15 express significantly higher levels of the stem cell marker sox2 and reduced levels of differentiation markers TuJ-1 and GFAP as measured by FACS analysis compared to negatively labeled cells (*$p<0.05$, **$p<0.01$, ***$p<0.10$, ****$p<0.2$).

Figure 5

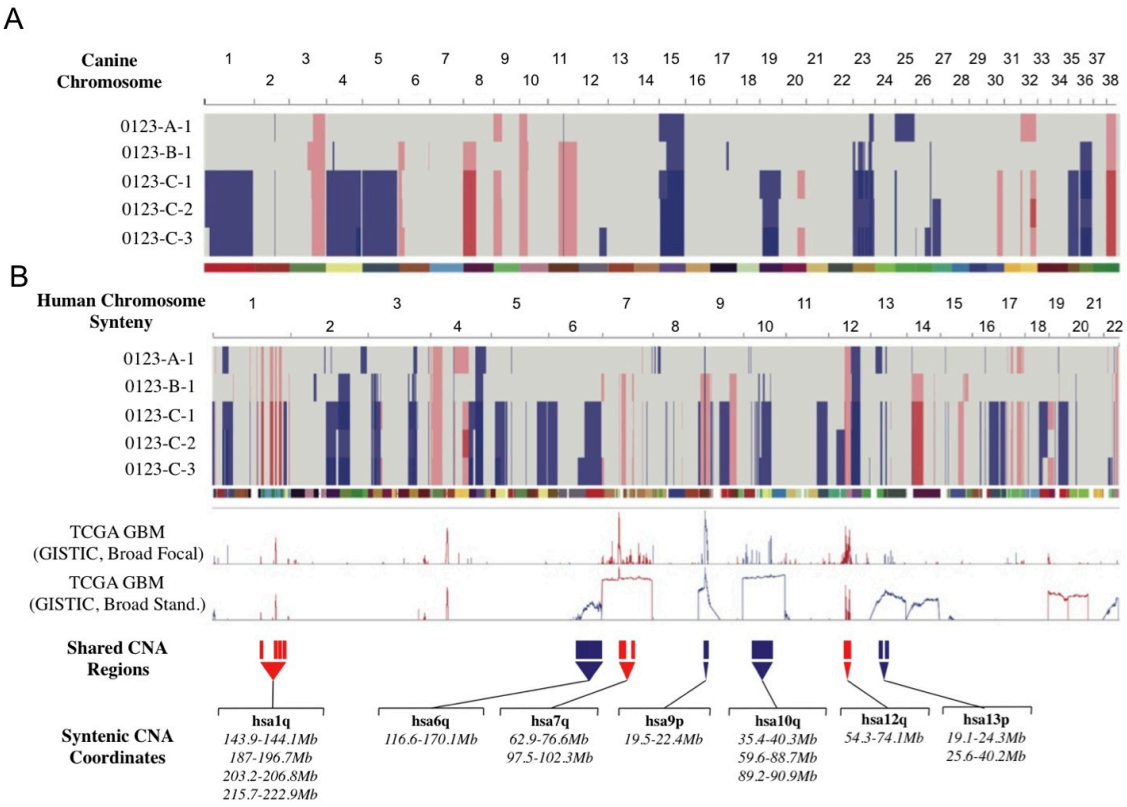

Figure 5. Comparative Genomic Hybridization of Canine GSCs over Serial Xenotransplantation Defines Shared Copy Number Alterations. A) Canine SNP array shows progressive copy number alterations (CNAs) across serial xenotransplantation (Amplifications are represented by red, deletions by blue. Intensity reflects call rate from SNP array. Canine chromosomes are color-coded). CNAs show significant conservation at cfa3 (corresponding to MDM2 amplification), cfa11 (corresponding to p16/Ink4a deletion), progressive CNAs at cfa8, cfa15, cfa23, cfa26 (corresponding to PTEN deletion), and cfa38 (corresponding to MDM4 amplification). B) When canine GSC CNAs are displayed according to their human syntenic analogs and are superimposed over commonly altered regions in glioblastoma (derived from TCGA database) multiple, shared CNAs in both amplified and deleted regions are evident in hsa1q, hsa6q, hsa7q, hsa9p, hsa10q, hsa12q, and hsa13p.

Figure 6

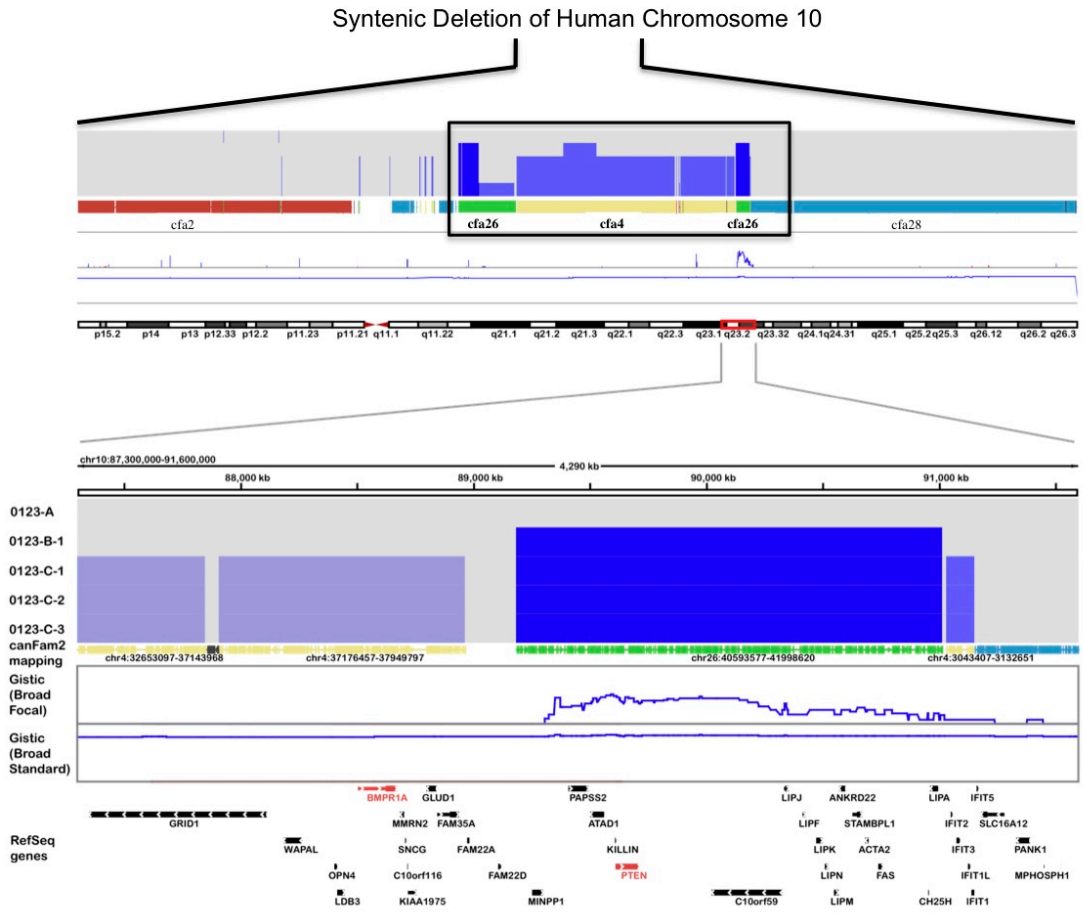

Figure 6. Minimal Regions of Alteration in Human Chromosome 10 are defined by Multiple, Separate Canine Chromosomes. The CNA corresponding to hsa10q23.1-23.3 is composed of syntenic regions including deletions of both canine cfa4 (yellow) and cfa26 (green). By closely examining these joints of independently deleted, separate canine chromosomes within shared CNAs, we can identify and investigate novel tumor suppressor gene or oncogene candidates, as the co-deletion across multiple canine chromosomes implies significant biological relevance within the syntenic human region. Surrounding *PTEN*, genes of suspected interest in glioma biology, such as *ANXA7*, *BMPR1A*, and *CCAR1*, among others are independently co-deleted in this case.

Figure 7

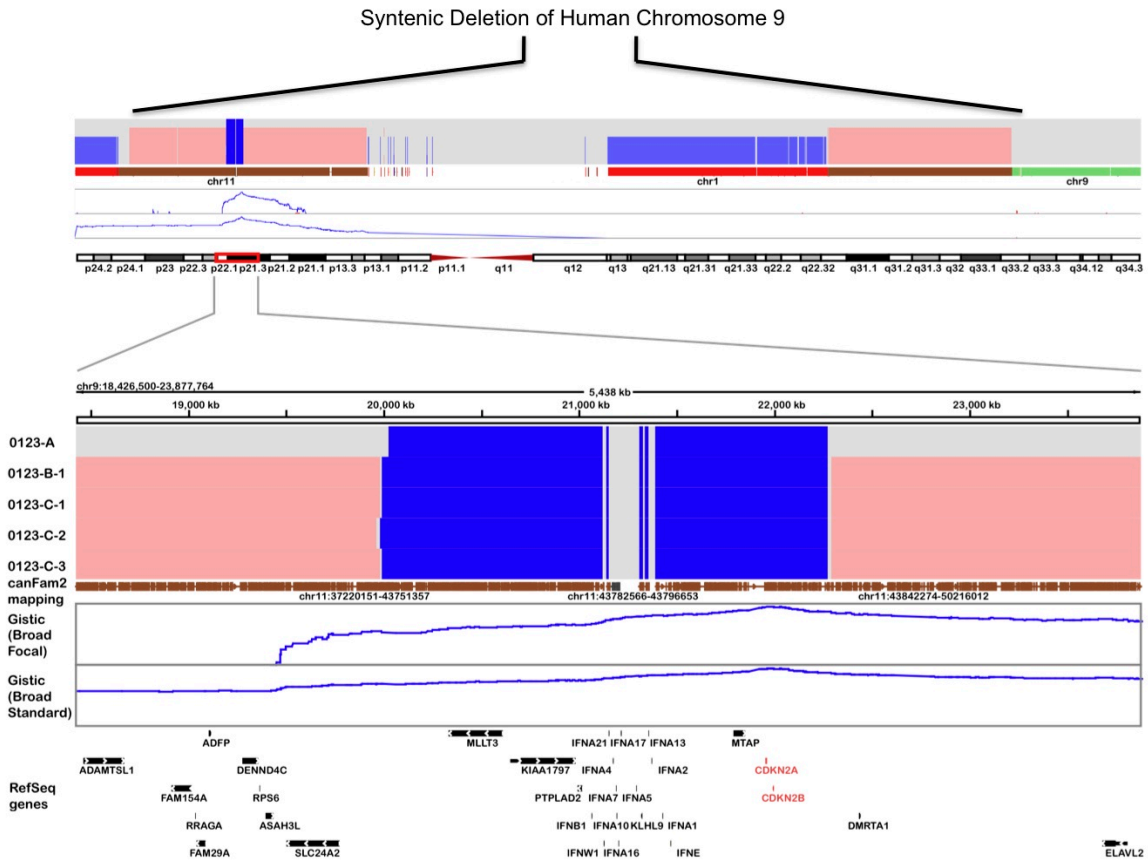

Figure 7: Deletion of Regions Syntenic to hsa9. Similar to our characterization of the altered foci surrounding *PTEN* in human chromosome 10, we compared the regions of alteration containing the *p16/ARF* locus (cfa11) to the syntenic regions along human chromosome 9 (Amplifications are represented by red, deletions by blue. Intensity reflects call rate from SNP array. Canine chromosomes are color-coded). The loss of *p16/ARF* corresponds to a small, focal alteration (in cfa 11, color coded in brown, above) containing the *p16/ARF* locus as well as numerous genes within the interferon cluster. A second, independent deletion of canine chromosome 1 (in red, above) suggests a progressive loss of a region syntenic to an upstream region of hsa9p also frequently deleted.

Figure 8

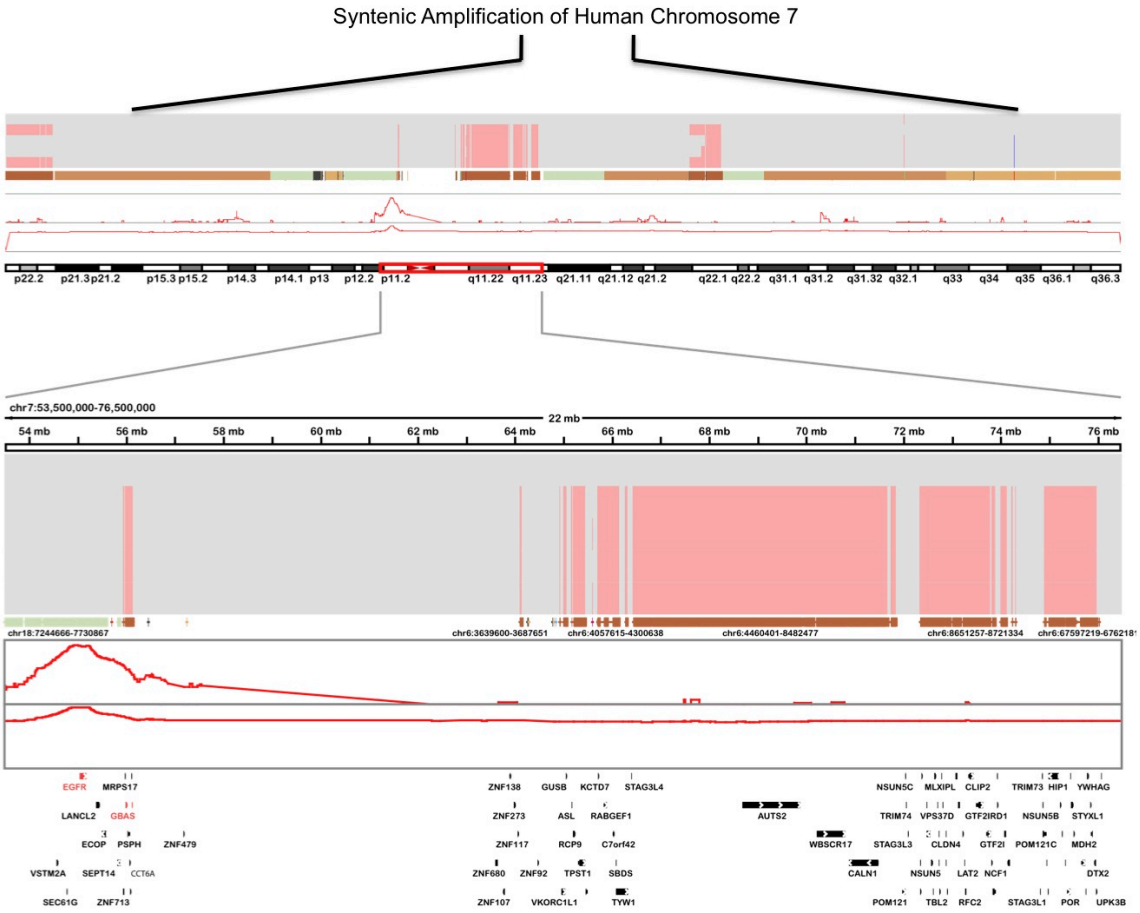

Figure 8: Amplification of Regions Syntenic to hsa7. Amplification of human chromosome 7 is a common event in human primary glioblastoma and is often attributed to the gain of function of EGFR. However, other putative oncogenes exist within this segment as well. We are able to identify progressive amplifications in regions of canine chromosome 6 (Amplifications are represented by red, deletions by blue. Intensity reflects call rate from SNP array. Canine chromosomes are color-coded). While EGFR is not implicated in this region (as is the case in most human secondary GBMs), other candidate oncogenes such as GBAS (glioblastoma amplified sequence) are present.

Figure 9

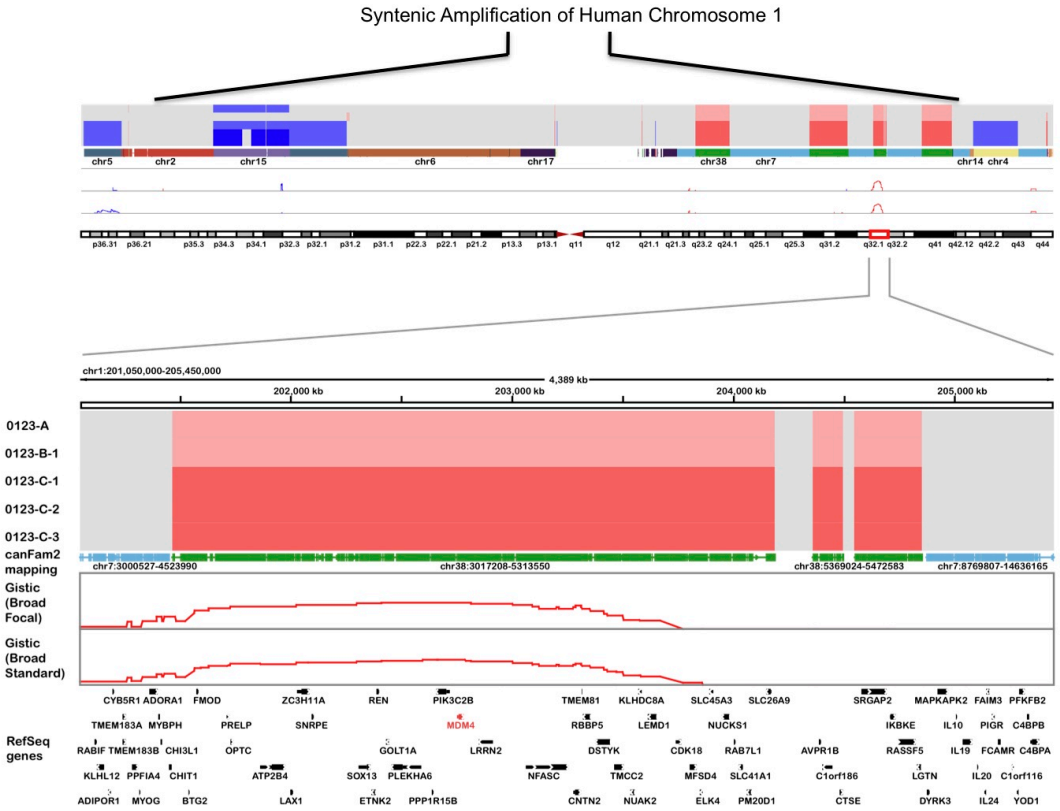

Figure 9: Amplification of Regions Syntenic to hsa1. Similar to our characterization of the altered foci surrounding PTEN in human chromosome 10, we compared the regions of alteration containing the mdm4 locus (cfa38) to the syntenic regions along human chromosome 1 (Amplifications are represented by red, deletions by blue. Intensity reflects call rate from SNP array. Canine chromosomes are color-coded). This region corresponds to a highly conserved area of deletion identified from the TCGA database containing MDM4 and numerous other genes and reveals progressive intensity of amplification of the segment containing mdm4 over serial xenograft progression.

Figure 10

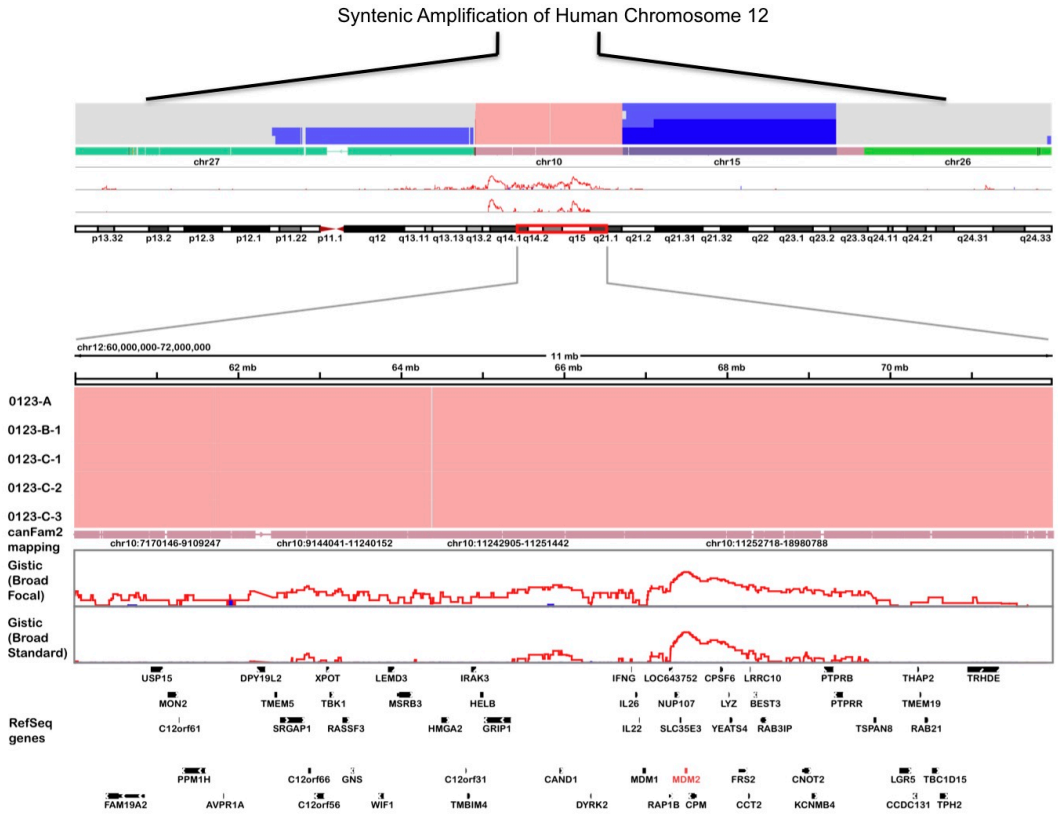

Figure 10: Amplification of Regions Syntenic to hsa12. Similar to our characterization of the altered foci surrounding PTEN in human chromosome 10, we compared the regions of alteration containing the mdm2 locus (cfa10) to the syntenic regions along human chromosome 12 (Amplifications are represented by red, deletions by blue. Intensity reflects call rate from SNP array. Canine chromosomes are color-coded). This region corresponds to a highly conserved area of deletion identified from the TCGA database containing MDM2 and numerous other genes.

Figure 11

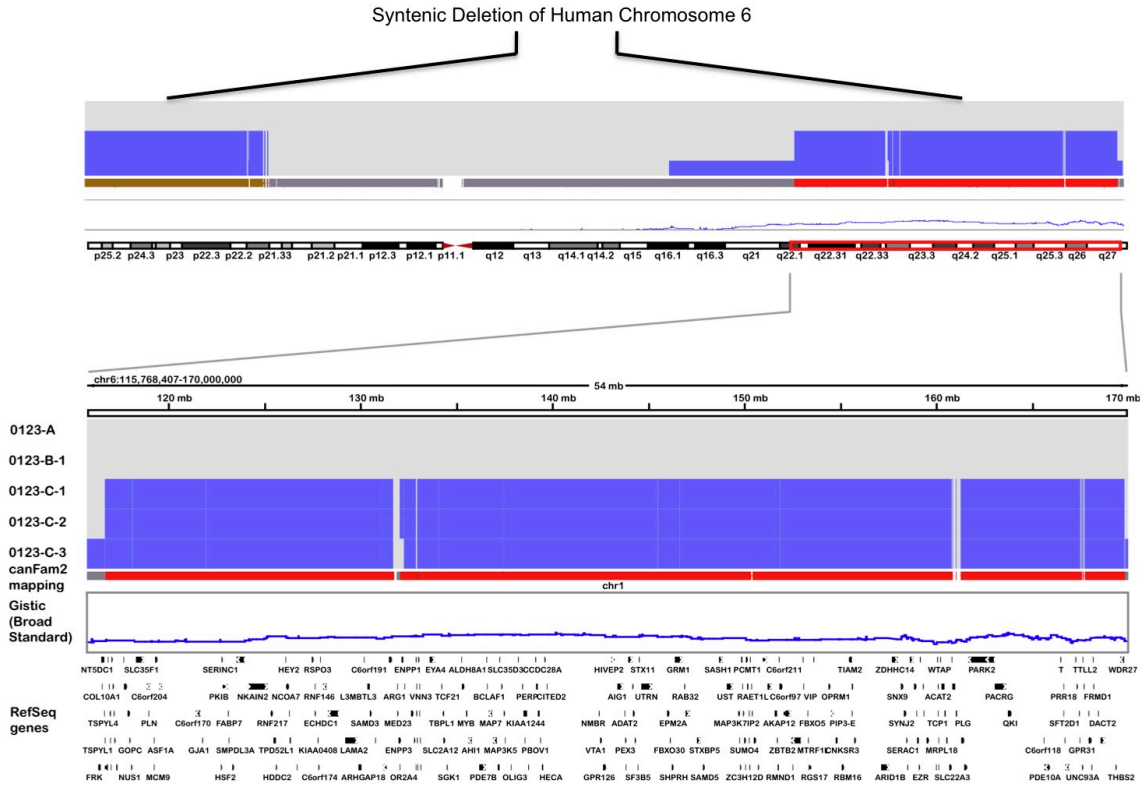

Figure 11: Deletion of Regions Syntenic to hsa6. While our investigation regarding foci of alteration surrounding PTEN, p16/ARF, and MDM2/4 concentrate on genes adjacent to known tumor suppressor genes, we also investigated the alteration of regions that, while commonly altered in human glioblastoma, as yet contain no defined tumor suppressor genes. One such region is the syntenic region along human chromosome 6q, comprised of progressive deletions in canine chromosome 1, 12, and 35 (Amplifications are represented by red, deletions by blue. Intensity reflects call rate from SNP array. Canine chromosomes are color-coded). Identification and examination of genes within these regions not only provides potential tumor suppressor gene candidates but also serves to highlight the similarity of disease between canine and human glioma tumors.

Figure 12

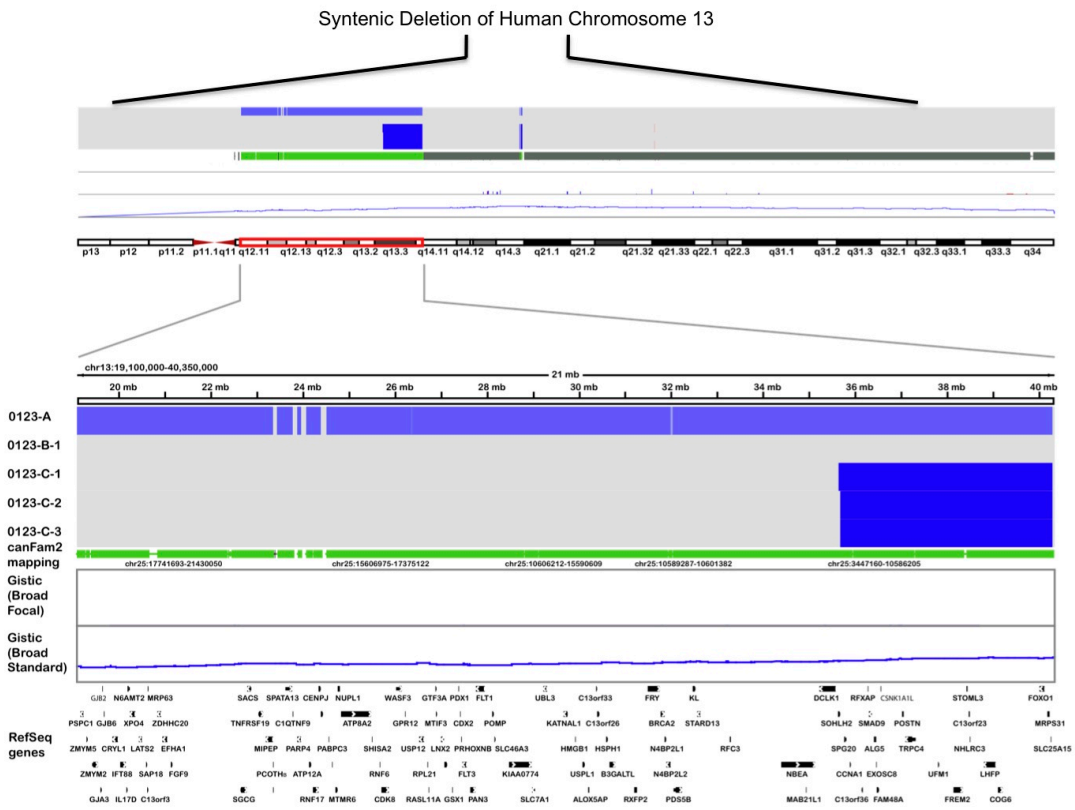

Figure 12: Deletion of Regions Syntenic to hsa13. Similar to our interest in investigating foci of alteration surrounding hsa6q, other regions that are commonly altered in human glioblastoma such as hsa13 were also compared across our canine GSCs (Amplifications are represented by red, deletions by blue. Intensity reflects call rate from SNP array. Canine chromosomes are color-coded). Serial xenograft progression in this population corresponds to deletion of a focal region of canine chromosome 25 within the tertiary GSC population, suggesting the presence of potential tumor suppressor genes relevant to glioma progression in this region.

Figure 13

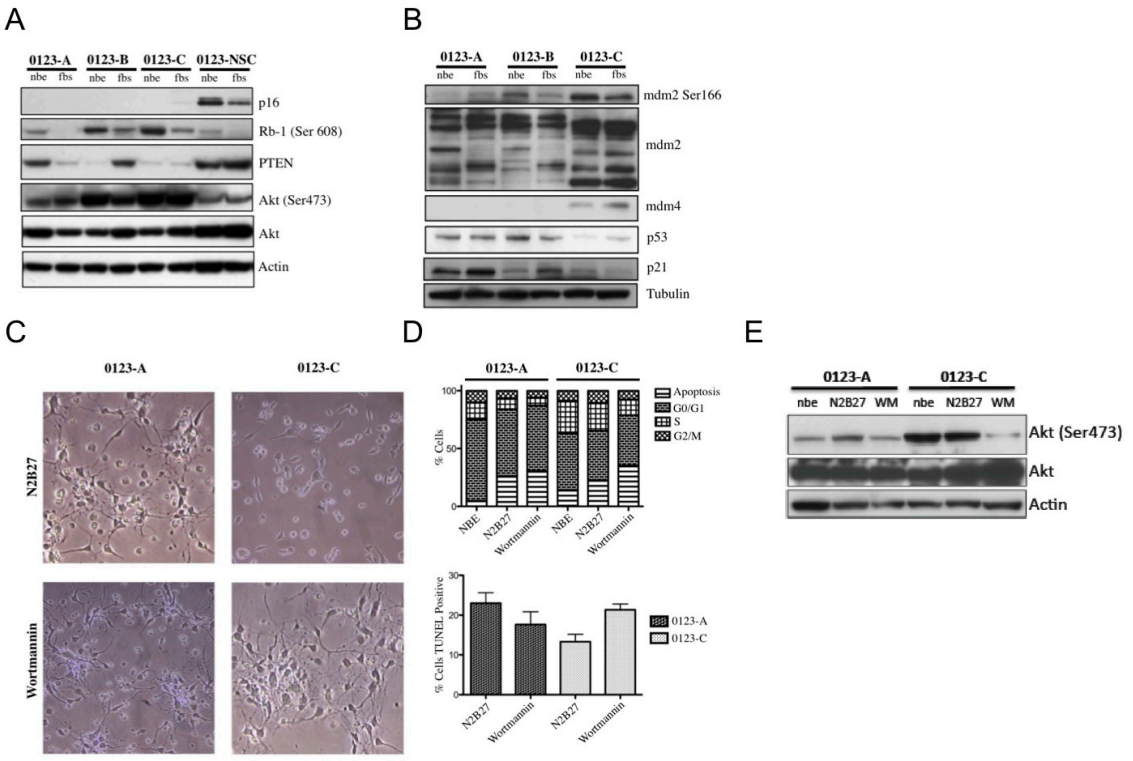

Figure 13. Progressive Genomic Alterations Are Critical for Increased Self-Renewal and Cell Survival in Canine GSCs Derived from Tertiary Xenografts. Consistent with our aCGH data, (A) canine GSCs exhibit a loss of p16 expression, reflected in an increase in Rb-1 inactivation, a progressive decrease in PTEN activity, and increased AKT phosphorylation. (B) Serial xenograft formation results in increased expression and activation of mdm2 and mdm4, corresponding to highly conserved regions of genomic amplification identified by the aCGH and reflected in a progressive decrease in p53 and p21 protein levels. (C) While growth factor withdrawal (N2B27) results in atrophic and apoptotic cells in primary GSCs, the cumulative increase in CNAs allows the tertiary 0123-C GSCs to survive in vitro. Blockade of PI3K activity by treating the cells with Wortmannin increases the apoptotic and senescence response of our 0123-C tertiary cells while failing to significantly affect 0123-A cells as measured by (D) cell cycle analysis or TUNEL assay. E) Immunoblot confirms wortmannin inhibition of AKT activity.

Table 1: Genes Deleted in 0123-C Samples Within Syntenic Regions of hsa10.

HUMAN GENOME (SYNTENIC REGION)					CANINE GENOME					
Chromosome	Strand	Start	End	Gene Name	Ensemble Canine Transcript ID or RefSeq ID	Chr	Strand	Start	End	RED = evidence from Ensemble, Blue = from tblastn (RefSeq), Black = both
chr10	-	51617005	51678376	ASAH2	ENSCAFT00000024747	chr26	-	40208372	40269120	ASAH2
chr10	-	51735350	52053743	SGMS1	ENSCAFT00000024774	chr26	-	40313149	40346886	SGMS1
chr10	+	52169713	52184575	ASAH2B	ENSCAFT00000042114	chr26	-	40304534	40304642	ENSCAFG00000027831
chr10	-	52236330	52315441	A1CF	ENSCAFT00000024715	chr26	+	40122760	40171929	A1CF
chr10	+	52420950	53725280	PRKG1	ENSCAFT00000024649	chr26	-	38807031	38838030	PRKG1
chr10	+	52729338	52729421	MIR605	ENSCAFT00000035994	chr26	-	40000521	40001770	ENSCAFG00000023425
chr10	-	53125251	53129361	CSTF2T	ENSCAFT00000024677	chr26	+	39333767	39335803	CSTF2T
chr10	+	53744046	53747423	DKK1	ENSCAFT00000024645	chr26	-	38767662	38946574	DKK1
chr10	-	55250865	56231057	PCDH15	ENSCAFT00000024635	chr26	+	37153676	37639408	PCDH15
chr10	-	57787204	57791040	ZWINT	ENSCAFT00000024605	chr26	+	35496433	35516619	ZWINT
chr10	-	59625619	59697700	IPMK	ENSCAFT00000019477	chr4	-	13607403	13662838	IPMK
chr10	+	59698900	59719025	CISD1	ENSCAFT00000019483	chr4	+	13671123	13680447	CISD1
chr10	+	59764744	59800515	UBE2D1	ENSCAFT00000019538	chr4	+	13724759	13753706	UBE2D1
chr10	+	59815181	59825903	TFAM	ENSCAFT00000038143	chr4	+	13787951	13800708	TFAM
chr10	+	59942909	60258851	BICC1	ENSCAFT00000019599	chr4	+	14171704	14206730	BICC1
chr10	+	60606353	60677538	PHYHIPL	ENSCAFT00000019692	chr4	+	14589915	14663009	PHYHIPL
chr10	-	60675895	60792358	FAM13C	ENSCAFT00000019728	chr4	-	14665000	14810304	FAM13C
chr10	-	61080528	61139655	SLC16A9	ENSCAFT00000019750	chr4	-	15069865	15098058	SLC16A9
chr10	-	61218526	61336824	CCDC6	ENSCAFT00000019769	chr4	-	15172453	15279794	CCDC6
chr10	-	61458164	61570752	ANK3	ENSCAFT00000020300	chr4	-	15369867	15590029	ANK3
chr10	+	62208094	62216833	CDK1	ENSCAFT00000020502	chr4	+	16091940	16224607	CDK1
chr10	-	62299205	62374039	RHOBTB1	ENSCAFT00000020539	chr4	-	16179601	16215590	RHOBTB1
chr10	-	62836406	62883214	TMEM26	ENSCAFT00000020586	chr4	-	16670202	16714431	TMEM26
chr10	+	63092724	63196095	C10orf107	ENSCAFT00000036219	chr4	+	16909268	17009024	C10orf107
chr10	+	63331018	63526713	ARID5B	ENSCAFT00000020628	chr4	+	17133136	17306880	ARID5B
chr10	-	63622958	63698472	RTKN2	ENSCAFT00000020670	chr4	-	17382154	17450938	RTKN2
chr10	+	63803921	63832223	ZNF365	ENSCAFT00000020684	chr4	+	17517209	17537463	ZNF365
chr10	+	64234521	64238245	ADO	ENSCAFT00000020687	chr4	+	17904501	17905314	XM_546121.2
chr10	-	64241765	64246132	EGR2	ENSCAFT00000020697	chr4	-	17912485	17915293	EGR2
chr10	+	64563012	64584792	NRBF2	ENSCAFT00000020716	chr4	+	18164111	18196211	NRBF2
chr10	-	64596993	64698988	JMJD1C	ENSCAFT00000020775	chr4	-	18213393	18301245	JMJD1C
chr10	+	64951128	65054887	REEP3	ENSCAFT00000020842	chr4	+	18604047	18629158	REEP3
chr10	-	67349730	69095422	CTNNA3	ENSCAFT00000021033	chr4		20577292	20755158	XM_844561.1
chr10	+	68355797	68530873	LRRTM3	ENSCAFT00000021048	chr4	+	21528242	21529784	LRRTM3
chr10	-	69226432	69267943	DNAJC12	ENSCAFT00000021116	chr4	-	22302891	22347623	DNAJC12
chr10	+	69314432	69348152	SIRT1	ENSCAFT00000021123	chr4	+	22394790	22424360	SIRT1
chr10	-	69351661	69505109	HERC4	ENSCAFT00000021421	chr4	-	22429641	22556496	HERC4
chr10	+	69539255	69641779	MYPN	ENSCAFT00000021485	chr4	+	22587609	22672111	MYPN
chr10	-	69660387	69661861	ATOH7	ENSCAFT00000021497	chr4	-	22684809	22685489	ATOH7
chr10	-	69712422	69762690	PBLD	ENSCAFT00000021563	chr4	-	22721170	22743081	PBLD
chr10	+	69761773	69772959	HNRNPH3	ENSCAFT00000000525	chr4	+	22770030	22775042	HNRNPH3
chr10	-	69773280	69836952	RUFY2	ENSCAFT00000021715	chr4	-	22778314	22827942	RUFY2
chr10	-	69843826	69901885	DNA2	ENSCAFT00000036654	chr4	-	22871200	22887253	ENSCAFG00000023722
chr10	-	69912102	69957590	SLC25A16	ENSCAFT00000021772	chr4	-	22903122	22944994	SLC25A16
chr10	+	69990122	70124245	TET1	ENSCAFT00000021794	chr4	+	22974337	23095986	TET1
chr10	+	70150976	70221315	CCAR1	ENSCAFT00000021848	chr4	+	23123055	23183178	CCAR1
chr10	+	70184934	70185001	SNORD98	ENSCAFT00000040993	chr4	+	23157901	23157966	ENSCAFG00000026710
chr10	+	70257299	70322821	STOX1	ENSCAFT00000021852	chr4	+	23220068	23270982	STOX1
chr10	+	70331039	70376609	DDX50	ENSCAFT00000021867	chr4	+	23278755	23308341	DDX50
chr10	+	70385897	70414285	DDX21	ENSCAFT00000021901	chr4	+	23315541	23338063	DDX21
chr10	+	70418482	70446745	KIAA1279	ENSCAFT00000021920	chr4	+	23345245	23383762	KIAA1279
chr10	+	70517833	70534573	SRGN	ENSCAFT00000001563	chr4	+	23436454	23450165	SRGN
chr10	+	70553913	70602622	VPS26A	ENSCAFT00000021943	chr4	+	23470890	23500376	VPS26A
chr10	+	70609998	70638855	SUPV3L1	ENSCAFT00000021963	chr4	+	23519560	23546602	SUPV3L1
chr10	+	70650064	70697321	HKDC1	NM_025130	chr4	+	23583654	23591512	HKDC1
chr10	+	70699761	70831643	HK1	ENSCAFT00000022120	chr4	+	23655777	23721856	HK1
chr10	-	70833963	70846680	TACR2	ENSCAFT00000022135	chr4	-	23724516	23736838	NK2R_CANFA
chr10	+	70881231	70937429	TSPAN15	ENSCAFT00000022143	chr4	+	23762801	23812985	TSPAN15
chr10	-	71001797	71003216	NEUROG3	ENSCAFT00000036379	chr4	-	23862146	23862975	NEUROG3
chr10	+	71060008	71063361	C10orf35	ENSCAFT00000022147	chr4	+	23901424	23903876	C10orf35
chr10	+	71231649	71388909	COL13A1	ENSCAFT00000022194	chr4	+	24116200	24194947	COL13A1
chr10	+	71482362	71542046	H2AFY2	ENSCAFT00000022230	chr4	+	24267755	24296477	H2AFY2
chr10	-	71542035	71562696	AIFM2	ENSCAFT00000022236	chr4	-	24297085	24306520	AIFM2
chr10	-	71567738	71576502	TYSND1	ENSCAFT00000035412	chr4	-	24327267	24327660	TYSND1
chr10	-	71579973	71600291	SAR1A	ENSCAFT00000022270	chr4	-	24332511	24342344	SAR1A
chr10	-	71632591	71663196	PPA1	ENSCAFT00000022283	chr4	-	24355343	24392361	PPA1
chr10	-	71684719	71713446	NPFFR1	ENSCAFT00000022287	chr4	-	24407898	24412670	NPFFR1
chr10	-	71728734	71811420	LRRC20	ENSCAFT00000022294	chr4	-	24439275	24484846	LRRC20
chr10	+	71833866	71858378	EIF4EBP2	ENSCAFT00000022299	chr4	+	24548861	24567887	EIF4EBP2
chr10	-	71861697	71871471	NODAL	ENSCAFT00000022302	chr4	-	24577397	24584438	NODAL
chr10	+	71908569	71998212	KIAA1274	ENSCAFT00000022336	chr4	+	24654132	24688460	KIAA1274
chr10	-	72027109	72032537	PRF1	ENSCAFT00000022343	chr4	-	24707281	24709814	PRF1
chr10	+	72102564	72192201	ADAMTS14	ENSCAFT00000022359	chr4	+	24743349	24820009	ADAMTS14
chr10	-	72201000	72215163	C10orf27	ENSCAFT00000022374	chr4	-	24846575	24859445	C10orf27
chr10	+	72245709	72310936	SGPL1	ENSCAFT00000022384	chr4	+	24877713	24926276	SGPL1
chr10	-	72313272	72318547	PCBD1	ENSCAFT00000022390	chr4	-	24931146	24935245	PCBD1
chr10	+	72642303	72730755	UNC5B	ENSCAFT00000022760	chr4	+	25214474	25291596	UNC5B
chr10	+	72749015	72793151	SLC29A3	ENSCAFT00000022774	chr4	+	25308760	25344185	SLC29A3
chr10	+	72826696	73047367	CDH23	ENSCAFT00000022666	chr4	+	25492870	25781226	CDH23
chr10	-	73177318	73203343	C10orf54	ENSCAFT00000022797	chr4	-	25718182	25730340	C10orf54

Table 1 (continued)

HUMAN GENOME (SYNTENIC REGION)					CANINE GENOME					RED = evidence from Ensemble, Blue = from tblastn (RefSeq), Black = both
Chromosome	Strand	Start	End	Gene Name	Ensemble Canine Transcript ID or RefSeq ID	Chr	Strand	Start	End	
chr10	-	73246060	73281088	PSAP	ENSCAFT00000022871	chr4	-	25782268	25798393	PSAP
chr10	+	73394125	73443327	CHST3	ENSCAFT00000022886	chr4	+	25902557	25905391	CHST3
chr10	-	73488798	73518796	SPOCK2	ENSCAFT00000022891	chr4	-	25959610	25968522	SPOCK2
chr10	-	73526283	73645700	ASCC1	ENSCAFT00000022904	chr4	-	25990743	26085178	ASCC1
chr10	+	73645811	73665624	ANAPC16	ENSCAFT00000022911	chr4	+	26092273	26099906	C10orf104
chr10	+	73703682	73705803	DDIT4	ENSCAFT00000022926	chr4	+	26128023	26129002	DDIT4
chr10	-	73762593	73784913	DNAJB12	ENSCAFT00000022966	chr4	-	26176932	26191155	DNAJB12
chr10	-	73797103	74055905	CBARA1	ENSCAFT00000023026	chr4	-	26201003	26391452	**CBARA1**
chr10	+	74121894	74317458	CCDC109A	ENSCAFT00000023057	chr4	+	26520354	26708024	CCDC109A
chr10	+	74323344	74362793	OIT3	ENSCAFT00000023087	chr4	+	26724643	26749887	OIT3
chr10	-	74364943	74384516	PLA2G12B	ENSCAFT00000023098	chr4	-	26752221	26772005	PLA2G12B
chr10	-	74436987	74526738	P4HA1	ENSCAFT00000023158	chr4	-	26812368	26873880	P4HA1
chr10	+	74540215	74561587	NUDT13	ENSCAFT00000023196	chr4	+	26906229	26922364	NUDT13
chr10	-	74564288	74597859	ECD	ENSCAFT00000023218	chr4	-	26924850	26951185	ECD
chr10	+	74597882	74671945	FAM149B1	ENSCAFT00000023246	chr4	+	26953415	27029837	**XM_847232.1**
chr10	-	74672587	74677031	DNAJC9	ENSCAFT00000023265	chr4	-	27031559	27036267	DNAJC9
chr10	-	74678606	74682457	MRPS16	NM_016065	chr4	-	27038625	27039485	**MRPS16**
chr10	-	74683522	74788623	TTC18	ENSCAFT00000023341	chr4	-	27041372	27134949	TTC18
chr10	-	74805194	74843847	ANXA7	ENSCAFT00000008812	chr4	-	27144646	27164166	ANXA7
chr10	-	74853342	74863325	ZMYND17	ENSCAFT00000023445	chr4	-	27176647	27180339	ZMYND17
chr10	-	74866569	74925788	PPP3CB	ENSCAFT00000023521	chr4	-	27187850	27238740	PPP3CB
chr10	-	74927301	75005439	USP54	ENSCAFT00000036041	chr4	-	27257439	27304464	USP54
chr10	-	75061417	75071521	MYOZ1	ENSCAFT00000023556	chr4	-	27369426	27374791	Q1AG03_CANFA
chr10	-	75074649	75080793	SYNPO2L	ENSCAFT00000023558	chr4	-	27380322	27388117	**SYNPO2L**
chr10	+	75174137	75201925	SEC24C	ENSCAFT00000023604	chr4	+	27396721	27418582	SEC24C
chr10	+	75202054	75205982	FUT11	ENSCAFT00000023609	chr4	+	27419886	27423131	FUT11
chr10	+	75211813	75213412	CHCHD1	ENSCAFT00000023617	chr4	+	27428048	27429355	CHCHD1
chr10	+	75215610	75231557	KIAA0913	ENSCAFT00000023812	chr4	+	27431412	27445548	**KIAA0913**
chr10	-	75231674	75241595	NDST2	ENSCAFT00000023910	chr4	-	27446175	27451259	NDST2
chr10	-	75242264	75304344	CAMK2G	ENSCAFT00000024094	chr4	-	27454678	27509971	CAMK2G
chr10	-	75339739	75352541	C10orf55	NM_001001791	chr4	+	27540227	27540656	**C10orf55**
chr10	+	75340867	75347262	PLAU	NM_002658	chr4	+	27540113	27544506	**PLAU**
chr10	+	75427877	75549920	VCL	ENSCAFT00000024269	chr4	+	27683819	27728897	VCL
chr10	-	75550020	75580832	AP3M1	ENSCAFT00000024342	chr4	-	27734273	27743398	AP3M1
chr10	+	75580970	76139066	ADK	ENSCAFT00000024344	chr4	+	27917606	28257261	ADK
chr10	+	76256384	76462645	MYST4	ENSCAFT00000024383	chr4	+	28445575	28512346	MYST4
chr10	-	76467599	76488278	DUPD1	NM_001003892	chr4	-	28518681	28539874	**DUPD1**
chr10	-	76524195	76538976	DUSP13	ENSCAFT00000024394	chr4	-	28570817	28575301	DUSP13
chr10	+	76541398	76611886	SAMD8	ENSCAFT00000024402	chr4	+	28609750	28630869	SAMD8
chr10	+	76639917	76661210	VDAC2	ENSCAFT00000024325	chr4	-	27621932	27623164	VDAC2
chr10	-	76663734	76665776	COMTD1	ENSCAFT00000024445	chr4	-	28675067	28676680	COMTD1
chr10	-	76827610	76831519	ZNF503	ENSCAFT00000024477	chr4	-	28795585	28798366	ZNF503
chr10	+	77212524	77987132	C10orf11	ENSCAFT00000024487	chr4	+	29388095	29410172	C10orf11
chr10	-	78299364	79067583	KCNMA1	ENSCAFT00000024544	chr4	-	30054840	30345318	KCMA1_CANFA
chr10	-	79220554	79356354	DLG5	ENSCAFT00000024600	chr4	-	30898933	31016619	DLG5
chr10	-	79404913	79459304	POLR3A	ENSCAFT00000024699	chr4	-	31046071	31093096	POLR3A
chr10	+	79463523	79470477	RPS24	ENSCAFT00000024732	chr4	+	31096894	31100080	XM_859408.1
chr10	+	80498797	80746291	ZMIZ1	ENSCAFT00000024855	chr4	+	32140515	32245239	ZMIZ1
chr10	+	80777225	80785095	PPIF	ENSCAFT00000024860	chr4	+	32284643	32289365	PPIF
chr10	-	80812090	80875389	ZCCHC24	ENSCAFT00000024863	chr4	-	32314687	32371486	ZCCHC24
chr10	+	81360646	81365150	SFTPA1	ENSCAFT00000035263	chr4	-	32629692	32643408	SFTPA_CANFA
chr10	-	81687475	81698841	SFTPD	ENSCAFT00000024966	chr4	+	32606666	32617100	SFTPD
chr10	+	81828405	81842287	C10orf57	ENSCAFT00000025136	chr4	+	32754760	32768521	C10orf57
chr10	-	81904859	81955308	ANXA11	ENSCAFT00000024935	chr4	+	32459978	32476324	ANXA11
chr10	-	82021555	82039414	MAT1A	ENSCAFT00000025100	chr4	-	32662407	32676736	MAT1A
chr10	-	82085841	82106480	DYDC1	ENSCAFT00000025120	chr4	-	32700011	32711152	DYDC1
chr10	+	82106537	82117809	DYDC2	ENSCAFT00000036524	chr4	+	32719411	32724569	DYDC2
chr10	+	82158221	82182733	C10orf58	NM_032333	chr4		32759475	32768518	**C10orf58**
chr10	+	82204017	82272371	TSPAN14	ENSCAFT00000025149	chr4	+	32818812	32843492	TSPAN14
chr10	+	82287637	82396296	SH2D4B	ENSCAFT00000025151	chr4	+	32861618	32944451	SH2D4B
chr10	+	83625049	84736915	NRG3	ENSCAFT00000025160	chr4	+	34732094	34765670	**NRG3**
chr10	+	85889164	85903291	GHITM	ENSCAFT00000025181	chr4	+	35611156	35625371	**GHITM**
chr10	+	85923533	85935030	C10orf99	ENSCAFT00000025187	chr4	+	35633347	35640629	C10orf99
chr10	+	85944391	85967099	CDHR1	NM_033100	chr4	+	35664794	35666219	**CDHR1**
chr10	-	85970228	85975264	LRIT2	ENSCAFT00000025221	chr4	-	35673653	35677805	**LRIT2**
chr10	-	85981255	85991197	LRIT1	ENSCAFT00000025227	chr4	-	35684299	35694426	LRIT1
chr10	+	85994788	86008924	RGR	NM_001012720	chr4	+	35699045	35707701	**RGR**
chr10	+	86078389	86268256	FAM190B	NM_018999	chr4	+	35794523	35938107	**FAM190B**
chr10	-	87349291	88116230	GRID1	NM_017551	chr4	-	36726198	37345301	**GRID1**
chr10	-	88184992	88271521	WAPAL	ENSCAFT00000025322	chr4	-	37409599	37488548	WAPAL
chr10	+	88404293	88416196	OPN4	ENSCAFT00000025328	chr4	+	37547449	37557537	OPN4
chr10	+	88418185	88485802	LDB3	ENSCAFT00000025464	chr4	+	37560261	37613516	LDB3
chr10	+	88506375	88674925	BMPR1A	ENSCAFT00000025524	chr4	+	37737051	37771245	BMPR1A
chr10	-	88685279	88707405	MMRN2	ENSCAFT00000025530	chr4	-	37781918	37786667	MMRN2
chr10	+	88708267	88712997	SNCG	ENSCAFT00000025533	chr4	+	37797727	37800748	SNCG
chr10	+	88718167	88720646	C10orf116	NM_006829	chr4		37804055	37806064	**C10orf116**
chr10	+	88844932	88941202	FAM35A	NM_019054	chr4		37901149	37932886	**FAM35A**
chr10	+	89254202	89303198	MINPP1	ENSCAFT00000024776	chr26	+	40694757	40695228	MINPP1
chr10	+	89409455	89497442	PAPSS2	ENSCAFT00000024810	chr26	+	40792834	40812606	PAPSS2
chr10	-	89502854	89567897	ATAD1	ENSCAFT00000024819	chr26	-	40820035	40859103	ATAD1
chr10	+	89613174	89718512	PTEN	ENSCAFT00000038008	chr26	+	40903726	40981745	PTEN_CANFA

Table 1 (continued)

HUMAN GENOME (SYNTENIC REGION)					CANINE GENOME					
Chromosome	Strand	Start	End	Gene Name	Ensemble Canine Transcript ID or RefSeq ID	Chr	Strand	Start	End	RED = evidence from Ensemble, Blue = from tblastn (RefSeq), Black = both
chr10	-	90023600	90333062	RNLS	ENSCAFT00000024823	chr26	-	41238654	41294666	XM_847958.1
chr10	+	90336498	90356713	LIPJ	ENSCAFT00000036576	chr26	+	41493381	41509766	LIPJ
chr10	+	90414073	90428552	LIPF	ENSCAFT00000024834	chr26	+	41538536	41555859	LIPG_CANFA
chr10	+	90474280	90502493	LIPK	ENSCAFT00000036401	chr26	+	41602750	41625551	LIPK
chr10	+	90511142	90527979	LIPN	ENSCAFT00000036272	chr26	+	41643252	41656524	LIPN
chr10	+	90552466	90570283	LIPM	ENSCAFT00000036170	chr26	+	41677107	41690949	LIPM
chr10	-	90569638	90601712	ANKRD22	ENSCAFT00000024847	chr26	-	41692312	41712468	ANKRD22
chr10	+	90630005	90673224	STAMBPL1	ENSCAFT00000024871	chr26	+	41746052	41762280	STAMBPL1
chr10	-	90684810	90702560	ACTA2	ENSCAFT00000024881	chr26	-	41769085	41779476	Q9GKL5_CANFA
chr10	+	90740267	90765522	FAS	ENSCAFT00000024887	chr26	+	41815742	41827374	FAS
chr10	-	90955673	90957051	CH25H	ENSCAFT00000024895	chr26	-	41949439	41950666	CH25H
chr10	-	90963305	91001640	LIPA	ENSCAFT00000035174	chr26	-	41958806	41983393	LIPA
chr10	+	91051685	91059013	IFIT2	ENSCAFT00000015279	chr4	+	3068325	3069849	**IFIT2**
chr10	+	91077581	91090705	IFIT3	NM_001549	chr4	+	3103827	3105258	**IFIT3**
chr10	+	91127792	91134942	IFIT1B	NM_001010987	chr4	+	3115494	3116874	**IFIT1B**
chr10	+	91142301	91153724	IFIT1	ENSCAFT00000015282	chr4	+	3130893	3132312	**IFIT1**

Table 2: Genes Deleted in 0123-C Samples Within Syntenic Regions of hsa9.

HUMAN GENOME (SYNTENIC REGION)					CANINE GENOME					
Chromosome	Strand	Start	End	Gene Name	Ensemble Canine Transcript ID or RefSeq ID	Chr	Strand	Start	End	RED = evidence from Ensemble, Blue = from tblastn (RefSeq), Black = both
chr9	-	20334967	20612514	MLLT3	ENSCAFT00000002590	chr11	-	42955977	43028884	MLLT3
chr9	+	20648308	20985954	KIAA1797	ENSCAFT00000039148	chr11	+	43328279	43605479	KIAA1797
chr9	+	20706103	20706187	MIR491	ENSCAFT00000034898	chr11	+	43329117	43329201	cfa-mir-491
chr9	-	20996364	21021635	PTPLAD2	ENSCAFT00000002593	chr11	-	43614245	43644169	PTPLAD2
chr9	-	21067103	21067943	IFNB1	ENSCAFT00000002595	chr11	-	43696387	43696948	B6E116_CANFA
chr9	-	21130630	21132144	IFNW1	NM_002177	chr11	-	43727611	43728148	IFNW1
chr9	-	21155635	21156659	IFNA21	NM_002175	chr11	-	43892930	43893491	IFNA21
chr9	-	21176617	21177598	IFNA4	NM_021068	chr11	-	43892930	43893491	IFNA4
chr9	-	21191467	21192204	IFNA7	NM_021057	chr11	-	43892945	43893491	IFNA7
chr9	-	21196179	21197142	IFNA10	NM_002171	chr11	-	43892930	43893491	IFNA10
chr9	-	21206371	21207310	IFNA16	NM_002173	chr11	-	43892930	43893491	IFNA16
chr9	-	21217241	21218221	IFNA17	NM_021268	chr11	-	43892930	43893491	IFNA17
chr9	-	21321017	21325429	KLHL9	ENSCAFT00000036531	chr11	+	43823003	43825337	KLHL9
chr9	-	21357370	21358075	IFNA13	ENSCAFT00000036382	chr11	+	43850779	43851991	XM_849076.1
chr9	-	21374254	21375396	IFNA2	NM_000605	chr11	-	43892930	43893491	IFNA2
chr9	+	21430439	21431315	IFNA1	ENSCAFT00000002602	chr11	-	43792443	43793007	IFNA1_CANFA
chr9	-	21470840	21472312	IFNE	ENSCAFT00000002615	chr11	-	43909685	43910249	IFNE
chr9	+	21792634	21855969	MTAP	ENSCAFT00000002620	chr11	+	44190904	44229901	MTAP
chr9	-	21957750	21965038	CDKN2A	ENSCAFT00000002623	chr11	-	44255704	44256013	ENSCAFG00000001675
chr9	-	21992901	21999312	CDKN2B	ENSCAFT00000002632	chr11	-	44291166	44294900	Q9GMF2_CANFA

Table 3: Genes Amplified in 0123-C Samples Within Syntenic Regions of hsa7.

HUMAN GENOME (SYNTENIC REGION)					CANINE GENOME					RED = evidence from Ensemble, Blue = from tblastn (RefSeq), Black = both
Chromosome	Strand	Start	End	Gene Name	Ensemble Canine Transcript ID or RefSeq ID	Chr	Strand	Start	End	
chr7	+	55947824	55975927	ZNF713	ENSCAFT00000016043	chr6	-	3360437	3371451	ZNF713
chr7	+	55987104	55990527	MRPS17	NM_015969	chr6	+	3447521	3449107	MRPS17
chr7	+	55999789	56035365	GBAS	ENSCAFT00000016070	chr6	+	3453647	3486311	GBAS
chr7	-	56046237	56086762	PSPH	ENSCAFT00000016091	chr6	-	3495206	3501133	PSPH
chr7	+	56086871	56099176	CCT6A	ENSCAFT00000016127	chr6	+	3548427	3558923	ENSCAFG00000010149
chr7	+	56099410	56115859	SUMF2	ENSCAFT00000037029	chr6	+	3559919	3569854	ENSCAFG00000010156
chr7	-	56116168	56128183	PHKG1	ENSCAFT00000016154	chr6	-	3570999	3577275	PHKG1
chr7	-	56136759	56141681	CHCHD2	ENSCAFT00000036609	chr6	-	3584008	3587327	CHCHD2
chr7	+	64975691	65057235	VKORC1L1	ENSCAFT00000016169	chr6	+	3722561	3727185	XM_843392.1
chr7	-	65063107	65084736	GUSB	ENSCAFT00000036132	chr6	-	3727032	3745879	BGLR_CANFA
chr7	+	65178210	65195764	ASL	ENSCAFT00000017006	chr6	-	3770528	3777651	XM_536832.2
chr7	+	65217239	65256988	CRCP	ENSCAFT00000038430	chr6	+	3808608	3843925	CRCP
chr7	+	65307693	65462873	TPST1	ENSCAFT00000017118	chr6	+	3951846	3953303	TPST1
chr7	+	65731302	65745473	KCTD7	ENSCAFT00000017139	chr6	+	4066206	4073510	ENSCAFG00000024640
chr7	+	65843077	65913883	RABGEF1	ENSCAFT00000017144	chr6	+	4116894	4159028	ENSCAFG00000010773
chr7	+	66023637	66060973	C7orf42	ENSCAFT00000017156	chr6	+	4212770	4221928	C7orf42
chr7	-	66090124	66098023	SBDS	ENSCAFT00000017228	chr6	-	4257576	4263768	SBDS
chr7	+	66099251	66341933	TYW1	ENSCAFT00000017631	chr6	+	4265616	4467571	ENSCAFG00000010867
chr7	+	68701840	69895411	AUTS2	ENSCAFT00000017875	chr6	-	5749987	5776825	AUTS2
chr7	+	70235724	70816520	WBSCR17	ENSCAFT00000017769	chr6	-	5133718	5412774	WBSCR17
chr7	-	70882411	71440144	CALN1	NM_031468	chr6	+	4700430	5067949	CALN1
chr7	+	71987871	72056774	POM121	ENSCAFT00000021143	chr6	-	9902782	9927292	ENSCAFG00000013253
chr7	-	72067951	72077933	TRIM74	ENSCAFT00000020820	chr6	+	9875289	9883711	ENSCAFG00000013047
chr7	-	72106962	72114391	STAG3L3	ENSCAFT00000023065	chr6	-	1.2E+07	1.2E+07	ENSCAFG00000014526
chr7	-	72354449	72360800	NSUN5	ENSCAFT00000021018	chr6	+	9889139	9900652	ENSCAFG00000013197
chr7	-	72364470	72380021	TRIM50	ENSCAFT00000020820	chr6	+	9875289	9883711	ENSCAFG00000013047
chr7	+	72380090	72410577	FKBP6	ENSCAFT00000020922	chr6	-	9854159	9869305	FKBP6
chr7	+	72486044	72488386	FZD9	ENSCAFT00000020894	chr6	-	9783778	9785563	FZD9
chr7	-	72492663	72574551	BAZ1B	ENSCAFT00000020881	chr6	+	9710856	9777837	BAZ1B
chr7	-	72588618	72609538	BCL7B	ENSCAFT00000020787	chr6	+	9681894	9701799	BCL7B
chr7	-	72621209	72630949	TBL2	ENSCAFT00000020676	chr6	+	9657381	9662123	TBL2
chr7	-	72645459	72676806	MLXIPL	ENSCAFT00000020619	chr6	+	9634957	9652688	MLXIPL
chr7	+	72720109	72724376	VPS37D	ENSCAFT00000020555	chr6	-	9604833	9607933	VPS37D
chr7	-	72733183	72735717	DNAJC30	ENSCAFT00000020549	chr6	+	9596497	9597169	DNAJC30
chr7	+	72735833	72750478	WBSCR22	ENSCAFT00000020540	chr6	-	9585005	9596297	WBSCR22
chr7	-	72751470	72771953	STX1A	ENSCAFT00000020411	chr6	+	9575887	9582889	STX1A
chr7	-	72788360	72791120	ABHD11	ENSCAFT00000020011	chr6	+	9552153	9554435	ENSCAFG00000012539
chr7	-	72821262	72822536	CLDN3	ENSCAFT00000019892	chr6	+	9535464	9536473	CLD3_CANFA
chr7	+	72883128	72884951	CLDN4	ENSCAFT00000019888	chr6	-	9494748	9495381	CLDN4
chr7	-	72886857	72894791	WBSCR27	ENSCAFT00000019870	chr6	+	9489583	9493475	WBSCR27
chr7	+	72913424	72918159	WBSCR28	ENSCAFT00000019822	chr6	-	9473764	9476214	WBSCR28
chr7	+	73136091	73174790	LIMK1	ENSCAFT00000019799	chr6	-	9265783	9286920	LIMK1
chr7	+	73226641	73249365	EIF4H	ENSCAFT00000019083	chr6	-	9182800	9193584	EIF4H
chr7	+	73262022	73282100	LAT2	ENSCAFT00000019064	chr6	-	9165900	9172570	LAT2
chr7	-	73283767	73306674	RFC2	ENSCAFT00000019010	chr6	+	9138055	9158373	RFC2
chr7	+	73341740	73458209	CLIP2	ENSCAFT00000018930	chr6	-	9035427	9082777	CLIP2
chr7	+	73506055	73654848	GTF2IRD1	ENSCAFT00000018878	chr6	-	8889844	8965279	GTF2IRD1
chr7	+	73826244	73841595	NCF1	ENSCAFT00000018106	chr6	-	8706103	8721194	A7E3M5_CANFA
chr7	-	73848419	73905777	GTF2IRD2	ENSCAFT00000018060	chr6	+	8659716	8696869	XM_844465.1
chr7	-	74094218	74127635	WBSCR16	ENSCAFT00000018027	chr6	-	8607457	8634235	WBSCR16
chr7	+	74146282	74203559	GTF2IRD2B	ENSCAFT00000018060	chr6	+	8659716	8696869	XM_844465.1
chr7	-	74645540	74705277	GATSL2	ENSCAFT00000019856	chr6	+	8585255	8599643	GATS
chr7	+	74826382	74834926	STAG3L1	NM_018991	chr6	+-	1.2E+07	1.2E+07	STAG3L1
chr7	-	74884000	74953504	POM121C	ENSCAFT00000021143	chr6	-	9902783	9927292	ENSCAFG00000013253
chr7	-	75001344	75206215	HIP1	ENSCAFT00000021231	chr6	-	9963063	1E+07	HIP1
chr7	-	75236777	75257000	CCL26	ENSCAFT00000021246	chr6	-	1E+07	1E+07	CCL26_CANFA
chr7	-	75279049	75280969	CCL24	ENSCAFT00000021262	chr6	-	1E+07	1E+07	CCL24_CANFA
chr7	+	75346252	75356180	RHBDD2	ENSCAFT00000021273	chr6	+	1E+07	1E+07	RHBDD2
chr7	+	75382355	75454109	POR	ENSCAFT00000021363	chr6	+	1E+07	1E+07	Q2EFX8_CANFA
chr7	-	75454090	75461928	TMEM120A	ENSCAFT00000021384	chr6	-	1E+07	1E+07	ENSCAFG00000013483
chr7	-	75463590	75515257	STYXL1	ENSCAFT00000036420	chr6	-	1E+07	1E+07	STYXL1
chr7	+	75515328	75533866	MDH2	ENSCAFT00000021459	chr6	+	1E+07	1E+07	Q0QF34_CANFA
chr7	+	75669151	75754541	SRRM3	ENSCAFT00000021471	chr6	+	1E+07	1E+07	SRRM3
chr7	+	75769810	75771550	HSPB1	ENSCAFT00000021478	chr6	+	1E+07	1.1E+07	HSPB1_CANFA
chr7	-	75794043	75826278	YWHAG	ENSCAFT00000021492	chr6	-	1.1E+07	1.1E+07	YWHAG
chr7	-	75856581	75876948	SRCRB4D	ENSCAFT00000021637	chr6	-	1.1E+07	1.1E+07	SRCRB4D
chr7	+	75864776	75909324	ZP3	ENSCAFT00000021646	chr6	+	1.1E+07	1.1E+07	ZP3_CANFA
chr7	+	75928907	75973248	DTX2	ENSCAFT00000021597	chr6	+	1.1E+07	1.1E+07	DTX2
chr7	+	75977680	75995135	UPK3B	ENSCAFT00000021651	chr6	+	1.1E+07	1.1E+07	UPK3B

Table 4: Genes Amplified in 0123-C Samples Within Syntenic Regions of hsa1.

HUMAN GENOME (SYNTENIC REGION)					CANINE GENOME					
Chromosome	Strand	Start	End	Gene Name	Ensemble Canine Transcript ID or RefSeq ID	Chr	Strand	Start	End	RED = evidence from Ensemble, Blue = from tblastn (RefSeq), Black = both
chr1	+	201541286	201545352	BTG2	ENSCAFT00000015026	chr38	+	3071069	3072867	BTG2
chr1	-	201576374	201586912	FMOD	ENSCAFT00000015038	chr38	-	3103689	3112372	FMOD
chr1	+	201711505	201727102	PRELP	ENSCAFT00000015041	chr38	+	3206312	3209828	PRELP
chr1	+	201729893	201744700	OPTC	ENSCAFT00000015046	chr38	+	3215294	3223138	OPT_CANFA
chr1	+	201862550	201979832	ATP2B4	ENSCAFT00000015202	chr38	+	3366526	3415843	ATP2B4
chr1	+	202000906	202012101	LAX1	ENSCAFT00000015207	chr38	+	3429508	3436587	LAX1
chr1	+	202031373	202089879	ZC3H11A	ENSCAFT00000015260	chr38	+	3477875	3503919	ZC3H11A
chr1	+	202097362	202106903	SNRPE	ENSCAFT00000015274	chr38	+	3515732	3521241	SNRPE
chr1	+	202308868	202363494	SOX13	ENSCAFT00000015281	chr38	+	3709350	3720096	SOX13
chr1	-	202366812	202387930	ETNK2	ENSCAFT00000015284	chr38	-	3726820	3740246	ETNK2
chr1	-	202390566	202402088	REN	ENSCAFT00000037807	chr38	-	3744477	3754876	RENI_CANFA
chr1	-	202433910	202449843	GOLT1A	ENSCAFT00000015295	chr38	-	3768838	3778625	GOLT1A
chr1	-	202454603	202595667	PLEKHA6	ENSCAFT00000015332	chr38	-	3804295	3839470	PLEKHA6
chr1	-	202639114	202647567	PPP1R15B	ENSCAFT00000015335	chr38	-	3959584	3965117	PPP1R15B
chr1	-	202658380	202726097	PIK3C2B	ENSCAFT00000015347	chr38	-	3988623	4016123	PIK3C2B
chr1	+	202752133	202793870	MDM4	ENSCAFT00000015363	chr38	+	4055972	4103319	**MDM4**
chr1	-	202852925	202921220	LRRN2	ENSCAFT00000015370	chr38	-	4164479	4166666	XM_545681.1
chr1	+	203064404	203258572	NFASC	ENSCAFT00000015800	chr38	+	4474563	4542491	NFASC
chr1	+	203278962	203313761	CNTN2	ENSCAFT00000037921	chr38	+	4576761	4596329	CNTN2
chr1	-	203318879	203320211	TMEM81	ENSCAFT00000015833	chr38	-	4604335	4605118	TMEM81
chr1	-	203322601	203357754	RBBP5	ENSCAFT00000015870	chr38	-	4608590	4634589	RBBP5
chr1	-	203378254	203447350	DSTYK	ENSCAFT00000015922	chr38	-	4669577	4715897	DUSTY_CANFA
chr1	+	203463660	203509093	TMCC2	ENSCAFT00000015952	chr38	+	4734043	4773669	**TMCC2**
chr1	-	203537813	203557506	NUAK2	ENSCAFT00000015965	chr38	-	4798849	4816487	NUAK2
chr1	-	203572270	203592662	KLHDC8A	ENSCAFT00000015976	chr38	-	4833445	4838972	KLHDC8A
chr1	-	203617135	203657804	LEMD1	ENSCAFT00000039078	chr38	-	4872059	4896801	LEMD1
chr1	-	203684052	203684149	MIR135B	ENSCAFT00000032723	chr38	-	4926412	4926501	**cfa-mir-135b**
chr1	+	203740306	203768543	CDK18	ENSCAFT00000016029	chr38	+	4993764	5001820	PCTK3
chr1	+	203804734	203838669	MFSD4	ENSCAFT00000016099	chr38	+	5037069	5063455	MFSD4
chr1	-	203851857	203868623	ELK4	ENSCAFT00000039294	chr38	-	5077862	5084309	ELK4
chr1	-	203893603	203916253	SLC45A3	ENSCAFT00000016118	chr38	-	5111404	5116718	SLC45A3
chr1	-	203948569	203985984	NUCKS1	ENSCAFT00000016150	chr38	-	5160105	5170400	**NUCKS1**
chr1	-	204003737	204011233	RAB7L1	ENSCAFT00000038496	chr38	-	5197894	5203751	RAB7L1
chr1	-	204024843	204048784	SLC41A1	ENSCAFT00000016167	chr38	-	5218599	5235872	SLC41A1
chr1	-	204063773	204085899	PM20D1	ENSCAFT00000016137	chr38	-	5250126	5270063	PM20D1
chr1	-	204148801	204179211	SLC26A9	NM_052934	chr38	-	5277229	5295877	**SLC26A9**
chr1	+	204390905	204398105	AVPR1B	ENSCAFT00000016207	chr38	-	5436783	5445898	AVPR1B
chr1	-	204405494	204455270	C1orf186	ENSCAFT00000016204	chr38	+	5429891	5433326	C1orf186
chr1	+	204484081	204498727	CTSE	ENSCAFT00000039604	chr38	-	5369143	5380314	CTSE
chr1	+	204710208	204736846	IKBKE	ENSCAFT00000039509	chr38	+	5749400	5771713	IKBKE
chr1	+	204747501	204829239	RASSF5	ENSCAFT00000016265	chr38	+	5842279	5846764	RASSF5
chr1	-	204831597	204852527	LGTN	ENSCAFT00000038953	chr38	-	5851832	5871265	LGTN

Table 5: Genes Amplified in 0123-C Samples Within Syntenic Regions of hsa12.

HUMAN GENOME (SYNTENIC REGION)					CANINE GENOME					
Chromosome	Strand	Start	End	Gene Name	Ensemble Canine Transcript ID or RefSeq ID	Chr	Strand	Start	End	RED = evidence from Ensemble, Blue = from tblastn (RefSeq), Black = both
chr12	+	54316942	54317884	OR10P1	ENSCAFT00000000071	chr10	+	3017177	3032873	OR10P1
chr12	+	54361596	54364661	METTL7B	ENSCAFT00000000074	chr10	+	3070596	3072610	METTL7B
chr12	-	54364622	54387953	ITGA7	ENSCAFT00000000090	chr10	-	3073564	3092166	ITGA7
chr12	+	54396086	54399754	BLOC1S1	ENSCAFT00000000098	chr10	+	3098395	3101514	BLOC1S1
chr12	+	54400417	54404792	RDH5	ENSCAFT00000000100	chr10	+	3102992	3106433	RDH5
chr12	-	54405496	54409177	CD63	ENSCAFT00000000112	chr10	-	3107718	3110156	CD63
chr12	+	54423330	54432931	GDF11	ENSCAFT00000000114	chr10	+	3126648	3127932	GDF11
chr12	-	54432513	54497807	SARNP	ENSCAFT00000000119	chr10	-	3134990	3184782	SARNP
chr12	+	54498072	54501226	ORMDL2	ENSCAFT00000000124	chr10	+	3185119	3187382	ORMDL2
chr12	-	54501010	54509687	DNAJC14	ENSCAFT00000000121	chr10	-	3188423	3194132	ENSCAFG00000000069
chr12	-	54515480	54523002	MMP19	ENSCAFT00000000127	chr10	-	3201034	3206078	MMP19
chr12	-	54581463	54607964	WIBG	ENSCAFT00000000129	chr10	-	3233226	3234388	WIBG
chr12	+	54611212	54634074	DGKA	ENSCAFT00000000131	chr10	+	3257138	3273882	DGKA
chr12	-	54634155	54646093	SILV	ENSCAFT00000000132	chr10	-	3273992	3281426	A7XY82_CANFA
chr12	+	54646822	54652835	CDK2	ENSCAFT00000000140	chr10	+	3282370	3286720	CDK2
chr12	+	54654128	54674755	RAB5B	ENSCAFT00000000142	chr10	+	3301638	3304811	RAB5B
chr12	+	54677309	54685576	SUOX	ENSCAFT00000000143	chr10	+	3310463	3312604	SUOX
chr12	+	54700955	54718486	IKZF4	ENSCAFT00000000148	chr10	+	3328716	3338637	IKZF4
chr12	+	54760158	54765668	ERBB3	ENSCAFT00000000159	chr10	+	3391588	3402928	ERBB3
chr12	+	54784369	54793961	PA2G4	ENSCAFT00000000163	chr10	+	3407167	3415173	PA2G4
chr12	+	54798296	54802545	ZC3H10	ENSCAFT00000000165	chr10	+	3422801	3424109	ZC3H10
chr12	+	54808252	54824727	ESYT1	ENSCAFT00000000170	chr10	+	3429267	3444353	ESYT1
chr12	+	54832601	54838038	MYL6B	ENSCAFT00000000173	chr10	-	3464833	3484579	SMARCC2
chr12	+	54838366	54841633	MYL6	ENSCAFT00000000180	chr10	+	3455562	3462241	MYL6B
chr12	-	54841902	54869618	SMARCC2	NM_003075	chr10	-	3465253	3484570	SMARCC2
chr12	-	54884552	54901971	RNF41	ENSCAFT00000000183	chr10	-	3497655	3504291	RNF41
chr12	+	54904391	54909904	OBFC2B	NM_024068	chr10	+	54904391	54909904	OBFC2B
chr12	+	54910086	54917894	SLC39A5	ENSCAFT00000000184	chr10	+	3535812	3540223	SLC39A5
chr12	-	54917857	54938410	ANKRD52	ENSCAFT00000000185	chr10	-	3545676	3557777	ANKRD52
chr12	+	54946908	54951017	COQ10A	ENSCAFT00000000187	chr10	+	3563586	3566080	COQ10A
chr12	-	54951749	54980442	CS	ENSCAFT00000037011	chr10	-	3568500	3594284	Q0QEK9_CANFA
chr12	-	54990480	54996395	CNPY2	ENSCAFT00000000190	chr10	-	3600731	3602942	CNPY2
chr12	-	54996273	55014104	PAN2	ENSCAFT00000000197	chr10	-	3604363	3617479	PAN2
chr12	+	55018929	55020461	IL23A	ENSCAFT00000000198	chr10	+	3621292	3623442	IL23A
chr12	-	55021650	55040304	STAT2	ENSCAFT00000000201	chr10	-	3625800	3641629	STAT2
chr12	-	55040621	55042850	APOF	ENSCAFT00000000202	chr10	-	3644966	3645760	XM_531636.2
chr12	-	55096424	55129467	TIMELESS	ENSCAFT00000000206	chr10	-	3655847	3669988	TIMELESS
chr12	-	55129552	55134702	MIP	ENSCAFT00000000211	chr10	-	3685926	3689200	MIP_CANFA
chr12	+	55148567	55151034	SPRYD4	ENSCAFT00000000213	chr10	+	3703269	3704202	SPRYD4
chr12	-	55151002	55168448	GLS2	ENSCAFT00000000215	chr10	-	3705202	3720836	GLS2
chr12	+	55201875	55276247	RBMS2	ENSCAFT00000000217	chr10	+	3785509	3811386	ENSCAFG00000000134
chr12	-	55275646	55316430	BAZ2A	ENSCAFT00000000220	chr10	-	3819747	3851812	BAZ2A
chr12	-	55318225	55326119	ATP5B	NM_001686	chr10	-	3853646	3859986	ATP5B
chr12	-	55343391	55368345	PTGES3	ENSCAFT00000000226	chr10	-	3869131	3892218	PTGES3
chr12	-	55392477	55405333	NACA	NM_005594	chr10	-	3922078	3931240	NACA
chr12	-	55411630	55432413	PRIM1	ENSCAFT00000000231	chr10	-	3935703	3958061	PRIM1
chr12	+	55443374	55467841	HSD17B6	ENSCAFT00000000235	chr10	+	3989037	3999343	HSD17B6
chr12	-	55603204	55614456	SDR9C7	ENSCAFT00000000241	chr10	-	4097291	4103734	SDR9C7
chr12	-	55631482	55637685	RDH16	ENSCAFT00000000246	chr10	-	4105413	4113763	RDH16
chr12	+	55674621	55676736	GPR182	ENSCAFT00000037911	chr10	+	4125950	4128084	GPR182
chr12	-	55678884	55686497	ZBTB39	ENSCAFT00000000247	chr10	-	4133499	4135636	ENSCAFG00000000153
chr12	-	55690047	55696611	TAC3	ENSCAFT00000000251	chr10	-	4145522	4148906	TAC3
chr12	-	55708567	55730160	MYO1A	ENSCAFT00000000253	chr10	-	4154597	4174290	MYO1A
chr12	-	55735693	55758841	TMEM194A	ENSCAFT00000000256	chr10	-	4185030	4201175	TMEM194A
chr12	+	55768943	55775526	NAB2	ENSCAFT00000000260	chr10	+	4209765	4214792	NAB2
chr12	-	55775461	55791463	STAT6	NM_003153	chr10	-	4216675	4226135	STAT6
chr12	+	55808548	55893392	LRP1	ENSCAFT00000000295	chr10	+	4243700	4323862	ENSCAFG00000000178
chr12	+	55909622	55914984	SHMT2	ENSCAFT00000000313	chr10	+	4340484	4345325	SHMT2
chr12	-	55914952	55920742	NDUFA4L2	ENSCAFT00000000319	chr10	-	4346146	4347529	NDUFA4L2
chr12	-	55923508	55931236	STAC3	ENSCAFT00000000323	chr10	-	4353694	4359905	STAC3
chr12	-	55933814	55990513	R3HDM2	ENSCAFT00000000344	chr10	-	4363402	4406779	R3HDM2
chr12	+	56114809	56130876	INHBC	ENSCAFT00000000305	chr10	+	4530082	4539543	INHBC
chr12	+	56135362	56138058	INHBE	ENSCAFT00000000350	chr10	+	4544017	4545293	INHBE
chr12	+	56140184	56152312	GLI1	ENSCAFT00000000352	chr10	+	4551656	4558763	GLI1
chr12	-	56152304	56159900	ARHGAP9	ENSCAFT00000000358	chr10	-	4559113	4567620	ARHGAP9
chr12	+	56168117	56196700	MARS	ENSCAFT00000000365	chr10	+	4571896	4589746	MARS
chr12	-	56196637	56200567	DDIT3	ENSCAFT00000000367	chr10	-	4589894	4590495	DDIT3
chr12	+	56202925	56210198	MBD6	NM_052897	chr10	+	4597828	4602646	MBD6
chr12	-	56210360	56227245	DCTN2	ENSCAFT00000000369	chr10	-	4603702	4617222	DCTN2
chr12	+	56230113	56264821	KIF5A	ENSCAFT00000000388	chr10	+	4620144	4647765	KIF5A
chr12	+	56271208	56283477	PIP4K2C	ENSCAFT00000000391	chr10	+	4655367	4662166	PIP4K2C
chr12	+	56284870	56289850	DTX3	ENSCAFT00000035912	chr10	+	4667389	4669194	DTX3
chr12	+	56290229	56297293	GEFT	ENSCAFT00000000393	chr10	+	4671016	4677239	ENSCAFG00000000250
chr12	+	56299959	56306201	SLC26A10	ENSCAFT00000005206	chr10	+	4679960	4686719	SLC26A10
chr12	-	56305817	56313252	B4GALNT1	ENSCAFT00000000401	chr10	-	4687169	4692367	B4GALNT1

Table 5 (continued)

HUMAN GENOME (SYNTENIC REGION)					CANINE GENOME					
Chromosome	Strand	Start	End	Gene Name	Ensemble Canine Transcript ID or RefSeq ID	Chr	Strand	Start	End	RED = evidence from Ensemble, Blue = from tblastn (RefSeq), Black = both
chr12	+	56374004	56401605	OS9	ENSCAFT00000000411	chr10	+	4740112	4770307	OS9
chr12	-	56405260	56422207	AGAP2	ENSCAFT00000000434	chr10	-	4775738	4785620	AGAP2
chr12	+	56425050	56428293	TSPAN31	ENSCAFT00000000436	chr10	+	4793196	4795694	Q9XST6_CANFA
chr12	-	56428269	56432431	CDK4	ENSCAFT00000036354	chr10	-	4795886	4798127	LOC612475
chr12	+	56435166	56439956	MARCH9	ENSCAFT00000000442	chr10	+	4802411	4804813	MARCH9
chr12	-	56442383	56447243	CYP27B1	ENSCAFT00000000446	chr10	-	4809049	4812912	CYP27B1
chr12	-	56448617	56452181	METTL1	ENSCAFT00000000448	chr10	-	4814091	4816648	METTL1
chr12	+	56452649	56462591	FAM119B	ENSCAFT00000000449	chr10	+	4818126	4824474	FAM119B
chr12	+	56462794	56477637	TSFM	ENSCAFT00000000451	chr10	+	4825597	4837939	TSFM
chr12	-	56477427	56496119	AVIL	ENSCAFT00000000466	chr10	-	4839148	4855280	AVIL
chr12	-	56499976	56527014	CTDSP2	ENSCAFT00000000474	chr10	-	4861860	4881275	CTDSP2
chr12	-	56504658	56504742	MIR26A2	ENSCAFT00000032738	chr10	-	4863490	4863550	cfa-mir-26a-2
chr12	+	56621711	56637319	XRCC6BP1	ENSCAFT00000000475	chr10	+	4967525	4981253	XRCC6BP1
chr12	-	61281797	61283481	C12orf61	ENSCAFT00000000526	chr10	-	9569184	9569424	C16orf61
chr12	-	61826482	61832857	AVPR1A	ENSCAFT00000000524	chr10	-	9253792	9257238	AVPR1A
chr12	+	62459903	62489154	TMEM5	ENSCAFT00000000529	chr10	+	9617300	9635557	TMEM5
chr12	+	62524807	62827880	SRGAP1	ENSCAFT00000000539	chr10	+	9799126	9929665	SRGAP1
chr12	-	62872685	62902343	C12orf66	ENSCAFT00000000549	chr10	-	9967769	9985284	C12orf66
chr12	-	62947031	63070612	C12orf56	ENSCAFT00000000550	chr10	-	10012506	10101270	C12orf56
chr12	+	63084499	63128730	XPOT	ENSCAFT00000000554	chr10	+	10112302	10150664	XPOT
chr12	+	63132203	63182158	TBK1	ENSCAFT00000000555	chr10	+	10156670	10195125	TBK1
chr12	+	63290559	63375459	RASSF3	ENSCAFT00000000559	chr10	+	10329794	10337855	RASSF3
chr12	-	63393488	63439493	GNS	ENSCAFT00000000563	chr10	-	10353157	10397858	Q32KH4_CANFA
chr12	-	63730670	63801613	WIF1	ENSCAFT00000000572	chr10	-	10646584	10712600	WIF1
chr12	+	63849617	63928406	LEMD3	ENSCAFT00000036610	chr10	+	10764528	10820664	LEMD3
chr12	+	63958754	64146954	MSRB3	ENSCAFT00000000573	chr10	+	10879352	11024318	MSRB3
chr12	+	64504506	64595574	HMGA2	NM_003483	chr10	+	11338630	11477665	HMGA2
chr12	-	64803116	64810800	LLPH	ENSCAFT00000000574	chr10	-	11618439	11625209	LLPH
chr12	-	64816983	64850074	TMBIM4	ENSCAFT00000000579	chr10	-	11630345	11657235	TMBIM4
chr12	+	64869244	64934659	IRAK3	ENSCAFT00000000586	chr10	+	11683611	11715516	IRAK3
chr12	+	64982622	65018225	HELB	NM_033647	chr10	+	11752158	11758850	HELB
chr12	-	65027478	65359192	GRIP1	ENSCAFT00000000607	chr10	-	11788386	11915927	GRIP1
chr12	+	65949327	65994655	CAND1	ENSCAFT00000000639	chr10	+	12637866	12676783	CAND1
chr12	+	66328778	66342711	DYRK2	ENSCAFT00000000642	chr10	+	12967074	12976524	DYRK2
chr12	-	66834816	66839788	IFNG	ENSCAFT00000000643	chr10	-	13391594	13396426	IFNG_CANFA
chr12	-	66881395	66905838	IL26	ENSCAFT00000000644	chr10	-	13441974	13456177	IL26
chr12	-	66928291	66933548	IL22	ENSCAFT00000000647	chr10	-	13472572	13477017	IL22
chr12	-	66974612	67012428	MDM1	ENSCAFT00000000649	chr10	-	13509169	13537590	MDM1
chr12	+	67290918	67340641	RAP1B	ENSCAFT00000000651	chr10	+	13789941	13801415	RAP1B
chr12	+	67366997	67422740	NUP107	ENSCAFT00000000659	chr10	+	13822941	13842599	NUP107
chr12	+	67488237	67525478	MDM2	ENSCAFT00000000663	chr10	+	13920605	13946580	MDM2_CANFA
chr12	-	67531224	67613246	CPM	ENSCAFT00000000665	chr10	-	13955750	13981764	CPM
chr12	+	67919583	67954405	CPSF6	ENSCAFT00000000672	chr10	+	14256048	14276951	CPSF6
chr12	+	68028400	68034280	LYZ	ENSCAFT00000000675	chr10	+	14330495	14334946	LYSC2_CANFA
chr12	+	68039798	68070843	YEATS4	ENSCAFT00000000678	chr10	+	14348644	14366352	YEATS4
chr12	+	68150395	68259829	FRS2	ENSCAFT00000000681	chr10	+	14529537	14536183	FRS2
chr12	+	68265474	68281624	CCT2	ENSCAFT00000000684	chr10	+	14544444	14562336	LOC607972
chr12	-	68288611	68291209	LRRC10	ENSCAFT00000000687	chr10	-	14568549	14569389	LRRC10
chr12	-	68333655	68369323	BEST3	ENSCAFT00000000688	chr10	-	14584456	14619781	BEST3
chr12	+	68418897	68503251	RAB3IP	ENSCAFT00000000695	chr10	+	14670980	14698165	RAB3IP
chr12	+	68923043	69035040	CNOT2	ENSCAFT00000000698	chr10	+	14708040	14830103	C12orf28
chr12	+	69046328	69111245	KCNMB4	ENSCAFT00000000699	chr10	+	14938188	14939178	ENSCAFG00000000440
chr12	-	69196898	69317486	PTPRB	ENSCAFT00000000717	chr10	-	15264753	15344313	PTPRB
chr12	-	69318128	69600851	PTPRR	ENSCAFT00000000721	chr10	-	15375536	15481818	PTPRR
chr12	-	69805143	69838046	TSPAN8	ENSCAFT00000000723	chr10	-	15775589	15806624	TSPAN8
chr12	+	70120079	70264888	LGR5	ENSCAFT00000000724	chr10	+	15996824	16107136	LGR5
chr12	-	70289648	70344016	ZFC3H1	ENSCAFT00000000728	chr10	-	16148461	16205051	ZFC3H1
chr12	+	70344050	70360686	THAP2	ENSCAFT00000000730	chr10	+	16205779	16216389	THAP2
chr12	+	70366144	70384106	TMEM19	ENSCAFT00000000731	chr10	+	16223779	16240010	TMEM19
chr12	+	70434924	70467417	RAB21	ENSCAFT00000038239	chr10	+	16276683	16313261	RAB21_CANFA
chr12	+	70519753	70606894	TBC1D15	ENSCAFT00000000735	chr10	+	16370072	16413667	TBC1D15
chr12	+	70618892	70712488	TPH2	ENSCAFT00000000740	chr10	+	16430948	16514219	B6EY12_CANFA
chr12	+	70952795	71345688	TRHDE	ENSCAFT00000000753	chr10	+	16931619	17102952	ENSCAFG00000000473
chr12	+	73217817	73221490	ATXN7L3B	ENSCAFT00000037473	chr10	+	18348370	18348664	ENSCAFG00000024260
chr12	-	73720162	73889778	KCNC2	ENSCAFT00000000758	chr10	-	18630367	18638947	KCNC2
chr12	-	73956025	74010103	CAPS2	ENSCAFT00000000762	chr10	-	18830524	18865417	CAPS2
chr12	+	74014729	74050436	GLIPR1L1	ENSCAFT00000035568	chr10	+	18887989	18902165	GLIPR1L1
chr12	+	74071155	74104087	GLIPR1L2	ENSCAFT00000000766	chr10	+	18912998	18927856	GLIPR1L2
chr12	+	74160779	74181983	GLIPR1	ENSCAFT00000000817	chr10	+	18947774	18965415	GLIPR1
chr12	-	74177685	74191685	KRR1	ENSCAFT00000000822	chr10	-	18966402	18980749	KRR1

Table 6: Genes Deleted in 0123-C Samples Within Syntenic Regions of hsa6.

HUMAN GENOME (SYNTENIC REGION)					CANINE GENOME					
Chromosome	Strand	Start	End	Gene Name	Ensemble Canine Transcript ID or RefSeq ID	Chr	Strand	Start	End	RED = evidence from Ensemble, Blue = from tblastn (RefSeq), Black = both
chr6	+	116798802	116866135	DSE	ENSCAFT00000001378	chr1	+	59864306	59916896	DSE
chr6	+	116889248	116891627	FAM26F	ENSCAFT00000035848	chr1	+	59944383	59946149	FAM26F
chr6	-	116924343	116973466	BET3L	ENSCAFT00000001382	chr1	-	59973809	60008060	BET3L
chr6	+	116939500	116946402	FAM26E	ENSCAFT00000001381	chr1	+	59978616	59983205	FAM26E
chr6	+	116956887	116986724	FAM26D	ENSCAFT00000001383	chr1	+	60022719	60027694	FAM26D
chr6	+	116999275	117021129	RWDD1	ENSCAFT00000001386	chr1	+	60036888	60056674	RWDD1
chr6	+	117044334	117060841	RSPH4A	ENSCAFT00000035490	chr1	+	60114268	60127176	RSHL1
chr6	-	117063473	117096666	ZUFSP	ENSCAFT00000001397	chr1	-	60129743	60156468	ZUFSP
chr6	+	117109059	117169723	KPNA5	ENSCAFT00000001405	chr1	+	60167456	60201256	KPNA5
chr6	-	117180052	117193579	FAM162B	ENSCAFT00000001408	chr1	-	60211841	60219162	FAM162B
chr6	-	117219940	117256891	GPRC6A	ENSCAFT00000001414	chr1	-	60240863	60261409	GPRC6A
chr6	+	117305068	117360019	RFX6	ENSCAFT00000001421	chr1	+	60291580	60346011	RFX6
chr6	+	117693413	117701421	VGLL2	ENSCAFT00000036780	chr1	+	60579585	60586174	VGLL2
chr6	-	117716222	117853711	ROS1	ENSCAFT00000001427	chr1	-	60605780	60726344	Q6JDH3_CANFA
chr6	+	117910512	117997713	DCBLD1	ENSCAFT00000001430	chr1	+	60783189	60822062	DCBLD1
chr6	-	117988125	118030398	GOPC	ENSCAFT00000001435	chr1	-	60842529	60878332	GOPC
chr6	+	118103309	118138579	NUS1	ENSCAFT00000001438	chr1	+	60918954	60944908	NUS1
chr6	+	118335381	118745532	SLC35F1	ENSCAFT00000001439	chr1	+	61307290	61451160	SLC35F1
chr6	-	118888627	119079713	C6orf204	ENSCAFT00000001441	chr1	-	61547829	61680636	C6orf204
chr6	+	118976134	118988280	PLN	ENSCAFT00000001443	chr1	+	61632414	61643805	PPLA_CANFA
chr6	+	119263627	119272034	ASF1A	ENSCAFT00000001453	chr1	+	61827956	61886947	ASF1A
chr6	-	119273460	119298002	MCM9	ENSCAFT00000001448	chr1	-	61820428	61912549	MCM9
chr6	-	119322694	119441511	FAM184A	ENSCAFT00000001463	chr1	-	61958108	62022160	FAM184A
chr6	-	119540965	119712625	MAN1A1	ENSCAFT00000001467	chr1	-	62162683	62326669	Q6JDJ4_CANFA
chr6	+	121798443	121812572	GJA1	NM_000165	chr1	+	63994950	63996093	GJA1
chr6	+	122762394	122795963	HSF2	ENSCAFT00000001507	chr1	+	64845053	64863856	Q6JDK4_CANFA
chr6	-	122806191	122834651	SERINC1	ENSCAFT00000001531	chr1	-	64870154	64900562	SERINC1
chr6	+	122834760	123089217	PKIB	ENSCAFT00000001533	chr1	+	65098535	65103729	PKIB
chr6	+	123142344	123146917	FABP7	ENSCAFT00000001539	chr1	+	65139822	65143881	FABP7
chr6	+	123151669	123172563	SMPDL3A	ENSCAFT00000001544	chr1	+	65147454	65165415	SMPDL3A
chr6	+	123359280	123426762	CLVS2	ENSCAFT00000001550	chr1	+	65273343	65337695	RLBP1L2
chr6	-	123579181	123999641	TRDN	ENSCAFT00000001573	chr1	-	65458042	65817870	TRDN_CANFA
chr6	+	124166767	125188485	NKAIN2	ENSCAFT00000001579	chr1	+	66278073	66908377	NKAIN2
chr6	+	125346212	125446360	RNF217	ENSCAFT00000001581	chr1	+	67099212	67141812	RNF217
chr6	+	125516577	125626343	TPD52L1	ENSCAFT00000013354	chr1	+	67240749	67273789	TPD52L1
chr6	-	125638194	125664981	HDDC2	ENSCAFT00000035528	chr1	-	67279512	67304450	HDDC2
chr6	+	126153693	126293959	NCOA7	ENSCAFT00000001606	chr1	+	67792941	67867503	NCOA7
chr6	+	126319553	126343082	HINT3	ENSCAFT00000001613	chr1	+	67693792	67902785	HINT3
chr6	+	126349268	126402113	TRMT11	ENSCAFT00000035268	chr1	+	67918137	67974135	TRMT11
chr6	+	127481740	127559877	RSPO3	ENSCAFT00000037685	chr1	+	68940899	69031073	RSPO3
chr6	+	127629712	127651197	RNF146	ENSCAFT00000001634	chr1	+	69065532	69066615	RNF146
chr6	-	127651549	127705245	ECHDC1	ENSCAFT00000001635	chr1	-	69069277	69110641	ECHDC1
chr6	-	127801243	127882193	C6orf174	ENSCAFT00000001637	chr1	-	69217193	69261104	ENSCAFG00000001071
chr6	-	127801243	127822228	KIAA0408	NM_014702	chr1	-	69188037	69195066	KIAA0408
chr6	+	127940011	127954653	C6orf58	ENSCAFT00000001639	chr1	+	69326956	69338755	ENSCAFG00000001072
chr6	-	128071031	128281469	THEMIS	ENSCAFT00000001645	chr1	-	69506890	69551307	THEMIS
chr6	-	128331616	128883512	PTPRK	ENSCAFT00000001682	chr1	-	69653330	69778386	PTPRK
chr6	+	129245978	129879403	LAMA2	ENSCAFT00000001697	chr1	+	70790696	71150490	Q6JDJ8_CANFA
chr6	-	129939932	130073063	ARHGAP18	NM_033515	chr1	-	71199655	71255741	ARHGAP18
chr6	-	130194081	130224109	C6orf191	NM_001010876	chr1	-	71431500	71438571	C6orf191
chr6	+	130381420	130504287	L3MBTL3	ENSCAFT00000001708	chr1	+	71616975	71712469	L3MBTL3
chr6	-	130507153	130585792	SAMD3	ENSCAFT00000001709	chr1	-	71716730	71753831	SAMD3
chr6	+	130799954	130805903	TMEM200A	ENSCAFT00000001710	chr1	+	71904319	71905798	TMEM200A
chr6	-	131202180	131426155	EPB41L2	ENSCAFT00000001740	chr1	-	72177842	72278445	EPB41L2
chr6	+	131508153	131646366	AKAP7	ENSCAFT00000001765	chr1	+	72537649	72537889	AKAP7
chr6	+	132170848	132257988	ENPP1	NM_006208	chr1	-	3252003	3321678	ENPP1
chr6	-	132311009	132314211	CTGF	ENSCAFT00000000288	chr1	-	28055665	28057076	CTGF
chr6	-	132658886	132764357	MOXD1	ENSCAFT00000000292	chr1	-	28454306	28548258	MOXD1
chr6	-	132820355	132876030	STX7	ENSCAFT00000000293	chr1	-	28598727	28643869	STX7
chr6	-	133007815	133008835	TAAR1	NM_138327	chr1	-	28681545	28682551	TAAR1
chr6	-	133043689	133076887	VNN1	ENSCAFT00000036358	chr1	-	28714676	28733472	VNN1_CANFA
chr6	-	133106701	133120715	VNN2	NM_004665	chr1	-	28715094	28811985	VNN2
chr6	-	133132199	133161440	C6orf192	ENSCAFT00000000298	chr1	-	28835229	28858477	C6orf192
chr6	+	133177400	133180396	RPS12	ENSCAFT00000000299	chr1	+	28873184	29001514	RPS12
chr6	+	133604187	133894951	EYA4	ENSCAFT00000000314	chr1	+	29482791	29549164	EYA4
chr6	+	134251951	134258368	TCF21	ENSCAFT00000000328	chr1	+	29895776	29898078	TCF21
chr6	+	134315993	134350322	TBPL1	ENSCAFT00000000332	chr1	+	29938687	29975897	TBPL1
chr6	-	134350411	134415482	SLC2A12	ENSCAFT00000000338	chr1	-	29979675	30014297	SLC2A12
chr6	-	134532076	134537727	SGK1	ENSCAFT00000000342	chr1	-	30126357	30194825	Q6JDG9_CANFA
chr6	-	135280220	135312953	ALDH8A1	ENSCAFT00000000353	chr1	-	30712020	30733865	ALDH8A1
chr6	-	135323213	135417729	HBS1L	ENSCAFT00000035155	chr1	-	30743800	30830202	HBS1L
chr6	+	135544145	135582003	MYB	ENSCAFT00000000363	chr1	+	30947385	30980426	Q9XT66_CANFA
chr6	-	135646802	135860596	AHI1	ENSCAFT00000000373	chr1	-	31158732	31221849	AHI1
chr6	+	136214526	136558402	PDE7B	ENSCAFT00000000378	chr1	+	31758274	31830775	PDE7B
chr6	-	136593860	136613142	FAM54A	ENSCAFT00000000380	chr1	-	31869807	31882476	FAM54A
chr6	-	136619693	136652682	BCLAF1	ENSCAFT00000000383	chr1	-	31894103	31912546	BCLAF1
chr6	-	136705564	136913485	MAP7	ENSCAFT00000000389	chr1	-	31975332	32031527	MAP7
chr6	-	136919879	137155349	MAP3K5	ENSCAFT00000000397	chr1	-	32170029	32349433	MAP3K5
chr6	+	137185394	137276765	PEX7	ENSCAFT00000000399	chr1	+	32380584	32461265	PEX7

Table 6 (continued)

HUMAN GENOME (SYNTENIC REGION)					CANINE GENOME Ensemble Canine					RED = evidence from Ensemble, Blue = from tblastn (RefSeq), Black = both
Chromosome	Strand	Start	End	Gene Name	Transcript ID or RefSeq ID	Chr	Strand	Start	End	
chr6	+	137285094	137288469	SLC35D3	ENSCAFT00000000400	chr1	+	32469193	32471385	SLC35D3
chr6	-	137362800	137407991	IL20RA	ENSCAFT00000000403	chr1	-	32549803	32568492	IL20RA
chr6	-	137506649	137536478	IL22RA2	ENSCAFT00000000408	chr1	-	32654963	32674715	IL22RA2
chr6	-	137560313	137582260	IFNGR1	ENSCAFT00000000413	chr1	-	32690793	32712820	IFNGR1
chr6	-	137855028	137857224	OLIG3	ENSCAFT00000000416	chr1	-	32963426	32964242	OLIG3
chr6	+	138230273	138246142	TNFAIP3	ENSCAFT00000000421	chr1	+	33294306	33304234	TNFAIP3
chr6	-	138451334	138470353	PERP	ENSCAFT00000000422	chr1	-	33463257	33478443	PERP
chr6	+	138524745	138707493	KIAA1244	ENSCAFT00000000423	chr1	+	33568203	33695313	KIAA1244
chr6	+	138767028	138776275	HEBP2	ENSCAFT00000000424	chr1	+	33759879	33767733	HEBP2
chr6	-	138784873	138862272	NHSL1	ENSCAFT00000000426	chr1	-	33783710	33849589	NHSL1
chr6	+	139136349	139156149	CCDC28A	ENSCAFT00000000433	chr1	+	34087361	34100917	CCDC28A
chr6	+	139158940	139267212	ECT2L	ENSCAFT00000035252	chr1	+	34133017	34136595	ECT2L
chr6	-	139267312	139351091	REPS1	ENSCAFT00000000437	chr1	-	34184744	34224766	REPS1
chr6	+	139391511	139406132	C6orf115	ENSCAFT00000000438	chr1	+	34298335	34310270	C6orf115
chr6	+	139497941	139543639	HECA	ENSCAFT00000000439	chr1	+	34406288	34416670	HECA
chr6	-	139602891	139654901	TXLNB	ENSCAFT00000000441	chr1	-	34460653	34507740	TXLNB
chr6	-	139735089	139737043	CITED2	ENSCAFT00000000443	chr1	-	34566914	34567736	ENSCAFG00000000285
chr6	-	142438437	142451629	NMBR	ENSCAFT00000000452	chr1	-	36816604	36833075	NMBR
chr6	+	142510102	142583778	VTA1	ENSCAFT00000000455	chr1	+	36894133	36937613	VTA1
chr6	+	142664748	142809096	GPR126	ENSCAFT00000000457	chr1	+	37076917	37147228	GPR126
chr6	-	143114296	143308031	HIVEP2	ENSCAFT00000000460	chr1	-	37412108	37433278	Q6JDK8_CANFA
chr6	+	143423715	143703134	AIG1	ENSCAFT00000000463	chr1	+	37686936	37920834	AIG1
chr6	-	143785661	143813534	ADAT2	ENSCAFT00000000467	chr1	-	38008649	38036784	ADAT2
chr6	+	143813610	143853444	PEX3	ENSCAFT00000000471	chr1	+	38037177	38066847	PEX3
chr6	-	143857641	143874713	FUCA2	ENSCAFT00000000476	chr1	-	38071314	38086165	FUCA2
chr6	+	143971009	144194015	PHACTR2	ENSCAFT00000000479	chr1	+	38297787	38374244	PHACTR2
chr6	+	144206200	144226636	LTV1	ENSCAFT00000000484	chr1	+	38404057	38416474	LTV1
chr6	+	144227265	144301176	C6orf94	ENSCAFT00000037949	chr1	+	38426963	38459468	C6orf94
chr6	-	144303129	144427428	PLAGL1	ENSCAFT00000000490	chr1	-	38462171	38467955	PLAGL1
chr6	-	144457710	144458447	SF3B5	NM_031287	chr1	+-	38601197	38601455	SF3B5
chr6	+	144513346	144554769	STX11	ENSCAFT00000000493	chr1	+	38686128	38687777	STX11
chr6	+	144654565	145215863	UTRN	ENSCAFT00000000501	chr1	+	38777103	39263729	NP_001012395.1
chr6	-	145988132	146098684	EPM2A	ENSCAFT00000035347	chr1	-	39913037	40019725	EPM2A_CANFA
chr6	-	146160964	146177614	FBXO30	ENSCAFT00000000507	chr1	-	40052472	40059426	FBXO30
chr6	-	146247636	146326926	SHPRH	ENSCAFT00000000517	chr1	-	40120671	40205370	SHPRH
chr6	+	146390474	146800424	GRM1	ENSCAFT00000000530	chr1	+	40250881	40251767	ENSCAFG00000024218
chr6	+	146906520	146917779	RAB32	ENSCAFT00000000532	chr1	+	40755312	40760311	RAB32
chr6	+	147567200	147750400	STXBP5	ENSCAFT00000000561	chr1	+	41313654	41475608	STXBP5
chr6	+	148705421	148914877	SASH1	ENSCAFT00000000575	chr1	+	42441515	42516604	SASH1
chr6	+	149109963	149439819	UST	ENSCAFT00000000577	chr1	+	42675437	42961301	UST
chr6	+	149681128	149774440	TAB2	NM_015093	chr1	+	43208888	43255952	TAB2
chr6	+	149763187	149763875	SUMO4	ENSCAFT00000000584	chr1	+	43208831	43256586	MAP3K7IP2
chr6	-	149810458	149847841	ZC3H12D	ENSCAFT00000000588	chr1	-	43295379	43312706	ZC3H12D
chr6	-	149867323	149908864	PPIL4	ENSCAFT00000000593	chr1	-	43339443	43383471	Q6JDI1_CANFA
chr6	+	149929220	149953760	C6orf72	ENSCAFT00000000596	chr1	+	43390788	43415634	C6orf72
chr6	-	149957864	150001421	KATNA1	ENSCAFT00000000603	chr1	-	43417719	43464002	KATNA1
chr6	-	150023743	150081085	LATS1	ENSCAFT00000000614	chr1	-	43474831	43499007	NP_001019806.1
chr6	-	150087149	150109381	NUP43	ENSCAFT00000000620	chr1	-	43525916	43535410	NUP43
chr6	+	150112523	150174250	PCMT1	ENSCAFT00000000625	chr1	+	43537859	43582336	PCMT1
chr6	-	150181586	150227173	LRP11	ENSCAFT00000000626	chr1	-	43590480	43634673	LRP11
chr6	-	150251293	150253790	RAET1E	ENSCAFT00000037310	chr1	-	43646285	43648524	RAET1E
chr6	-	150279706	150285907	RAET1G	NM_001001788	chr1	-	43647197	43647921	RAET1G
chr6	+	150304828	150312061	ULBP2	NM_025217	chr1	-	43647197	43647921	ULBP2
chr6	+	150326835	150336539	ULBP1	NM_025218	chr1	-	43647200	43647921	ULBP1
chr6	+	150505880	150613221	PPP1R14C	ENSCAFT00000000631	chr1	+	43754381	43838944	PPP1R14C
chr6	+	150731720	150767458	IYD	ENSCAFT00000000633	chr1	+	43933596	43951500	IYD
chr6	+	150962691	151206492	PLEKHG1	ENSCAFT00000000638	chr1	+	44250292	44340718	PLEKHG1
chr6	+	151228383	151464716	MTHFD1L	ENSCAFT00000000656	chr1	+	44362051	44533921	MTHFD1L
chr6	+	151602826	151721390	AKAP12	ENSCAFT00000000664	chr1	+	44660605	44754574	AKAP12
chr6	-	151726942	151754370	ZBTB2	ENSCAFT00000000667	chr1	-	44766326	44773632	ZBTB2
chr6	-	151767681	151815009	RMND1	ENSCAFT00000000670	chr1	-	44800742	44839066	RMND1
chr6	+	151815114	151832925	C6orf211	ENSCAFT00000000674	chr1	+	44845504	44859403	C6orf211
chr6	+	151856867	151984021	C6orf97	ENSCAFT00000000677	chr1	+	44921552	44977888	C6orf97
chr6	+	152053323	152466101	ESR1	ENSCAFT00000000680	chr1	+	45129992	45409811	ESR1
chr6	-	152484514	152542294	SYNE1	ENSCAFT00000000760	chr1	-	45429640	45773768	SYNE1
chr6	+	153060722	153087408	MYCT1	ENSCAFT00000000829	chr1	+	45932250	45952025	MYCT1
chr6	+	153113625	153122593	VIP	ENSCAFT00000000831	chr1	+	45988521	45993428	VIP_CANFA
chr6	-	153333350	153345896	FBXO5	ENSCAFT00000000840	chr1	-	46184142	46194160	FBXO5
chr6	-	153350092	153365618	MTRF1L	ENSCAFT00000000841	chr1	-	46200672	46211909	MTRF1L
chr6	-	153373724	153494082	RGS17	ENSCAFT00000000847	chr1	-	46220147	46249324	RGS17
chr6	+	154373328	154482286	OPRM1	ENSCAFT00000036590	chr1	+	47018027	47066130	OPRM1
chr6	-	154517309	154719592	IPCEF1	ENSCAFT00000000861	chr1	-	47116628	47186909	IPCEF1
chr6	-	154768124	154873445	CNKSR3	ENSCAFT00000000867	chr1	-	47327575	47361284	CNKSR3
chr6	+	155096203	155196886	RBM16	ENSCAFT00000000878	chr1	+	47633528	47681831	Q6JDJ9_CANFA
chr6	+	155453114	155620549	TIAM2	ENSCAFT00000000892	chr1	+	47940412	48045215	TIAM2
chr6	-	155620481	155677318	TFB1M	ENSCAFT00000000895	chr1	-	48045720	48115883	TFB1M
chr6	+	155626838	155639374	CLDN20	ENSCAFT00000000897	chr1	+	48062727	48063387	CLDN20
chr6	-	155758193	155818729	NOX3	ENSCAFT00000000923	chr1	-	48173744	48231143	A7E3L1_CANFA
chr6	+	157140755	157573605	ARID1B	ENSCAFT00000000940	chr1	+	49718285	49843245	ARID1B
chr6	+	157722544	158014965	ZDHHC14	NM_024630	chr1	+	49986429	50258873	ZDHHC14
chr6	+	158164281	158286097	SNX9	ENSCAFT00000000969	chr1	+	50436289	50498735	SNX9

Table 6 (continued)

HUMAN GENOME (SYNTENIC REGION)					CANINE GENOME Ensemble Canine					RED = evidence from Ensemble, Blue =
Chromosome	Strand	Start	End	Gene Name	Transcript ID or RefSeq ID	Chr	Strand	Start	End	from tblastn (RefSeq), Black = both
chr6	+	158322875	158440195	SYNJ2	ENSCAFT00000000998	chr1	+	50550971	50622090	SYNJ2
chr6	-	158450523	158509300	SERAC1	ENSCAFT00000000999	chr1	-	50642817	50692684	SERAC1
chr6	+	158509366	158540364	GTF2H5	ENSCAFT00000001001	chr1	+	50711828	50723839	GTF2H5
chr6	+	158653679	158852844	TULP4	ENSCAFT00000001007	chr1	+	50919149	50993873	TULP4
chr6	+	158877455	158976455	TMEM181	ENSCAFT00000001010	chr1	+	51025868	51097443	TMEM181
chr6	-	158977494	158985792	DYNLT1	ENSCAFT00000001013	chr1	-	51101240	51108740	DYNLT1
chr6	+	158991033	159105889	SYTL3	ENSCAFT00000001014	chr1	+	51125124	51202177	SYTL3
chr6	-	159106760	159159328	EZR	ENSCAFT00000001022	chr1	-	51203784	51252401	VIL2
chr6	-	159318253	159341186	RSPH3	ENSCAFT00000001027	chr1	-	51371554	51392086	RSPH3
chr6	-	159376014	159386172	TAGAP	ENSCAFT00000001032	chr1	-	51425889	51433831	TAGAP
chr6	+	159510416	159613130	FNDC1	ENSCAFT00000001034	chr1	+	51570226	51644667	FNDC1
chr6	-	160020138	160034343	SOD2	ENSCAFT00000001037	chr1	-	51988448	51997380	SOD2
chr6	+	160068141	160090443	WTAP	NM_152858	chr1	+	52026654	52038998	WTAP
chr6	+	160102978	160120077	ACAT2	ENSCAFT00000001128	chr1	+	52054081	52071488	ACAT2
chr6	-	160119519	160130725	TCP1	ENSCAFT00000001141	chr1	-	52071623	52080203	TCP1
chr6	+	160131481	160139451	MRPL18	NM_014161	chr1	+	52081299	52085691	MRPL18
chr6	+	160141290	160161725	PNLDC1	ENSCAFT00000001145	chr1	+	52087556	52105147	PNLDC1
chr6	+	160247963	160249097	MAS1	ENSCAFT00000001147	chr1	+	52146609	52147589	ENSCAFG00000000742
chr6	+	160310120	160447573	IGF2R	ENSCAFT00000001105	chr1	+	52221868	52303183	B1H0W0_CANFA
chr6	+	160462852	160499740	SLC22A1	ENSCAFT00000001164	chr1	+	52311576	52340730	SLC22A1
chr6	-	160557783	160599953	SLC22A2	NM_003058	chr1	+	52311576	52338195	SLC22A2
chr6	+	160689414	160796004	SLC22A3	ENSCAFT00000001165	chr1	+	52452474	52539630	SLC22A3
chr6	+	161043214	161095075	PLG	ENSCAFT00000001179	chr1	-	52541713	52579725	PLMN_CANFA
chr6	+	161332811	161458407	MAP3K4	ENSCAFT00000035541	chr1	+	52635423	52746115	MAP3K4
chr6	-	161471046	161615097	AGPAT4	ENSCAFT00000001195	chr1	-	52754083	52785720	AGPAT4
chr6	-	161688579	163068824	PARK2	ENSCAFT00000035270	chr1	-	52932982	52971374	XM_850059.1
chr6	+	163068153	163656514	PACRG	NM_152410	chr1	+	54246129	54760613	PACRG
chr6	+	163755664	163919618	QKI	ENSCAFT00000035144	chr1	+	54843700	54994615	QKI_CANFA
chr6	-	165613142	165643101	C6orf118	ENSCAFT00000001217	chr1	-	56460540	56480903	C6orf118
chr6	-	165660767	165995574	PDE10A	ENSCAFT00000001259	chr1	-	56505858	56596845	PDE10A
chr6	-	166491075	166502121	T	ENSCAFT00000001265	chr1	-	57228891	57237728	BRAC_CANFA
chr6	-	166653505	166675981	SFT2D1	ENSCAFT00000001268	chr1	-	57381330	57399484	SFT2D1
chr6	-	166742843	166960716	RPS6KA2	ENSCAFT00000001310	chr1	-	57464894	57627005	RPS6KA2
chr6	-	167262993	167290067	RNASET2	ENSCAFT00000001318	chr1	-	57848731	57866619	ENSCAFG00000000842
chr6	+	167332805	167374056	FGFR1OP	ENSCAFT00000001325	chr1	+	57900888	57925220	FGFR1OP
chr6	+	167445284	167472619	CCR6	ENSCAFT00000035698	chr1	+	57980037	58006381	CCR6
chr6	-	167490349	167491309	GPR31	ENSCAFT00000001332	chr1	-	58022503	58024290	GPR31
chr6	+	167624792	167649492	UNC93A	ENSCAFT00000001341	chr1	+	58482631	58580899	Q6JDJ2_CANFA
chr6	+	168161401	168188618	KIF25	ENSCAFT00000001345	chr1	+	58585083	58635386	KIF25
chr6	-	168199312	168222688	FRMD1	ENSCAFT00000001346	chr1	-	58645361	58657463	FRMD1
chr6	-	168450432	168463251	DACT2	ENSCAFT00000001347	chr1	-	58776992	58786667	DACT2
chr6	+	168584679	168810599	SMOC2	ENSCAFT00000001348	chr1	+	58876267	59034371	SMOC2
chr6	-	169357799	169396062	THBS2	ENSCAFT00000001365	chr1	-	59454408	59477077	THBS2
chr6	-	169857307	170102159	WDR27	ENSCAFT00000001373	chr1	-	59714992	59730235	WDR27

Table 7: Genes Deleted in 0123-C Samples Within Syntenic Regions of hsa13.

HUMAN GENOME (SYNTENIC REGION)					CANINE GENOME					RED = evidence from Ensemble, Blue = from tblastn (RefSeq), Black = both
Chromosome	Strand	Start	End	Gene Name	Ensemble Canine Transcript ID or RefSeq ID	Chr	Strand	Start	End	
chr13	+	19105787	19145599	MPHOSPH8	ENSCAFT00000011808	chr25	-	21376192	21426386	MPHOSPH8
chr13	-	19146895	19255083	PSPC1	ENSCAFT00000039169	chr25	+	21280120	21372007	PSPC1
chr13	-	19295623	19335776	ZMYM5	ENSCAFT00000011776	chr25	+	21214501	21230792	ZMYM5
chr13	+	19430973	19563968	ZMYM2	ENSCAFT00000011765	chr25	-	21035545	21110709	ZMYM2
chr13	-	19610394	19633183	GJA3	ENSCAFT00000011715	chr25	+	20986634	20987933	ENSCAFG00000007321
chr13	-	19659603	19665114	GJB2	ENSCAFT00000011711	chr25	+	20940046	20940727	Q8SPL9_CANFA
chr13	-	19694100	19703372	GJB6	ENSCAFT00000011709	chr25	+	20904637	20906184	GJB6
chr13	-	19875805	19998012	CRYL1	ENSCAFT00000011676	chr25	+	20572718	20717134	CRYL1
chr13	+	20039207	20163576	IFT88	ENSCAFT00000011646	chr25	-	20399293	20535083	IFT88
chr13	-	20201072	20246057	N6AMT2	ENSCAFT00000011595	chr25	+	20354782	20365927	N6AMT2
chr13	-	20249467	20374913	XPO4	ENSCAFT00000011580	chr25	+	20215183	20332563	XPO4
chr13	-	20445175	20533722	LATS2	ENSCAFT00000011560	chr25	+	20095332	20152438	LATS2
chr13	-	20625733	20648741	SKA3	ENSCAFT00000011522	chr25	+	19966790	19985673	SKA3
chr13	+	20648371	20651220	MRP63	ENSCAFT00000041346	chr25	-	19908561	19908668	ENSCAFG00000027063
chr13	-	20848507	20931423	ZDHHC20	ENSCAFT00000038556	chr25	+	19867625	19936565	ZDHHC20
chr13	-	20964827	21076355	EFHA1	ENSCAFT00000011503	chr25	+	19712660	19838320	EFHA1
chr13	+	21143214	21176640	FGF9	ENSCAFT00000011481	chr25	-	19346062	19649017	FGF9
chr13	+	22653059	22797304	SGCG	ENSCAFT00000011472	chr25	-	18288302	18366570	SGCG_CANFA
chr13	-	22800964	22905841	SACS	ENSCAFT00000011461	chr25	+	18236070	18259278	SACS
chr13	+	23051638	23141412	TNFRSF19	ENSCAFT00000011444	chr25	-	17978934	18041520	TNFRSF19
chr13	-	23202327	23361587	MIPEP	ENSCAFT00000011440	chr25	+	17743869	17916519	MIPEP
chr13	+	23361027	23364242	PCOTH	NM_001014442	chr25	-	17733165	17733465	PCOTH
chr13	+	23632860	23779212	SPATA13	ENSCAFT00000011396	chr25	+	17660785	17714660	SPATA13
chr13	+	23781715	23794669	C1QTNF9	ENSCAFT00000011399	chr25	+	17726880	17733805	XM_846206.1
chr13	-	23893068	23984948	PARP4	ENSCAFT00000011825	chr25	-	21432112	21521270	PARP4
chr13	+	24152548	24183923	ATP12A	NM_001676	chr25	-	21736512	21761320	ATP12A
chr13	+	24236300	24352058	RNF17	ENSCAFT00000011897	chr25	-	21597501	21710956	RNF17
chr13	-	24354411	24395085	CENPJ	ENSCAFT00000011844	chr25	+	21545147	21593788	CENPJ
chr13	-	24640671	24643857	FAM123A	NM_152704	chr25	+	17273005	17275075	FAM123A
chr13	-	24718340	24759704	MTMR6	ENSCAFT00000011353	chr25	+	17169049	17204675	MTMR6
chr13	+	24773665	24814561	NUPL1	ENSCAFT00000011338	chr25	-	17106195	17144526	NUPL1
chr13	+	24844208	25493420	ATP8A2	ENSCAFT00000011254	chr25	-	16623302	16702647	ENSCAFG00000007007
chr13	-	25516734	25523198	SHISA2	ENSCAFT00000011144	chr25	+	16458367	16463576	TMEM46
chr13	-	25684904	25693840	RNF6	ENSCAFT00000011085	chr25	+	16185756	16193587	RNF6
chr13	+	25726755	25876569	CDK8	ENSCAFT00000011055	chr25	-	16046024	16165769	CDK8
chr13	+	26029839	26161082	WASF3	ENSCAFT00000019238	chr25	-	15792432	15834308	WASF3
chr13	-	26227338	26232922	GPR12	ENSCAFT00000010970	chr25	+	15725214	15726219	GPR12
chr13	-	26538286	26644033	USP12	ENSCAFT00000024112	chr25	+	15376364	15461321	USP12
chr13	+	26723691	26728702	RPL21	ENSCAFT00000010959	chr25	-	15314090	15318456	XM_859407.1
chr13	+	26742463	26745827	RASL11A	ENSCAFT00000010941	chr25	-	15303298	15305658	RASL11A
chr13	+	26896680	26907846	GTF3A	ENSCAFT00000010938	chr25	-	15158723	15171044	GTF3A
chr13	-	26907775	26922326	MTIF3	ENSCAFT00000010929	chr25	+	15154464	15158801	MTIF3
chr13	-	27018049	27092720	LNX2	ENSCAFT00000010916	chr25	+	15026765	15061732	LNX2
chr13	+	27094028	27095585	POLR1D	ENSCAFT00000010876	chr25	-	14984768	14986221	POLR1D
chr13	+	27264779	27266089	GSX1	ENSCAFT00000010870	chr25	-	14841463	14842723	GSX1
chr13	+	27392167	27398451	PDX1	ENSCAFT00000010866	chr25	-	14729982	14734368	PDX1
chr13	-	27434277	27441317	CDX2	ENSCAFT00000010860	chr25	+	14688806	14694705	CDX2
chr13	-	27450242	27460774	PRHOXNB	ENSCAFT00000010846	chr25	+	14669997	14680543	PRHOXNB
chr13	-	27475410	27572729	FLT3	ENSCAFT00000010813	chr25	+	14603184	14658045	NP_001018647.1
chr13	+	27610642	27767475	PAN3	ENSCAFT00000010833	chr25	-	14406734	14517087	PAN3
chr13	-	27857687	27967265	FLT1	ENSCAFT00000010807	chr25	+	14246903	14395230	Q9N0N1_CANFA
chr13	-	28172217	28191150	SLC46A3	ENSCAFT00000010772	chr25	+	14020226	14036750	SLC46A3
chr13	+	28900776	28978084	MTUS2	ENSCAFT00000038628	chr25	-	13357525	13546575	MTUS2
chr13	-	28981550	29067825	SLC7A1	ENSCAFT00000010744	chr25	+	13325825	13347121	SLC7A1
chr13	-	29236544	29322820	UBL3	ENSCAFT00000010690	chr25	+	13088522	13154546	UBL3
chr13	-	29674766	29779163	KATNAL1	ENSCAFT00000010676	chr25	+	12699177	12775231	KATNAL1
chr13	-	29930878	29938081	HMGB1	ENSCAFT00000010639	chr25	+	12540085	12545288	HMGB1_CANFA
chr13	+	30089829	30131686	USPL1	ENSCAFT00000010632	chr25	-	12385954	12415555	USPL1
chr13	+	30207668	30236556	ALOX5AP	ENSCAFT00000010626	chr25	-	12307267	12333329	ALOX5AP
chr13	+	30378311	30397709	C13orf33	ENSCAFT00000010612	chr25	-	12169724	12186228	C13orf33
chr13	+	30404833	30447153	C13orf26	ENSCAFT00000010602	chr25	-	12131700	12157018	C13orf26
chr13	-	30608762	30634117	HSPH1	ENSCAFT00000039011	chr25	+	11958958	11983946	HSPH1
chr13	+	30672111	30804411	B3GALTL	ENSCAFT00000010529	chr25	-	11803583	11900874	B3GALTL
chr13	+	31211678	31275009	RXFP2	ENSCAFT00000010501	chr25	-	11294670	11340203	RXFP2_CANFA
chr13	+	31503436	31768776	FRY	ENSCAFT00000010464	chr25	-	10938828	11050973	ENSCAFG00000006435
chr13	+	31787616	31871809	BRCA2	ENSCAFT00000010309	chr25	-	10719192	10782555	NP_001006654.2
chr13	-	31872859	31900315	N4BP2L1	ENSCAFT00000010304	chr25	+	10712528	10716387	N4BP2L1
chr13	+	32058563	32250158	PDS5B	ENSCAFT00000010289	chr25	-	10395258	10510956	PDS5B
chr13	+	32488570	32538282	KL	ENSCAFT00000010228	chr25	-	10141076	10184300	KL
chr13	-	32575271	32658216	STARD13	ENSCAFT00000010220	chr25	+	10040918	10100442	STARD13
chr13	+	33290205	33309644	RFC3	ENSCAFT00000010156	chr25	-	9455068	9472034	RFC3
chr13	+	34414423	35144873	NBEA	ENSCAFT00000010121	chr25	-	7950109	8522345	NBEA
chr13	-	34945925	34948832	MAB21L1	ENSCAFT00000010124	chr25	+	8041099	8042179	MAB21L1
chr13	-	35240789	35327998	DCLK1	ENSCAFT00000010068	chr25	+	7432978	7450492	ENSCAFG00000024986
chr13	-	35640344	35686752	SOHLH2	NM_017826	chr25	+	7341383	7380228	SOHLH2
chr13	-	35703214	35769992	C13orf38	ENSCAFT00000010028	chr25	+	7341359	7381679	ENSCAFG00000006206
chr13	-	35773774	35818646	SPG20	ENSCAFT00000010004	chr25	+	7245613	7301877	SPG20
chr13	+	35904408	35915019	CCNA1	ENSCAFT00000010017	chr25	-	7161889	7181159	CCNA1
chr13	+	36146048	36169975	C13orf36	ENSCAFT00000009985	chr25	-	6946977	6947301	C13orf36
chr13	+	36291338	36301740	RFXAP	ENSCAFT00000009980	chr25	-	6846329	6854988	RFXAP
chr13	-	36316967	36392409	SMAD9	ENSCAFT00000009977	chr25	+	6800178	6824973	SMAD9
chr13	-	36421907	36471504	ALG5	ENSCAFT00000009926	chr25	+	6690074	6737647	ALG5
chr13	+	36472677	36481751	EXOSC8	ENSCAFT00000009898	chr25	-	6682134	6688921	EXOSC8
chr13	-	36481450	36531850	FAM48A	ENSCAFT00000009889	chr25	+	6642526	6681772	FAM48A
chr13	-	37034718	37070981	POSTN	ENSCAFT00000039502	chr25	+	6151437	6192512	POSTN

Table 7 (continued):

HUMAN GENOME (SYNTENIC REGION)					CANINE GENOME Ensemble Canine					RED = evidence from Ensemble, Blue = from tblastn (RefSeq), Black = both
Chromosome	Strand	Start	End	Gene Name	Transcript ID or RefSeq ID	Chr	Strand	Start	End	
chr13	-	37108772	37341939	TRPC4	ENSCAFT00000009795	chr25	+	5965770	6116884	TRPC4
chr13	+	37821941	37835143	UFM1	ENSCAFT00000009717	chr25	-	5519774	5531234	UFM1
chr13	+	38159172	38359267	FREM2	ENSCAFT00000009710	chr25	-	5087612	5248158	FREM2
chr13	-	38438061	38462996	STOML3	ENSCAFT00000009698	chr25	+	5067391	5076639	STOML3
chr13	-	38482001	38510252	C13orf23	ENSCAFT00000009688	chr25	+	5022203	5046664	C13orf23
chr13	+	38510454	38522246	NHLRC3	ENSCAFT00000009678	chr25	-	5010781	5020826	NHLRC3
chr13	-	38815028	39075356	LHFP	ENSCAFT00000009676	chr25	+	4553789	4554285	ENSCAFG00000005998
chr13	+	39127763	39224765	COG6	ENSCAFT00000009672	chr25	-	4413770	4509422	COG6
chr13	-	40027800	40138734	FOXO1	ENSCAFT00000009632	chr25	+	3588307	3687610	FOXO1
chr13	-	40201431	40243347	MRPS31	ENSCAFT00000009625	chr25	+	3506246	3540442	MRPS31
chr13	+	40261546	40284596	SLC25A15	ENSCAFT00000009612	chr25	-	3457718	3477925	ENSCAFG00000005955

4) ISOLATION AND COMPARISON OF CANINE GLIAL AND NON-GLIAL NEUROEPITHELIAL TUMOR STEM CELLS.

Abstract

All neuroepithelial tissue arises from a shared embryonic structure, the neural plate and developing neural tube, eventually forming neurons, glia, ependymal cells, and the choroid plexus. Extending this relationship to the tumors formed by these structures would imply a shared origin as well. Accordingly glioblastoma tumors occasionally exhibit foci of ependymal differentiation, implying the reacquisition or persistence of some degree of plasticity in the differentiation along multiple neuroepithelial cell fates. Indeed, cancer stem cells have been isolated from several human neuroepithelial tumors, including glioma, ependymoma, and medulloblastomas. The domestic dog develops neuroepithelial tumors in every lineage documented in humans, recapitulating the salient histologic features of each. Here, we characterize for the first time the isolation of tumor stem cells from low-grade canine gliomas, an anaplastic canine ependymoma, and a canine choroid plexus carcinoma. These cells share similar growth characteristics *in vitro* and express similar stem cell markers as well as differentiation potential, implying shared regulatory pathways governing self-renewal across canine and human neuroepithelial tumors.

Introduction

Neuroepithelial tumors include neoplasms of glial, ependymal, primitive neuroectodermal tumors (medulloblastomas), and those of choroid plexus origin (17). Developmentally, these tumors arise from tissues that share a common cell of origin, the neural plate (468). The neural plate arises in the gastrulating embryo through the inhibition of the bone morphogenetic protein (BMP) and other related pathways within the transforming growth factor-β (TGF-β) superfamily (372-374). This inhibition, in concert with the local production of mitogenic growth factors such as members of the fibroblast growth factor (FGF) family promotes neural speciation and forms the primitive neural tube (379). Once closed, the neuroectoderm expands to form the ventricular zone (VZ), a germinal structure composed of primitive neural stem cells arranged in a pseudo-stratified arrangement with radial processes on some cells (radial glia) and other cells which divide symmetrically to populate the developing prosencephalon (neural stem cells) (383, 385, 390). How radial glia and neural stem cells interact with each other and what properties are shared between the two populations are currently unknown.

While the precise role of these cells in the developing mammalian brain remains obscure, they share many regulatory pathways with neuroepithelial cancers, such as bmi-1, notch, hedgehog, Wnt, and growth factor receptor signaling such as EGFR activation (262, 469, 470). The cancer stem cell hypothesis posits that many tumors are driven by a rare subpopulation of cells capable of self-renewal and recapitulating the heterogeneous cell

population of the tumor through the generation of more lineage-restricted progeny in asymmetric cell divisions (297, 299). Cells satisfying at least some of these characteristics have been described in many human neuroepithelial tumors, including glioma, ependymoma, and medulloblastomas, suggesting the possibility for shared pathways governing tumorigenesis given their common ancestry (3, 471, 472).

Glioma stem cells (GSCs) have been identified using the putative neural stem or progenitor cell markers CD133 and CD15, express shared neural stem cell markers such as sox2, nestin, and are capable of expressing markers of both neuronal and glial differentiation, just as neural stem cells (4, 323). These cells behave similarly in vitro as well, growing as non-adherent neurosphere-like structures in serum free media supplemented with bFGF and EGF. Most importantly, they are capable of forming highly infiltrative tumors in immunocompromised mouse orthografts that recapitulate the features of the parental tumor, often by injecting very small numbers of cells (156).

Ependymomas arise from the ependymal cells lining the ventricles of the brain and spinal cord or radial glia within the subependymal layer. Radial glia share many features with neural stem cells, and a good degree of functional overlap may be shared between the two populations *in vivo*. Ependymal cells and radial glia may express GFAP and the cell surface marker CD133, similar to neural stem cells (428). Accordingly, cells with radial glia features have been isolated from human ependymomas which are clonogenic, exhibit multipotential differentiation potential, and grow in an analogous manner to GSCs in

serum free media (471). These cells also demonstrate similar genomic copy number alterations to glioma, including loss of the Ink4A/ARF locus, and overexpression of the notch signaling pathway (473, 474).

Medulloblastoma and other primitive neuroectodermal tumors (PNETs) are less characterized genomically and functionally than gliomas or ependymomas. A majority of cells in these tumors lack expression of neuronal or glial differentiation, suggesting shared stem-like properties (475). Cells from these tumors also express CD133 and CD15, and are capable of differentiating into neuronal and glial lineage in vitro, and express similar cell regulatory pathways, such as Wnt, notch, and specifically sonic hedgehog signaling involved in cell self-renewal (476-478).

Choroid plexus cells originate from the roof of the neural tube early in fetal brain development, primarily in response to BMP stimulation (479, 480). These cells ultimately produce cerebrospinal fluid within the lateral, third, and fourth ventricles and are somewhat unique among other neuroepithelial tumor subtypes in that choroid plexus cells express cytokeratin and tight junctions. While uncommon tumors in adults, choroid plexus carcinomas may arise throughout the ventricular system and may also be regulated by similar self-renewal pathways, including notch (479, 481).

The domestic dog develops spontaneous neuroepithelial tumors that recapitulate the salient histologic and biologic features of all human neuroepithelial tumors (482). We

have previously characterized the significant similarities between human and canine GSCs, suggesting that similarities may lie in canine ependymal or choroid plexus tumors. Here, we report for the first time the isolation of canine ependymal tumor stem cells and the isolation of cells capable of self-renewal and multipotential differentiation from a canine choroid plexus carcinoma. Finally, we compare these to canine GSCs isolated from grade II astrocytomas.

Materials and Methods

GSC and NSC Cultures

Following identification of a spontaneously occurring choroid plexus carcinoma, an anaplastic ependymoma, and two grade II astrocytomas by MRI, the brain was removed immediately after death and the tumor sectioned. All samples were briefly enzymatically dissociated into single cells. Red blood cells and cellular debris were removed by ACK lysis buffer and differential centrifugation. Cells were each placed into culture in NBE medium comprised of Neurobasal-A medium (Invitrogen), N2 and B27 supplements (0.5x concentration, each; Invitrogen), heparin (2ug/mL, Sigma), and recombinant human bFGF and EGF (25ng/mL each; R&D systems). Recombinant human PDGF-BB (20ng/mL, R&D systems) was also supplemented to choroid plexus carcinoma cultures. Differentiation was induced by either growth factor withdrawal or by culturing cells in DMEM medium (Invitrogen) containing 10% fetal bovine serum (Invitrogen). Cells were

cultured as neurospheres in uncoated tissue culture flasks or as adherent cells on plates pre-coated with a poly-ornithine/poly-D-lysine mixture.

Intracranial Tumor Cell Injection into SCID Mice

5000 cells were orthotopically implanted as previously described(367). Cells were enzymatically dissociated and resuspended in 40-80ul of HBSS containing EDTA (Invitrogen). Cells were then injected stereotactically into the striatum of anesthetized adult mice using a stereotactic frame (coordinates: 2 mm anterior, 2 mm lateral, 2.5 mm depth from bregma). There was no injection-procedure-related animal mortality. Animals were sacrificed at given time points for the analysis of tumor histology and immunohistochemistry or for culture of cells from the xenograft tumor. Brains were perfused with 4% paraformaldehyde by cardiac perfusion and further fixed at 4℃ overnight.

FACS Analysis

Cultured cells were dissociated into single-cell suspensions and labeled with the following antibodies; anti-CD133 (Santa Cruz sc-30220), CD-15-FITC (MMA clone, BD) as previously described. Staining for CD133 was performed by labeling one million cells with 2ug of antibody at 4ºC for 10 minutes. Concentrations of other antibodies and the staining conditions were followed per the manufacturers recommendation. Non-conjugated primary antibodies were subsequently labeled with PE- or FITC-conjugated secondary antibodies (BD). Antibodies against mouse immunoglobulin conjugated to PE

or FITC were used as antibody isotype controls (BD). The stained cells were analyzed on the FACS Vantage SE flow cytometer (BD).

Antibodies for Western Blot Analysis and Immunohistochemistry

The following antibodies were used as primary antibodies: Nestin (IBL America and Covance), Sox2 (R&D Systems and Santa Cruz Biotechnology; sc-20088), Olig2 (Santa Cruz Biotechnology; sc-48817), a-tubulin (Sigma), GFAP (Dako), Tuj1 (Covance), cytokeratin 7 (Millipore), cytokeratin 20 (Dako), pan-cytokeratin (Dako), EMA (Sigma), vimentin (Novus biological).

Karyotype Analysis

Canine GSCs were briefly trypsinized to single cell suspension, recovered for 6 hours in NBE medium at 37°C, and then incubated with colcemid (final concentration 50-100ng/mL, Invitrogen) for 4-6 hours at 37°C. Cells were then suspended and fixed in methanol and glacial acetic acid. Fixed cells were then sent to the NCI Cytogenetic Core for metaphase analysis and karyotype determination (Frederick, MD).

Results

Canine Grade II Astrocytomas Also Contain GSCs

The role of GSCs in low-grade astrocytomas is still unknown in human glioma tumors, as detailed studies of non-GBM GSCs are largely lacking. We have isolated GSCs from two

separate, grade II astrocytomas in the domestic dog however, which display similar characteristics to our prior characterization of canine GSCs in high-grade glioma tumors. The first grade II astrocytoma, 0712, was collected from a well-demarcated mass in the brainstem of a dog (Figure 1A and 1B). This tumor is composed of sheets of well-differentiated astrocytes (Figures 1C and 1D). Despite the low grade of the astrocytoma, GSCs were isolated that grew as neurosphere-like structures in NBE medium (Figure 1E), similar to those isolated from physiologic NSC niches in the same dog, such as the subventricular zone (Figure 1F).

0712 GSCs are capable of forming xenograft tumors in immunocompromised mice, although these tumors are well-demarcated, lack significant invasion, and exhibit minimal cellular pleomorphism (Figures 2A and 2B). These GSCs form these xenograft tumors at a low rate as well, with only 2 of 10 mice injected intracerebrally with 50,000 cells forming tumors (Figure 2C). Those xenograft tumors that did form expressed low levels of stem cell markers such as sox2 (Figure 2D) and high markers of differentiated astrocytes such as GFAP (Figure 2E). Consistent with this, 0712 GSCs in vitro express low amounts of either sox2 or olig2, while constitutively expressing markers of either glial (GFAP) or neuronal (TuJ-1) differentiation (Figure 2F) in either NBE or FBS, and express undetectable levels of GSC cell surface markers CD133 or CD15 (Figure 2G). Karyotype analysis of 0712 GSCs versus patient-matched physiologic NSCs isolated from the subventricular zone identifies a focal anomaly involving a chromosomal inversion of canine chromosome 9 (Figure 3), which may contribute to their tumorigenic

potential, although as these GSCs express low levels of stem-cell associated markers, they have a much lower tumorigenic potential than either our high-grade canine GSCs or human GSCs derived from GBMs.

We also isolated GSCs from a second canine grade-II astrocytoma, 0514. This tumor also arose in the brainstem region of a dog (Figure 4A). This neoplasm was comprised of well-differentiated neoplastic astrocytes, which exhibit focal infiltration into the adjacent neuropil (Figures 4B and 4C). These GSCs form xenograft tumors that are moderately infiltative, but exhibit cellular pleomorphism and focal regions of necrosis (Figures 4D-F). Xenograft tumors formed by 0504 GSCs highly express nestin, GFAP, and sox2 (Figures 4G-I). Despite the modest xenograft tumor burden, 0504 GSCs efficiently form xenograft tumors in all mice injected, with a median survival time of 108 days (Figure 5A). Consistent with this efficient xenograft formation, 0504 GSCs express both CD133 and CD15 (Figure 5B). Both primary 0504 and xenograft-derived 0504-A-1 GSCs express the stem cell markers nestin, sox2, and olig2, while expressing low levels of either TuJ-1 or GFAP in NBE conditions (Figure 5C).

Canine grade II astrocytomas do contain GSCs, as we are able to isolate and expand them from two individual tumors. Their tumorigenic potential and similarities to either human GBM or high-grade canine GSCs appears to vary widely, however.

Canine Ependymomas Contain Cells with GSC-like Properties

Given our ability to isolate GSCs from low- and high-grade glioma tumors, we next sought to identify any similar cells in canine ependymoma, as has been postulated in human ependymoma tumors. We were able to isolate cells from a poorly demarcated, periventricular mass from a dog (Figures 6A-B), 0302, that was composed of sheets of poorly demarcated round to oval cells that form occasional rosettes and pseudo-rosettes, consistent with an anaplastic ependymoma (Figures 6C-D). These cells proliferate in serum-free media identical to our GSCs, forming nonadherent neurosphere-like structures (Figure 6E).

0302 ependymal stem cells (EPSCs) co-express both TuJ-1 and GFAP in vitro, although at low levels (Figure 7A), and express high levels of nestin (Figure 7B). Interestingly, some nestin-positive cell have an elongate, polarized appearance consistent with radial glia, the speculated progenitor cell for many human ependymal tumors (Figure 7C). Canine EPSCs also express CD133 and CD15 in a manner similar to both human ependymoma stem cells and GSCs. 0302 EPSCs are able to form xenograft tumors in all immunocompromised mice injected, although the latency to tumor formation is considerably longer than even grade II canine GSCs (Figure 7E). 0302 EPSCs in vitro express sox2 and olig2 as well as GFAP in both NBE and FBS conditions (Figure 6F). Radial glia, the purported stem cell for human ependymoma also strongly express GFAP, suggesting similarities with our canine EPSCs.

The xenograft tumors formed by 0302 EPSCs expand and fill the lateral and third ventricles of mice, consistent with their ependymal etiology (Figure 8). All mice develop significant, secondary obstructive hydrocephalus due to intraventricular masses. Xenograft tumors are similar to the parental tumor, with sheets of poorly differentiated ependymal cells arranged either in a myxomatous matrix or into crude rosettes and pseudo-rosettes (Figures 8C-D). While a majority of cells are located within the ventricles, cells also invade into the adjacent neuropil from the lateral ventricles (Figure 8B). Xenograft tumors express variable amounts of GFAP, although the highest tumor burdens within the myxomatous regions exhibit sparse immunoreactivity (Figures 9B, G, and L). These regions, while expressing low GFAP do express sox2 and nestin (Figures 9M and N), as well as the ependymal marker EMA (Figure 9O) (483).

Canine ependymomas therefore contain EPSCs that exhibit remarkable similarities to GSCs in both the methods used to isolate and expand the cells, the expression of neural stem cell markers, and their ability to recapitulate the original tumor.

Isolation of GSC-like Cells from a Canine Choroid Plexus Carcinoma

Finally, we examined a third intracranial tumor of neuroepithelial origin in the dog, a choroid plexus tumor in an effort to expand similar cells using serum free media. We were able to isolate such a tumor from a dog, 0818 from the ventral floor of the right lateral ventricle (Figure 10A). This tumor was arranged into an arboribform pattern of fronds and multiple projections lined by high cuboidal to columnar, neoplastic epithelial

cells (Figures 10B-C). This tumor was negative for GFAP (Figure 10D) and nestin (Figure 10E), but strongly positive for both pan-cytokeratin (Figure 10F) and sox2 (Figure 10G), consistent with a choroid plexus carcinoma (CPC).

We were able to isolate and expand cells in serum free NBE media supplemented with PDGF-BB that exhibit remarkable similarities to both our canine GSCs and EPSCs, including the ability to grow as non-adherent neurosphere-like structures (Figure 11A). Only cultures containing PDGF-BB were successful, suggesting a similar importance to PDGF signaling to that reported in human CPCs (484). Despite the injection of 200,000 cells per mouse however, these cells failed to produce any xenograft tumors in immunocompromised mice (Figure 11B). Analysis of these cells in vitro confirms selective expression of cytokeratin 7 and an absence of cytokeratin 20, which has been reported in human CPCs (Figure 11C) (485). Notably, these cells also fail to express either vimentin or GFAP in vitro (Figure 11D).

Discussion

Despite sharing a common embryonic origin of the neural plate, little information is known regarding the relatedness of neuroepithelial tumors in humans. The domestic dog not only develops spontaneous glioma tumors with remarkably similar incidence rates and pathologic features, but also develops ependymal and choroid plexus tumors that share significant homology to the human disease. Recent investigations of canine

neuroepithelial tumors indicate that many stem-cell proteins associated with human and canine GSCs are also shared in these other neuroepithelial tumor types (482).

Here, we identify and characterize for the first time tumor stem cells in both grade II canine astrocytomas as well as in a canine anaplastic ependymoma, as well as similar cells isolated from a canine choroid plexus carcinoma. Canine GSCs from low-grade astrocytomas appear to vary widely in their tumorigenic potential, as while 0712 GSCs have very little tumor forming capacity in immunocompromised mice, 0514 GSCs readily form xenograft tumors. As 0712 GSCs are negative for both CD133 and CD15, while 0514 express low levels of each, this may further support the notion that these markers enrich for glioma tumor stem cells in both human and canine tumors. Human GSCs negative for CD133 or expressing low levels of CD15 are capable of forming xenograft tumors however, suggesting the explanation may include other complicating factors (319, 323). 0514 GSCs also express increased markers of sox2 and olig2 compared to 0712, while expressing less TuJ-1 or GFAP in NBE conditions. While a definitive mechanism of sox2 regulation in human or canine GSCs remains elusive, inhibition of sox2 expression in human GSCs dramatically reduces their tumorigenic potential and may induce apoptosis (335). These observations add to the importance of neural stem cell marker expression in the regulation of tumorigenic potential in GSCs, suggesting a potential marker-independent association for transcription factors such as sox2 or olig2.

While 0712 GSCs do not express CD133, CD15, or high levels of stem-cell associated proteins, karyotype analysis does reveal a focal chromosomal translocation on cfa9. This region is syntenic to hsa17, which does exhibit loss of heterozygosity in human GBMs, although this is most frequently present within the region containing p53 (486). This region is syntenic to cfa5, not cfa9, although it is possible that other tumor suppressor genes may be present within this region corresponding to cfa9.

Human ependymoma tumors often have significant similarities to glioma tumors, and high-grade glioma tumors may often contain foci of apparent ependymal differentiation (487-489). Such observations may imply either a shared, transformed progenitor cell or similar regulatory mechanisms governing each tumor progenitor cell, allowing for a degree of plasticity between the two tumor types. Ependymomas have been suggested to arise from transformed radial glia cells, neural progenitors that share significant similarities and may have functional overlap with neural stem cells (a putative cell of origin for gliomas) (471). For the first time, we have characterized tumor stem cells from a canine anaplastic ependymoma, 0302, and documented significant similarities to both canine and human GSCs.

Canine EPSCs express the markers CD133 and CD15, consistent with both human GSCs and cells isolated form ependymoma. EPSCs in vitro also express nestin and co-express markers of neuronal and glial differentiation, and often have phenotypic characteristics of

radial glia, including long, polarized cell processes, suggesting a similar cell of origin may produce canine ependymomas (471).

Interestingly, our ependymoma stem cells form xenograft tumors exclusively within the ventricular system of immunocompromised mice, often occluding cerebrospinal fluid outflow and producing obstructive hydrocephalus in these mice. This suggests that tissue microenvironment is of critical importance for the regulation of this tumor, as even though the EPSCs were injected anterior to the lateral ventricle, the tumor only forms within the ventricle, suggesting the cells migrate first to the lateral ventricle prior to tumor expansion. This profound influence by the microenvironment may suggest how gliomas contain foci of ependymal differentiation, as they may be exposed to these cues within intraventricular tumor mass. Further comparisons between human and canine EPSCs may help identify the interaction between putative radial stem cell progenitors and growth factors within the CSF.

Cells comprising the choroid plexus differentiate from modified ependymal cells and therefore like glioma and ependymal tumors, they originate from the neural plate developmentally (479). Accordingly, we were able to isolate cells from a canine choroid plex carcinoma that have similar properties to our ependymal and glioma stem cells, although they fail to produce tumors when injected orthotopically. This may be because the microenvironment of the choroid plexus is still poorly defined, as well as the molecular events governing choroid plexus tumor initiation.

Glioma, ependymoma, and choroid plexus tumors all arise from tissues developmentally related to the neural plate. This shared ontogeny of these tumors may imply shared functional characteristics governing the initiation of these tumors, especially with the growing evidence of cells with stem like properties in numerous solid neoplasms. Here, we report for the first time the isolation and expansion of tumor initiating cells or cells with similar functional properties in vitro from gliomas, an anplastic ependymoma, and a choroid plexus carcinoma. These cells expand in identical, serum-free media, express similar markers associated with neural stem cells, as well as the putative tumor stem cell markers CD133 and CD15, further supporting the evidence that these are relevant in both human and canine neuroepithelial tumor biology. Further characterization and analysis of multiple neuroepithelial-derived tumors in canine and human tumor subtypes may enable the identification of shared pathways involved in self-renewal.

References

1. Louis, D.N., et al., *The 2007 WHO classification of tumours of the central nervous system.* Acta Neuropathol, 2007. **114**(2): p. 97-109.

2. Vieira, C., et al., *Molecular mechanisms controlling brain development: an overview of neuroepithelial secondary organizers.* Int J Dev Biol, 2010. **54**(1): p. 7-20.

3. Pera, M.F., et al., *Regulation of human embryonic stem cell differentiation by BMP-2 and its antagonist noggin.* J Cell Sci, 2004. **117**(Pt 7): p. 1269-80.

4. Kawasaki, H., et al., *Induction of midbrain dopaminergic neurons from ES cells by stromal cell-derived inducing activity.* Neuron, 2000. **28**(1): p. 31-40.

5. Chambers, S.M., et al., *Highly efficient neural conversion of human ES and iPS cells by dual inhibition of SMAD signaling.* Nat Biotechnol, 2009. **27**(3): p. 275-80.

6. Gaspard, N. and P. Vanderhaeghen, *Mechanisms of neural specification from embryonic stem cells.* Curr Opin Neurobiol, 2010. **20**(1): p. 37-43.

7. Ajioka, I., T. Maeda, and K. Nakajima, *Identification of ventricular-side-enriched molecules regulated in a stage-dependent manner during cerebral cortical development.* Eur J Neurosci, 2006. **23**(2): p. 296-308.

8. Bystron, I., C. Blakemore, and P. Rakic, *Development of the human cerebral cortex: Boulder Committee revisited.* Nat Rev Neurosci, 2008. **9**(2): p. 110-22.

9. Rakic, P., *Specification of cerebral cortical areas.* Science, 1988. **241**(4862): p. 170-6.

10. Taipale, J. and P.A. Beachy, *The Hedgehog and Wnt signalling pathways in cancer.* Nature, 2001. **411**(6835): p. 349-54.

11. Pardal, R., M.F. Clarke, and S.J. Morrison, *Applying the principles of stem-cell biology to cancer.* Nat Rev Cancer, 2003. **3**(12): p. 895-902.

12. Reya, T., et al., *Stem cells, cancer, and cancer stem cells.* Nature, 2001. **414**(6859): p. 105-11.

13. Jordan, C.T., M.L. Guzman, and M. Noble, *Cancer stem cells.* N Engl J Med, 2006. **355**(12): p. 1253-61.

14. Dick, J.E., *Stem cell concepts renew cancer research.* Blood, 2008. **112**(13): p. 4793-807.

15. Taylor, M.D., et al., *Radial glia cells are candidate stem cells of ependymoma.* Cancer Cell, 2005. **8**(4): p. 323-35.

16. Huang, X., et al., *Isolation, enrichment, and maintenance of medulloblastoma stem cells.* J Vis Exp, 2010(43).

17. Galli, R., et al., *Isolation and characterization of tumorigenic, stem-like neural precursors from human glioblastoma.* Cancer Res, 2004. **64**(19): p. 7011-21.

18. Son, M.J., et al., *SSEA-1 is an enrichment marker for tumor-initiating cells in human glioblastoma.* Cell Stem Cell, 2009. **4**(5): p. 440-52.

19. Singh, S.K., et al., *Identification of human brain tumour initiating cells.* Nature, 2004. **432**(7015): p. 396-401.

20. Bao, S., et al., *Glioma stem cells promote radioresistance by preferential activation of the DNA damage response.* Nature, 2006. **444**(7120): p. 756-60.

21. Coskun, V., et al., *CD133+ neural stem cells in the ependyma of mammalian postnatal forebrain.* Proc Natl Acad Sci U S A, 2008. **105**(3): p. 1026-31.

22. Johnson, R.A., et al., *Cross-species genomics matches driver mutations and cell compartments to model ependymoma.* Nature, 2010. **466**(7306): p. 632-6.

23. Rousseau, E., et al., *CDKN2A, CDKN2B and p14ARF are frequently and differentially methylated in ependymal tumours.* Neuropathol Appl Neurobiol, 2003. **29**(6): p. 574-83.

24. Molenaar, W.M., et al., *Molecular markers of primitive neuroectodermal tumors and other pediatric central nervous system tumors. Monoclonal antibodies to neuronal and glial antigens distinguish subsets of primitive neuroectodermal tumors.* Lab Invest, 1989. **61**(6): p. 635-43.

25. Onvani, S., et al., *Genetics of medulloblastoma: clues for novel therapies.* Expert Rev Neurother, 2010. **10**(5): p. 811-23.

26. Read, T.A., et al., *Identification of CD15 as a marker for tumor-propagating cells in a mouse model of medulloblastoma.* Cancer Cell, 2009. **15**(2): p. 135-47.

27. Enguita-German, M., et al., *CD133+ cells from medulloblastoma and PNET cell lines are more resistant to cyclopamine inhibition of the sonic hedgehog signaling pathway than CD133- cells.* Tumour Biol, 2010. **31**(5): p. 381-90.

28. Wolburg, H. and W. Paulus, *Choroid plexus: biology and pathology.* Acta Neuropathol, 2010. **119**(1): p. 75-88.

29. Hunter, N.L. and S.M. Dymecki, *Molecularly and temporally separable lineages form the hindbrain roof plate and contribute differentially to the choroid plexus.* Development, 2007. **134**(19): p. 3449-60.

30. Dang, L., et al., *Notch3 signaling initiates choroid plexus tumor formation.* Oncogene, 2006. **25**(3): p. 487-91.

31. Ide, T., et al., *Immunohistochemical characterization of canine neuroepithelial tumors.* Vet Pathol, 2010. **47**(4): p. 741-50.

32. Lee, J., et al., *Tumor stem cells derived from glioblastomas cultured in bFGF and EGF more closely mirror the phenotype and genotype of primary tumors than do serum-cultured cell lines.* Cancer Cell, 2006. **9**(5): p. 391-403.

33. Mahfouz, S., et al., *Immunohistochemical study of CD99 and EMA expression in ependymomas.* Medscape J Med, 2008. **10**(2): p. 41.

34. Nupponen, N.N., et al., *Platelet-derived growth factor receptor expression and amplification in choroid plexus carcinomas.* Mod Pathol, 2008. **21**(3): p. 265-70.

35. Gyure, K.A. and A.L. Morrison, *Cytokeratin 7 and 20 expression in choroid plexus tumors: utility in differentiating these neoplasms from metastatic carcinomas.* Mod Pathol, 2000. **13**(6): p. 638-43.

36. Beier, D., et al., *CD133(+) and CD133(-) glioblastoma-derived cancer stem cells show differential growth characteristics and molecular profiles.* Cancer Res, 2007. **67**(9): p. 4010-5.

37. Gangemi, R.M., et al., *SOX2 silencing in glioblastoma tumor-initiating cells causes stop of proliferation and loss of tumorigenicity.* Stem Cells, 2009. **27**(1): p. 40-8.

38. Sarkar, C., et al., *Loss of heterozygosity of a locus in the chromosomal region 17p13.3 is associated with increased cell proliferation in astrocytic tumors.* Cancer Genet Cytogenet, 2003. **144**(2): p. 156-64.

39. Kano, T., et al., *A case of an anaplastic ependymoma with gliosarcomatous components.* Brain Tumor Pathol, 2009. **26**(1): p. 11-7.

40. Jacobsen, P.F., T.J. Parker, and J.M. Papadimitriou, *Ependymal differentiation of a glioblastoma multiforme after heterotransplantation into nude mice.* J Natl Cancer Inst, 1987. **79**(4): p. 771-9.

41. Poppleton, H. and R.J. Gilbertson, *Stem cells of ependymoma.* Br J Cancer, 2007. **96**(1): p. 6-10.

Figure 1

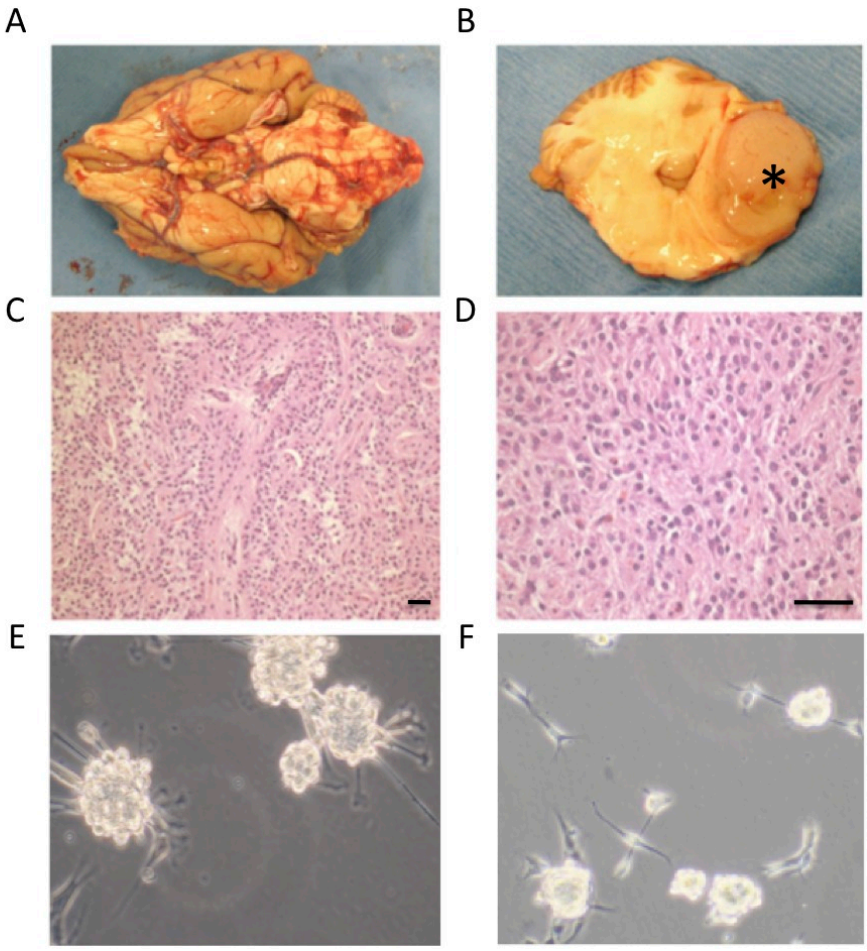

Figure 1. Isolation of GSCs from a Canine Grade II Astrocytoma, 0712. A) An asymmetric expansion of the ventral brainstem was caused by B) a well-demarcated, expansile neoplastic mass (asterisk). C) This mass was composed of sheets and chords of D) well-differentiated neoplastic astrocytes (bar=20μm). E) Cells cultured in serum-free NBE media grew as non-adherent neurosphere-like structures, similar to F) physiologic neural stem cells isolated from the subventricular zone.

Figure 2

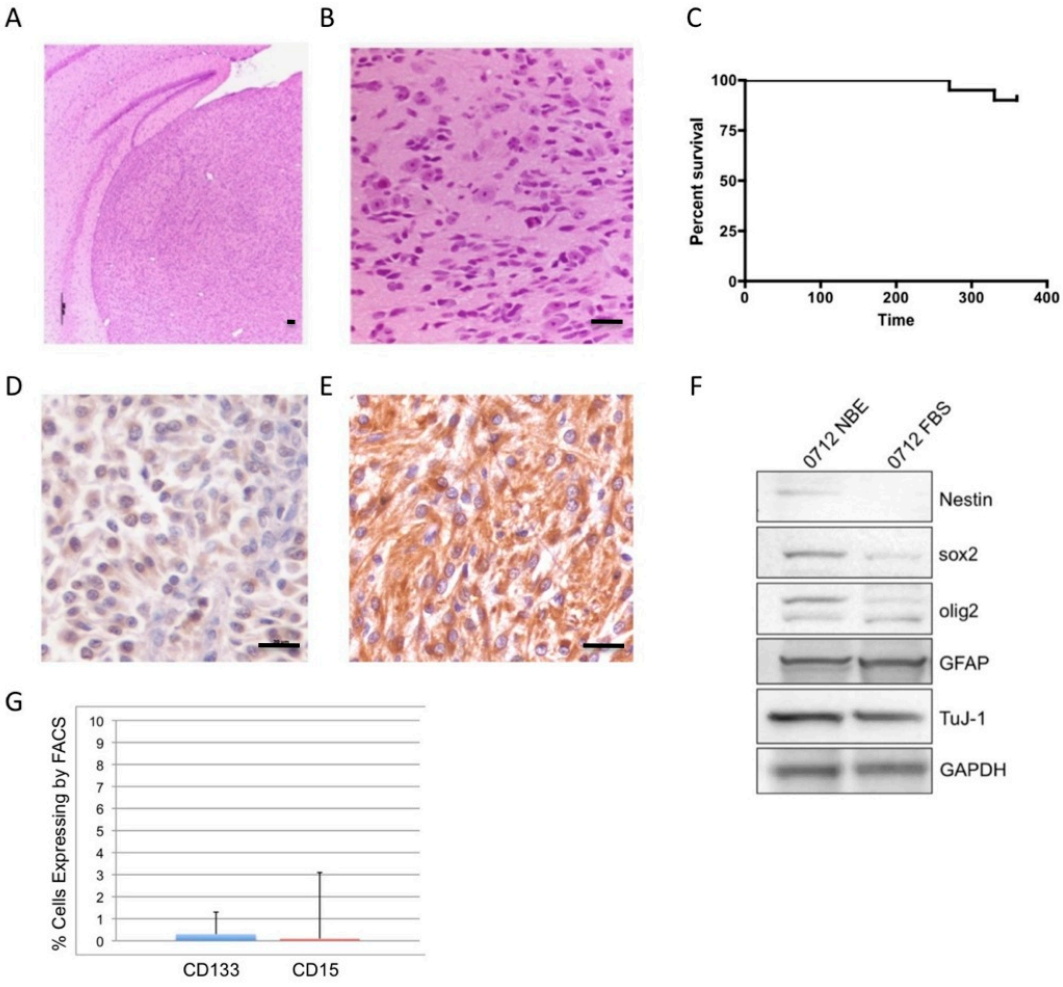

Figure 2. Characterization of 0712 GSCs *in vivo* and *in vitro*. A) Xenograft tumor formed by intracerebral injection of 0712 canine GSCs is characterized by a well-demarcated, expansile tumor. B) This tumor exhibits minimal cellular pleomorphism and is of moderate cellularity. C) 0712 GSCs are poorly tumorigenic, forming only two xenograft tumors in ten mice injected. D) Xenograft tumors formed express low levels of sox2 in vivo while E) expressing high levels of GFAP (bar=5μm). F) Similarly, 0712 GSCs in vitro express low amounts of stem cell markers sox2, olig2, and nestin, while constitutively expressing TuJ-1 and GFAP. G) 0712 GSCs do not express either CD133 or CD15.

Figure 3

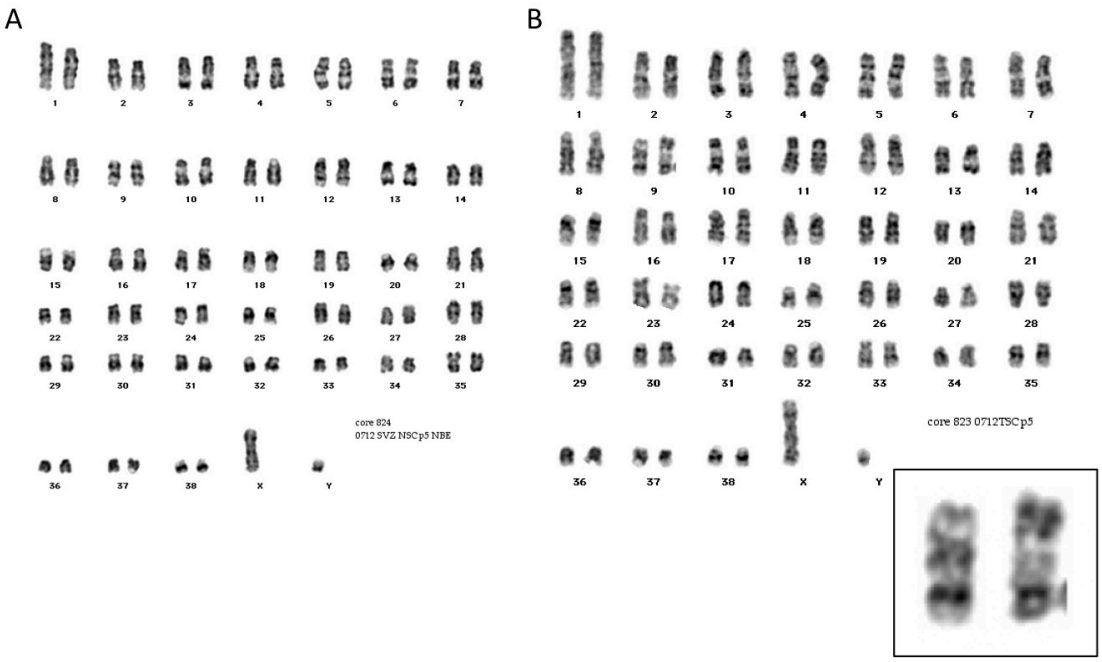

Figure 3. Karyotype of 0712 NSCs and GSCs. A) Physiologic NSCs contain a wild-type karyotype while B) 0712 GSCs contain a focal chromosomal inversion on chromosome 9 (inset).

Figure 4

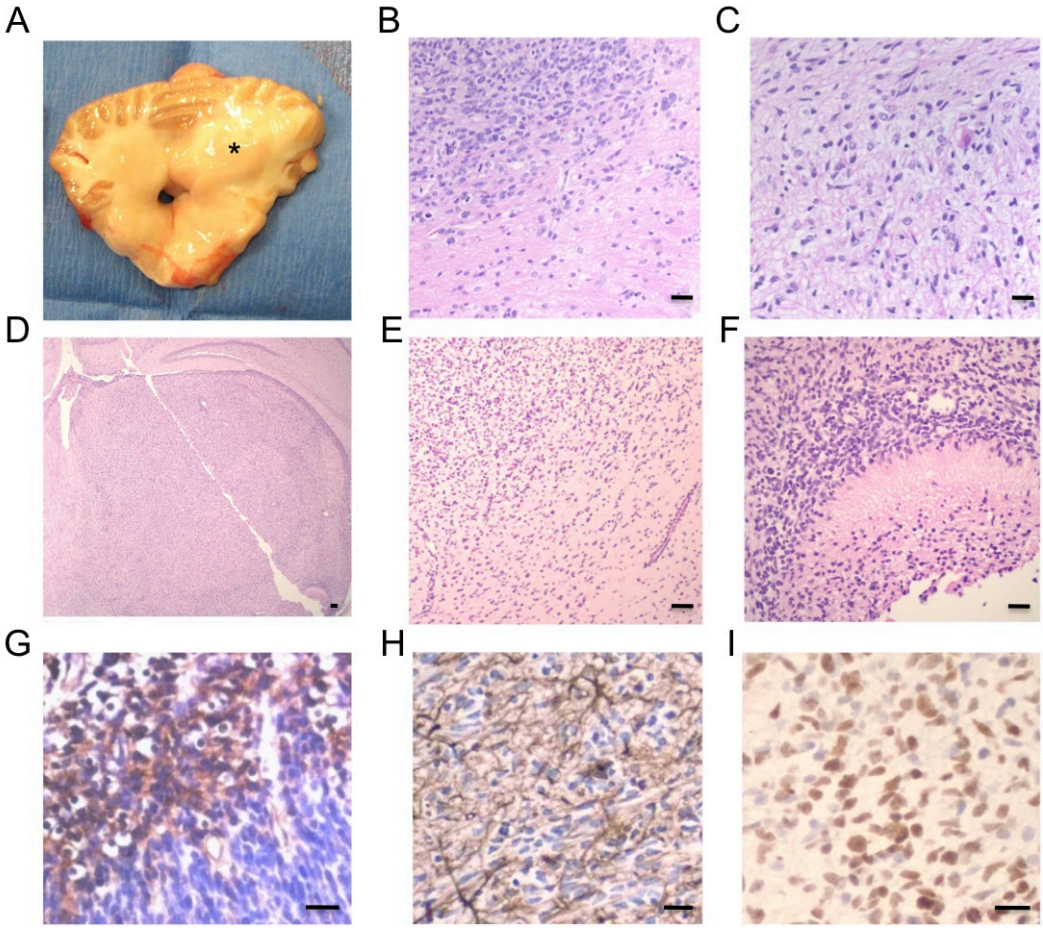

Figure 4. Isolation of GSCs from a Canine Grade II Astrocytoma, 0504. A) A poorly demarcated, expansile mass was dissected from the brainstem. B) Neoplastic cells are moderately infiltrative but C) are minimally pleomorphic. D) Xenograft tumors formed by 0504 cells are moderately well demarcated, E) exhibit moderate cellular pleomorphism, and F) contain focal regions of necrosis. F) Xenograft tumors express nestin, H) GFAP, and I) sox2 (bar=5μm).

Figure 5

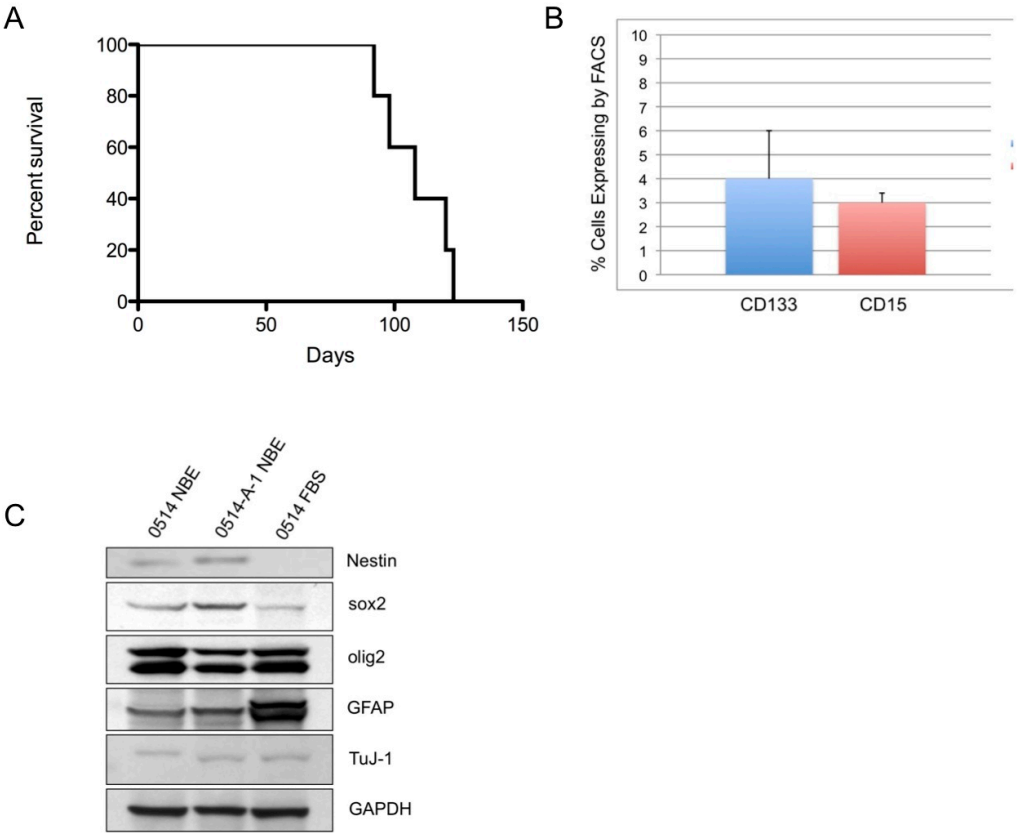

Figure 5. Canine 0504 GSCs are Tumorigenic and Express Stem Cell Markers *in vitro*. A) Canine 0504 GSCs are tumorigenic in all mice injected, with a median survival time of xenograft mice of 108 days. B) 0504 GSCs express both CD133 and CD15. C) These cells express nestin, sox2, and olig2 in NBE conditions, and upregulate GFAP expression when cultured in serum.

Figure 6

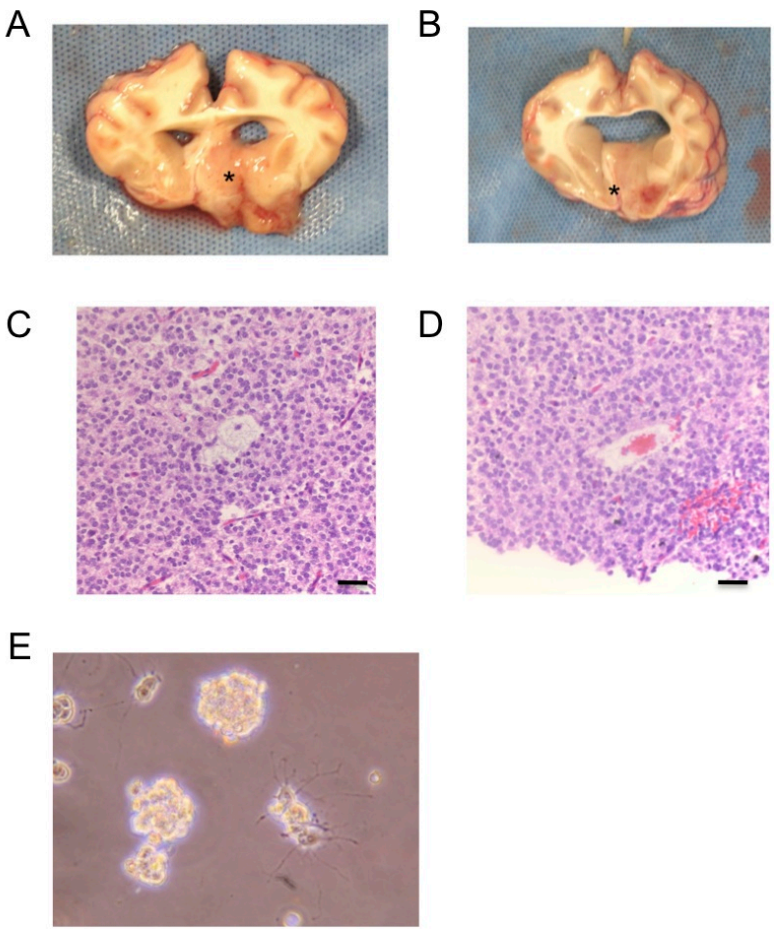

Figure 6. Tumor Stem Cells Are Present in a Canine Ependymoma. 0302. A) A poorly demarcated mass was dissected free from the floor of a lateral ventricle in a dog. This mass was intimately associated with the ventricle and produced B) hydrocephalus. C) This mass is composed of sheets of poorly differentiated ependymal cells arranged in rosettes and D) pseudo-rossettes (bar=20μm). E) Cells cultured in NBE medium grow as non-adherent neurosphere-like structures similar to canine GSCs and NSCs.

Figure 7

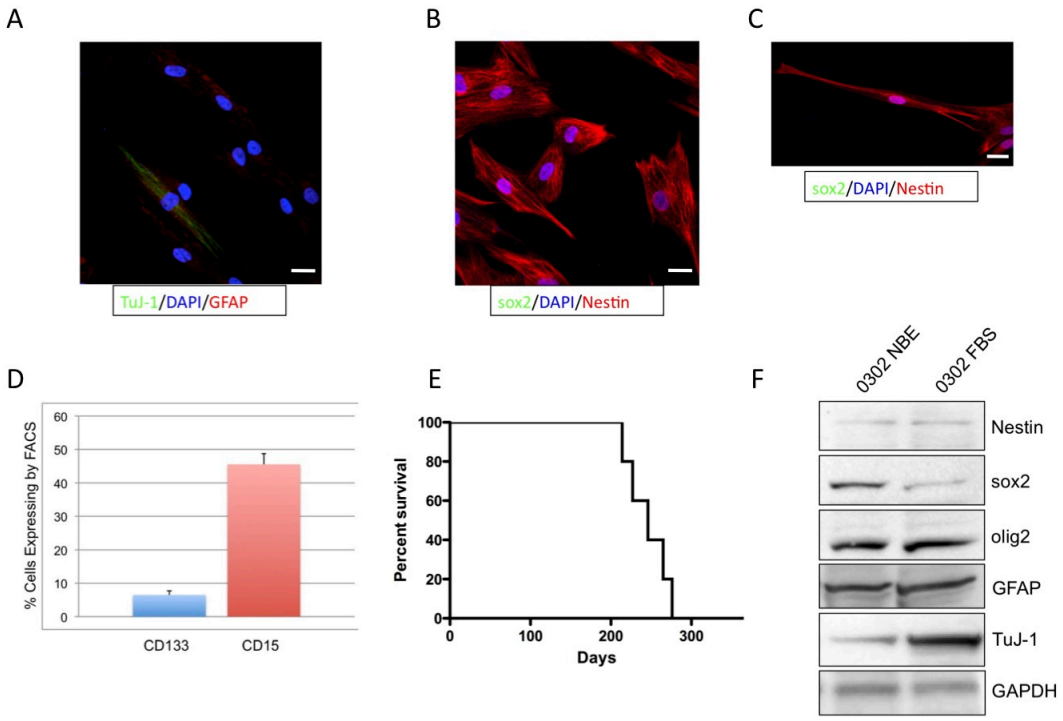

Figure 7. Characterization of 0302 Canine Ependymoma Stem Cells (EPSCs). A) 0302 EPSCs cultured in NBE co-express low amounts of TuJ-1 and GFAP, while B) prominently expressing nestin. C) Some cells exhibit a polarized, elongate phenotype reminiscent of radial glia cells, the putative stem cell of human ependymomas (bar=5μm). D) 0302 EPSCs express both CD133 and CD15. E) While xenograft tumors form in all mice injected intracerebrally, these tumors form with prolonged latency, exhibiting a median survival time of 246d. F) 0302 EPSCs in vitro express sox2 and olig2 and constitutively express GFAP, similar to radial glia.

Figure 8

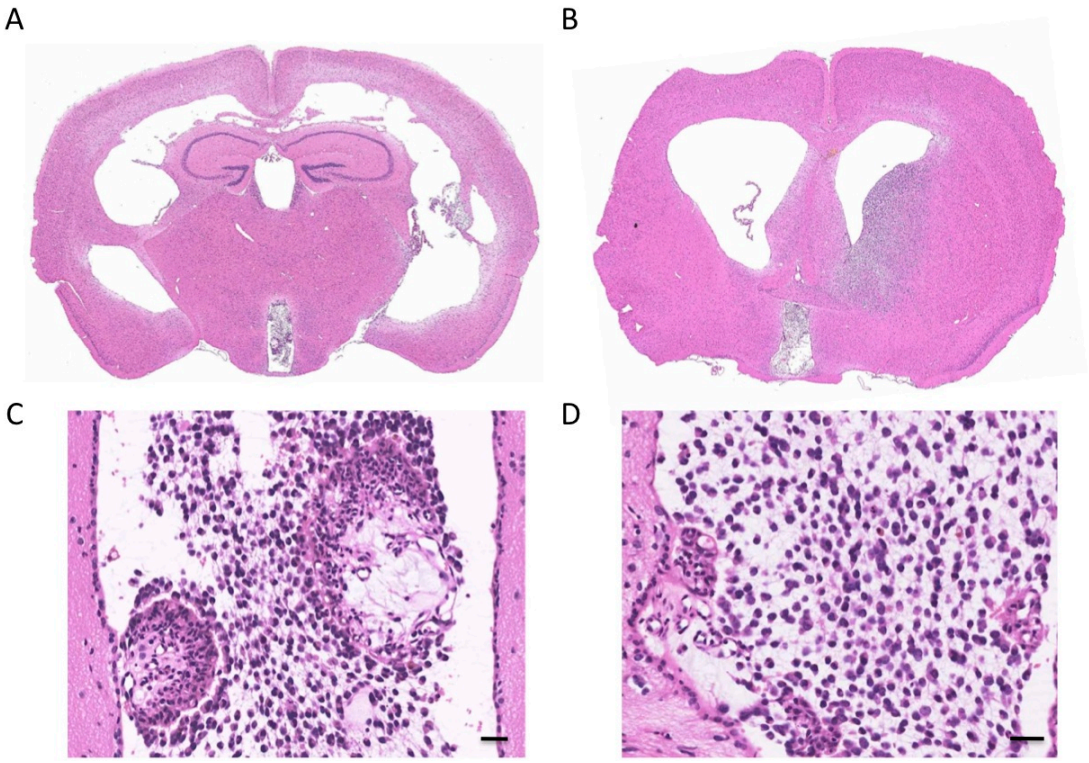

Figure 8. Canine 0302 EPSCs Form Large Intraventricular Xenograft Tumors. A) All mice containing xenograft tumors exhibit prominent hydrocephalus and intraventricular tumor masses. B) These tumors often infiltrate into adjacent neuropil. C) Intraventricular masses contain poorly organized rosettes and D) neoplastic cells within a myxomatous extracellular matrix (bar=10μm).

Figure 9

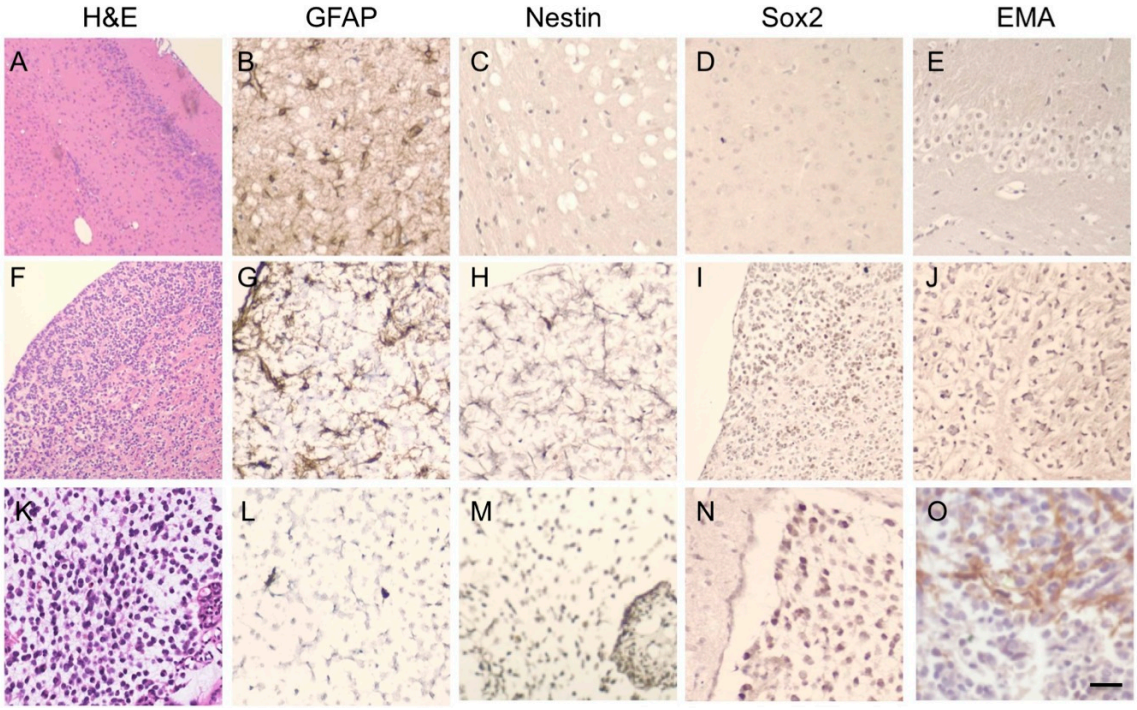

Figure 9. Immunohistochemical evaluation of 0302 EPSC Xenograft Tumors. The murine cortex expresses high amounts of GFAP but lacks nestin, sox2, or EMA expression (A-E). Infiltrative regions of the xenograft express GFAP, low amounts of nestin, sox2, but lack significant EMA expression (F-J). Intraventricular portions of the xenograft tumor in contrast express no GFAP, but do express nestin, prominent sox2, but strong EMA reactivity (bar=10μm).

Figure 10

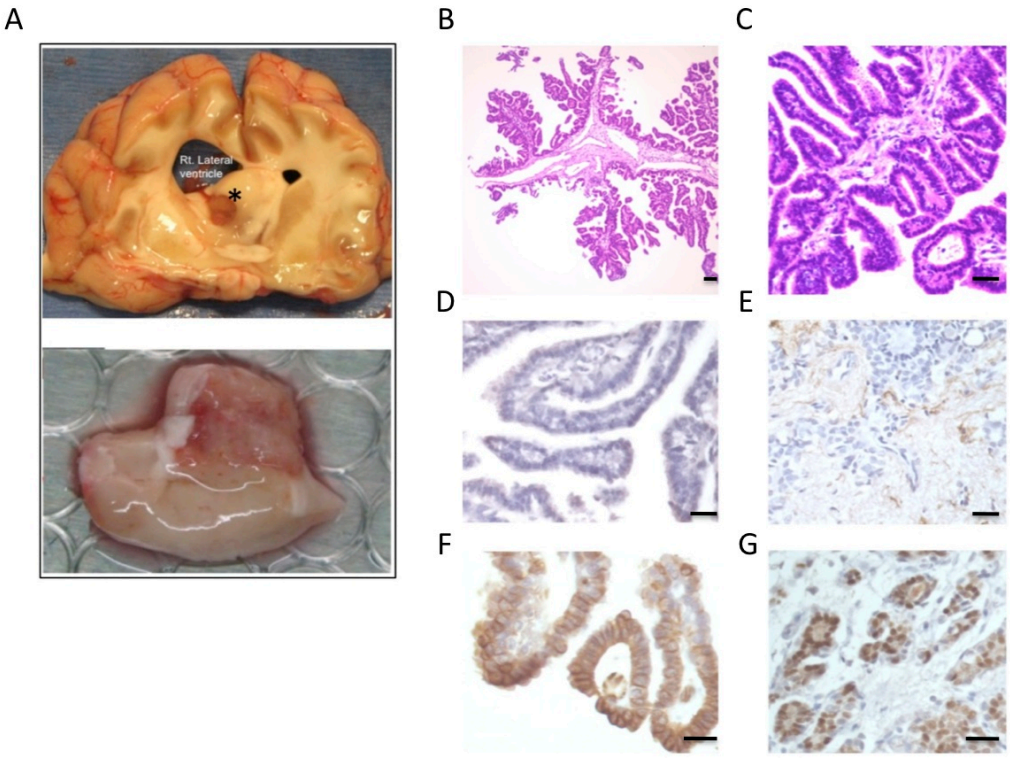

Figure 10. Canine Choroid Plexus Carcinoma, 0818 Expresses Cytokeratin *in situ*. A) A poorly demarcated, expansive mass was isolated from the ventral floor of the right ventricle in a dog. B) This mass was composed of multiple fronds of neoplastic epithelial cells C) arranged on fibrovascular projections. These cells do not express D) GFAP or E) nestin, but strongly express F) cytokeratin and G) sox2 (bar=30μm).

Figure 11

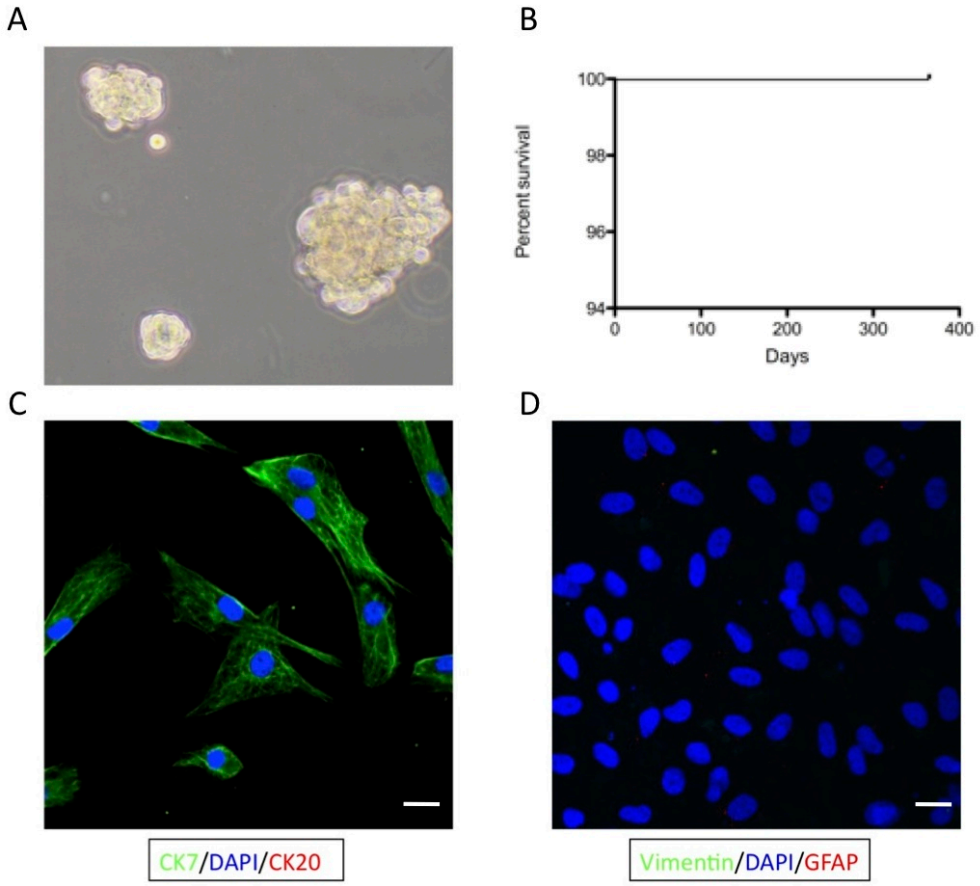

Figure 11. Cells Derived from Canine Choroid Plexus Carcinoma are Similar to GSCs *in vitro*. A) 0818 tumor cells grow as non-adherent neurosphere-like structures in NBE medium, similar to canine GSCs and EPSCs. B) Injection of these cells intracerebrally however, fail to produce any xenograft tumors. C) Consistent with human choroid plexus carcinoma, canine 0818 cells express cytokeratin 7 but not cytokeratin 20. D) 0818 cells do not express either vimentin or GFAP (bar=5μm).

5) ISOLATION AND CHARACTERIZATION OF CANINE EMBRYONIC NEURAL STEM CELLS IDENTIFIES TEMPORALLY REGULATED DIFFERENTIATION POTENTIAL THROUGHOUT GESTATION.

Abstract

Mammalian neural stem cells (NSCs) are derived from the primitive neuroepithelium of the neural crest. Following fate commitment to neural tissue, these cells enter temporally regulated periods of first proliferation, then neuronal, and finally glial differentiation throughout the embryonic brain development. Many of the cellular events governing the transition from each period remain unknown however. Here, we characterize for the first time embryonic NSCs from the developing brain of the domestic dog. Similar to other mammalian NSCs, canine NSCs proliferate in serum free media and are able to differentiate along first neuronal and ultimately glial cell fates through gestation. Canine NSCs isolated early in gestation are more resistant to differentiation, have a significantly higher clonogenic potential, and express high levels of CD133. Interestingly, early canine NSCs express low levels of sox2, a protein identified in murine embryonic and neural stem cells. Canine NSCs from early gestation instead express high levels of sox3, and acquisition of sox2 expression coincides with neuronal differentiation in early canine NSCs. Finally, we perform global gene expression analysis and identify key regulatory pathways including the TGF-β and Wnt pathway governing early neural stem cell self-renewal.

Introduction

During mammalian brain development, embryonic neural stem cells represent a dynamic cell population derived from primitive neuroepithelial cells and are capable of both self-renewal and multilineage differentiation. NSCs differentiate first into neurons and then into astrocytes or oligodendroglial cells in a temporally regulated fashion (16, 431). These neuroepithelial cells demonstrate a remarkable plasticity, with a capacity of generating a wide variety of terminally differentiated cells from a small original population. These cells may be isolated and expanded *in vitro* as neurospheres, allowing for the identification of cell markers or regulatory signaling mechanisms associated with self-renewal and with cell differentiation (490).

The onset of neurogenesis within NSCs marks a switch from symmetric divisions of primitive, lineage-negative cells to asymmetric cell divisions that generate an increasingly heterogeneous population of cells expressing various neuronal markers (390). Combinations of growth factors (bFGF and EGF) and secreted proteins in the TGF-β superfamily (chiefly BMPs) or Wnt pathway govern early neurogenesis in combination with basic helix-loop-helix (bHLH) transcription factors such as sox2, other transcription factors such as paired box 6 (Pax6), forkhead box G1 (FOXG1), LIM homeobox 2 (LHX2), and empty spiracles homologue 2 (EMX2) (404, 407, 409-411, 491).

Glial differentiation follows neuronal patterning and is regulated by a combination of cytokine signaling and changes in gene expression. BMP signaling through BMPR-1B, in addition to causing terminal differentiation of NSCs to neurons results in the fate-switching from neuronal to astrocytic differentiation. BMP signaling induces inhibitory bHLH transcription factors such as Hes-5, Id1, and Id3 (407, 409). These factors rapidly downregulate the expression of Mash1 and neurogenin and thus inhibit neuronal differentiation (410, 411). Receptors for cytokines such as leukemia inhibitory factor (LIF) and ciliary neurotrophic factor (CNTF) phosphorylate STAT3 upon binding of their ligand, activating genes associated with glial differentiation (409, 413-415, 492). Epigenetic regulation of chromatin helps in the coordination of these signaling events as opening or compaction of chromatin structures may reveal or conceal binding sites for STAT3 (460).

In contrast, much less is known regarding regulation of self-renewal and pathways governing cell division in more primitive neuroepithelial cells or lineage-negative NSCs. These cells express bHLH transcription factors and signaling through the Notch pathway is operative in early patterning of the developing ventricular zone, but other regulatory pathways and how these may interact with these transcription factors to govern symmetric cell division and then the transition to neurogenesis is unknown (342, 343, 387, 414, 493).

The domestic dog (Canis familiaris) represents a powerful, untapped species for the comparative analysis of early neural stem cell or neuroepithelial regulation in man. As the domesticated dog and humans have co-evolved over centuries, both species show shared evolutionary traits in genes associated with brain development that are not shared in rodents (13). Dogs and humans also develop numerous spontaneous nervous system disorders with remarkable similarity, suggesting shared regulatory pathways between the two species (494). Here, we report for the first time the characterization of neural stem cells isolated from canine embryos harvested from the time of neural tube closure through fetal development, including times of peak neuronal and astroglial differentiation. NSCs isolated early in development express CD133, are lineage negative, more clonogenic *in vitro*, and are refractory to differentiation in the presence of serum. Analysis of gene expression microarrays reveals significant differences in early passage eNSCs isolated from e27 embryos compared to those harvested from later in gestation. By comparing gene expression networks from our e20 and e27 eNSCs to those more primed for differentiation, we hope to identify shared self-renewal pathways or similar mechanisms involved in the inhibition of differentiation or cellular senescence.

Materials and Methods

Isolation of Canine Embryos and Culture of NSCs

Female beagle dogs aged 2-5 years were mated over three consecutive days after the onset of estrus. The second day of mating was established as day zero for gestational

timing. Following this, at 20, 27, 40, or 60 days gestation, the dog was anesthetized and an ovariohysterectomy performed under aseptic conditions. The gravid uterus was transferred to a surgical operating microscope (Zeiss) where the embryo was microdissected from the fetal membranes and immediately placed into ice-cold PBS supplemented with 0.5% glucose. The prosencephalon (e20) or telencephalon (e27, e40, e60) were then microdissected free and briefly enzymatically dissociated into single cells. Red blood cells and cellular debris were removed by ACK lysis buffer (Gibco) and differential centrifugation. Cells were placed into culture in Neurobasal-A medium (Invitrogen), N2 and B27 supplements (0.5x concentration, each; Invitrogen), heparin (2ug/mL, Sigma), and containing either recombinant human bFGF alone (bFGF) or bFGF and EGF (NBE, 25ng/mL each; R&D systems). Differentiation was induced by either growth factor withdrawal or by culturing cells in DMEM medium (Invitrogen) containing 10% fetal bovine serum (Invitrogen). Cells were cultured as neurospheres in uncoated tissue culture flasks or as adherent cells on plates pre-coated with a poly-ornithine/poly-D-lysine mixture.

FACS Analysis

Cultured NSCs were dissociated into single-cell suspensions and labeled with anti-CD133 (Santa Cruz **sc-30220**) and CD-15-FITC (MMA clone, BD) as previously described. Staining for CD133 was performed by labeling one million cells with 2ug of antibody at 4ºC for 10 minutes. Concentrations of other antibodies and the staining conditions were followed per the manufacturers recommendation. Non-conjugated

primary antibodies were subsequently labeled with PE- or FITC-conjugated secondary antibodies (BD). Antibodies against mouse immunoglobulin conjugated to PE or FITC were used as antibody isotype controls (BD). The stained cells were analyzed on the FACS Vantage SE flow cytometer (BD).

Immunocytochemistry

Cells were dissociated into single-cell suspensions and plated onto optical glass coverslips coated with polyornithine, poly-D-lysine, and laminin (BD Biosciences). Cells were maintained at 37°C for either 2-3 days (bFGF and NBE conditions) or for 10 days during serum-induced differentiation. Cells were then washed with PBS and fixed for 20 minutes at room temperature with 4% paraformaldehyde (PFA). The coverglass was then washed with PBS, blocked for 1 hour at room temperature with 5% FBS in PBS and labeled with primary antibodies. The following primary antibodies were used: Nestin (Covance PRB-336c), Sox2 (R&D systems: MAB2018), GFAP (Dako ZO334), Tuj1 (Covance MMS-435p), and Vimentin (Novus NB200-622), all used according to manufacturer's recommended dilutions. Fluorescent-conjugated anti-mouse and anti-rabbit secondary antibodies were then applied for 1 hour at room temperature and the coverslips mounted with DAPI-containing mounting medium (Vector Labs). Images were visualized through a Zeiss LSM510 confocal microscope.

Limiting Dilution Assay

NSCs cultured in either bFGF or NBE were dissociated into single-cell suspensions and then plated into 96 well plates with various seeding densities (1 to 50 cells per well). Cells were incubated at 37°C for two to three weeks. At the time of quantification, each well was examined for the formation of spheres.

Antibodies for Western Blot Analysis

The following antibodies were used as primary antibodies: Nestin (IBL America), Sox2 (Santa Cruz Biotechnology; sc-20088), sox3 (Aviva; ARP38649), sox9 (Abcam; ab71762), sox10 (Santa Cruz Biotechnology; sc-48824), sox17 (Lifespan Biosciences), GFAP (Dako ZO334), Tuj1 (Covance MMS-435P), Vimentin (Novus), Cleaved Caspase 3 (Cell Signaling), GAPDH (Abcam), STAT3 (Invitrogen), pSTAT3 (Cell Signaling), pSMAD1/5/8 (Cell Signaling), SMAD1 (Chemicon), ERK1/2 (Cell Signaling), MEK1/2 (Cell Signaling), p38 (Cell Signaling), osteonectin (Abcam ab61383), and BMPR1A (R&D), BMPR1B (R&D).

Telomerase Activity (TRAP) Assay

Telomerase activity was assessed by using the TeloTAGGG PCR ELISA according to manufacturer's recommendations (Roche 11 854 666 910). NSCs were grown to passage 2, 6, or 12, enzymatically dissociated and enumerated such that $2x10^5$ cells were lysed. The lysate was subsequently amplified by PCR reaction according to the manufacturer protocol, hybridized to the ELISA microplate, and the colormetric reaction developed

and analyzed on a microplate reader set at 450 and 690nm wavelengths. Absorbance readings are reported as A_{450}-A_{690}. Human embryonic kidney cells (HEK 293) were used as a positive control.

Gene Expression Microarray Analysis

Total RNA from e27, e40, and e60 NSCs cultured either in NBE or FBS was isolated using Trizol (Invitrogen) and then further purified using RNeasy Mini Kit (Qiagen). The integrity and quality of RNA obtained was verified with the Bioanalyzer System (Agilent Technologies, Palo Alto, CA) using the RNA Pico Chips. Total RNA was then converted to cDNA with Superscript reverse transcriptase (Invitrogen) using T7-linked Oligo (dT) primer. Complementary DNA was transcribed *in vitro* using the T7 Bioarray High Yield RNA Transcript Labeling Kit (ENZO Diagnostics) to generate biotinylated cRNA. Purified cRNA (20 μg) was fragmented and hybridized to the Canine Genome 2.0 expression array (Affymetrix). Arrays were processed according to manufacturer's recommendations. After hybridization, the chips were processed using fluidics station 450 and high-resolution microarray scanner 3000. The initial gene expression analysis data files (.dat, .cel, .txt and .rpt files) were generated using Affymetrix GeneChip Operating Software (GCOS) version 1.3. All RNA samples and arrays met standard quality control metrics.

Gene Expression Data Analysis

The .cel files and detection calls were imported into Partek software version 6.2 (Partek Inc.) and normalized using the dChip PM/MM average difference model. Arrays with percentage of outliers >5% were excluded for data analysis. Two filters were then applied to the normalized and cleaned data set to filter the probe sets with "present" calls <10% of the total number of samples or probe sets containing >10% of the zeros across samples with signal intensities of mismatch > perfect match. Hierarchical clustering was done using distance matrix of Pearson correlation with average linkage method and principal component analysis (PCA) done with correlation dispersion matrix and normalized eigenvector scaling using Partek software version 6.2 (Partek, Inc.).

Statistical Analysis

All values are shown as mean ± standard deviation (SD). Kaplan-Meier survival analysis was performed in Prism 4.0 software.

Results

Isolation of Canine NSCs and Their Differentiation Potential

In order to evaluate neural stem cells through periods of expansion, neuronal differentiation, and glial differentiation, we isolated NSCs from timed gestation lengths of 20, 27, 40, and 60 days (normal gestation length of the domestic dog is approximately 62 days, Figure 1). NSCs isolated from early in development at either 20 or 27 days (E20,

E27, respectively) proliferate rapidly in serum-free medium (either bFGF or NBE medium) as a mixed population containing both adherent and non-adherent, neurosphere structures. In contrast, NSCs isolated from either 40 or 60 days gestation proliferate exclusively as non-adherent neurospheres under identical culture conditions (Figure 2).

Lacking definitive markers for mammalian neural stem cells, many studies rely on the expression of nestin and sox2 to identify NSCs. How these proteins are regulated throughout embryonic brain development remains unknown, however- particularly within the time period of neural fate commitment from embryonic stem cells or uncommitted neuroepithelial cells. We therefore examined the expression of the intermediate filaments nestin and vimentin along with expression of sox2 in our canine NSCs throughout embryonic brain development. NSCs isolated from E40 and E60 ubiquitously express both nestin and sox2 in NBE conditions, both of which are downregulated significantly when cultured in the presence of FBS in a similar manner to murine E14 NSCs. Interestingly, NSCs isolated from earlier developmental periods, E20 and E27 lack significant expression of sox2 (Figure 3). The intermediate filament expression in E20 NSCs is also in contrast to E27, E40, and E60 NSCs, as these early neural progenitor cells lack significant nestin expression while maintaining strong vimentin expression. Vimentin is also expressed early in human neuroepithelial development. Our canine E20 NSCs may therefore represent a pre-nestin neural progenitor cell.

As the neural tube closes at approximately 18.5d gestation in the dog, we next investigated the differentiation capacity of early canine NSCs and compared them to those isolated from either 40 or 60 days gestation (382). To minimize the impact of time *in vitro* during NSC expansion, all cells were analyzed at 7-10 days *in vitro* (d.i.v). Consistent with NSCs isolated form murine embryos early in gestation (e8-e8.5), canine NSCs from e20 express no markers associated with either neuronal (β-III-Tubulin/TuJ-1) or astrocytic (GFAP) differentiation in either NBE or FBS (Figure 3). NSCs isolated at 27d gestation also fail to demonstrate any TuJ-1 or GFAP expression in NBE conditions, although scattered cells express TuJ-1 in FBS, suggesting this time point is associated with the onset of neurogenesis (beginning of neuronal differentiation capacity). In contrast to either E20 or E27, NSCs from E40 strongly express TuJ-1 in both NBE and FBS conditions, confirming these cells are similar to murine E14 NSCs and represent the peak time for neurogenesis. NSCs from E60 express both TuJ-1 and GFAP in NBE conditions, but strongly and exclusively express GFAP in FBS, consistent with the astroglial-competent differentiation status of other mammalian NSCs near parturition. Canine embryonic NSCs therefore exhibit temporally regulated differentiation potential along first neuronal and then astroglial differentiation similar to both human and murine NSCs. NSCs isolated early in development (E20) appear refractory to differentiation even in the presence of serum while the expression of TuJ-1 by small numbers of NSCs from E27 in FBS suggest these cells are acquiring the ability to differentiate into neurons.

Expression of NSC Markers and Evaluation of Clonogenic Potential

Along with nestin and sox2 expression, the cell surface markers CD133 (also known as prominin-1) and CD15 (also known as SSEA-1 or LeX) have been used to prospectively identify mammalian NSCs (321, 428, 431, 495). How the expression of these markers is regulated through brain development and the relationship of each marker to the other is still unknown however. We therefore examined the expression of both CD133 and CD15 in our canine NSCs. CD133 is expressed in high amounts only in our E20 NSCs, suggesting this marker is limited to early neuroepithelial progenitor cells. In contrast, CD15 is expressed in a manner that correlates with peak time points of either neuronal (E40) or glial (E60) differentiation (Figure 4A). These data suggest that CD133 is limited to non-committed canine NSCs while CD15 is expressed only in differentiation-competent cells.

The restricted expression of CD133 to cells isolated early in neuroepithelial development would therefore suggest these cells contain more of a stem cell component than those populations rich in CD15 (E40 and E60 NSCs). Consistent with this, limiting dilution assays of our canine NSCs reveal a significantly enhanced self-renewal capacity in E20 or E27 NSCs compared to E40 and E60 NSCs (Figure 4B). Expression of telomerase, an enzyme expressed in embryonic neural stem cells and many immortalized cells responsible for the maintenance of chromosome ends, is also significantly upregulated in both E20 and E27 NSCs compared to either E40 or E60 NSCs (Figure 4C). Finally, the onset of differentiation in the mammalian forebrain is also associated with upregulation

of apoptosis as cells exit the proliferative phase in order to control the cell number of the developing brain. Consistent with this, activation of caspase 3 is identified only in late passage E27 or E40 NSCs and not in acutely isolated E27 cells (Figure 4D).

Expression of Proteins Governing NSC Development in Canine NSCs

As our canine NSCs isolated early in gestation surprisingly lack significant sox2 expression, we sought to more fully characterize the expression of other proteins related to mammalian neural crest or NSC development. Immunoblots confirmed significantly reduced sox2 expression in both E20 and E27 NSCs compared to E40 or E60 NSCs. Other members of the β1-Sox family of transcription factors are highly expressed in early gestation canine NSCs however, including sox3. Similarly, other members of the sox transcription factor family involved in neuroepithelial fate commitment from embryonic stem cells, sox9 and sox10 are increased in E20 and E27 canine NSCs. The expression of BMPR-1A in NSCs *in vivo* induces the expression of BMPR-1B and is vital for the fate commitment of neural precursors. Accordingly, E20 NSCs express high levels of both BMPR1A and BMPR1B compared to NSCs isolated from other gestational time periods.

Similar to the observations made on immunofluorescence, immunoblots confirm E20 NSCs express very low levels of nestin intermediate filament. Interestingly, these cells, along with E27 NSCs express high levels of the intermediate filament vimentin and the structural protein osteonectin (Figure 5). Expression of vimentin and osteonectin is associated with epithelial-to-mesenchymal transition (EMT) in many cancers, and a

similar process occurs early during brain development associated with migration of early neural precursors (98, 339). E20 and E27 canine NSCs may therefore represent early neural progenitor cells at the transition from proliferative, differentiation resistant, highly migratory cells to lineage-committed progenitor cells.

Canine NSCs Mature *In Vitro* in a Regulated Temporal Manner

In order to examine whether early, lineage-negative canine NSCs are capable of recapitulating the temporal events governing first neuronal and then astroglial differentiation *in vivo*, we serially passaged E27 NSCs to compare the expression of TuJ-1 and GFAP over time (Figure 6). Indeed, serial passage of these cells first increases the expression of TuJ-1 by passage 6, and ultimately the expression of GFAP by passage 12. Through long-term serial passage, GFAP expression becomes prominent by passage 22, suggesting that the differentiation capacity of NSCs is genomically imprinted following neural fate commitment and may proceed independently of exogenous cues or differentiation signals. Interestingly, sox2 expression coincides with the onset of differentiation over this serial passage (Figure 7). Early E27 NSCs are largely lineage negative, yet express low amounts of sox2. At the time of neural differentiation, cells positive for TuJ-1 co-express sox2, and at late passages all cells co-express both. Sox2 expression *in vivo* is upregulated at the time of neural differentiation, although a specific role for the transcription factor driving neurogenesis has not yet been elucidated. These data suggest that sox2 may induce neural differentiation from canine neuroepithelial cells.

As E27 NSCs are capable of following a similar differentiation pattern *in vitro* over serial passage as that documented *in vivo*, we investigated whether the cytokine signaling pathways governing NSC differentiation status matured in an analogous manner. Bone morphogenetic protein (BMP) mediated SMAD signaling and STAT3 signaling through either activation of the leukemia inhibitory factor (LIF) or the ciliary neurotrophic factor (CNTF) receptors coordinate the transition from neurogenesis to astroglial differentiation (414-416, 492). Prolonged STAT3 activation in particular is associated with the acquisition of astrocytic differentiation. Consistent with our other observations regarding serial passage *in vitro*, our E27 NSCs gradually acquire prolonged activation of STAT3 in response to CNTF signaling at a time (passage) corresponding to widespread GFAP expression. Early canine NSCs (E20) fail to demonstrate any STAT3 activation in response to CNTF treatment, consistent with the differentiation refractory nature of these cells (Figure 8).

Finally, we examined the activation of the mitogen-activated-kinase (MAP) pathway over serial passage. The onset of neuronal differentiation is associated with the phosphorylation of p38 in murine NSCs (496, 497). While early passage E27 NSCs express little endogenous p38 activity, treatment of BMP2, a potent physiologic inducer of neural induction *in vivo* dramatically upregulates p38 activity (Figure 9). Serial passage of E27 NSCs also results in the acquisition of p38 activity, consistent with the ability of early, lineage negative NSCs to follow physiologically relevant differentiation

pathways through endogenous regulatory means. As p38 phosphorylation governs only the onset of neurogenesis, its ability to be induced by neurogenic stimuli is lost by the time of peak neurogenesis at E40.

Early Gestation NSCs are Resistant to Serum-Induced Differentiation

While culturing E40 and E60 NSCs in the presence of FBS produces morphologic changes consistent with differentiation (acquisition of a neuronal and/or astrocytic phenotype) and the cessation of proliferation, both E20 and E27 cells continue to proliferate in FBS, even forming neurospheres similar to NBE conditions (Figure 10A). When we compare the differentiation capacity of E27 cells maintained in NBE versus FBS however, we observe a dramatic acceleration in the onset of neuronal differentiation. Cells maintained simultaneously in either NBE or FBS were examined for TuJ-1 expression. While cells maintained in NBE still express minimal levels of TuJ-1, those passaged three times in FBS strongly express TuJ-1 (Figure 10B). This accelerated onset of differentiation is also reflected in STAT3 phosphorylation in response to CNTF (Figure 10C). While cells cultured in NBE have only a transient STAT3 activation to CNTF stimulation, those cultured for an identical time in FBS now have a prolonged STAT3 activation similar to late passage NBE-cultured E27 cells and consistent with a more differentiation competent cell. Canine NSCs early in gestation are therefore resistant to differentiation, although the presence of differentiation cues in FBS greatly accelerates the acquisition of neuronal and glial differentiation (Figure 10D).

Changes in Gene Expression in Canine NSC Development

Early canine NSCs are resistant to differentiation initially, yet acquire differentiation capacity through serial passage *in vitro*. Global gene expression analysis of E27, E40, and E60 canine NSCs reveals significant differences in both the genes expressed at these gestational times as well as in the differential gene expression in response to serum induced differentiation conditions. E27 NSCs highly express numerous genes associated with embryonic stem cells, self-renewal, and early neuroepithelial development, including the transcription factor KLF4, Frizzled-1 and -2, BMP-4 and BMP-5, and members of the TGF-β superfamily. Both TGF-β2 and its receptor, TGF-β2-R, as well as Activin receptors are upregulated in E27 cells. E27 cells also highly express IL-6 and the pro-angiogenic mediators Angiopoietin-like 4 and Dkk3.

Genes associated with neuronal and astroglial differentiation are significantly downregulated in E27 NSCs compared to either E40 or E60 NSCs. These cells express less TuJ-1, MAP2, and GFAP, consistent with our observations on immunofluorescence. Early NSCs also express less neural cell adhesion molecules (NCAM-1 and NCAM-2), glutamate receptors GluR-1 and GluR-2, doublecortin, and the early neuronal transcription factor Pax6. E40 NSCs also express increased retinoic acid receptors and retinol binding proteins over E27, consistent with the suspected role of these proteins in neuronal induction (402, 403, 413).

In an effort to visualize the relatedness of canine NSCs over serial passage and between gestation lengths, we performed unsupervised principle component analysis (PCA) on the global gene expression of E27 NSCs over serial passage from p2 through p22, E40 p2, and E60 p2. Interestingly, E27 NSCs from passage 2, 5, and 11 cluster separately from either late passage (p22) E27 NSCs, E40, or E60 NSCs, suggesting significantly different patterns of gene expression within this group (Figure 11A). In contrast, E27 NSCs from later passage (p14, p22) cluster together with E40 and E60, suggesting similar gene expression profiles in this group, consistent with the observation of aging *in vitro* mimicking the maturation of differentiation capabilities *in vivo*. This is also supported by the observation that treatment of NSCs with NBE or FBS has dichotomous effects on E27 NSCs based on passage. While both NBE and FBS cultured E27 NSCs in early passage cluster together in PCA, they separate significantly at passage 14 and 22, just as E40 and E60 NSCs do. Unsupervised hierarchical clustering of this gene expression data further demonstrates that, while there is a treatment effect of culturing early passage E27 NSCs in FBS versus NBE, these cells still cluster more similar to each other when compared to late passage E27 NSCs (p14, p22), which are more similar to E40 and E60 NSCs, which also share similar differentiation capacities (Figure 11B).

Metaplastic Differentiaion Potential in Early Canine NSCs

Given the unique ability of NCSs derived early in gestation to proliferate in the presence of FBS and the lack of endogenous markers of either neuronal or astroglial differentiation, we investigated whether E27 NSCs could be induced to differentiate

along non-neural cell fates. We cultured E27, passage 2 NSCs in Neurobasal medium supplemented with ITS supplement (R&D Systems) and TGF-β3 for 21 days. Following this period, E27 NSCs expressed a significant amount of both intracellular and extracellular aggrecan, consistent with chondrogenic differentiation and suggesting significant plasticity towards the developmental potential of early canine NSCs (Figure 12).

Discussion

Here, we have for the first time demonstrated that neural stem cells may be isolated from the developing canine embryo from the time of neural tube closure through the onset and peak of neurogenesis, and from times of peak glial differentiation. Canine embryos are significantly larger than murine embryos at comparable gestation points, yet the dog is still a litter-bearing species, allowing for the isolation of significant numbers of NSCs immediately upon harvesting of the embryo. Much more thorough characterization may therefore be performed using these early gestation canine NSCs at early passages, without the need for prolonged, *in vitro* expansion as is the case with murine NSCs. These cells demonstrate significant similarities to murine NSCs in their growth characteristics and expression of neural and glial markers, as well as the temporal nature of neuronal and then glial differentiation *in vivo*. Canine NSCs also express identical cell surface markers identified on murine NSCs through various stages of development, CD133 (Prominin-1) and CD15 (SSEA-1) (321, 428, 429, 431, 495). How the expression

of these markers is regulated through neural development is still unknown however, as is the relationship of each marker to the other. The identification of these markers in an additional mammalian NSC model such as the dog is therefore beneficial towards the establishment of a hierarchy in NSC development, as we identify significant CD133 expression only in our E20 and E27 NSCs, with the expression of CD15 coinciding with the onset of differentiation potential. Significant differences do exist however, in both ability to interrogate NSCs early in development and in proteins expressed associated with murine NSC self-renewal, suggesting alternative pathways in mammalian brain development.

The intermediate filament nestin was originally described as a marker of rodent NSCs (330). Subsequent investigations have identified non-neural cells that also express nestin, including vascular progenitor cells, hair follicle cells, and bone marrow stromal cells, suggesting the role of nestin in NSCs may be more complicated than originally envisioned (313, 316, 332, 333). The expression of nestin and its role *in vivo* is also unclear regarding neural fate commitment from primitive neuroectoderm or embryonic stem cells. Our canine NSCs isolated from early in gestation express markedly reduced levels of nestin compared to E40 and E60 NSCs, instead expressing vimentin intermediate filaments. Vimentin is also a primitive intermediate filament and one of the most ubiquitously expressed in embryonic development (498-500). It is possible that our E20 NSCs represent a early timepoint in NSC development prior to nestin expression. It is also interesting to note the expression of the structural protein osteonectin with

vimentin, as both are upregulated with epithelial-to-mesenchymal transition (EMT) in certain neoplasms (98). In addition to neoplastic EMT, similar processes occur developmentally in the brain as cells migrate from the neural crest to form the early prosencephalon, further supporting the evidence that E20 and E27 NSCs are derived from primitive neuroepithelial tissue (339, 390).

Similarly, sox2 is expressed in murine NSCs and in embryonic stem cells, suggesting it has a prominent role in cell self-renewal (336, 337, 339, 343). Our canine NSCs however, express low levels of sox2 at early passages, when they are the most clonogenic, have high telomerase activity, and lack significant markers of either neuronal or glial differentiation (suggesting these populations have the most stem-like characteristics). These E20 and E27 NSCs do express other members of the β1-group of the sox transcription factor family, including sox3, supporting the suspected functional similarities between the β1-sox transcription factors and suggesting that species differences governing their expression may occur (342, 343). One such difference may explain the gradual expression of sox2 in our E27 NSCs over serial passage as they acquired neuronal differentiation capabilities. Sox2 is upregulated experimentally in murine NSCs differentiated into neurons, but the activity of this transcription factor in a differentiation versus a self-renewal scenario is unexplored (344). Our data suggests that sox2 may act to promote both a self-renewal and differentiation pattern in mammalian NSCs.

Early canine NSCs, expressing low levels of sox2 are resistant to differentiation in the presence of serum when compared to E40 and E60 NSCs that express high levels of sox2. In contrast to murine NSCs, these cells continue to proliferate in the presence of serum, although *in vitro* aging and the onset of differentiation capabilities is greatly accelerated. E27 cells express other genes associated with stem cell self-renewal or early neural crest development, including KLF4. KLF4 was identified as a key regulator of embryonic stem cell self-renewal and is a member of the four transcription factors originally used by Yamanaka et. al to induce pluripotency in murine fibroblasts (iPS cells) (337). The Wnt pathway is also critical for early neuroepithelial patterning in the developing brain (420). E27 NSCs express the Frizzled-1 and -2 receptors for Wnt, suggesting that Wnt signaling is also critical for self-renewal in early canine NSCs. Furthermore, early NSCs appear able to differentiate along mesenchymal lineage by expressing the chondrocyte-associated aggrecan protein *in vitro*. Interestingly, a recent report of generating iPS cells from murine neural stem cells suggest these cells have a propensity to differentiate towards chondrocytic lineage and may imply shared regulatory pathways between these iPS cells and early canine NSCs (501).

Characterization of canine embryonic NSCs allows the comparison of an additional, non-rodent species to investigate mammalian brain development. The embryo size and litter-bearing nature of dogs allows for significant acute analysis of these cells and the identification of primitive neural precursor cells, as we have reported here. These cells are resistant to differentiation, yet appear epigenetically imprinted early in neural fate

commitment to produce endogenous signals driving both neuronal and glial differentiation, as we are able to replicate this through serial passage *in vitro*. Investigations into gene regulatory networks driving the proliferation as well as the onset and maturation of differentiation of canine NSCs may identify novel gene interactions important for mammalian neurogenesis.

References

1. Tait MJ, Petrik V, Loosemore A, Bell BA, Papadopoulos MC. Survival of patients with glioblastoma multiforme has not improved between 1993 and 2004: analysis of 625 cases. Br J Neurosurg 2007;21:496-500.

2. Vescovi AL, Galli R, Reynolds BA. Brain tumour stem cells. Nat Rev Cancer 2006;6:425-36.

3. Galli R, Binda E, Orfanelli U, et al. Isolation and characterization of tumorigenic, stem-like neural precursors from human glioblastoma. Cancer Res 2004;64:7011-21.

4. Singh SK, Hawkins C, Clarke ID, et al. Identification of human brain tumour initiating cells. Nature 2004;432:396-401.

5. Frese KK, Tuveson DA. Maximizing mouse cancer models. Nat Rev Cancer 2007;7:645-58.

6. Stoica G, Kim HT, Hall DG, Coates JR. Morphology, immunohistochemistry, and genetic alterations in dog astrocytomas. Vet Pathol 2004;41:10-9.

7. Stoica G, Lungu G, Martini-Stoica H, Waghela S, Levine J, Smith R, 3rd. Identification of cancer stem cells in dog glioblastoma. Vet Pathol 2009;46:391-406.

8. Lipsitz D, Higgins RJ, Kortz GD, et al. Glioblastoma multiforme: clinical findings, magnetic resonance imaging, and pathology in five dogs. Vet Pathol 2003;40:659-69.

9. Thomas R, Duke SE, Wang HJ, et al. 'Putting our heads together': insights into genomic conservation between human and canine intracranial tumors. J Neurooncol 2009;94:333-49.

10. TCGA. Comprehensive genomic characterization defines human glioblastoma genes and core pathways. Nature 2008;455:1061-8.

11. Freire P, Vilela M, Deus H, et al. Exploratory analysis of the copy number alterations in glioblastoma multiforme. PLoS One 2008;3:e4076.

12. Rapaport F, Leslie C. Determining frequent patterns of copy number alterations in cancer. PLoS One 2007;5:e12028.

13. Lindblad-Toh K, Wade CM, Mikkelsen TS, et al. Genome sequence, comparative analysis and haplotype structure of the domestic dog. Nature 2005;438:803-19.

14. Liu W, Shen G, Shi Z, et al. Brain tumour stem cells and neural stem cells: still explored by the same approach? J Int Med Res 2008;36:890-5.

15. Sanai N, Alvarez-Buylla A, Berger MS. Neural stem cells and the origin of gliomas. N Engl J Med 2005;353:811-22.

16. Abramova N, Charniga C, Goderie SK, Temple S. Stage-specific changes in gene expression in acutely isolated mouse CNS progenitor cells. Dev Biol 2005;283:269-81.

17. Louis DN, Ohgaki H, Wiestler OD, et al. The 2007 WHO classification of tumours of the central nervous system. Acta Neuropathol 2007;114:97-109.

18. Michotte A, Neyns B, Chaskis C, Sadones J, In 't Veld P. Neuropathological and molecular aspects of low-grade and high-grade gliomas. Acta Neurol Belg 2004;104:148-53.

19. Huang H, Colella S, Kurrer M, Yonekawa Y, Kleihues P, Ohgaki H. Gene expression profiling of low-grade diffuse astrocytomas by cDNA arrays. Cancer Res 2000;60:6868-74.

20. Bourne TD, Schiff D. Update on molecular findings, management and outcome in low-grade gliomas. Nat Rev Neurol.

21. Dreyfuss JM, Johnson MD, Park PJ. Meta-analysis of glioblastoma multiforme versus anaplastic astrocytoma identifies robust gene markers. Mol Cancer 2009;8:71.

22. Ohgaki H. Epidemiology of brain tumors. Methods Mol Biol 2009;472:323-42.

23. Deorah S, Lynch CF, Sibenaller ZA, Ryken TC. Trends in brain cancer incidence and survival in the United States: Surveillance, Epidemiology, and End Results Program, 1973 to 2001. Neurosurg Focus 2006;20:E1.

24. Maher EA, Brennan C, Wen PY, et al. Marked genomic differences characterize primary and secondary glioblastoma subtypes and identify two distinct molecular and clinical secondary glioblastoma entities. Cancer Res 2006;66:11502-13.

25. Ohgaki H, Kleihues P. Genetic pathways to primary and secondary glioblastoma. Am J Pathol 2007;170:1445-53.

26. Phillips HS, Kharbanda S, Chen R, et al. Molecular subclasses of high-grade glioma predict prognosis, delineate a pattern of disease progression, and resemble stages in neurogenesis. Cancer Cell 2006;9:157-73.

27. Shinojima N, Tada K, Shiraishi S, et al. Prognostic value of epidermal growth factor receptor in patients with glioblastoma multiforme. Cancer Res 2003;63:6962-70.

28. Heimberger AB, Hlatky R, Suki D, et al. Prognostic effect of epidermal growth factor receptor and EGFRvIII in glioblastoma multiforme patients. Clin Cancer Res 2005;11:1462-6.

29. Zhu Y, Guignard F, Zhao D, et al. Early inactivation of p53 tumor suppressor gene cooperating with NF1 loss induces malignant astrocytoma. Cancer Cell 2005;8:119-30.

30. Jackson EL, Garcia-Verdugo JM, Gil-Perotin S, et al. PDGFR alpha-positive B cells are neural stem cells in the adult SVZ that form glioma-like growths in response to increased PDGF signaling. Neuron 2006;51:187-99.

31. Dai C, Celestino JC, Okada Y, Louis DN, Fuller GN, Holland EC. PDGF autocrine stimulation dedifferentiates cultured astrocytes and induces oligodendrogliomas and oligoastrocytomas from neural progenitors and astrocytes in vivo. Genes Dev 2001;15:1913-25.

32. Ma D, Nutt CL, Shanehsaz P, Peng X, Louis DN, Kaetzel DM. Autocrine platelet-derived growth factor-dependent gene expression in glioblastoma cells is mediated largely by activation of the transcription factor sterol regulatory element binding protein and is associated with altered genotype and patient survival in human brain tumors. Cancer Res 2005;65:5523-34.

33. Hunter T. Signaling--2000 and beyond. Cell 2000;100:113-27.

34. Schlessinger J. Cell signaling by receptor tyrosine kinases. Cell 2000;103:211-25.

35. Ohgaki H, Dessen P, Jourde B, et al. Genetic pathways to glioblastoma: a population-based study. Cancer Res 2004;64:6892-9.

36. Watanabe K, Tachibana O, Sata K, Yonekawa Y, Kleihues P, Ohgaki H. Overexpression of the EGF receptor and p53 mutations are mutually exclusive in the evolution of primary and secondary glioblastomas. Brain Pathol 1996;6:217-23; discussion 23-4.

37. Ekstrand AJ, Sugawa N, James CD, Collins VP. Amplified and rearranged epidermal growth factor receptor genes in human glioblastomas reveal deletions of sequences encoding portions of the N- and/or C-terminal tails. Proc Natl Acad Sci U S A 1992;89:4309-13.

38. Fankhauser R, Luginbuhl H, McGrath JT. Tumours of the nervous system. Bull World Health Organ 1974;50:53-69.

39. Koestner A HR. Tumors of the nervous syste. In: Meuten D (ed) Tumors in Domestic Animals. Blackwell Publishing 2002:697.

40. Dickinson PJ, Sturges BK, Higgins RJ, et al. Vascular endothelial growth factor mRNA expression and peritumoral edema in canine primary central nervous system tumors. Vet Pathol 2008;45:131-9.

41. Obermaier G, Reihlen A, Dahme E, Weis S. Rhinencephalic glial cell nests and their possible role in glioma formation: morphometric studies do not reveal significant differences between brachycephalic and dolichocephalic dogs. Acta Neuropathol 1995;89:258-61.

42. Thomas R, Duke SE, Karlsson EK, et al. A genome assembly-integrated dog 1 Mb BAC microarray: a cytogenetic resource for canine cancer studies and comparative genomic analysis. Cytogenet Genome Res 2008;122:110-21.

43. Engelman JA, Luo J, Cantley LC. The evolution of phosphatidylinositol 3-kinases as regulators of growth and metabolism. Nat Rev Genet 2006;7:606-19.

44. Easton RM, Cho H, Roovers K, et al. Role for Akt3/protein kinase Bgamma in attainment of normal brain size. Mol Cell Biol 2005;25:1869-78.

45. Tschopp O, Yang ZZ, Brodbeck D, et al. Essential role of protein kinase B gamma (PKB gamma/Akt3) in postnatal brain development but not in glucose homeostasis. Development 2005;132:2943-54.

46. Franca-Koh J, Kamimura Y, Devreotes PN. Leading-edge research: PtdIns(3,4,5)P3 and directed migration. Nat Cell Biol 2007;9:15-7.

47. Alessi DR, Deak M, Casamayor A, et al. 3-Phosphoinositide-dependent protein kinase-1 (PDK1): structural and functional homology with the Drosophila DSTPK61 kinase. Curr Biol 1997;7:776-89.

48. Alessi DR, James SR, Downes CP, et al. Characterization of a 3-phosphoinositide-dependent protein kinase which phosphorylates and activates protein kinase Balpha. Curr Biol 1997;7:261-9.

49. Sarbassov DD, Guertin DA, Ali SM, Sabatini DM. Phosphorylation and regulation of Akt/PKB by the rictor-mTOR complex. Science 2005;307:1098-101.

50. Mora A, Komander D, van Aalten DM, Alessi DR. PDK1, the master regulator of AGC kinase signal transduction. Semin Cell Dev Biol 2004;15:161-70.

51. Yang L, Qiao G, Ying H, Zhang J, Yin F. TCR-induced Akt serine 473 phosphorylation is regulated by protein kinase C-alpha. Biochem Biophys Res Commun 2010;400:16-20.

52. Cross DA, Alessi DR, Cohen P, Andjelkovich M, Hemmings BA. Inhibition of glycogen synthase kinase-3 by insulin mediated by protein kinase B. Nature 1995;378:785-9.

53. Alessi DR, Caudwell FB, Andjelkovic M, Hemmings BA, Cohen P. Molecular basis for the substrate specificity of protein kinase B; comparison with MAPKAP kinase-1 and p70 S6 kinase. FEBS Lett 1996;399:333-8.

54. Hutchinson JN, Jin J, Cardiff RD, Woodgett JR, Muller WJ. Activation of Akt-1 (PKB-alpha) can accelerate ErbB-2-mediated mammary tumorigenesis but suppresses tumor invasion. Cancer Res 2004;64:3171-8.

55. Arboleda MJ, Lyons JF, Kabbinavar FF, et al. Overexpression of AKT2/protein kinase Bbeta leads to up-regulation of beta1 integrins, increased invasion, and metastasis of human breast and ovarian cancer cells. Cancer Res 2003;63:196-206.

56. Yoeli-Lerner M, Yiu GK, Rabinovitz I, Erhardt P, Jauliac S, Toker A. Akt blocks breast cancer cell motility and invasion through the transcription factor NFAT. Mol Cell 2005;20:539-50.

57. Mure H, Matsuzaki K, Kitazato KT, et al. Akt2 and Akt3 play a pivotal role in malignant gliomas. Neuro Oncol 2010;12:221-32.

58. Manning BD, Cantley LC. AKT/PKB signaling: navigating downstream. Cell 2007;129:1261-74.

59. Marte BM, Downward J. PKB/Akt: connecting phosphoinositide 3-kinase to cell survival and beyond. Trends Biochem Sci 1997;22:355-8.

60. Wang M, Zhang X, Zhao H, Wang Q, Pan Y. FoxO gene family evolution in vertebrates. BMC Evol Biol 2009;9:222.

61. Hoekman MF, Jacobs FM, Smidt MP, Burbach JP. Spatial and temporal expression of FoxO transcription factors in the developing and adult murine brain. Gene Expr Patterns 2006;6:134-40.

62. Lein ES, Hawrylycz MJ, Ao N, et al. Genome-wide atlas of gene expression in the adult mouse brain. Nature 2007;445:168-76.

63. Brunet A, Bonni A, Zigmond MJ, et al. Akt promotes cell survival by phosphorylating and inhibiting a Forkhead transcription factor. Cell 1999;96:857-68.

64. Yang X, Cao W, Lin H, et al. Isoform-specific expression of 14-3-3 proteins in human astrocytoma. J Neurol Sci 2009;276:54-9.

65. Cao L, Cao W, Zhang W, et al. Identification of 14-3-3 protein isoforms in human astrocytoma by immunohistochemistry. Neurosci Lett 2008;432:94-9.

66. Maiese K, Chong ZZ, Shang YC. OutFOXOing disease and disability: the therapeutic potential of targeting FoxO proteins. Trends Mol Med 2008;14:219-27.

67. Dijkers PF, Birkenkamp KU, Lam EW, et al. FKHR-L1 can act as a critical effector of cell death induced by cytokine withdrawal: protein kinase B-enhanced cell survival through maintenance of mitochondrial integrity. J Cell Biol 2002;156:531-42.

68. Medema RH, Kops GJ, Bos JL, Burgering BM. AFX-like Forkhead transcription factors mediate cell-cycle regulation by Ras and PKB through p27kip1. Nature 2000;404:782-7.

69. Datta SR, Dudek H, Tao X, et al. Akt phosphorylation of BAD couples survival signals to the cell-intrinsic death machinery. Cell 1997;91:231-41.

70. Datta SR, Katsov A, Hu L, et al. 14-3-3 proteins and survival kinases cooperate to inactivate BAD by BH3 domain phosphorylation. Mol Cell 2000;6:41-51.

71. del Peso L, Gonzalez-Garcia M, Page C, Herrera R, Nunez G. Interleukin-3-induced phosphorylation of BAD through the protein kinase Akt. Science 1997;278:687-9.

72. Danial NN. BAD: undertaker by night, candyman by day. Oncogene 2008;27 Suppl 1:S53-70.

73. Mayo LD, Donner DB. A phosphatidylinositol 3-kinase/Akt pathway promotes translocation of Mdm2 from the cytoplasm to the nucleus. Proc Natl Acad Sci U S A 2001;98:11598-603.

74. Zhou BP, Liao Y, Xia W, Zou Y, Spohn B, Hung MC. HER-2/neu induces p53 ubiquitination via Akt-mediated MDM2 phosphorylation. Nat Cell Biol 2001;3:973-82.

75. Liang J, Zubovitz J, Petrocelli T, et al. PKB/Akt phosphorylates p27, impairs nuclear import of p27 and opposes p27-mediated G1 arrest. Nat Med 2002;8:1153-60.

76. Viglietto G, Motti ML, Bruni P, et al. Cytoplasmic relocalization and inhibition of the cyclin-dependent kinase inhibitor p27(Kip1) by PKB/Akt-mediated phosphorylation in breast cancer. Nat Med 2002;8:1136-44.

77. Sekimoto T, Fukumoto M, Yoneda Y. 14-3-3 suppresses the nuclear localization of threonine 157-phosphorylated p27(Kip1). EMBO J 2004;23:1934-42.

78. Rossig L, Badorff C, Holzmann Y, Zeiher AM, Dimmeler S. Glycogen synthase kinase-3 couples AKT-dependent signaling to the regulation of p21Cip1 degradation. J Biol Chem 2002;277:9684-9.

79. Peterson TR, Laplante M, Thoreen CC, et al. DEPTOR is an mTOR inhibitor frequently overexpressed in multiple myeloma cells and required for their survival. Cell 2009;137:873-86.

80. Hara K, Maruki Y, Long X, et al. Raptor, a binding partner of target of rapamycin (TOR), mediates TOR action. Cell 2002;110:177-89.

81. Kim DH, Sarbassov DD, Ali SM, et al. mTOR interacts with raptor to form a nutrient-sensitive complex that signals to the cell growth machinery. Cell 2002;110:163-75.

82. Gingras AC, Raught B, Sonenberg N. eIF4 initiation factors: effectors of mRNA recruitment to ribosomes and regulators of translation. Annu Rev Biochem 1999;68:913-63.

83. Rousseau D, Gingras AC, Pause A, Sonenberg N. The eIF4E-binding proteins 1 and 2 are negative regulators of cell growth. Oncogene 1996;13:2415-20.

84. Corradetti MN, Inoki K, Guan KL. The stress-inducted proteins RTP801 and RTP801L are negative regulators of the mammalian target of rapamycin pathway. J Biol Chem 2005;280:9769-72.

85. Shahbazian D, Roux PP, Mieulet V, et al. The mTOR/PI3K and MAPK pathways converge on eIF4B to control its phosphorylation and activity. EMBO J 2006;25:2781-91.

86. Acosta-Jaquez HA, Keller JA, Foster KG, et al. Site-specific mTOR phosphorylation promotes mTORC1-mediated signaling and cell growth. Mol Cell Biol 2009;29:4308-24.

87. Inoki K, Li Y, Zhu T, Wu J, Guan KL. TSC2 is phosphorylated and inhibited by Akt and suppresses mTOR signalling. Nat Cell Biol 2002;4:648-57.

88. Manning BD, Tee AR, Logsdon MN, Blenis J, Cantley LC. Identification of the tuberous sclerosis complex-2 tumor suppressor gene product tuberin as a target of the phosphoinositide 3-kinase/akt pathway. Mol Cell 2002;10:151-62.

89. Cai SL, Tee AR, Short JD, et al. Activity of TSC2 is inhibited by AKT-mediated phosphorylation and membrane partitioning. J Cell Biol 2006;173:279-89.

90. Huang J, Dibble CC, Matsuzaki M, Manning BD. The TSC1-TSC2 complex is required for proper activation of mTOR complex 2. Mol Cell Biol 2008;28:4104-15.

91. Tee AR, Anjum R, Blenis J. Inactivation of the tuberous sclerosis complex-1 and -2 gene products occurs by phosphoinositide 3-kinase/Akt-dependent and -independent phosphorylation of tuberin. J Biol Chem 2003;278:37288-96.

92. Ghosh HS, McBurney M, Robbins PD. SIRT1 negatively regulates the mammalian target of rapamycin. PLoS One 2010;5:e9199.

93. McBride SM, Perez DA, Polley MY, et al. Activation of PI3K/mTOR pathway occurs in most adult low-grade gliomas and predicts patient survival. J Neurooncol 2010;97:33-40.

94. Wang L, Harris TE, Lawrence JC, Jr. Regulation of proline-rich Akt substrate of 40 kDa (PRAS40) function by mammalian target of rapamycin complex 1 (mTORC1)-mediated phosphorylation. J Biol Chem 2008;283:15619-27.

95. Wang L, Harris TE, Roth RA, Lawrence JC, Jr. PRAS40 regulates mTORC1 kinase activity by functioning as a direct inhibitor of substrate binding. J Biol Chem 2007;282:20036-44.

96. Sanchez Canedo C, Demeulder B, Ginion A, et al. Activation of the cardiac mTOR/p70(S6K) pathway by leucine requires PDK1 and correlates with PRAS40 phosphorylation. Am J Physiol Endocrinol Metab 2010;298:E761-9.

97. Molina JR, Hayashi Y, Stephens C, Georgescu MM. Invasive glioblastoma cells acquire stemness and increased Akt activation. Neoplasia 2010;12:453-63.

98. Cheng GZ, Chan J, Wang Q, Zhang W, Sun CD, Wang LH. Twist transcriptionally up-regulates AKT2 in breast cancer cells leading to increased migration, invasion, and resistance to paclitaxel. Cancer Res 2007;67:1979-87.

99. Elias MC, Tozer KR, Silber JR, et al. TWIST is expressed in human gliomas and promotes invasion. Neoplasia 2005;7:824-37.

100. Zhang J, Han L, Zhang A, et al. AKT2 expression is associated with glioma malignant progression and required for cell survival and invasion. Oncol Rep 2010;24:65-72.

101. Zhang B, Gu F, She C, et al. Reduction of Akt2 inhibits migration and invasion of glioma cells. Int J Cancer 2009;125:585-95.

102. Yan W, Qian C, Zhao P, et al. Expression pattern of osteopontin splice variants and its functions on cell apoptosis and invasion in glioma cells. Neuro Oncol 2010;12:765-75.

103. Fu Y, Zhang Q, Kang C, et al. Inhibitory effects of adenovirus mediated Akt1 and PIK3R1 shRNA on the growth of malignant tumor cells in vitro and in vivo. Cancer Biol Ther 2009;8:1002-9.

104. Park CM, Park MJ, Kwak HJ, et al. Ionizing radiation enhances matrix metalloproteinase-2 secretion and invasion of glioma cells through Src/epidermal growth factor receptor-mediated p38/Akt and phosphatidylinositol 3-kinase/Akt signaling pathways. Cancer Res 2006;66:8511-9.

105. Kubiatowski T, Jang T, Lachyankar MB, et al. Association of increased phosphatidylinositol 3-kinase signaling with increased invasiveness and gelatinase activity in malignant gliomas. J Neurosurg 2001;95:480-8.

106. Brunckhorst MK, Wang H, Lu R, Yu Q. Angiopoietin-4 promotes glioblastoma progression by enhancing tumor cell viability and angiogenesis. Cancer Res 2010;70:7283-93.

107. Gordan JD, Simon MC. Hypoxia-inducible factors: central regulators of the tumor phenotype. Curr Opin Genet Dev 2007;17:71-7.

108. Semenza GL. Targeting HIF-1 for cancer therapy. Nat Rev Cancer 2003;3:721-32.

109. Maiuri F, Del Basso De Caro M, Siciliano A, et al. Expression of growth factors in brain tumors: correlation with tumor grade, recurrence and survival. Clin Neuropathol 2010;29:109-14.

110. Dimmeler S, Fleming I, Fisslthaler B, Hermann C, Busse R, Zeiher AM. Activation of nitric oxide synthase in endothelial cells by Akt-dependent phosphorylation. Nature 1999;399:601-5.

111. Fulton D, Gratton JP, McCabe TJ, et al. Regulation of endothelium-derived nitric oxide production by the protein kinase Akt. Nature 1999;399:597-601.

112. Towner RA, Smith N, Doblas S, et al. In vivo detection of inducible nitric oxide synthase in rodent gliomas. Free Radic Biol Med 2010;48:691-703.

113. Broholm H, Rubin I, Kruse A, et al. Nitric oxide synthase expression and enzymatic activity in human brain tumors. Clin Neuropathol 2003;22:273-81.

114. Warburg O. On the origin of cancer cells. Science 1956;123:309-14.

115. Calera MR, Martinez C, Liu H, Jack AK, Birnbaum MJ, Pilch PF. Insulin increases the association of Akt-2 with Glut4-containing vesicles. J Biol Chem 1998;273:7201-4.

116. Kohn AD, Summers SA, Birnbaum MJ, Roth RA. Expression of a constitutively active Akt Ser/Thr kinase in 3T3-L1 adipocytes stimulates glucose uptake and glucose transporter 4 translocation. J Biol Chem 1996;271:31372-8.

117. Eguez L, Lee A, Chavez JA, et al. Full intracellular retention of GLUT4 requires AS160 Rab GTPase activating protein. Cell Metab 2005;2:263-72.

118. Deprez J, Vertommen D, Alessi DR, Hue L, Rider MH. Phosphorylation and activation of heart 6-phosphofructo-2-kinase by protein kinase B and other protein kinases of the insulin signaling cascades. J Biol Chem 1997;272:17269-75.

119. Sundqvist A, Bengoechea-Alonso MT, Ye X, et al. Control of lipid metabolism by phosphorylation-dependent degradation of the SREBP family of transcription factors by SCF(Fbw7). Cell Metab 2005;1:379-91.

120. Berwick DC, Hers I, Heesom KJ, Moule SK, Tavare JM. The identification of ATP-citrate lyase as a protein kinase B (Akt) substrate in primary adipocytes. J Biol Chem 2002;277:33895-900.

121. Kotliarova S, Pastorino S, Kovell LC, et al. Glycogen synthase kinase-3 inhibition induces glioma cell death through c-MYC, nuclear factor-kappaB, and glucose regulation. Cancer Res 2008;68:6643-51.

122. Korur S, Huber RM, Sivasankaran B, et al. GSK3beta regulates differentiation and growth arrest in glioblastoma. PLoS One 2009;4:e7443.

123. Chakravarti A, Delaney MA, Noll E, et al. Prognostic and pathologic significance of quantitative protein expression profiling in human gliomas. Clin Cancer Res 2001;7:2387-95.

124. Broderick DK, Di C, Parrett TJ, et al. Mutations of PIK3CA in anaplastic oligodendrogliomas, high-grade astrocytomas, and medulloblastomas. Cancer Res 2004;64:5048-50.

125. Samuels Y, Wang Z, Bardelli A, et al. High frequency of mutations of the PIK3CA gene in human cancers. Science 2004;304:554.

126. Knobbe CB, Reifenberger G. Genetic alterations and aberrant expression of genes related to the phosphatidyl-inositol-3'-kinase/protein kinase B (Akt) signal transduction pathway in glioblastomas. Brain Pathol 2003;13:507-18.

127. Endersby R, Baker SJ. PTEN signaling in brain: neuropathology and tumorigenesis. Oncogene 2008;27:5416-30.

128. Zheng H, Ying H, Yan H, et al. p53 and Pten control neural and glioma stem/progenitor cell renewal and differentiation. Nature 2008;455:1129-33.

129. Taylor BS, Barretina J, Socci ND, et al. Functional copy-number alterations in cancer. PLoS One 2008;3:e3179.

130. Beroukhim R, Getz G, Nghiemphu L, et al. Assessing the significance of chromosomal aberrations in cancer: methodology and application to glioma. Proc Natl Acad Sci U S A 2007;104:20007-12.

131. Yadav AK, Renfrow JJ, Scholtens DM, et al. Monosomy of chromosome 10 associated with dysregulation of epidermal growth factor signaling in glioblastomas. JAMA 2009;302:276-89.

132. Bredel M, Scholtens DM, Harsh GR, et al. A network model of a cooperative genetic landscape in brain tumors. JAMA 2009;302:261-75.

133. Lane DP. Cancer. p53, guardian of the genome. Nature 1992;358:15-6.

134. Kirpensteijn J, Kik M, Teske E, Rutteman GR. TP53 gene mutations in canine osteosarcoma. Vet Surg 2008;37:454-60.

135. Yonemaru K, Sakai H, Murakami M, et al. The significance of p53 and retinoblastoma pathways in canine hemangiosarcoma. J Vet Med Sci 2007;69:271-8.

136. Lee CH, Kim WH, Lim JH, Kang MS, Kim DY, Kweon OK. Mutation and overexpression of p53 as a prognostic factor in canine mammary tumors. J Vet Sci 2004;5:63-9.

137. Talos F, Moll UM. Role of the p53 family in stabilizing the genome and preventing polyploidization. Adv Exp Med Biol 2010;676:73-91.

138. Soussi T, Ishioka C, Claustres M, Beroud C. Locus-specific mutation databases: pitfalls and good practice based on the p53 experience. Nat Rev Cancer 2006;6:83-90.

139. Daee DL, Mertz TM, Shcherbakova PV. A cancer-associated DNA polymerase delta variant modeled in yeast causes a catastrophic increase in genomic instability. Proc Natl Acad Sci U S A 2010;107:157-62.

140. Robertson AB, Klungland A, Rognes T, Leiros I. DNA repair in mammalian cells: Base excision repair: the long and short of it. Cell Mol Life Sci 2009;66:981-93.

141. Baute J, Depicker A. Base excision repair and its role in maintaining genome stability. Crit Rev Biochem Mol Biol 2008;43:239-76.

142. Weissman L, de Souza-Pinto NC, Stevnsner T, Bohr VA. DNA repair, mitochondria, and neurodegeneration. Neuroscience 2007;145:1318-29.

143. Campisi J, d'Adda di Fagagna F. Cellular senescence: when bad things happen to good cells. Nat Rev Mol Cell Biol 2007;8:729-40.

144. Finkel T, Serrano M, Blasco MA. The common biology of cancer and ageing. Nature 2007;448:767-74.

145. Gorgoulis VG, Vassiliou LV, Karakaidos P, et al. Activation of the DNA damage checkpoint and genomic instability in human precancerous lesions. Nature 2005;434:907-13.

146. Bartkova J, Horejsi Z, Koed K, et al. DNA damage response as a candidate anti-cancer barrier in early human tumorigenesis. Nature 2005;434:864-70.

147. Smith J, Tho LM, Xu N, Gillespie DA. The ATM-Chk2 and ATR-Chk1 pathways in DNA damage signaling and cancer. Adv Cancer Res 2010;108:73-112.

148. Limbo O, Porter-Goff ME, Rhind N, Russell P. Mre11 Nuclease Activity and Ctp1 Regulate Chk1 Activation by Rad3ATR and Tel1ATM Checkpoint Kinases at Double-Strand Breaks. Mol Cell Biol 2010.

149. Guo Z, Kozlov S, Lavin MF, Person MD, Paull TT. ATM activation by oxidative stress. Science 2010;330:517-21.

150. Lamarche BJ, Orazio NI, Weitzman MD. The MRN complex in double-strand break repair and telomere maintenance. FEBS Lett 2010;584:3682-95.

151. Williams RS, Dodson GE, Limbo O, et al. Nbs1 flexibly tethers Ctp1 and Mre11-Rad50 to coordinate DNA double-strand break processing and repair. Cell 2009;139:87-99.

152. Yoo HY, Kumagai A, Shevchenko A, Dunphy WG. The Mre11-Rad50-Nbs1 complex mediates activation of TopBP1 by ATM. Mol Biol Cell 2009;20:2351-60.

153. Wilsker D, Bunz F. Chk1 phosphorylation during mitosis: a new role for a master regulator. Cell Cycle 2009;8:1161-3.

154. Fragkos M, Jurvansuu J, Beard P. H2AX is required for cell cycle arrest via the p53/p21 pathway. Mol Cell Biol 2009;29:2828-40.

155. Carlessi L, De Filippis L, Lecis D, Vescovi A, Delia D. DNA-damage response, survival and differentiation in vitro of a human neural stem cell line in relation to ATM expression. Cell Death Differ 2009;16:795-806.

156. Bao S, Wu Q, McLendon RE, et al. Glioma stem cells promote radioresistance by preferential activation of the DNA damage response. Nature 2006;444:756-60.

157. Ashcroft M, Kubbutat MH, Vousden KH. Regulation of p53 function and stability by phosphorylation. Mol Cell Biol 1999;19:1751-8.

158. Hublarova P, Greplova K, Holcakova J, Vojtesek B, Hrstka R. Switching p53-dependent growth arrest to apoptosis via the inhibition of DNA damage-activated kinases. Cell Mol Biol Lett 2010;15:473-84.

159. Helt CE, Cliby WA, Keng PC, Bambara RA, O'Reilly MA. Ataxia telangiectasia mutated (ATM) and ATM and Rad3-related protein exhibit selective target specificities in response to different forms of DNA damage. J Biol Chem 2005;280:1186-92.

160. Brooks CL, Gu W. Ubiquitination, phosphorylation and acetylation: the molecular basis for p53 regulation. Curr Opin Cell Biol 2003;15:164-71.

161. Bode AM, Dong Z. Post-translational modification of p53 in tumorigenesis. Nat Rev Cancer 2004;4:793-805.

162. Nie L, Sasaki M, Maki CG. Regulation of p53 nuclear export through sequential changes in conformation and ubiquitination. J Biol Chem 2007;282:14616-25.

163. Sasaki M, Nie L, Maki CG. MDM2 binding induces a conformational change in p53 that is opposed by heat-shock protein 90 and precedes p53 proteasomal degradation. J Biol Chem 2007;282:14626-34.

164. Shieh SY, Ikeda M, Taya Y, Prives C. DNA damage-induced phosphorylation of p53 alleviates inhibition by MDM2. Cell 1997;91:325-34.

165. Di Stefano V, Soddu S, Sacchi A, D'Orazi G. HIPK2 contributes to PCAF-mediated p53 acetylation and selective transactivation of p21Waf1 after nonapoptotic DNA damage. Oncogene 2005;24:5431-42.

166. Knights CD, Catania J, Di Giovanni S, et al. Distinct p53 acetylation cassettes differentially influence gene-expression patterns and cell fate. J Cell Biol 2006;173:533-44.

167. Sakaguchi K, Herrera JE, Saito S, et al. DNA damage activates p53 through a phosphorylation-acetylation cascade. Genes Dev 1998;12:2831-41.

168. Millau JF, Bastien N, Bouchard EF, Drouin R. p53 Pre- and post-binding event theories revisited: stresses reveal specific and dynamic p53-binding patterns on the p21 gene promoter. Cancer Res 2009;69:8463-71.

169. Menendez D, Inga A, Resnick MA. The expanding universe of p53 targets. Nat Rev Cancer 2009;9:724-37.

170. Sauer M, Bretz AC, Beinoraviciute-Kellner R, et al. C-terminal diversity within the p53 family accounts for differences in DNA binding and transcriptional activity. Nucleic Acids Res 2008;36:1900-12.

171. Yakovleva T, Pramanik A, Kawasaki T, et al. p53 Latency. C-terminal domain prevents binding of p53 core to target but not to nonspecific DNA sequences. J Biol Chem 2001;276:15650-8.

172. Gu W, Malik S, Ito M, et al. A novel human SRB/MED-containing cofactor complex, SMCC, involved in transcription regulation. Mol Cell 1999;3:97-108.

173. Xing J, Sheppard HM, Corneillie SI, Liu X. p53 Stimulates TFIID-TFIIA-promoter complex assembly, and p53-T antigen complex inhibits TATA binding protein-TATA interaction. Mol Cell Biol 2001;21:3652-61.

174. Maltzman W, Czyzyk L. UV irradiation stimulates levels of p53 cellular tumor antigen in nontransformed mouse cells. Mol Cell Biol 1984;4:1689-94.

175. Vaseva AV, Moll UM. The mitochondrial p53 pathway. Biochim Biophys Acta 2009;1787:414-20.

176. Li YZ, Lu DY, Tan WQ, Wang JX, Li PF. p53 initiates apoptosis by transcriptionally targeting the antiapoptotic protein ARC. Mol Cell Biol 2008;28:564-74.

177. Lee JH, Kang Y, Khare V, et al. The p53-inducible gene 3 (PIG3) contributes to early cellular response to DNA damage. Oncogene 2010;29:1431-50.

178. Haupt S, Berger M, Goldberg Z, Haupt Y. Apoptosis - the p53 network. J Cell Sci 2003;116:4077-85.

179. Kuribayashi K, Krigsfeld G, Wang W, et al. TNFSF10 (TRAIL), a p53 target gene that mediates p53-dependent cell death. Cancer Biol Ther 2008;7:2034-8.

180. Hung AC, Porter AG. p53 mediates nitric oxide-induced apoptosis in murine neural progenitor cells. Neurosci Lett 2009;467:241-6.

181. Wang P, Yu J, Zhang L. The nuclear function of p53 is required for PUMA-mediated apoptosis induced by DNA damage. Proc Natl Acad Sci U S A 2007;104:4054-9.

182. Yu J, Zhang L, Hwang PM, Kinzler KW, Vogelstein B. PUMA induces the rapid apoptosis of colorectal cancer cells. Mol Cell 2001;7:673-82.

183. Kuwana T, Bouchier-Hayes L, Chipuk JE, et al. BH3 domains of BH3-only proteins differentially regulate Bax-mediated mitochondrial membrane permeabilization both directly and indirectly. Mol Cell 2005;17:525-35.

184. Chen L, Willis SN, Wei A, et al. Differential targeting of prosurvival Bcl-2 proteins by their BH3-only ligands allows complementary apoptotic function. Mol Cell 2005;17:393-403.

185. Letai A, Bassik MC, Walensky LD, Sorcinelli MD, Weiler S, Korsmeyer SJ. Distinct BH3 domains either sensitize or activate mitochondrial apoptosis, serving as prototype cancer therapeutics. Cancer Cell 2002;2:183-92.

186. Moll UM, Wolff S, Speidel D, Deppert W. Transcription-independent pro-apoptotic functions of p53. Curr Opin Cell Biol 2005;17:631-6.

187. Green DR, Kroemer G. Cytoplasmic functions of the tumour suppressor p53. Nature 2009;458:1127-30.

188. Hayflick L. The Limited in Vitro Lifetime of Human Diploid Cell Strains. Exp Cell Res 1965;37:614-36.

189. Serrano M, Lin AW, McCurrach ME, Beach D, Lowe SW. Oncogenic ras provokes premature cell senescence associated with accumulation of p53 and p16INK4a. Cell 1997;88:593-602.

190. Dimri GP. What has senescence got to do with cancer? Cancer Cell 2005;7:505-12.

191. Campisi J. Suppressing cancer: the importance of being senescent. Science 2005;309:886-7.

192. d'Adda di Fagagna F, Reaper PM, Clay-Farrace L, et al. A DNA damage checkpoint response in telomere-initiated senescence. Nature 2003;426:194-8.

193. Herbig U, Jobling WA, Chen BP, Chen DJ, Sedivy JM. Telomere shortening triggers senescence of human cells through a pathway involving ATM, p53, and p21(CIP1), but not p16(INK4a). Mol Cell 2004;14:501-13.

194. Tkemaladze J, Chichinadze K. Centriole, differentiation, and senescence. Rejuvenation Res 2010;13:339-42.

195. Sahin E, Depinho RA. Linking functional decline of telomeres, mitochondria and stem cells during ageing. Nature 2010;464:520-8.

196. Liu D, Xu Y. p53, oxidative stress and aging. Antioxid Redox Signal 2010.

197. Hunziker A, Jensen MH, Krishna S. Stress-specific response of the p53-Mdm2 feedback loop. BMC Syst Biol 2010;4:94.

198. Bondar T, Medzhitov R. p53-mediated hematopoietic stem and progenitor cell competition. Cell Stem Cell 2010;6:309-22.

199. Collado M, Gil J, Efeyan A, et al. Tumour biology: senescence in premalignant tumours. Nature 2005;436:642.

200. Dannenberg JH, van Rossum A, Schuijff L, te Riele H. Ablation of the retinoblastoma gene family deregulates G(1) control causing immortalization and increased cell turnover under growth-restricting conditions. Genes Dev 2000;14:3051-64.

201. Sage J, Miller AL, Perez-Mancera PA, Wysocki JM, Jacks T. Acute mutation of retinoblastoma gene function is sufficient for cell cycle re-entry. Nature 2003;424:223-8.

202. Harvey M, Sands AT, Weiss RS, et al. In vitro growth characteristics of embryo fibroblasts isolated from p53-deficient mice. Oncogene 1993;8:2457-67.

203. Warmerdam DO, Freire R, Kanaar R, Smits VA. Cell cycle-dependent processing of DNA lesions controls localization of Rad9 to sites of genotoxic stress. Cell Cycle 2009;8:1765-74.

204. Bhatia P, Menigatti M, Brocard M, Morley S, Ferrari S. Mitotic DNA damage targets the Aurora A/TPX2 complex. Cell Cycle 2010;9.

205. Meyer M, Rubsamen D, Slany R, et al. Oncogenic RAS enables DNA damage- and p53-dependent differentiation of acute myeloid leukemia cells in response to chemotherapy. PLoS One 2009;4:e7768.

206. Smogorzewska A, de Lange T. Different telomere damage signaling pathways in human and mouse cells. EMBO J 2002;21:4338-48.

207. Chan YW, On KF, Chan WM, et al. The kinetics of p53 activation versus cyclin E accumulation underlies the relationship between the spindle-assembly checkpoint and the postmitotic checkpoint. J Biol Chem 2008;283:15716-23.

208. Levine AJ, Hu W, Feng Z. The P53 pathway: what questions remain to be explored? Cell Death Differ 2006;13:1027-36.

209. Jin S, Antinore MJ, Lung FD, et al. The GADD45 inhibition of Cdc2 kinase correlates with GADD45-mediated growth suppression. J Biol Chem 2000;275:16602-8.

210. Zhan Q, Antinore MJ, Wang XW, et al. Association with Cdc2 and inhibition of Cdc2/Cyclin B1 kinase activity by the p53-regulated protein Gadd45. Oncogene 1999;18:2892-900.

211. Malkin D, Li FP, Strong LC, et al. Germ line p53 mutations in a familial syndrome of breast cancer, sarcomas, and other neoplasms. Science 1990;250:1233-8.

212. Louis DN. The p53 gene and protein in human brain tumors. J Neuropathol Exp Neurol 1994;53:11-21.

213. Soussi T. The p53 pathway and human cancer. Br J Surg 2005;92:1331-2.

214. Kato S, Han SY, Liu W, et al. Understanding the function-structure and function-mutation relationships of p53 tumor suppressor protein by high-resolution missense mutation analysis. Proc Natl Acad Sci U S A 2003;100:8424-9.

215. Jones PA, Rideout WM, 3rd, Shen JC, Spruck CH, Tsai YC. Methylation, mutation and cancer. Bioessays 1992;14:33-6.

216. Hainaut P, Hollstein M. p53 and human cancer: the first ten thousand mutations. Adv Cancer Res 2000;77:81-137.

217. Olivier M, Hussain SP, Caron de Fromentel C, Hainaut P, Harris CC. TP53 mutation spectra and load: a tool for generating hypotheses on the etiology of cancer. IARC Sci Publ 2004:247-70.

218. Hinds PW, Finlay CA, Quartin RS, et al. Mutant p53 DNA clones from human colon carcinomas cooperate with ras in transforming primary rat cells: a comparison of the "hot spot" mutant phenotypes. Cell Growth Differ 1990;1:571-80.

219. Lang GA, Iwakuma T, Suh YA, et al. Gain of function of a p53 hot spot mutation in a mouse model of Li-Fraumeni syndrome. Cell 2004;119:861-72.

220. Oren M, Rotter V. Mutant p53 gain-of-function in cancer. Cold Spring Harb Perspect Biol 2010;2:a001107.

221. Gu J, Kawai H, Nie L, et al. Mutual dependence of MDM2 and MDMX in their functional inactivation of p53. J Biol Chem 2002;277:19251-4.

222. Carter S, Bischof O, Dejean A, Vousden KH. C-terminal modifications regulate MDM2 dissociation and nuclear export of p53. Nat Cell Biol 2007;9:428-35.

223. Candeias MM, Malbert-Colas L, Powell DJ, et al. P53 mRNA controls p53 activity by managing Mdm2 functions. Nat Cell Biol 2008;10:1098-105.

224. Giono LE, Manfredi JJ. Mdm2 is required for inhibition of Cdk2 activity by p21, thereby contributing to p53-dependent cell cycle arrest. Mol Cell Biol 2007;27:4166-78.

225. Reifenberger G, Reifenberger J, Ichimura K, Meltzer PS, Collins VP. Amplification of multiple genes from chromosomal region 12q13-14 in human malignant gliomas: preliminary mapping of the amplicons shows preferential involvement of CDK4, SAS, and MDM2. Cancer Res 1994;54:4299-303.

226. Wood NT, Meek DW, Mackintosh C. 14-3-3 Binding to Pim-phosphorylated Ser166 and Ser186 of human Mdm2--Potential interplay with the PKB/Akt pathway and p14(ARF). FEBS Lett 2009;583:615-20.

227. Kawai H, Lopez-Pajares V, Kim MM, Wiederschain D, Yuan ZM. RING domain-mediated interaction is a requirement for MDM2's E3 ligase activity. Cancer Res 2007;67:6026-30.

228. Riemenschneider MJ, Buschges R, Wolter M, et al. Amplification and overexpression of the MDM4 (MDMX) gene from 1q32 in a subset of malignant gliomas without TP53 mutation or MDM2 amplification. Cancer Res 1999;59:6091-6.

229. Tanimura S, Ohtsuka S, Mitsui K, Shirouzu K, Yoshimura A, Ohtsubo M. MDM2 interacts with MDMX through their RING finger domains. FEBS Lett 1999;447:5-9.

230. Okamoto K, Kashima K, Pereg Y, et al. DNA damage-induced phosphorylation of MdmX at serine 367 activates p53 by targeting MdmX for Mdm2-dependent degradation. Mol Cell Biol 2005;25:9608-20.

231. Solomon DA, Kim JS, Jean W, Waldman T. Conspirators in a capital crime: co-deletion of p18INK4c and p16INK4a/p14ARF/p15INK4b in glioblastoma multiforme. Cancer Res 2008;68:8657-60.

232. Quelle DE, Zindy F, Ashmun RA, Sherr CJ. Alternative reading frames of the INK4a tumor suppressor gene encode two unrelated proteins capable of inducing cell cycle arrest. Cell 1995;83:993-1000.

233. Wang S, Tian C, Xing G, et al. ARF-dependent regulation of ATM and p53 associated KZNF (Apak) protein activity in response to oncogenic stress. FEBS Lett 2010;584:3909-15.

234. Hochegger H, Takeda S, Hunt T. Cyclin-dependent kinases and cell-cycle transitions: does one fit all? Nat Rev Mol Cell Biol 2008;9:910-6.

235. Malumbres M, Barbacid M. Mammalian cyclin-dependent kinases. Trends Biochem Sci 2005;30:630-41.

236. Harbour JW, Luo RX, Dei Santi A, Postigo AA, Dean DC. Cdk phosphorylation triggers sequential intramolecular interactions that progressively block Rb functions as cells move through G1. Cell 1999;98:859-69.

237. Lundberg AS, Weinberg RA. Functional inactivation of the retinoblastoma protein requires sequential modification by at least two distinct cyclin-cdk complexes. Mol Cell Biol 1998;18:753-61.

238. Johnson DG, Schwarz JK, Cress WD, Nevins JR. Expression of transcription factor E2F1 induces quiescent cells to enter S phase. Nature 1993;365:349-52.

239. Murray AW. Recycling the cell cycle: cyclins revisited. Cell 2004;116:221-34.

240. DeGregori J, Johnson DG. Distinct and Overlapping Roles for E2F Family Members in Transcription, Proliferation and Apoptosis. Curr Mol Med 2006;6:739-48.

241. Dimova DK, Dyson NJ. The E2F transcriptional network: old acquaintances with new faces. Oncogene 2005;24:2810-26.

242. Gaubatz S, Lindeman GJ, Ishida S, et al. E2F4 and E2F5 play an essential role in pocket protein-mediated G1 control. Mol Cell 2000;6:729-35.

243. Rane SG, Cosenza SC, Mettus RV, Reddy EP. Germ line transmission of the Cdk4(R24C) mutation facilitates tumorigenesis and escape from cellular senescence. Mol Cell Biol 2002;22:644-56.

244. Sotillo R, Dubus P, Martin J, et al. Wide spectrum of tumors in knock-in mice carrying a Cdk4 protein insensitive to INK4 inhibitors. EMBO J 2001;20:6637-47.

245. Malumbres M, Barbacid M. To cycle or not to cycle: a critical decision in cancer. Nat Rev Cancer 2001;1:222-31.

246. Knudson AG, Jr. Mutation and cancer: statistical study of retinoblastoma. Proc Natl Acad Sci U S A 1971;68:820-3.

247. Cobrinik D, Francis RO, Abramson DH, Lee TC. Rb induces a proliferative arrest and curtails Brn-2 expression in retinoblastoma cells. Mol Cancer 2006;5:72.

248. Serrano M, Hannon GJ, Beach D. A new regulatory motif in cell-cycle control causing specific inhibition of cyclin D/CDK4. Nature 1993;366:704-7.

249. Schmidt EE, Ichimura K, Reifenberger G, Collins VP. CDKN2 (p16/MTS1) gene deletion or CDK4 amplification occurs in the majority of glioblastomas. Cancer Res 1994;54:6321-4.

250. Jeffrey PD, Tong L, Pavletich NP. Structural basis of inhibition of CDK-cyclin complexes by INK4 inhibitors. Genes Dev 2000;14:3115-25.

251. Russo AA, Tong L, Lee JO, Jeffrey PD, Pavletich NP. Structural basis for inhibition of the cyclin-dependent kinase Cdk6 by the tumour suppressor p16INK4a. Nature 1998;395:237-43.

252. Ortega S, Malumbres M, Barbacid M. Cyclin D-dependent kinases, INK4 inhibitors and cancer. Biochim Biophys Acta 2002;1602:73-87.

253. Pavletich NP. Mechanisms of cyclin-dependent kinase regulation: structures of Cdks, their cyclin activators, and Cip and INK4 inhibitors. J Mol Biol 1999;287:821-8.

254. Sherr CJ. The Pezcoller lecture: cancer cell cycles revisited. Cancer Res 2000;60:3689-95.

255. Foijer F, Wolthuis RM, Doodeman V, Medema RH, te Riele H. Mitogen requirement for cell cycle progression in the absence of pocket protein activity. Cancer Cell 2005;8:455-66.

256. Meuwissen R, Linn SC, Linnoila RI, Zevenhoven J, Mooi WJ, Berns A. Induction of small cell lung cancer by somatic inactivation of both Trp53 and Rb1 in a conditional mouse model. Cancer Cell 2003;4:181-9.

257. Munakata T, Liang Y, Kim S, et al. Hepatitis C virus induces E6AP-dependent degradation of the retinoblastoma protein. PLoS Pathog 2007;3:1335-47.

258. Ranade K, Hussussian CJ, Sikorski RS, et al. Mutations associated with familial melanoma impair p16INK4 function. Nat Genet 1995;10:114-6.

259. Singh SK, Clarke ID, Terasaki M, et al. Identification of a cancer stem cell in human brain tumors. Cancer Res 2003;63:5821-8.

260. Becker AJ, Mc CE, Till JE. Cytological demonstration of the clonal nature of spleen colonies derived from transplanted mouse marrow cells. Nature 1963;197:452-4.

261. Siminovitch L, McCulloch EA, Till JE. The Distribution of Colony-Forming Cells among Spleen Colonies. J Cell Physiol 1963;62:327-36.

262. Reya T, Morrison SJ, Clarke MF, Weissman IL. Stem cells, cancer, and cancer stem cells. Nature 2001;414:105-11.

263. Wu AM, Till JE, Siminovitch L, McCulloch EA. Cytological evidence for a relationship between normal hemotopoietic colony-forming cells and cells of the lymphoid system. J Exp Med 1968;127:455-64.

264. Spangrude GJ, Heimfeld S, Weissman IL. Purification and characterization of mouse hematopoietic stem cells. Science 1988;241:58-62.

265. Lang SH, Anderson E, Fordham R, Collins AT. Modeling the prostate stem cell niche: an evaluation of stem cell survival and expansion in vitro. Stem Cells Dev 2010;19:537-46.

266. Liu S, Dontu G, Wicha MS. Mammary stem cells, self-renewal pathways, and carcinogenesis. Breast Cancer Res 2005;7:86-95.

267. Vries RG, Huch M, Clevers H. Stem cells and cancer of the stomach and intestine. Mol Oncol 2010;4:373-84.

268. Waters JM, Richardson GD, Jahoda CA. Hair follicle stem cells. Semin Cell Dev Biol 2007;18:245-54.

269. Shackleton M, Quintana E, Fearon ER, Morrison SJ. Heterogeneity in cancer: cancer stem cells versus clonal evolution. Cell 2009;138:822-9.

270. Coons SW, Johnson PC. Regional heterogeneity in the DNA content of human gliomas. Cancer 1993;72:3052-60.

271. Fey MF, Zimmermann A, Borisch B, Tobler A. Studying clonal heterogeneity in human cancers. Cancer Res 1993;53:921.

272. Hill SA, Wilson S, Chambers AF. Clonal heterogeneity, experimental metastatic ability, and p21 expression in H-ras-transformed NIH 3T3 cells. J Natl Cancer Inst 1988;80:484-90.

273. Benard J, Da Silva J, Riou G. Culture of clonogenic cells from various human tumors: drug sensitivity assay. Eur J Cancer Clin Oncol 1983;19:65-72.

274. Boccadoro M, Gavarotti P, Fossati G, Massaia M, Pileri A, Durie BG. Kinetics of circulating B lymphocytes in human myeloma. Blood 1983;61:812-4.

275. Durie BG, Young LA, Salmon SE. Human myeloma in vitro colony growth: interrelationships between drug sensitivity, cell kinetics, and patient survival duration. Blood 1983;61:929-34.

276. Hamburger AW, Salmon SE. Primary bioassay of human tumor stem cells. Science 1977;197:461-3.

277. Nomura Y, Tashiro H, Hisamatsu K. In vitro clonogenic growth and metastatic potential of human operable breast cancer. Cancer Res 1989;49:5288-93.

278. Fialkow PJ, Faguet GB, Jacobson RJ, Vaidya K, Murphy S. Evidence that essential thrombocythemia is a clonal disorder with origin in a multipotent stem cell. Blood 1981;58:916-9.

279. Griffin JD, Lowenberg B. Clonogenic cells in acute myeloblastic leukemia. Blood 1986;68:1185-95.

280. Bonnet D, Dick JE. Human acute myeloid leukemia is organized as a hierarchy that originates from a primitive hematopoietic cell. Nat Med 1997;3:730-7.

281. Blair A, Hogge DE, Sutherland HJ. Most acute myeloid leukemia progenitor cells with long-term proliferative ability in vitro and in vivo have the phenotype CD34(+)/CD71(-)/HLA-DR. Blood 1998;92:4325-35.

282. Cobaleda C, Gutierrez-Cianca N, Perez-Losada J, et al. A primitive hematopoietic cell is the target for the leukemic transformation in human philadelphia-positive acute lymphoblastic leukemia. Blood 2000;95:1007-13.

283. Cox CV, Evely RS, Oakhill A, Pamphilon DH, Goulden NJ, Blair A. Characterization of acute lymphoblastic leukemia progenitor cells. Blood 2004;104:2919-25.

284. Sell S. On the stem cell origin of cancer. Am J Pathol 2010;176:2584-494.

285. Neumuller RA, Knoblich JA. Dividing cellular asymmetry: asymmetric cell division and its implications for stem cells and cancer. Genes Dev 2009;23:2675-99.

286. Quintana E, Shackleton M, Sabel MS, Fullen DR, Johnson TM, Morrison SJ. Efficient tumour formation by single human melanoma cells. Nature 2008;456:593-8.

287. Shah NP, Skaggs BJ, Branford S, et al. Sequential ABL kinase inhibitor therapy selects for compound drug-resistant BCR-ABL mutations with altered oncogenic potency. J Clin Invest 2007;117:2562-9.

288. Tomasetti C, Levy D. Role of symmetric and asymmetric division of stem cells in developing drug resistance. Proc Natl Acad Sci U S A 2010;107:16766-71.

289. Barabe F, Kennedy JA, Hope KJ, Dick JE. Modeling the initiation and progression of human acute leukemia in mice. Science 2007;316:600-4.

290. van de Geijn GJ, Hersmus R, Looijenga LH. Recent developments in testicular germ cell tumor research. Birth Defects Res C Embryo Today 2009;87:96-113.

291. Baba T, Convery PA, Matsumura N, et al. Epigenetic regulation of CD133 and tumorigenicity of CD133+ ovarian cancer cells. Oncogene 2009;28:209-18.

292. Li C, Lee CJ, Simeone DM. Identification of human pancreatic cancer stem cells. Methods Mol Biol 2009;568:161-73.

293. Lukacs RU, Memarzadeh S, Wu H, Witte ON. Bmi-1 is a crucial regulator of prostate stem cell self-renewal and malignant transformation. Cell Stem Cell 2010;7:682-93.

294. Shipitsin M, Campbell LL, Argani P, et al. Molecular definition of breast tumor heterogeneity. Cancer Cell 2007;11:259-73.

295. Yeung TM, Gandhi SC, Wilding JL, Muschel R, Bodmer WF. Cancer stem cells from colorectal cancer-derived cell lines. Proc Natl Acad Sci U S A 2010;107:3722-7.

296. Greaves M. Cancer stem cells: back to Darwin? Semin Cancer Biol 2010;20:65-70.

297. Dick JE. Stem cell concepts renew cancer research. Blood 2008;112:4793-807.

298. Dick JE. Looking ahead in cancer stem cell research. Nat Biotechnol 2009;27:44-6.

299. Jordan CT, Guzman ML, Noble M. Cancer stem cells. N Engl J Med 2006;355:1253-61.

300. Baguley BC. Multiple drug resistance mechanisms in cancer. Mol Biotechnol 2010;46:308-16.

301. Bleau AM, Hambardzumyan D, Ozawa T, et al. PTEN/PI3K/Akt pathway regulates the side population phenotype and ABCG2 activity in glioma tumor stem-like cells. Cell Stem Cell 2009;4:226-35.

302. Charles N, Holland EC. The perivascular niche microenvironment in brain tumor progression. Cell Cycle 2010;9:3012-21.

303. Jamal M, Rath BH, Williams ES, Camphausen K, Tofilon PJ. Microenvironmental regulation of glioblastoma radioresponse. Clin Cancer Res 2010.

304. Peng H, Dong Z, Qi J, et al. A novel two mode-acting inhibitor of ABCG2-mediated multidrug transport and resistance in cancer chemotherapy. PLoS One 2009;4:e5676.

305. Scharenberg CW, Harkey MA, Torok-Storb B. The ABCG2 transporter is an efficient Hoechst 33342 efflux pump and is preferentially expressed by immature human hematopoietic progenitors. Blood 2002;99:507-12.

306. Quinones-Hinojosa A, Sanai N, Soriano-Navarro M, et al. Cellular composition and cytoarchitecture of the adult human subventricular zone: a niche of neural stem cells. J Comp Neurol 2006;494:415-34.

307. Alvarez-Buylla A, Kohwi M, Nguyen TM, Merkle FT. The heterogeneity of adult neural stem cells and the emerging complexity of their niche. Cold Spring Harb Symp Quant Biol 2008;73:357-65.

308. Doetsch F, Garcia-Verdugo JM, Alvarez-Buylla A. Cellular composition and three-dimensional organization of the subventricular germinal zone in the adult mammalian brain. J Neurosci 1997;17:5046-61.

309. Aguirre A, Rubio ME, Gallo V. Notch and EGFR pathway interaction regulates neural stem cell number and self-renewal. Nature 2010;467:323-7.

310. Garcia AD, Doan NB, Imura T, Bush TG, Sofroniew MV. GFAP-expressing progenitors are the principal source of constitutive neurogenesis in adult mouse forebrain. Nat Neurosci 2004;7:1233-41.

311. Park D, Xiang AP, Mao FF, et al. Nestin is Required for the Proper Self-Renewal of Neural Stem Cells. Stem Cells 2010.

312. Witusik M, Gresner SM, Hulas-Bigoszewska K, et al. Neuronal and astrocytic cells, obtained after differentiation of human neural GFAP-positive progenitors, present heterogeneous expression of PrPc. Brain Res 2007;1186:65-73.

313. Fusi A, Reichelt U, Busse A, et al. Expression of the Stem Cell Markers Nestin and CD133 on Circulating Melanoma Cells. J Invest Dermatol 2010.

314. Guo R, Wu Q, Liu F, Wang Y. Description of the CD133+ subpopulation of the human ovarian cancer cell line OVCAR3. Oncol Rep 2011;25:141-6.

315. Hou NY, Yang K, Chen T, et al. CD133(+)CD44 (+) subgroups may be human small intestinal stem cells. Mol Biol Rep 2010.

316. Krupkova O, Jr., Loja T, Zambo I, Veselska R. Nestin expression in human tumors and tumor cell lines. Neoplasma 2010;57:291-8.

317. Bidlingmaier S, Zhu X, Liu B. The utility and limitations of glycosylated human CD133 epitopes in defining cancer stem cells. J Mol Med 2008;86:1025-32.

318. Liu G, Yuan X, Zeng Z, et al. Analysis of gene expression and chemoresistance of CD133+ cancer stem cells in glioblastoma. Mol Cancer 2006;5:67.

319. Beier D, Hau P, Proescholdt M, et al. CD133(+) and CD133(-) glioblastoma-derived cancer stem cells show differential growth characteristics and molecular profiles. Cancer Res 2007;67:4010-5.

320. Ogden AT, Waziri AE, Lochhead RA, et al. Identification of A2B5+CD133-tumor-initiating cells in adult human gliomas. Neurosurgery 2008;62:505-14; discussion 14-5.

321. Capela A, Temple S. LeX is expressed by principle progenitor cells in the embryonic nervous system, is secreted into their environment and binds Wnt-1. Dev Biol 2006;291:300-13.

322. Mao XG, Zhang X, Xue XY, et al. Brain Tumor Stem-Like Cells Identified by Neural Stem Cell Marker CD15. Transl Oncol 2009;2:247-57.

323. Son MJ, Woolard K, Nam DH, Lee J, Fine HA. SSEA-1 is an enrichment marker for tumor-initiating cells in human glioblastoma. Cell Stem Cell 2009;4:440-52.

324. Sun Y, Kong W, Falk A, et al. CD133 (Prominin) negative human neural stem cells are clonogenic and tripotent. PLoS One 2009;4:e5498.

325. Lin T, Islam O, Heese K. ABC transporters, neural stem cells and neurogenesis--a different perspective. Cell Res 2006;16:857-71.

326. Mouthon MA, Fouchet P, Mathieu C, et al. Neural stem cells from mouse forebrain are contained in a population distinct from the 'side population'. J Neurochem 2006;99:807-17.

327. Kelly PN, Dakic A, Adams JM, Nutt SL, Strasser A. Tumor growth need not be driven by rare cancer stem cells. Science 2007;317:337.

328. Guerrero-Cazares H, Chaichana KL, Quinones-Hinojosa A. Neurosphere culture and human organotypic model to evaluate brain tumor stem cells. Methods Mol Biol 2009;568:73-83.

329. Pollard SM, Conti L, Sun Y, Goffredo D, Smith A. Adherent neural stem (NS) cells from fetal and adult forebrain. Cereb Cortex 2006;16 Suppl 1:i112-20.

330. Lendahl U, Zimmerman LB, McKay RD. CNS stem cells express a new class of intermediate filament protein. Cell 1990;60:585-95.

331. Zhang M, Song T, Yang L, et al. Nestin and CD133: valuable stem cell-specific markers for determining clinical outcome of glioma patients. J Exp Clin Cancer Res 2008;27:85.

332. Amoh Y, Kanoh M, Niiyama S, et al. Human hair follicle pluripotent stem (hfPS) cells promote regeneration of peripheral-nerve injury: an advantageous alternative to ES and iPS cells. J Cell Biochem 2009;107:1016-20.

333. Kim SY, Lee S, Hong SW, et al. Nestin action during insulin-secreting cell differentiation. J Histochem Cytochem 2010;58:567-76.

334. Suzuki S, Namiki J, Shibata S, Mastuzaki Y, Okano H. The neural stem/progenitor cell marker nestin is expressed in proliferative endothelial cells, but not in mature vasculature. J Histochem Cytochem 2010;58:721-30.

335. Gangemi RM, Griffero F, Marubbi D, et al. SOX2 silencing in glioblastoma tumor-initiating cells causes stop of proliferation and loss of tumorigenicity. Stem Cells 2009;27:40-8.

336. Pevny LH, Nicolis SK. Sox2 roles in neural stem cells. Int J Biochem Cell Biol 2010;42:421-4.

337. Takahashi K, Tanabe K, Ohnuki M, et al. Induction of pluripotent stem cells from adult human fibroblasts by defined factors. Cell 2007;131:861-72.

338. Agathocleous M, Iordanova I, Willardsen MI, et al. A directional Wnt/beta-catenin-Sox2-proneural pathway regulates the transition from proliferation to differentiation in the Xenopus retina. Development 2009;136:3289-99.

339. Germana A, Montalbano G, Guerrera MC, et al. Developmental changes in the expression of sox2 in the zebrafish brain. Microsc Res Tech 2010.

340. Lim JH, Boozer L, Mariani CL, Piedrahita JA, Olby NJ. Generation and characterization of neurospheres from canine adipose tissue-derived stromal cells. Cell Reprogram 2010;12:417-25.

341. Favaro R, Valotta M, Ferri AL, et al. Hippocampal development and neural stem cell maintenance require Sox2-dependent regulation of Shh. Nat Neurosci 2009;12:1248-56.

342. Pevny L, Placzek M. SOX genes and neural progenitor identity. Curr Opin Neurobiol 2005;15:7-13.

343. Wegner M, Stolt CC. From stem cells to neurons and glia: a Soxist's view of neural development. Trends Neurosci 2005;28:583-8.

344. Cavallaro M, Mariani J, Lancini C, et al. Impaired generation of mature neurons by neural stem cells from hypomorphic Sox2 mutants. Development 2008;135:541-57.

345. Ge Y, Zhou F, Chen H, et al. Sox2 is translationally activated by eukaryotic initiation factor 4E in human glioma-initiating cells. Biochem Biophys Res Commun 2010;397:711-7.

346. Lu QR, Sun T, Zhu Z, et al. Common developmental requirement for Olig function indicates a motor neuron/oligodendrocyte connection. Cell 2002;109:75-86.

347. Molofsky AV, He S, Bydon M, Morrison SJ, Pardal R. Bmi-1 promotes neural stem cell self-renewal and neural development but not mouse growth and survival by repressing the p16Ink4a and p19Arf senescence pathways. Genes Dev 2005;19:1432-7.

348. Molofsky AV, Pardal R, Iwashita T, Park IK, Clarke MF, Morrison SJ. Bmi-1 dependence distinguishes neural stem cell self-renewal from progenitor proliferation. Nature 2003;425:962-7.

349. Zhou Q, Anderson DJ. The bHLH transcription factors OLIG2 and OLIG1 couple neuronal and glial subtype specification. Cell 2002;109:61-73.

350. Orzan F, Pellegatta S, Poliani L, et al. Enhancer of Zeste 2 (Ezh2) Is up-Regulated in Malignant Gliomas and in Glioma Stem-Like Cells. Neuropathol Appl Neurobiol 2010.

351. Rhee W, Ray S, Yokoo H, et al. Quantitative analysis of mitotic Olig2 cells in adult human brain and gliomas: implications for glioma histogenesis and biology. Glia 2009;57:510-23.

352. Bruggeman SW, Hulsman D, Tanger E, et al. Bmi1 controls tumor development in an Ink4a/Arf-independent manner in a mouse model for glioma. Cancer Cell 2007;12:328-41.

353. Schwartz YB, Pirrotta V. Polycomb silencing mechanisms and the management of genomic programmes. Nat Rev Genet 2007;8:9-22.

354. Valk-Lingbeek ME, Bruggeman SW, van Lohuizen M. Stem cells and cancer; the polycomb connection. Cell 2004;118:409-18.

355. Wang H, Wang L, Erdjument-Bromage H, et al. Role of histone H2A ubiquitination in Polycomb silencing. Nature 2004;431:873-8.

356. Guo WJ, Zeng MS, Yadav A, et al. Mel-18 acts as a tumor suppressor by repressing Bmi-1 expression and down-regulating Akt activity in breast cancer cells. Cancer Res 2007;67:5083-9.

357. Abdouh M, Facchino S, Chatoo W, Balasingam V, Ferreira J, Bernier G. BMI1 sustains human glioblastoma multiforme stem cell renewal. J Neurosci 2009;29:8884-96.

358. Ohtsubo M, Yasunaga S, Ohno Y, et al. Polycomb-group complex 1 acts as an E3 ubiquitin ligase for Geminin to sustain hematopoietic stem cell activity. Proc Natl Acad Sci U S A 2008;105:10396-401.

359. Maertens GN, El Messaoudi-Aubert S, Racek T, et al. Several distinct polycomb complexes regulate and co-localize on the INK4a tumor suppressor locus. PLoS One 2009;4:e6380.

360. Fasano CA, Phoenix TN, Kokovay E, et al. Bmi-1 cooperates with Foxg1 to maintain neural stem cell self-renewal in the forebrain. Genes Dev 2009;23:561-74.

361. Cao R, Wang L, Wang H, et al. Role of histone H3 lysine 27 methylation in Polycomb-group silencing. Science 2002;298:1039-43.

362. Czermin B, Melfi R, McCabe D, Seitz V, Imhof A, Pirrotta V. Drosophila enhancer of Zeste/ESC complexes have a histone H3 methyltransferase activity that marks chromosomal Polycomb sites. Cell 2002;111:185-96.

363. Kirmizis A, Bartley SM, Kuzmichev A, et al. Silencing of human polycomb target genes is associated with methylation of histone H3 Lys 27. Genes Dev 2004;18:1592-605.

364. Zhang Y, Cao R, Wang L, Jones RS. Mechanism of Polycomb group gene silencing. Cold Spring Harb Symp Quant Biol 2004;69:309-17.

365. Zhao S, Chai X, Frotscher M. Balance between neurogenesis and gliogenesis in the adult hippocampus: role for reelin. Dev Neurosci 2007;29:84-90.

366. Piccirillo SG, Reynolds BA, Zanetti N, et al. Bone morphogenetic proteins inhibit the tumorigenic potential of human brain tumour-initiating cells. Nature 2006;444:761-5.

367. Lee J, Kotliarova S, Kotliarov Y, et al. Tumor stem cells derived from glioblastomas cultured in bFGF and EGF more closely mirror the phenotype and genotype of primary tumors than do serum-cultured cell lines. Cancer Cell 2006;9:391-403.

368. von Bohlen Und Halbach O. Immunohistological markers for staging neurogenesis in adult hippocampus. Cell Tissue Res 2007;329:409-20.

369. Prestegarden L, Svendsen A, Wang J, et al. Glioma cell populations grouped by different cell type markers drive brain tumor growth. Cancer Res 2010;70:4274-9.

370. Menn B, Garcia-Verdugo JM, Yaschine C, Gonzalez-Perez O, Rowitch D, Alvarez-Buylla A. Origin of oligodendrocytes in the subventricular zone of the adult brain. J Neurosci 2006;26:7907-18.

371. Levine AJ, Brivanlou AH. Proposal of a model of mammalian neural induction. Dev Biol 2007;308:247-56.

372. Pera MF, Andrade J, Houssami S, et al. Regulation of human embryonic stem cell differentiation by BMP-2 and its antagonist noggin. J Cell Sci 2004;117:1269-80.

373. Kawasaki H, Mizuseki K, Nishikawa S, et al. Induction of midbrain dopaminergic neurons from ES cells by stromal cell-derived inducing activity. Neuron 2000;28:31-40.

374. Chambers SM, Fasano CA, Papapetrou EP, Tomishima M, Sadelain M, Studer L. Highly efficient neural conversion of human ES and iPS cells by dual inhibition of SMAD signaling. Nat Biotechnol 2009;27:275-80.

375. Ben-Zvi D, Shilo BZ, Fainsod A, Barkai N. Scaling of the BMP activation gradient in Xenopus embryos. Nature 2008;453:1205-11.

376. Fan X, Xu H, Cai W, Yang Z, Zhang J. Spatial and temporal patterns of expression of Noggin and BMP4 in embryonic and postnatal rat hippocampus. Brain Res Dev Brain Res 2003;146:51-8.

377. Sterneckert J, Stehling M, Bernemann C, et al. Neural induction intermediates exhibit distinct roles of Fgf signaling. Stem Cells 2010;28:1772-81.

378. Maric D, Fiorio Pla A, Chang YH, Barker JL. Self-renewing and differentiating properties of cortical neural stem cells are selectively regulated by basic fibroblast growth factor (FGF) signaling via specific FGF receptors. J Neurosci 2007;27:1836-52.

379. Gaspard N, Vanderhaeghen P. Mechanisms of neural specification from embryonic stem cells. Curr Opin Neurobiol 2010;20:37-43.

380. O'Rahilly R, Muller F. Neurulation in the normal human embryo. Ciba Found Symp 1994;181:70-82; discussion -9.

381. Juriloff DM, Harris MJ, Tom C, MacDonald KB. Normal mouse strains differ in the site of initiation of closure of the cranial neural tube. Teratology 1991;44:225-33.

382. Houston ML. The early brain development of the dog. J Comp Neurol 1968;134:371-84.

383. Ajioka I, Maeda T, Nakajima K. Identification of ventricular-side-enriched molecules regulated in a stage-dependent manner during cerebral cortical development. Eur J Neurosci 2006;23:296-308.

384. Committee TB. Embryonic vertebrate central nervous system: revised terminology. The Boulder Committee. Anat Rec 1970;166:257-61.

385. Rakic P. Specification of cerebral cortical areas. Science 1988;241:170-6.

386. Caviness VS, Jr., Rakic P. Mechanisms of cortical development: a view from mutations in mice. Annu Rev Neurosci 1978;1:297-326.

387. Gotz M, Huttner WB. The cell biology of neurogenesis. Nat Rev Mol Cell Biol 2005;6:777-88.

388. Iacopetti P, Michelini M, Stuckmann I, Oback B, Aaku-Saraste E, Huttner WB. Expression of the antiproliferative gene TIS21 at the onset of neurogenesis identifies single neuroepithelial cells that switch from proliferative to neuron-generating division. Proc Natl Acad Sci U S A 1999;96:4639-44.

389. Malatesta P, Appolloni I, Calzolari F. Radial glia and neural stem cells. Cell Tissue Res 2008;331:165-78.

390. Bystron I, Blakemore C, Rakic P. Development of the human cerebral cortex: Boulder Committee revisited. Nat Rev Neurosci 2008;9:110-22.

391. Zhong W, Jiang MM, Weinmaster G, Jan LY, Jan YN. Differential expression of mammalian Numb, Numblike and Notch1 suggests distinct roles during mouse cortical neurogenesis. Development 1997;124:1887-97.

392. Rakic P. A small step for the cell, a giant leap for mankind: a hypothesis of neocortical expansion during evolution. Trends Neurosci 1995;18:383-8.

393. Chenn A, McConnell SK. Cleavage orientation and the asymmetric inheritance of Notch1 immunoreactivity in mammalian neurogenesis. Cell 1995;82:631-41.

394. Taverna E, Huttner WB. Neural progenitor nuclei IN motion. Neuron 2010;67:906-14.

395. Del Bene F, Wehman AM, Link BA, Baier H. Regulation of neurogenesis by interkinetic nuclear migration through an apical-basal notch gradient. Cell 2008;134:1055-65.

396. Corbin JG, Gaiano N, Juliano SL, Poluch S, Stancik E, Haydar TF. Regulation of neural progenitor cell development in the nervous system. J Neurochem 2008;106:2272-87.

397. Clay MR, Halloran MC. Regulation of cell adhesions and motility during initiation of neural crest migration. Curr Opin Neurobiol 2010.

398. Okano H, Temple S. Cell types to order: temporal specification of CNS stem cells. Curr Opin Neurobiol 2009;19:112-9.

399. Noctor SC, Martinez-Cerdeno V, Kriegstein AR. Neural stem and progenitor cells in cortical development. Novartis Found Symp 2007;288:59-73; discussion -8, 96-8.

400. Brody T, Odenwald WF. Cellular diversity in the developing nervous system: a temporal view from Drosophila. Development 2002;129:3763-70.

401. Molyneaux BJ, Arlotta P, Menezes JR, Macklis JD. Neuronal subtype specification in the cerebral cortex. Nat Rev Neurosci 2007;8:427-37.

402. Engberg N, Kahn M, Petersen DR, Hansson M, Serup P. Retinoic acid synthesis promotes development of neural progenitors from mouse embryonic stem cells by suppressing endogenous, Wnt-dependent nodal signaling. Stem Cells 2010;28:1498-509.

403. Siegenthaler JA, Ashique AM, Zarbalis K, et al. Retinoic acid from the meninges regulates cortical neuron generation. Cell 2009;139:597-609.

404. Englund C, Fink A, Lau C, et al. Pax6, Tbr2, and Tbr1 are expressed sequentially by radial glia, intermediate progenitor cells, and postmitotic neurons in developing neocortex. J Neurosci 2005;25:247-51.

405. Mira H, Andreu Z, Suh H, et al. Signaling through BMPR-IA regulates quiescence and long-term activity of neural stem cells in the adult hippocampus. Cell Stem Cell 2010;7:78-89.

406. Di-Gregorio A, Sancho M, Stuckey DW, et al. BMP signalling inhibits premature neural differentiation in the mouse embryo. Development 2007;134:3359-69.

407. Brederlau A, Faigle R, Elmi M, et al. The bone morphogenetic protein type Ib receptor is a major mediator of glial differentiation and cell survival in adult hippocampal progenitor cell culture. Mol Biol Cell 2004;15:3863-75.

408. Fei T, Xia K, Li Z, et al. Genome-wide mapping of SMAD target genes reveals the role of BMP signaling in embryonic stem cell fate determination. Genome Res 2010;20:36-44.

409. Takizawa T, Ochiai W, Nakashima K, Taga T. Enhanced gene activation by Notch and BMP signaling cross-talk. Nucleic Acids Res 2003;31:5723-31.

410. Vinals F, Reiriz J, Ambrosio S, Bartrons R, Rosa JL, Ventura F. BMP-2 decreases Mash1 stability by increasing Id1 expression. EMBO J 2004;23:3527-37.

411. Hollnagel A, Oehlmann V, Heymer J, Ruther U, Nordheim A. Id genes are direct targets of bone morphogenetic protein induction in embryonic stem cells. J Biol Chem 1999;274:19838-45.

412. Imayoshi I, Sakamoto M, Yamaguchi M, Mori K, Kageyama R. Essential roles of Notch signaling in maintenance of neural stem cells in developing and adult brains. J Neurosci 2010;30:3489-98.

413. Asano H, Aonuma M, Sanosaka T, Kohyama J, Namihira M, Nakashima K. Astrocyte differentiation of neural precursor cells is enhanced by retinoic acid through a change in epigenetic modification. Stem Cells 2009;27:2744-52.

414. Androutsellis-Theotokis A, Leker RR, Soldner F, et al. Notch signalling regulates stem cell numbers in vitro and in vivo. Nature 2006;442:823-6.

415. He F, Ge W, Martinowich K, et al. A positive autoregulatory loop of Jak-STAT signaling controls the onset of astrogliogenesis. Nat Neurosci 2005;8:616-25.

416. Fan G, Martinowich K, Chin MH, et al. DNA methylation controls the timing of astrogliogenesis through regulation of JAK-STAT signaling. Development 2005;132:3345-56.

417. Nottebohm F. The road we travelled: discovery, choreography, and significance of brain replaceable neurons. Ann N Y Acad Sci 2004;1016:628-58.

418. Breunig JJ, Arellano JI, Macklis JD, Rakic P. Everything that glitters isn't gold: a critical review of postnatal neural precursor analyses. Cell Stem Cell 2007;1:612-27.

419. Song H, Stevens CF, Gage FH. Astroglia induce neurogenesis from adult neural stem cells. Nature 2002;417:39-44.

420. Lie DC, Colamarino SA, Song HJ, et al. Wnt signalling regulates adult hippocampal neurogenesis. Nature 2005;437:1370-5.

421. Filippov V, Kronenberg G, Pivneva T, et al. Subpopulation of nestin-expressing progenitor cells in the adult murine hippocampus shows electrophysiological and morphological characteristics of astrocytes. Mol Cell Neurosci 2003;23:373-82.

422. Fukuda S, Kato F, Tozuka Y, Yamaguchi M, Miyamoto Y, Hisatsune T. Two distinct subpopulations of nestin-positive cells in adult mouse dentate gyrus. J Neurosci 2003;23:9357-66.

423. Seri B, Garcia-Verdugo JM, Collado-Morente L, McEwen BS, Alvarez-Buylla A. Cell types, lineage, and architecture of the germinal zone in the adult dentate gyrus. J Comp Neurol 2004;478:359-78.

424. Cameron HA, Tanapat P, Gould E. Adrenal steroids and N-methyl-D-aspartate receptor activation regulate neurogenesis in the dentate gyrus of adult rats through a common pathway. Neuroscience 1998;82:349-54.

425. Gould E, Cameron HA, McEwen BS. Blockade of NMDA receptors increases cell death and birth in the developing rat dentate gyrus. J Comp Neurol 1994;340:551-65.

426. Monje ML, Toda H, Palmer TD. Inflammatory blockade restores adult hippocampal neurogenesis. Science 2003;302:1760-5.

427. Santarelli L, Saxe M, Gross C, et al. Requirement of hippocampal neurogenesis for the behavioral effects of antidepressants. Science 2003;301:805-9.

428. Coskun V, Wu H, Blanchi B, et al. CD133+ neural stem cells in the ependyma of mammalian postnatal forebrain. Proc Natl Acad Sci U S A 2008;105:1026-31.

429. Corti S, Nizzardo M, Nardini M, et al. Isolation and characterization of murine neural stem/progenitor cells based on Prominin-1 expression. Exp Neurol 2007;205:547-62.

430. Dromard C, Guillon H, Rigau V, et al. Adult human spinal cord harbors neural precursor cells that generate neurons and glial cells in vitro. J Neurosci Res 2008;86:1916-26.

431. Capela A, Temple S. LeX/ssea-1 is expressed by adult mouse CNS stem cells, identifying them as nonependymal. Neuron 2002;35:865-75.

432. Yang XT, Bi YY, Feng DF. From the vascular microenvironment to neurogenesis. Brain Res Bull 2010.

433. Kokovay E, Goderie S, Wang Y, et al. Adult SVZ lineage cells home to and leave the vascular niche via differential responses to SDF1/CXCR4 signaling. Cell Stem Cell 2010;7:163-73.

434. Furnari FB, Fenton T, Bachoo RM, et al. Malignant astrocytic glioma: genetics, biology, and paths to treatment. Genes Dev 2007;21:2683-710.

435. Chen R, Nishimura MC, Bumbaca SM, et al. A hierarchy of self-renewing tumor-initiating cell types in glioblastoma. Cancer Cell 2010;17:362-75.

436. Xie Z, Chin LS. Molecular and cell biology of brain tumor stem cells: lessons from neural progenitor/stem cells. Neurosurg Focus 2008;24:E25.

437. Stoica G, Lungu G, Stoica H, Waghela S, Levine J, Smith R, 3rd. Identification of cancer stem cells in dog glioblastoma. Vet Pathol 2009.

438. Chu LL, Rutteman GR, Kong JM, et al. Genomic organization of the canine p53 gene and its mutational status in canine mammary neoplasia. Breast Cancer Res Treat 1998;50:11-25.

439. Piccirillo SG, Binda E, Fiocco R, Vescovi AL, Shah K. Brain cancer stem cells. J Mol Med 2009;87:1087-95.

440. Tate MC, Aghi MK. Biology of angiogenesis and invasion in glioma. Neurotherapeutics 2009;6:447-57.

441. Tchougounova E, Kastemar M, Brasater D, Holland EC, Westermark B, Uhrbom L. Loss of Arf causes tumor progression of PDGFB-induced oligodendroglioma. Oncogene 2007;26:6289-96.

442. Martinho O, Longatto-Filho A, Lambros MB, et al. Expression, mutation and copy number analysis of platelet-derived growth factor receptor A (PDGFRA) and its ligand PDGFA in gliomas. Br J Cancer 2009;101:973-82.

443. Fan X, Khaki L, Zhu TS, et al. NOTCH pathway blockade depletes CD133-positive glioblastoma cells and inhibits growth of tumor neurospheres and xenografts. Stem Cells;28:5-16.

444. Chiba T, Seki A, Aoki R, et al. Bmi1 promotes hepatic stem cell expansion and tumorigenicity in both Ink4a/Arf-dependent and -independent manners in Mice. Hepatology.

445. Facchino S, Abdouh M, Chatoo W, Bernier G. BMI1 confers radioresistance to normal and cancerous neural stem cells through recruitment of the DNA damage response machinery. J Neurosci;30:10096-111.

446. Ligon KL, Huillard E, Mehta S, et al. Olig2-regulated lineage-restricted pathway controls replication competence in neural stem cells and malignant glioma. Neuron 2007;53:503-17.

447. Hoenerhoff MJ, Chu I, Barkan D, et al. BMI1 cooperates with H-RAS to induce an aggressive breast cancer phenotype with brain metastases. Oncogene 2009;28:3022-32.

448. Jen J, Harper JW, Bigner SH, et al. Deletion of p16 and p15 genes in brain tumors. Cancer Res 1994;54:6353-8.

449. Sherr CJ, McCormick F. The RB and p53 pathways in cancer. Cancer Cell 2002;2:103-12.

450. Rao SK, Edwards J, Joshi AD, Siu IM, Riggins GJ. A survey of glioblastoma genomic amplifications and deletions. J Neurooncol;96:169-79.

451. Ali IU, Schriml LM, Dean M. Mutational spectra of PTEN/MMAC1 gene: a tumor suppressor with lipid phosphatase activity. J Natl Cancer Inst 1999;91:1922-32.

452. Kwon CH, Zhao D, Chen J, et al. Pten haploinsufficiency accelerates formation of high-grade astrocytomas. Cancer Res 2008;68:3286-94.

453. Salmena L, Carracedo A, Pandolfi PP. Tenets of PTEN tumor suppression. Cell 2008;133:403-14.

454. Parsons DW, Jones S, Zhang X, et al. An integrated genomic analysis of human glioblastoma multiforme. Science 2008;321:1807-12.

455. Zheng H, Ying H, Wiedemeyer R, et al. PLAGL2 regulates Wnt signaling to impede differentiation in neural stem cells and gliomas. Cancer Cell;17:497-509.

456. Hou Y, Gupta N, Schoenlein P, et al. An anti-tumor role for cGMP-dependent protein kinase. Cancer Lett 2006;240:60-8.

457. Swartling FJ, Ferletta M, Kastemar M, Weiss WA, Westermark B. Cyclic GMP-dependent protein kinase II inhibits cell proliferation, Sox9 expression and Akt phosphorylation in human glioma cell lines. Oncogene 2009;28:3121-31.

458. Chen L, Daum G, Chitaley K, et al. Vasodilator-stimulated phosphoprotein regulates proliferation and growth inhibition by nitric oxide in vascular smooth muscle cells. Arterioscler Thromb Vasc Biol 2004;24:1403-8.

459. Kodach LL, Bleuming SA, Musler AR, et al. The bone morphogenetic protein pathway is active in human colon adenomas and inactivated in colorectal cancer. Cancer 2008;112:300-6.

460. Lee J, Son MJ, Woolard K, et al. Epigenetic-mediated dysfunction of the bone morphogenetic protein pathway inhibits differentiation of glioblastoma-initiating cells. Cancer Cell 2008;13:69-80.

461. Downey C, Alwan K, Thamilselvan V, et al. Pressure stimulates breast cancer cell adhesion independently of cell cycle and apoptosis regulatory protein (CARP)-1 regulation of focal adhesion kinase. Am J Surg 2006;192:631-5.

462. Rishi AK, Zhang L, Yu Y, et al. Cell cycle- and apoptosis-regulatory protein-1 is involved in apoptosis signaling by epidermal growth factor receptor. J Biol Chem 2006;281:13188-98.

463. Cerami E, Demir E, Schultz N, Taylor BS, Sander C. Automated network analysis identifies core pathways in glioblastoma. PLoS One 2010;5:e8918.

464. Wang XY, Smith DI, Liu W, James CD. GBAS, a novel gene encoding a protein with tyrosine phosphorylation sites and a transmembrane domain, is co-amplified with EGFR. Genomics 1998;49:448-51.

465. Lo HW, Zhu H, Cao X, Aldrich A, Ali-Osman F. A novel splice variant of GLI1 that promotes glioblastoma cell migration and invasion. Cancer Res 2009;69:6790-8.

466. Sidransky D, Mikkelsen T, Schwechheimer K, Rosenblum ML, Cavanee W, Vogelstein B. Clonal expansion of p53 mutant cells is associated with brain tumour progression. Nature 1992;355:846-7.

467. Noushmehr H, Weisenberger DJ, Diefes K, et al. Identification of a CpG island methylator phenotype that defines a distinct subgroup of glioma. Cancer Cell;17:510-22.

468. Vieira C, Pombero A, Garcia-Lopez R, Gimeno L, Echevarria D, Martinez S. Molecular mechanisms controlling brain development: an overview of neuroepithelial secondary organizers. Int J Dev Biol 2010;54:7-20.

469. Taipale J, Beachy PA. The Hedgehog and Wnt signalling pathways in cancer. Nature 2001;411:349-54.

470. Pardal R, Clarke MF, Morrison SJ. Applying the principles of stem-cell biology to cancer. Nat Rev Cancer 2003;3:895-902.

471. Taylor MD, Poppleton H, Fuller C, et al. Radial glia cells are candidate stem cells of ependymoma. Cancer Cell 2005;8:323-35.

472. Huang X, Ketova T, Litingtung Y, Chiang C. Isolation, enrichment, and maintenance of medulloblastoma stem cells. J Vis Exp 2010.

473. Johnson RA, Wright KD, Poppleton H, et al. Cross-species genomics matches driver mutations and cell compartments to model ependymoma. Nature 2010;466:632-6.

474. Rousseau E, Ruchoux MM, Scaravilli F, et al. CDKN2A, CDKN2B and p14ARF are frequently and differentially methylated in ependymal tumours. Neuropathol Appl Neurobiol 2003;29:574-83.

475. Molenaar WM, Jansson DS, Gould VE, et al. Molecular markers of primitive neuroectodermal tumors and other pediatric central nervous system tumors. Monoclonal antibodies to neuronal and glial antigens distinguish subsets of primitive neuroectodermal tumors. Lab Invest 1989;61:635-43.

476. Onvani S, Etame AB, Smith CA, Rutka JT. Genetics of medulloblastoma: clues for novel therapies. Expert Rev Neurother 2010;10:811-23.

477. Read TA, Fogarty MP, Markant SL, et al. Identification of CD15 as a marker for tumor-propagating cells in a mouse model of medulloblastoma. Cancer Cell 2009;15:135-47.

478. Enguita-German M, Schiapparelli P, Rey JA, Castresana JS. CD133+ cells from medulloblastoma and PNET cell lines are more resistant to cyclopamine inhibition of the sonic hedgehog signaling pathway than CD133- cells. Tumour Biol 2010;31:381-90.

479. Wolburg H, Paulus W. Choroid plexus: biology and pathology. Acta Neuropathol 2010;119:75-88.

480. Hunter NL, Dymecki SM. Molecularly and temporally separable lineages form the hindbrain roof plate and contribute differentially to the choroid plexus. Development 2007;134:3449-60.

481. Dang L, Fan X, Chaudhry A, Wang M, Gaiano N, Eberhart CG. Notch3 signaling initiates choroid plexus tumor formation. Oncogene 2006;25:487-91.

482. Ide T, Uchida K, Kikuta F, Suzuki K, Nakayama H. Immunohistochemical characterization of canine neuroepithelial tumors. Vet Pathol 2010;47:741-50.

483. Mahfouz S, Aziz AA, Gabal SM, el-Sheikh S. Immunohistochemical study of CD99 and EMA expression in ependymomas. Medscape J Med 2008;10:41.

484. Nupponen NN, Paulsson J, Jeibmann A, et al. Platelet-derived growth factor receptor expression and amplification in choroid plexus carcinomas. Mod Pathol 2008;21:265-70.

485. Gyure KA, Morrison AL. Cytokeratin 7 and 20 expression in choroid plexus tumors: utility in differentiating these neoplasms from metastatic carcinomas. Mod Pathol 2000;13:638-43.

486. Sarkar C, Chattopadhyay P, Ralte AM, Mahapatra AK, Sinha S. Loss of heterozygosity of a locus in the chromosomal region 17p13.3 is associated with increased cell proliferation in astrocytic tumors. Cancer Genet Cytogenet 2003;144:156-64.

487. Kano T, Ikota H, Wada H, Iwasa S, Kurosaki S. A case of an anaplastic ependymoma with gliosarcomatous components. Brain Tumor Pathol 2009;26:11-7.

488. Jacobsen PF, Parker TJ, Papadimitriou JM. Ependymal differentiation of a glioblastoma multiforme after heterotransplantation into nude mice. J Natl Cancer Inst 1987;79:771-9.

489. Poppleton H, Gilbertson RJ. Stem cells of ependymoma. Br J Cancer 2007;96:6-10.

490. Vescovi AL, Parati EA, Gritti A, et al. Isolation and cloning of multipotential stem cells from the embryonic human CNS and establishment of transplantable human neural stem cell lines by epigenetic stimulation. Exp Neurol 1999;156:71-83.

491. Rosenzweig BL, Imamura T, Okadome T, et al. Cloning and characterization of a human type II receptor for bone morphogenetic proteins. Proc Natl Acad Sci U S A 1995;92:7632-6.

492. Sherry MM, Reeves A, Wu JK, Cochran BH. STAT3 is required for proliferation and maintenance of multipotency in glioblastoma stem cells. Stem Cells 2009;27:2383-92.

493. Scott CE, Wynn SL, Sesay A, et al. SOX9 induces and maintains neural stem cells. Nat Neurosci 2010;13:1181-9.

494. Karlsson EK, Lindblad-Toh K. Leader of the pack: gene mapping in dogs and other model organisms. Nat Rev Genet 2008;9:713-25.

495. Pfenninger CV, Roschupkina T, Hertwig F, et al. CD133 is not present on neurogenic astrocytes in the adult subventricular zone, but on embryonic neural stem cells, ependymal cells, and glioblastoma cells. Cancer Res 2007;67:5727-36.

496. Miloso M, Scuteri A, Foudah D, Tredici G. MAPKs as mediators of cell fate determination: an approach to neurodegenerative diseases. Curr Med Chem 2008;15:538-48.

497. Aouadi M, Bost F, Caron L, Laurent K, Le Marchand Brustel Y, Binetruy B. p38 mitogen-activated protein kinase activity commits embryonic stem cells to either neurogenesis or cardiomyogenesis. Stem Cells 2006;24:1399-406.

498. Alonso G. Proliferation of progenitor cells in the adult rat brain correlates with the presence of vimentin-expressing astrocytes. Glia 2001;34:253-66.

499. Shin TK, Lee YD, Sim KB. Embryonic intermediate filaments, nestin and vimentin, expression in the spinal cords of rats with experimental autoimmune encephalomyelitis. J Vet Sci 2003;4:9-13.

500. Tolstonog GV, Shoeman RL, Traub U, Traub P. Role of the intermediate filament protein vimentin in delaying senescence and in the spontaneous immortalization of mouse embryo fibroblasts. DNA Cell Biol 2001;20:509-29.

501. Medvedev SP, Grigor'eva EV, Shevchenko AI, et al. Human Induced Pluripotent Stem Cells Derived from Fetal Neural Stem Cells Successfully Undergo Directed Differentiation into Cartilage. Stem Cells Dev 2010.

Figure 1

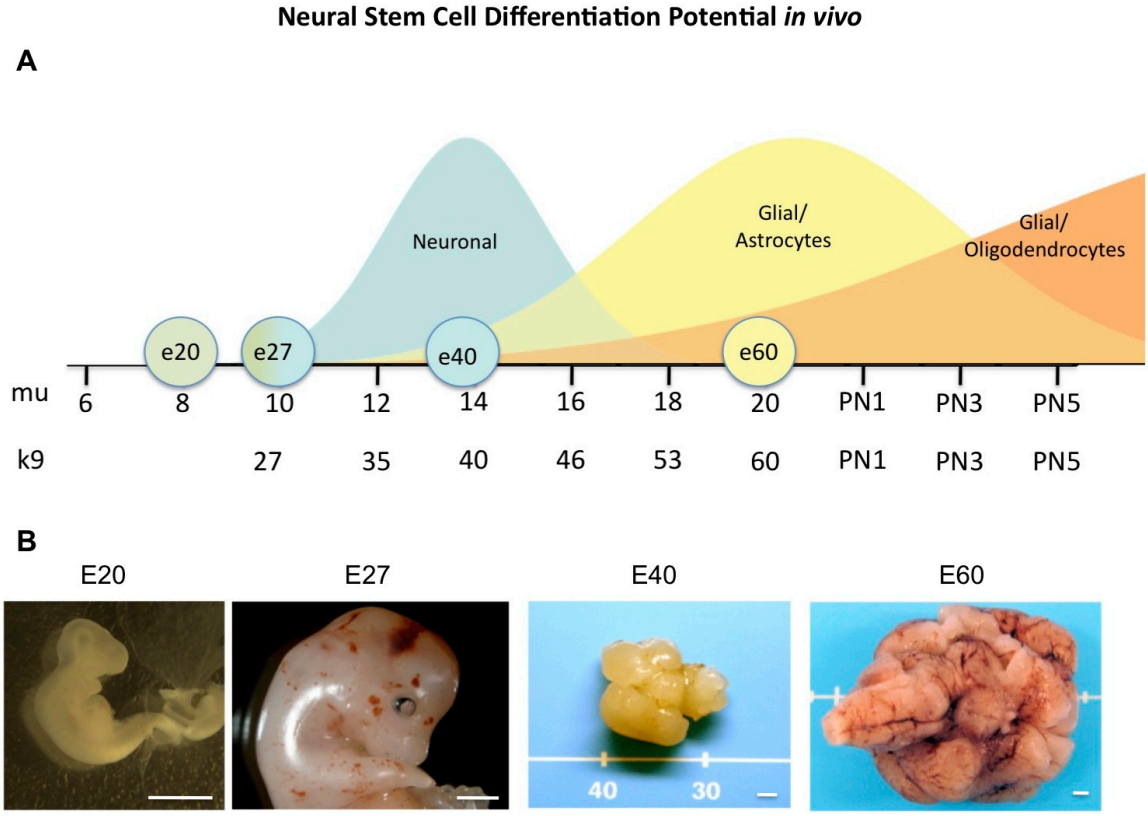

Figure 1. Canine NSCs are Isolated Throughout Gestation and Follow Temporal Differentiation Cues Similar to Murine NSCs. A) Canine NSCs were isolated from embryos at timed gestation lengths of 20, 27, 40, and 60 days. These time points correspond to the developmental periods of proliferation, the onset of neuronal differentiation, the peak of neuronal differentiaton, and the peak of astrocytic differentiation, respectively. The estimated gestational equivalency of murine (mu) NSCs is overlaid against canine (k9) NSCs. B) Canine embryos from gestational timepoints show maturation of the developing prosencephalon at E20 to a developing forebrain with craniofacial structures and eye development at E27. By E40, the telencephalon is developed into two cerebral hemispheres and at E60 the midbrain and telencephalon development are nearly complete (bar=2mm).

Figure 2

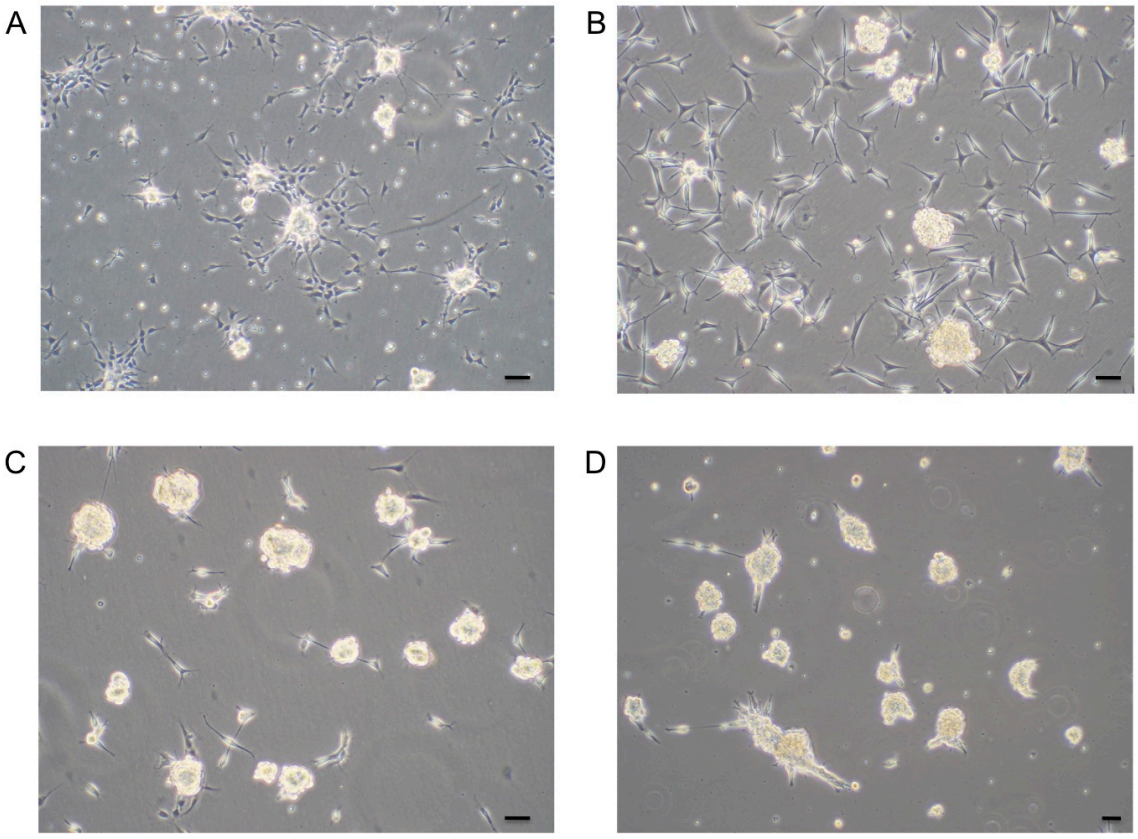

Figure 2. Canine NSCs Proliferate *in vitro* in Serum Free Media. Canine NSCs isolated from A) E20, B) E27, C) E40, and D) E60 expanded in serum free media supplemented with bFGF and EGF proliferate as non-adherent neurospheres. Early gestation canine NSCs (A and B) also exhibit an adherent, proliferative cell population (bar= 20μm).

Figure 3A

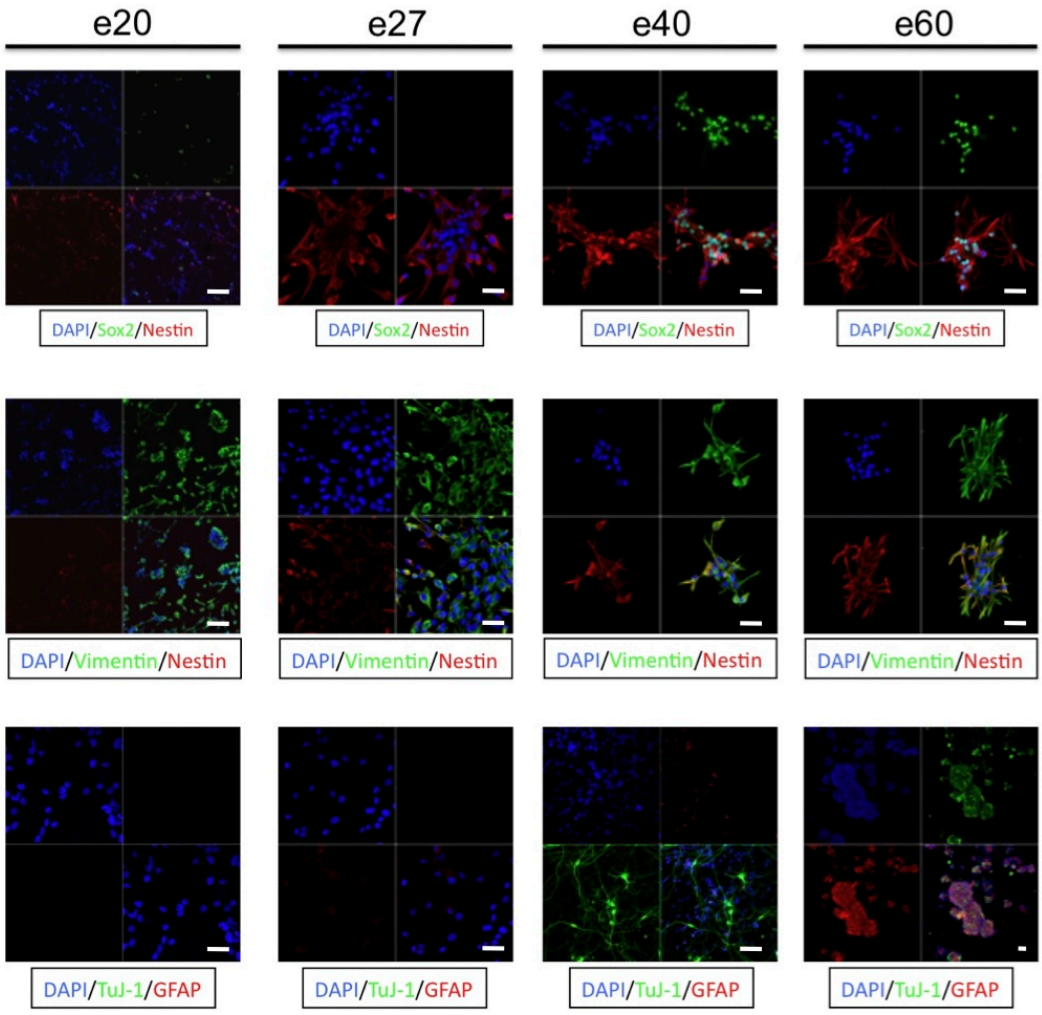

Figure 3. Expression of Neuronal or Glial Markers is Restricted to Late Gestation ***NSCs***. A) Canine NSCs cultured in NBE media show differential expression of sox2, which is expressed strongly only in E40 and E60 NSCs. Nestin is weakly expressed at E20, while all NSCs express vimentin. E20 and E27 NSCs are negative for either TuJ-1 or GFAP, while neuronal E40 NSCs express TuJ-1 and glial E60 NSCs express both TuJ-1 and GFAP (bar=20μm).

Figure 3B

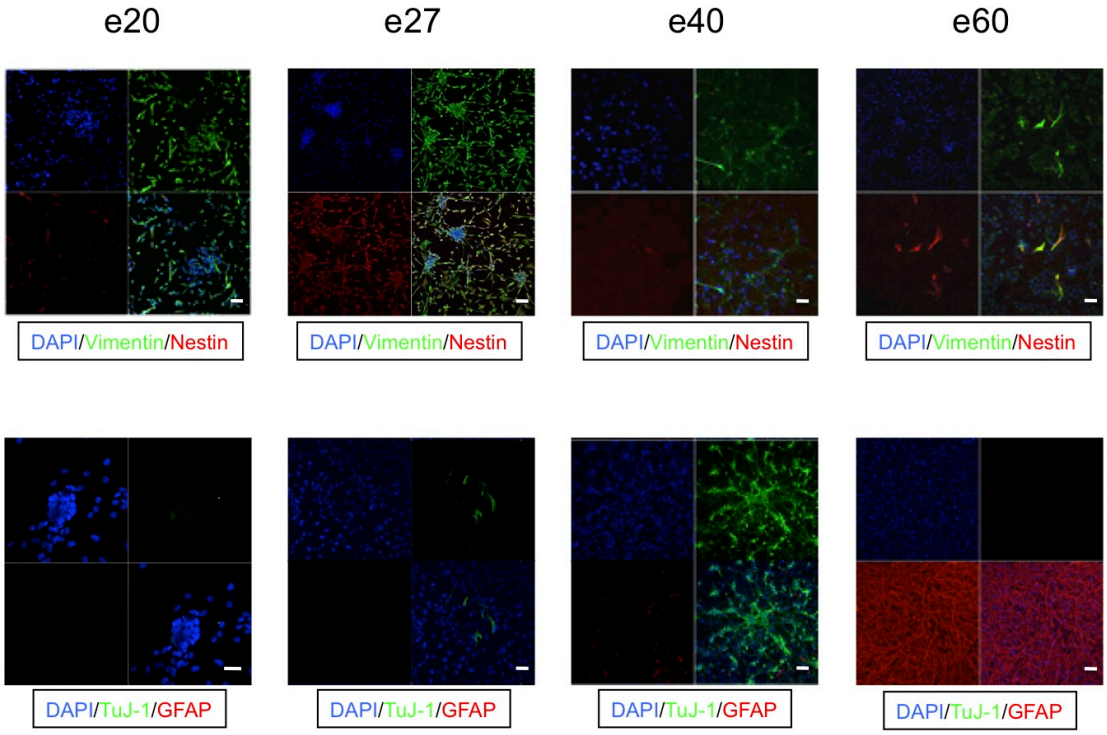

Figure 3 (Continued). Expression of Neuronal or Glial Markers is Restricted to Late Gestation NSCs. B)When cultured in the presence of serum, E20 and E27 maintain strong vimentin expression while E40 and E60 NSCs downregulate both vimentin and nestin while dramatically upregulating either TuJ-1 or GFAP, respectively. Serum results in the upregulation of TuJ-1 in rare E27 NSCs (bar=20μm).

Figure 4

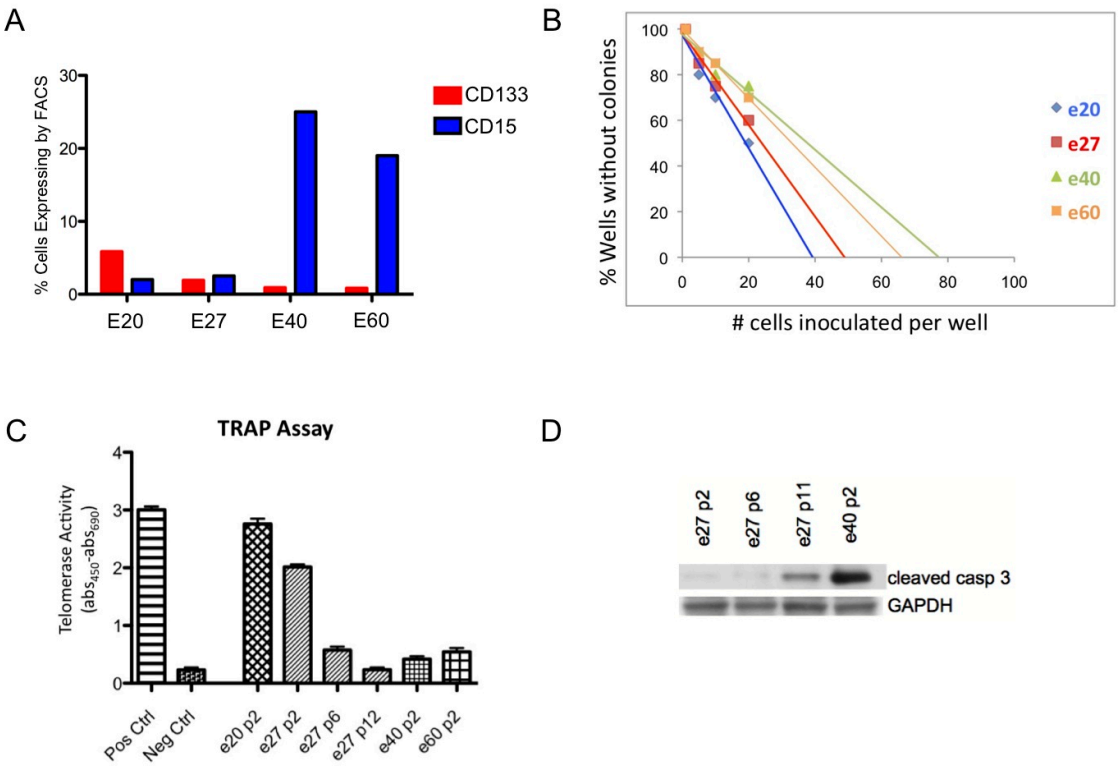

Figure 4. Canine GSCs from Early Gestation Exhibit Markers of Self-Renewal *in vitro*. A) Expression of putative neural stem cell marker CD133 is restricted to E20 NSCs, while the state-specific embryonic antigen CD15 is expressed only after the onset of neurogenesis at E40. Early gestation NSCs are more clonogenic as measured by B) limiting dilution assay at passage 2. C) E20 and E27 NSCs also express significantly more telomerase activity as compared to either E40 or E60 NSCs, although serial passage of E27 cells rapidly reduces telomerase activity. Apoptosis as measured by D) cleaved caspase 3 coincides with the onset of differentiation in either serially passaged E27 NSCs or neuronal E40 NSCs.

Figure 5

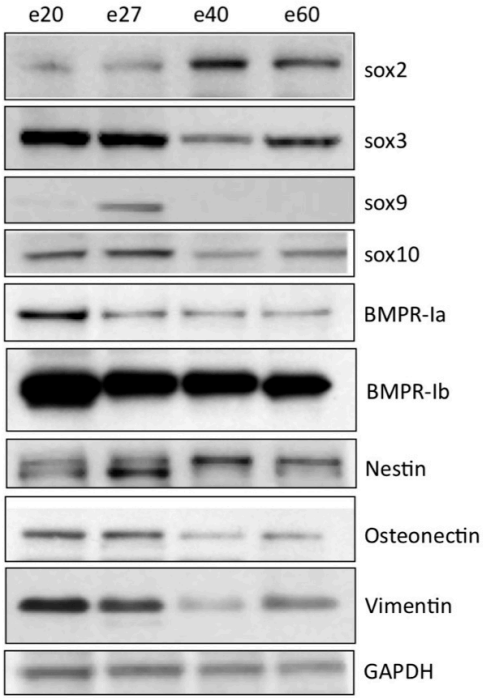

Figure 5. Canine GSCs from Early and Late Gestation Differentially Express Proteins Associated with NSC Development. Both E20 and E27 NSCs express significantly less sox2 compared to E40 or E60 NSCs. E20 and E27 NSCs express increased levels of another member of the β1-sox family, sox3, as well as sox10. E27 cells specifically express the neuroepithelial marker sox9. BMPR-1A and its induced target BMPR-1B, important for the induction of neuroepithelial cells, is expressed in E20 NSCs. While nestin is expressed in low amount in early NSCs compared to E40 or E60, these cells do express high levels of vimentin and osteonectin.

Figure 6

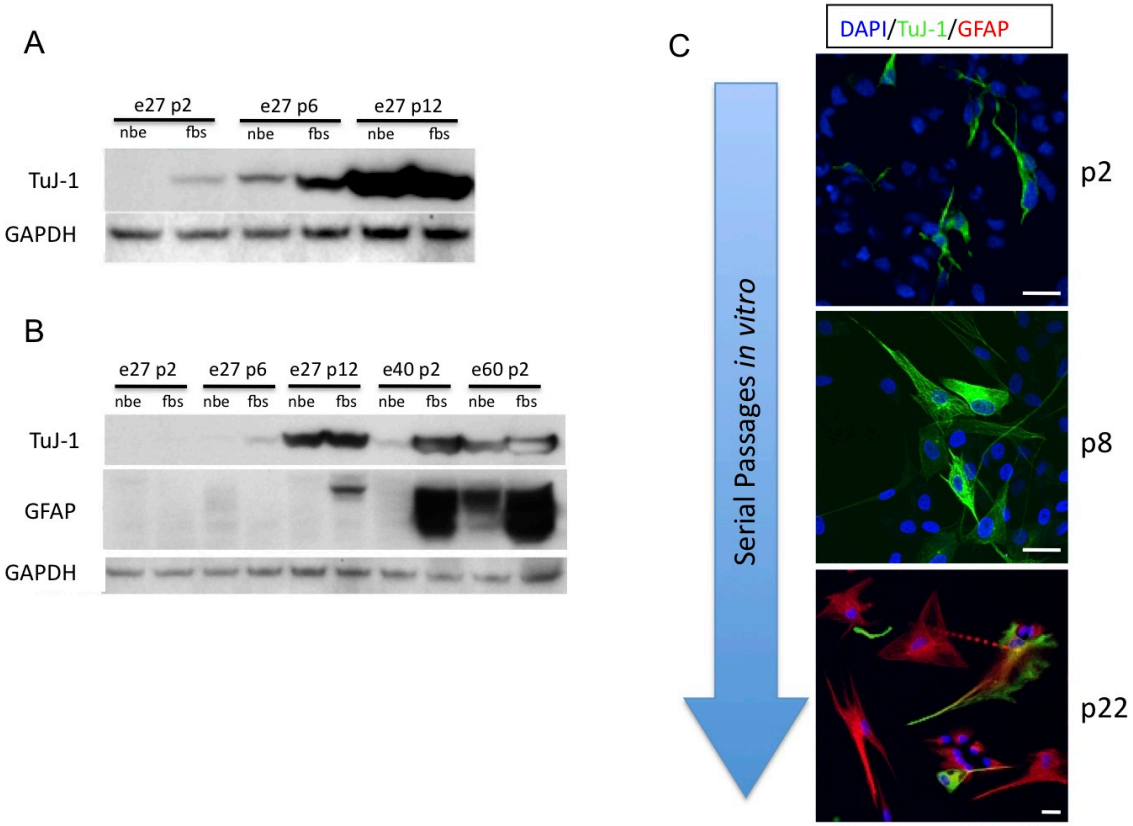

Figure 6. NSCs Derived Early in Gestation Mature *in vitro* to Neuronal and Glial Progenitor Cells. While E27 NSCs are largely lineage negative in early passage, they A) gradually acquire the ability to differentiate into neurons over serial passage, and B) demonstrate the acquition of GFAP co-expression by passage 12. C) By late passage these cells co-express significant levels of both TuJ-1 and GFAP (bar=10μm).

Figure 7

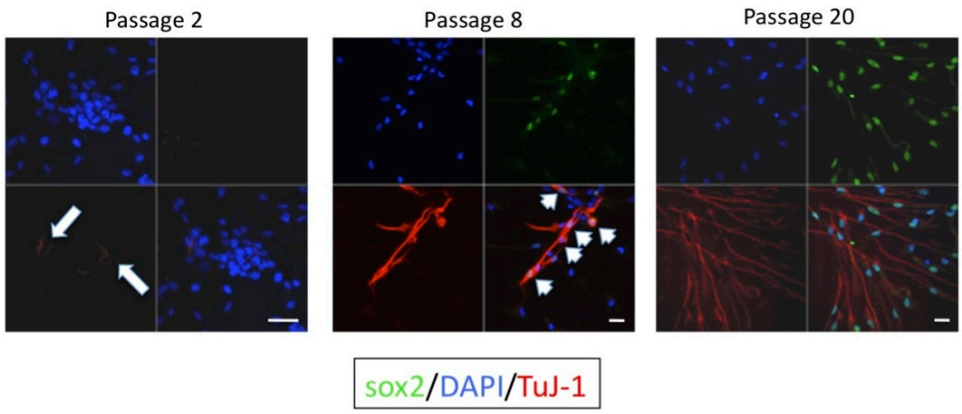

Figure 7. Serial Maturation *in vitro* Coincides with Sox2 Upregulation. While early passage, lineage negative E27 NSCs express low levels of sox2 and TuJ-1 (arrows), cells at passage 8 acquire sox2 expression as they begin to differentiate into neurons (arrowheads). By late passage, cells ubiquitously express both sox2 and TuJ-1 (bar=5μm).

Figure 8

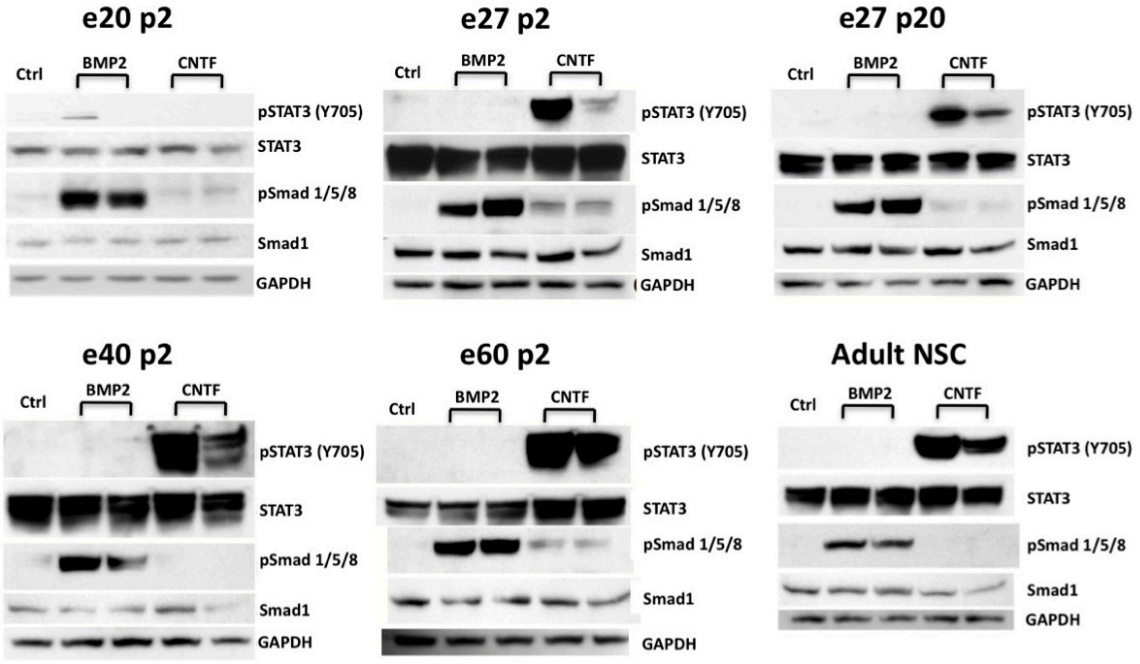

Figure 8. Cytokine Signaling through SMAD and STAT3 Pathways Regulate the Onset of Gliogenesis in Canine NSCs. While E20 NSCs exhibit a lack of STAT3 phosphorylation in response to CNTF stimulation at either 10 or 60 minutes, E27 cells at passage 2 exhibit STAT3 phosphorylation at 10 minutes but lack sustained activation at 60 minutes. In contrast, late passage E27 NSCs display similar cytokine mediated STAT3 phosphorylation to differentiation competent E40, E60, and adult canine NSCs.

Figure 9

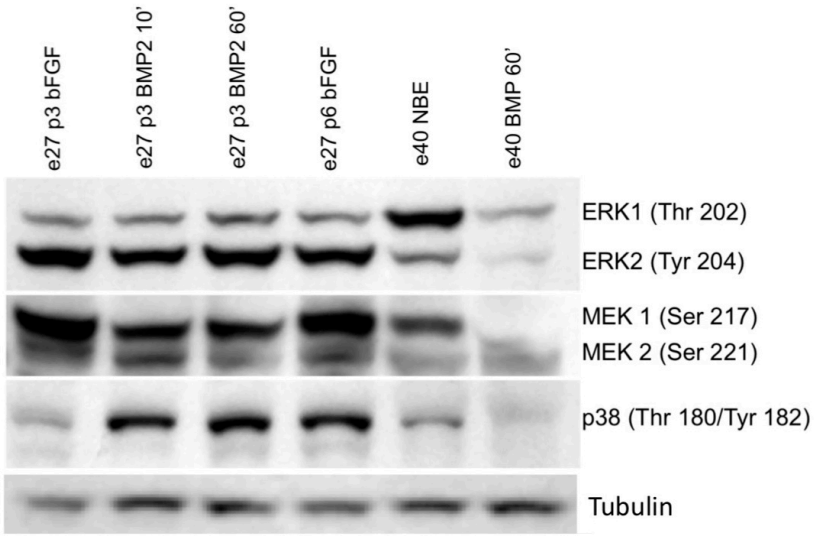

Figure 9. Differential MAP Kinase Activation Coincides with Neurogenesis in Canine NSCs. While E27 NSCs at passage 2 express little endogenous p38 phosphorylation, treatment of the neurogenic cytokine BMP2 induces p38 activation. At the time E27 NSCs spontaneously differentiate to neurons at passage 6, they are capable of endogenously phosphorylating p38. E27 cells also preferentially phosphorylate ERK2 over ERK1, in contrast to E40 NSCs.

Figure 10

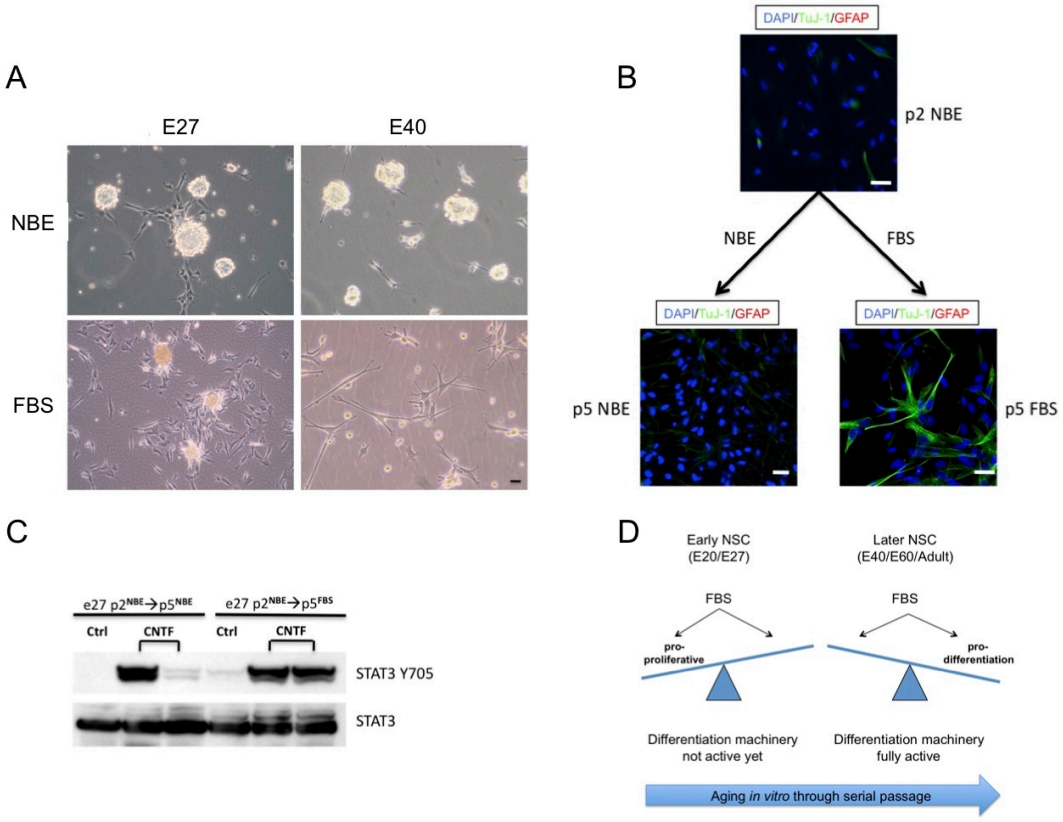

Figure 10. E27 NSCs are Resistant to Serum Induced Differentiation. A) Exposure of E40 NSC to FBS rapidly induces a phenotypic switch to neuronal or glial morphology and halts proliferation, while E27 cells continue to proliferate and form neurospheres (bar=10μm). While proliferative, E27 NSCs cultured in FBS B) express TuJ-1 at a much earlier rate than those maintained in NBE conditions (bar= 5μm). Consistent with this accelerated onset of neurogenesis, C) E27 cells in FBS more rapidly acquire sustained STAT3 phosphorylation in response to CNTF. D) Thus, while E20 and E27 cells are initially only able to respond to the proliferative cues in serum, these NSCs are able to differentiate as they mature *in vitro*.

Figure 11A

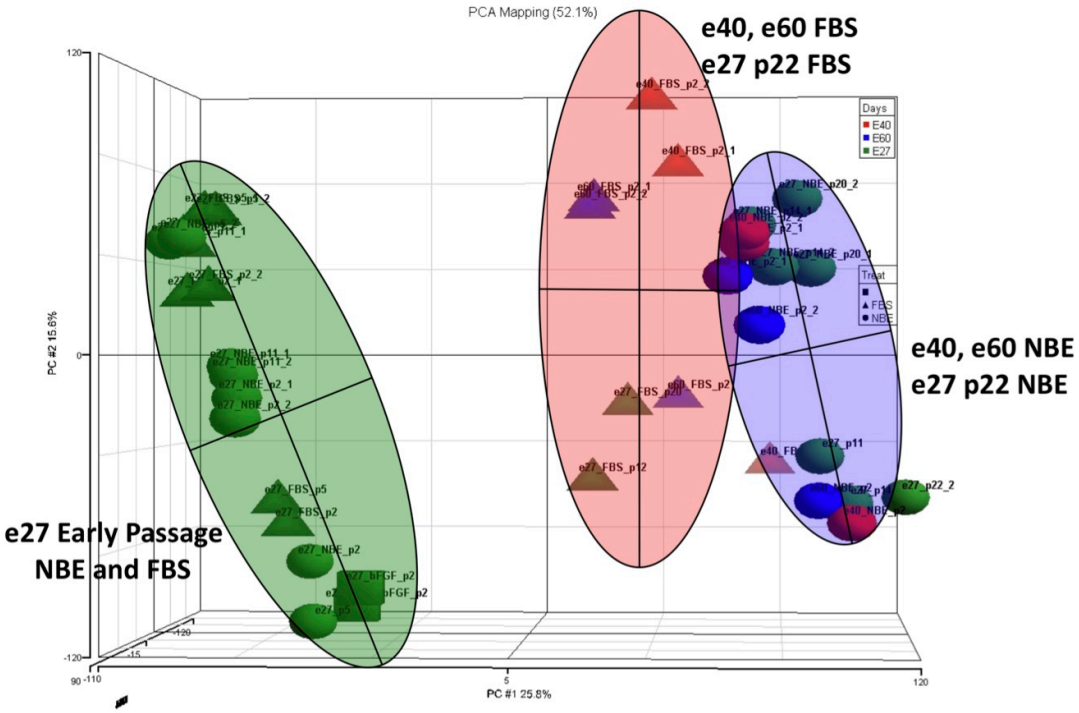

Figure 11. Analysis of Global Gene Expression Reveals Significantly Different Gene Expression in E27 NSCs at Early Passage. A) Unsupervised principle component analysis (PCA) of global gene expression between E40, E60, and E27 NSCs over serial passage indicates that E27 NSCs from passage 2 through 12 cluster together, while E27 at passage 14 and 22 cluster alongside E40 and E60. These differentiation-competent cells also demonstrate a similar treatment effect to serum, where FBS-cultured E40, E60, E27p14, and E27p22 dramatically alter their gene expression profiles. In contrast, differentiation resistant E27 NSCs at early passage cluster similarly in either NBE or FBS, highlighting their resistance to differentiation.

Figure 11B

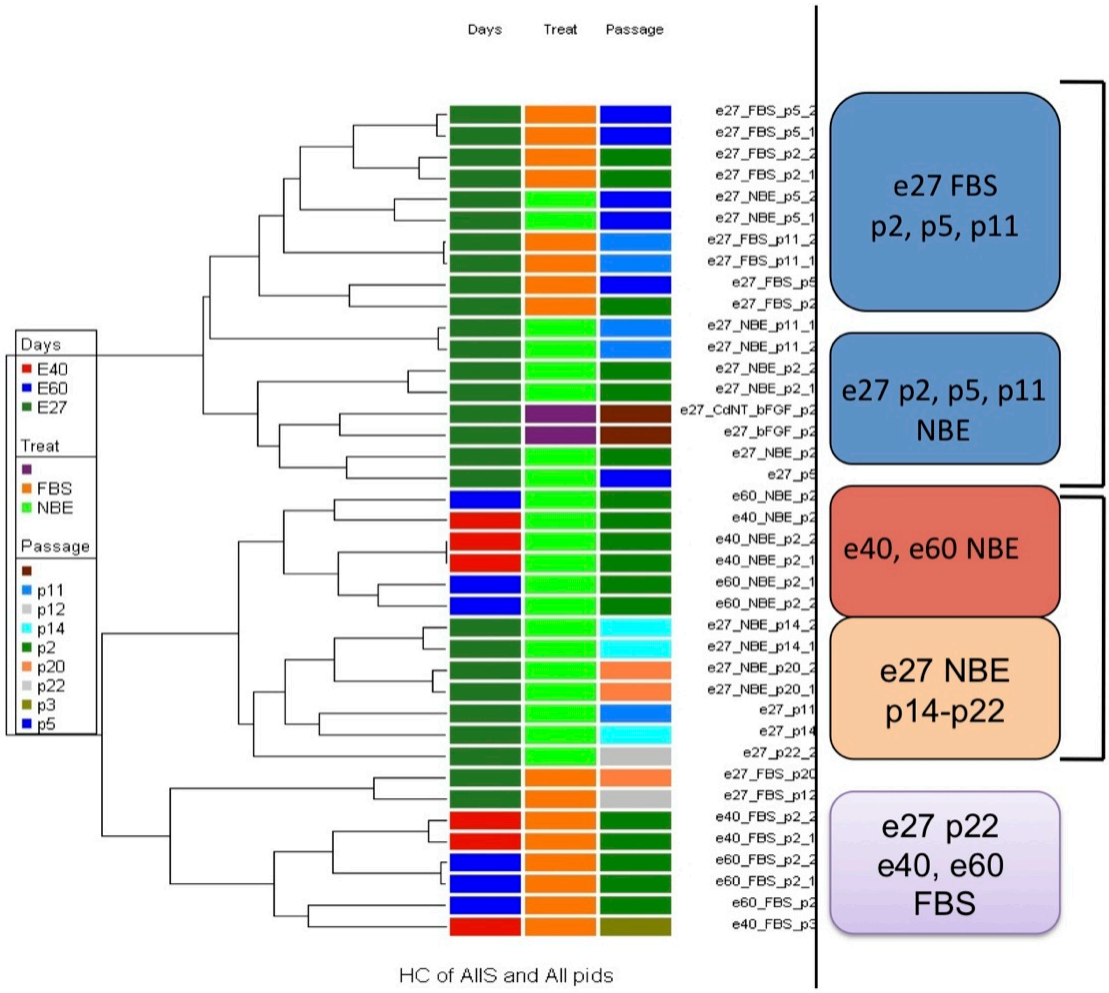

Figure 11 (Continued). Analysis of Global Gene Expression Reveals Significantly Different Gene Expression in E27 NSCs at Early Passage. B) Unsupervised hierarchical clustering of the same data further defines subclusters of NSCs and demonstrates the similarities between early passage E27 NSCs compared to late passage E27, E40, and E60 NSCs.

Figure 12

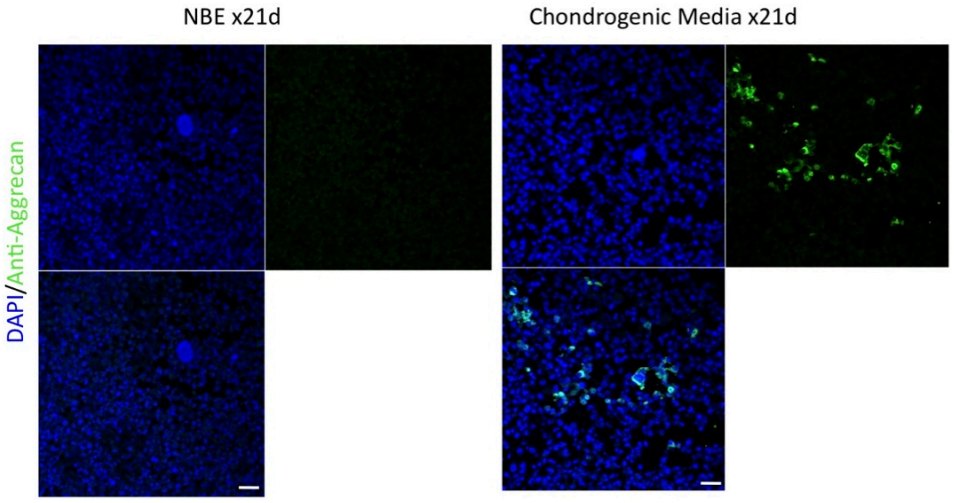

Figure 12. E27 NSCs are able to Differentiate along Chondrogenic Cell Fates. E27 NSCs cultured in TGF-β3 for prolonged periods of time express the proteoglycan aggrecan both intra- and extracellularly, suggesting significant plasticity in differentiation potential of these early NSCs.

6) SUMMARY AND CONCLUSIONS

This study addressed the following aims:

1) Determine the functional similarities between glioma stem cells isolated from human GBMs and canine glioma tumors and characterize the molecular events driving tumor formation.

2) Characterize the progressive genomic alterations within canine glioma stem cells over serial xenograft tumor formation and compare them to human GBMs through high-density array-based comparative genomic hybridization to identify shared copy number alterations.

3) Determine if canine glioma stem cells may be isolated from low-grade gliomas and other tumors of neuroepithelial origin and compare the functional and molecular similarities to glioma stem cells isolated form high-grade canine gliomas and human glioma stem cells.

4) Isolate canine embryonic neural stem cells from multiple timepoints through gestation to establish periods of temporally regulated neuronal and glial differentiation, and compare the differentiation-resistant neural stem cells isolated early in gestation to canine and human glioma stem cells.

These questions were answered as follows:

1) Canine gliomas are driven by glioma stem cells that are functionally identical to human glioma stem cells. We are able to propogate these cells using the same methodologies and they express similar stem cell markers, are able to differentiate along multiple cell lineages, and efficiently form serially transplantable tumors in immunocompromised mice using orthologous xenografts.
2) Canine GSCs exhibit progressive genomic copy number alterations over serial xenograft formation that correlate with increased xenograft tumor malignancy. This is analagous to malignant progression in human secondary glioblastoma formation, and is strongly associated with highly conserved genomic amplifications and deletions relevant to human GBM.
3) Tumor stem cells may be isolated from canine low-grade glial and other neuroepithelial tumors. These cells share significant similarities to high-grade canine and human GSCs, although low-grade GSCs express significantly less stem-cell related markers and are often less tumorigenic using xenograft models.
4) Canine embryonic neural stem cells isolated from 20, 27, 40, and 60 days gestation indicate temporally regulated maturation through expansion, neuronal, and then glial differentiation phases, similar to other mammalian neural stem cells. NSCs isolated early in gestation share significant similarities to GSCs,

including expression of stem cell markers and an intrinsic resistance serum-induced differentaition.

The cancer stem cell hypothesis attributes tumorigenicity to a specific sub-population of cells within the tumor. In many cases, these cancer stem cells share certain functional properties with normal tissue-restricted and embryonic stem cells. Others and we have demonstrated the existence of a subpopulation of tumor-derived glioma cells that self-renew, have the potential for both glial and neuronal differentiation and posses significantly increased tumorigenic potential in immunocompromised orthotopic xenograft mice models. Many key questions persist, however, regarding the relatedness of these "glioma stem cells" (GSCs) to normal neural stem cells and their exact role in GBM progression in patients. A spontaneous non-human glioma model that adequately recapitulates the disease would significantly enhance finding answers to these questions.

The domestic dog represents a unique and potentially powerful opportunity for the study of spontaneously occurring intracranial tumors, particularly in glioma. It has long been recognized that canine glial tumors are remarkably similar in growth and histologic appearance when compared to their human counterpart. Canine gliomas range from grade I pilocytic to grade IV GBMs, faithfully reproducing the salient histopathologic features of each grade of human gliomas. In this respect, the dog essentially represents the only non-human animal that is currently suitable for comparative study of naturally occurring gliomagenesis. Finally, brachycephalic dog breeds exhibit a significantly higher

incidence of gliomas providing an excellent opportunity for studying polymorphic gene variation controlling disease susceptibility.

Here, we report the isolation and characterization of GSCs from a canine anaplastic astrocytoma and demonstrate their remarkable similarities to human glioma GSCs. These GSCs exhibit shared markers of neural stem cells, are capable of differentiating along both glial and neuronal cell lineages and form invasive serial xenografts when orthotopically transplanted into immunocompromised mice. Most importantly, these xenografts progress in malignancy over serial xenotransplantation and this transformation is associated with stepwise genomic aberration of key oncogenes implicated in the progression of low-grade human astrocytomas to secondary GBMs. Most notably, canine glioma GSCs with an initial genomic deletion of p16/ARF further develop deletion of PTEN and deregulation of p53 pathway through genomic amplification and overexpression of MDM2 and MDM4; events functionally equivalent to those seen in the progression to secondary human GBMs. Thus, this study documents for the first time the key role of specific, serial genetic aberrations across species in two naturally occurring analogous tumor types and is the first study to demonstrate that these genetic aberrations are accrued within the GSC population during the progression of glial neoplasm.